UREAS IN MOLECULAR RECOGNITION: COMPLEXATION AND ENCAPSULATION

by

Blake Hamann

B.S., Chemistry

University of Iowa

Iowa City, IA

submitted to the Department of Chemistry in partial fulfillment of the requirements for the degree of

Doctor of Philosophy

at the

Massachusetts Institute of Technology

June 1996

© 1996 Massachusetts Institute of Technology

Signature of Author...

Department of Chemistry

May 15 1996

Certified by...

Professor Julius Rebek, Jr.

Thesis, Supervisor

Accepted by ....

Professor Dietmar Seyferth

Chairman, Departmental Committee on Graduate Students

Science

This doctoral thesis has been examined by a Committee of the Department of Chemistry as follows:

Professor S. Masamune ....

Chairman

Professor J. Rebek, Jr. ....

Thesis Supervisor

Professor S. C. Virgil

to Tami,
whose love and support made this possible

UREAS IN MOLECULAR RECOGNITION: COMPLEXATION AND ENCAPSULATION

by Blake Hamann

Submitted to the Department of Chemistry on May 15, 1996 in partial fulfillment of the requirements for the degree of a Doctor of Philosophy in Chemistry.

Abstract

A dicarboxylic acid cleft is presented that uses an optically active N,N'-dibenzylurea spacer. The acids are held apart by a moderately rigid structure that forms part of a C-shaped cleft. The urea offers a third binding site that is flanked by a chiral environment located in the 'floor' of the binding pocket between the diacids. Evidence for the complexation of dibasic guests through chelation of the acids is presented. Studies of optically active dibasic guests show that complexation differs between the R,R and S,S enantiomers of the host.

Ureas were also used in the development of an oxy-anion hole. Xanthene is used as a rigid U-turn to properly position two ureas so that they are unable to collapse on one another and directs the hydrogen bond donors of the ureas 'inwards' to create an oxy-anion hole. The anionic receptor has high affinity for carboxylates and phosphates in non-polar environments. Functionality at the periphery of the host is able to interact with complexed carboxylates and phosphates. The host is used as a receptor in a transesterification of a phosphodiester and to transfer information from its asymmetric auxiliaries to guests bound within the oxy-anion hole.

The self-complementarity of ureas is exploited in the formation of a dimeric capsule capable of encapsulating other organic species. A bowl-shaped calix[4]arene is used to arrange four aryl ureas in a circular fashion. Each urea is separated by enough space to allow another urea between them, giving a perfect setup for a cylindrical head-to-tail arrangement of ureas in the formation of a self-assembling dimeric capsule. Evidence for its assembly is presented. Additional data show that the newly created cavity encapsulates a variety of guests and catalyzes the Claisen rearrangement of allyl vinyl ether.

Thesis Supervisor: Dr. Julius Rebek, Jr.
Title: Camille Dreyfus Professor of Chemistry

Acknowledgments

During my graduate studies I have had the great fortune to work and play with a diverse group of world class chemists/friends. For this, I am grateful to Julius Rebek for his ability to bring such people together to create a stimulating environment for research and life. I am also indebted to Professor Rebek for his vast patience and willingness to let us explore our ideas. Thank you.

I owe much to many members of the Rebek group, past and present. Particularly, I thank Park for all the time he spent giving me chemistry advise, leading me down the correct path and for the hours of chalk-talk arguments. I enjoyed every minute and learned much. I am also grateful to Vince Rotello for always being there to lengthen the chalk-talks to marathon proportions and stirring them up the Rotello way. It is always entertaining to learning from you.

Thanks to Neil and Erica Branda for shared food, drink and television. You were always there to help enjoy these staples in my life. In addition I thank Neil, Torin Dewey and Robert Grotzfeld for the Pete's chemistry talks; there's just something about a Bunsen burner espresso. Also to Robert for shared panic attacks and the general 'hardships' in writing these things.

Many thanks to my classmates: Ken and Linda Shimizu, Roland Pieters, Anthony England and Alex Huboux. It was nice to cross the finish line with you cheering me across. And, of course, the afternoon coffee—I guess you just had to be there.

Lastly, I thank my parents and my wife, Tami, for all of her help with my thesis. Their love and hard work over the years brought me here today. I owe you everything.

Table of Contents

Chapter I

Convergent Diacids & Asymmetric Selectivity

Introduction

Diacid cleft **1** was designed so that an asymmetric microenvironment in the floor of the binding pocket would offer enantioselective complexation of dibasic guests. Stephan Luebben connected two well defined rigid U-turns, xanthene diacids, to an optically active dibenzyl urea spacer. A revised synthesis of this host, in multigram quantities, is presented here and studies show that this design gives a moderately preorganized cleft that is capable of strong binding of guests like 4,4'-dipyridyl through chelation. The extra flexibility in the host allows for multiple complexation conformers, which in turn limits the possibility of enantioselectivity in the binding studies.

1
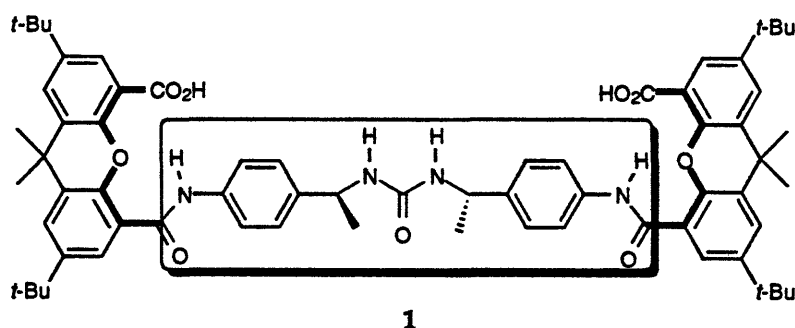
Background

Rebek and coworkers introduced molecular clefts in 1985.[1] The advantage of the cleft design over macrocycles is in the comparative ease with which they can be synthesized and their interior functionalized. An important feature in the design is an inability of convergent recognition elements to collapse on one another thereby producing a well defined binding pocket. The first generation of diacids were structurally rigid with well-defined, shallow binding sites (figure I-1).
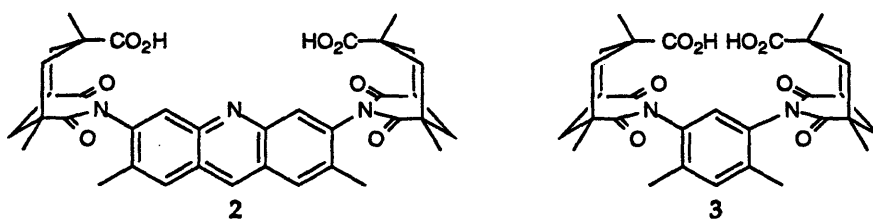

Figure I-1. *First generation of highly preorganized diacid clefts.*

Previous research found applications for these hosts as receptors for organic guests[2] and metals.[3] Diacid 3 was recently used to probe the energetics of low barrier hydrogen bonds in solution.[4] Studies with ^{1}H NMR found that an anhydrous $CDCl_3$ solution of the mono anion gave a low barrier hydrogen bond between the carboxylate and the remaining carboxylic acid. In fact, the unusual behavior of the this diacid system was first observed in a pKa determination in an ethanol/water mixture. The first deprotonation of cleft 3 has a pKa=4.8 while the second deprotonation has a pKa=11.1.[5] This large

---

1   Rebek, J. Jr.; Askew, B.; Islam, N.; Killoran, M.; Nemeth, D.; Wolak, R. *J. Am. Chem. Soc.* **1985**, *107*, 6736. Rebek, J., Jr.; Marshall, L.; Wolak, R.; Parris, K.; Killoran, M.; Askew, B.; Nemeth, D.; Islam, N. *J. Am. Chem. Soc.* **1985**, *107*, 7476-7481. Rebek, J., Jr.; Askew, B.; Islam, N.; Killoran, M.; Nemeth, D.; Wolak, R. *J. Am. Chem. Soc.* **1985**, *107*, 6736-6738.

2   Rebek, J., Jr. *Topics Curr. Chem.* **1988**, *149*, 189-210.

3   Watton, S. P.; Masschelein, A.; Rebek, J., Jr.; Lippard, S. J. *J. Am. Chem. Soc.* **1994**, *116*, 5196-5205. Yun, J.; Lippard, S. J. unpublished results.

4   Kato, Y. PhD Thesis, Massachussetts Institute of Technology, **1996**.

5   Rebek, J. Jr.; Duff, R. J.; Gordon, W. E.; Parris, K. *J. Am. Chem. Soc.* **1986**, *108*, 6068.

decrease in acidity suggests that the carboxylate is likely to be interacting with the remaining acid.

Wolfe and Nemeth put to use diacid **2** as a highly effective catalyst for enolization and hemiacetal cleavage (figure I–2). Enolization of quinuclidinone is accelerated by a factor of 60 in deuterochloroform in the presence of 10% **2**. Competitive inhibition of catalyst **2** is observed in the presence of diazabicylooctane (DABCO).[6] The decomposition of glycolaldehyde hemiacetal dimer is greatly accelerated by diacid **2** and 0.25% catalyst is sufficient to cause a 1.4×10^8 fold increase in the rate of decomposition of a hemiacetal.[7]
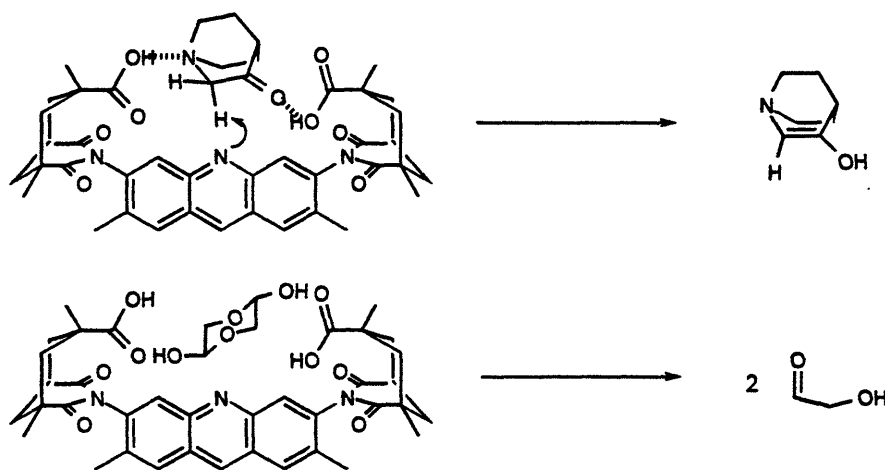
Figure I–2. *Diacid acridine clefts used in the catalysis of enolization and hemiacetal decomposition.*

Since the introduction of these clefts by Rebek a variety of diacid clefts were developed that offer a wide range of shapes, sizes and applications. Wilcox developed a V-shaped cleft based on Tröger's base, **5**. This shape was found to have excellent complementarity with that of 2-aminopyridine and similar structures (figure I–3).[8] Zimmerman developed a 'Tweezer' approach

6 Wolfe, J.; Muehldorf, A.; Rebek, J. Jr. . *Am. Chem. Soc.* **1991**, *113*, 1453-1454.

7 Nemeth, D. J. Ph.D. Thesis University of Pittsburgh, **1987**.

8 Adrian, J. C.; Wilcox, C. S. *J. Am. Chem. Soc.* **1989**, *111*, 8055-8057.

for the complexation of 9-propyladenosine.[9] Two aromatic surfaces of the host sandwich the flat guest while a carboxylic acid deep within the cavity provides hydrogen bonds 4. Jorgensen's calculations show that there are approximately equal contributions from the hydrogen bonds and aromatic stacking interactions to the affinity.[10] Experimentally the affinity between 4 and 9-propyladenosine was determined to be about 6.0 kcal/mol.
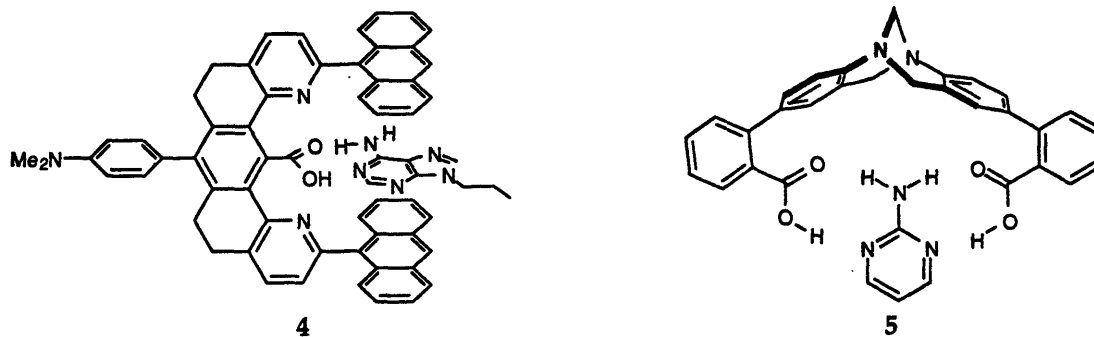

Figure I-3. *Carboxylic acid based clefts used to bind adenine and related heterocycles.*

Rebek and coworkers developed a second generation of diacid clefts using a different U-turn molecule, the xanthene. The xanthene was first introduced as a covalently linked rigid U-turn for templated peptide bond formation.[11] The xanthene offers the advantage of providing a deeper cleft than can be obtained with the use of Kemp's triacid (figure I-4), which enables the binding of larger guests within the cavity without experiencing strong steric repulsion from the spacer. One of the first xanthene based diacid clefts used a biphenyl spacer. Despite this spacer's flexibility, 6 proved to be quite successful at bonding diamines.[12] The flexibility in cleft 6 is not as great as it might first appear. The three rotations about the amide–aryl and aryl–aryl bonds only give rise to S-shaped and C-shaped molecules (figure I-4) and the cleft does not need to access a high energy state to reach the binding conformer. Extra conformational stabilization is also seen in an

9   Zimmerman, S.; Wu, W. *J. Am. Chem. Soc.* 1989, *111*, 8054-8055.

10   Blake, J. F.; Jorgensen, W. L. *J. Am. Chem. Soc.*, 1990, *112*, 7269

11   Kemp, D. S.; Buckler, D. R. *Tetrahedron Lett.* 1991, *32*, 3009-3012.

12   Nowick, J. S.; Ballester, P.; Ebmeyer, F.; Rebek, J., Jr. *J. Am. Chem. Soc.* 1990, *112*, 8902-8906.

intramolecular hydrogen bond between the amide N–H and the ether oxygen of the xanthene.
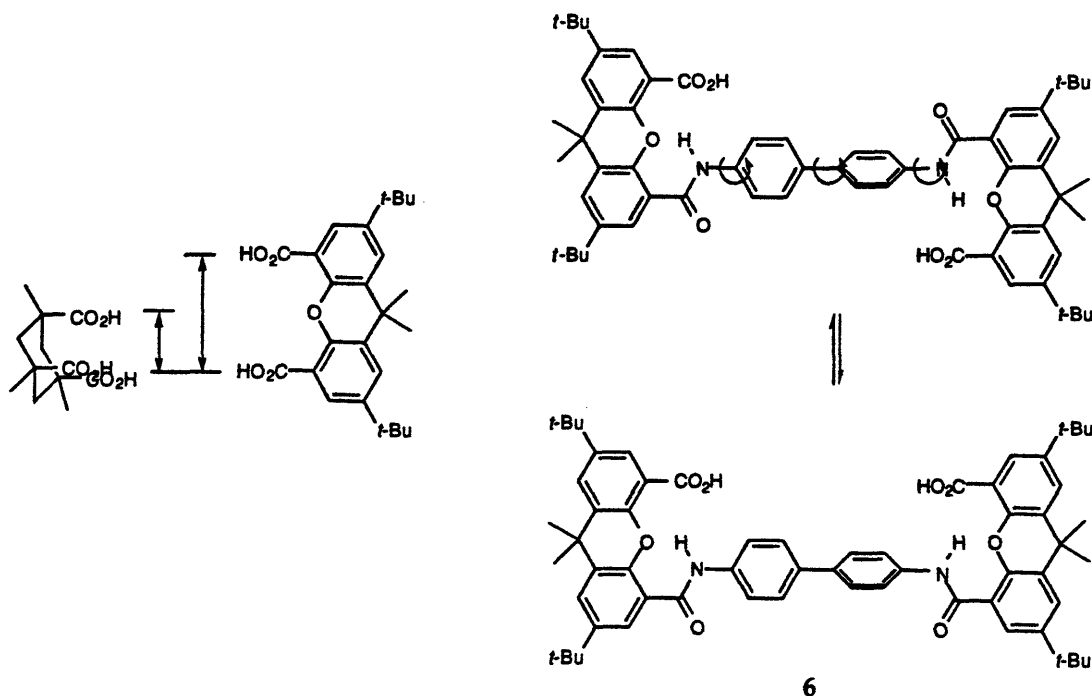
Figure I–4. *The deeper xanthene combined with limited conformational flexibility of the biphenyl spacer produced a larger cleft than was previously seen.*

Two other diacid clefts with similarly flexible spacers were synthesized by Gokel[13] and Vögtle.[14] Gokel uses a biphenyl spacer to link two ferrocene dicarboxylic acid units. The ferrocenes permit even more non-productive conformers to exist than does either **6** or **8** (figure I–5). Despite this extra flexibility strong binding affinity is still observed for diamine guests. Vögtle uses a diacetylene bridge to link two cyclophane units in a convergent fashion (figure I–5). This geometry was found to be a good fit for purines and pyrimidines which, is similar to Wilcox observation with diacid **5**.

[13] Medina, J. C.; Li, C.; Bott, S. G.; Atwood, J. L.; Gokel, G. W. *J. Am. Chem. Soc.* **1991**, *113*, 366-367.

[14] Güther, R.; Nieger, M.; Vögtle, F. *Angew. Chem. Int. Ed.* **1993**, *32*, 601-603.
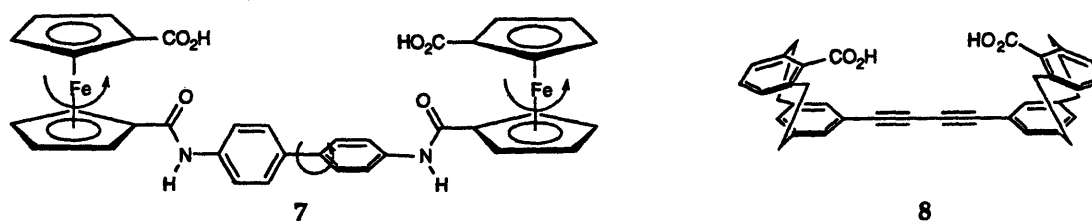
Figure I–5. *Diacid clefts which use moderately flexible spacers.*

Recently Rebek reported two highly preorganized diacid clefts (figure I–6).[15] Each uses xanthenes linked to a naphthalene (9) or perylene (10) spacer through an imide bond. The rotation about the nitrogen–aryl bond is frozen out at room temperature and the S-shaped and C-shaped clefts can be isolated as separate species. This gives a cleft that is locked in the desired C-shaped orientation. The flat spacer in conjunction with the depth provided by the xanthene U-turn produces a large binding pocket. Perylene diacid 10 is an elegant example of how modular synthesis and proper design can be combined to produce a well-defined spacious cleft that is readily prepared on multigram scale.

Figure I–6. *Extremely rigid diacid clefts that contain deep binding pockets.*

Design

The design of asymmetric microenvironments capable of enantioselection of optically active guests requires incorporation of at least

15 Shimizu, K. D.; Rebek, J. Jr. *Proc. Nat. Acad. Sci. USA*, **1995**, *92*, 12403-12407. Shimizu, K. D. Ph.D. Thesis Massachusetts Institute of Technology, **1995**.

three contacts between host and guest.[16] Each point of contact can be an attractive force, such as a hydrogen bond, or a negative int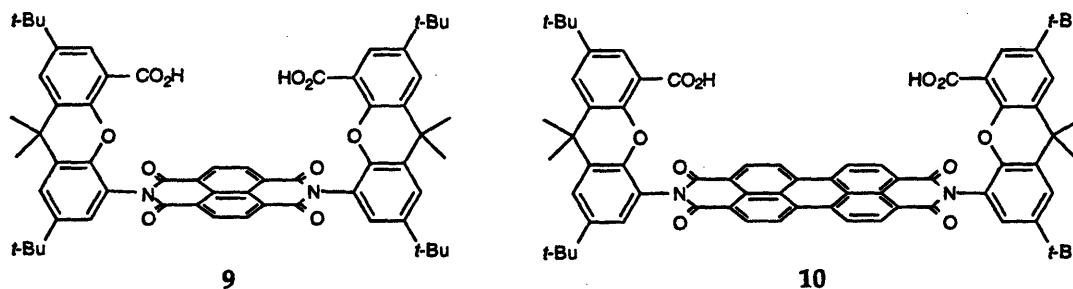eraction, such as steric repulsion. Multipoint contacts are also possible at a given binding site. An example of multipoint interactions is seen in aryl–aryl stacking.

A popular approach in the design of enantioselective molecular hosts often utilizes two or more attractive interactions and a repulsive steric force. Attractive forces serve to bring host and guest together and orient the chiral guest so that it will experience the host's asymmetric microenvironment. The 'good' enantiomer of the guest forms a tight complex which the 'bad' enantiomer cannot form due to steric repulsion.

Design of host **1** incorporates several useful features: convergent carboxylic acids, an oxy-anion hole in the 'floor' of the molecule, placement of chiral centers between the recognition sites and a convenient modular synthesis (figure I-7).
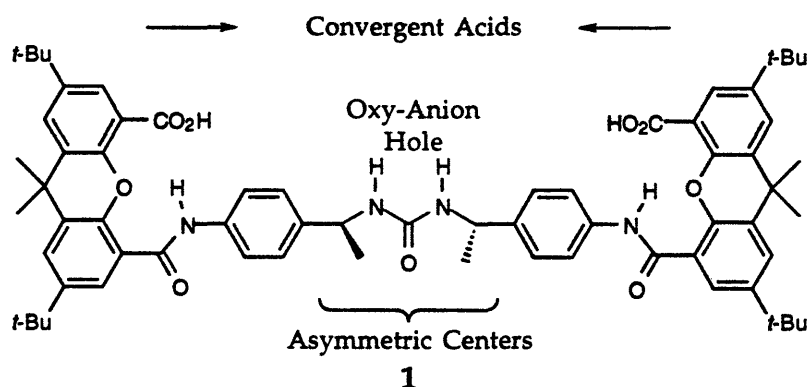
Figure I–7. *Optically acitive cleft that offers three binding sites.*

Synthesis

Synthesis of chiral cleft **1** utilizes the readily available U-turn molecule, 4,5-xanthene diacid **11**. Synthesis of mono protected benzyl ester **13** was previously worked-out by conversion of diacid **11** to dibenzyl ester **12**

---

16 Pirkle, W. H.; Pochapsky, T. C. *Chem. Rev.* **1989**, *89*, 347. Salem, L.; Chapuisat, X.; Segal, G.; Hiberty, P. C.; Minot, C.; Leforrestier, C.; Sautet, P. *J. Am. Chem. Soc.* **1987**, *109*, 2887.

followed by mono deprotection with hydrogen bromide in methylene chloride (scheme I-1).[17]
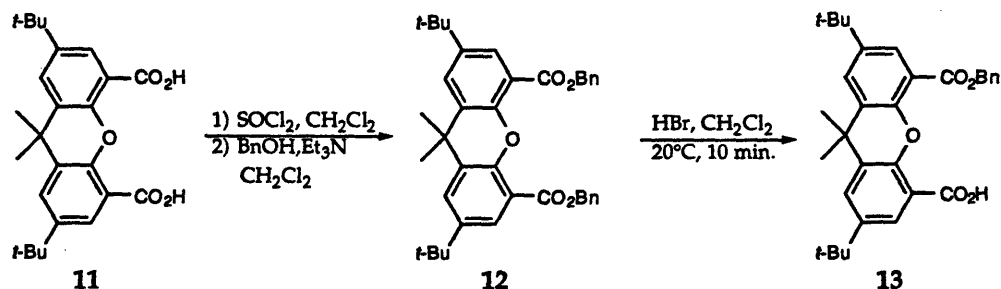
Scheme I-1. *Synthesis of xanthene monobenylester/monocarboxylic acid.*

Synthesis of chiral spacer **16** starts from optically active α-methylbenzyl amine (scheme I-2). The amine is protected by acylation with acetic anhydride. The acetamide was then nitrated in a cold sulfuric/nitric acid mixture.[18] The acetamide was cleaved under acidic conditions to yield the ammonium salt **14** which was symmetrically coupled to the phosgene equivalent phenylchloroformate in anhydrous tetrahydrofuran. Dinitro urea **15** was converted to the amine via Raney nickel catalyzed reduction with hydrazine in refluxing ethanol.[19]
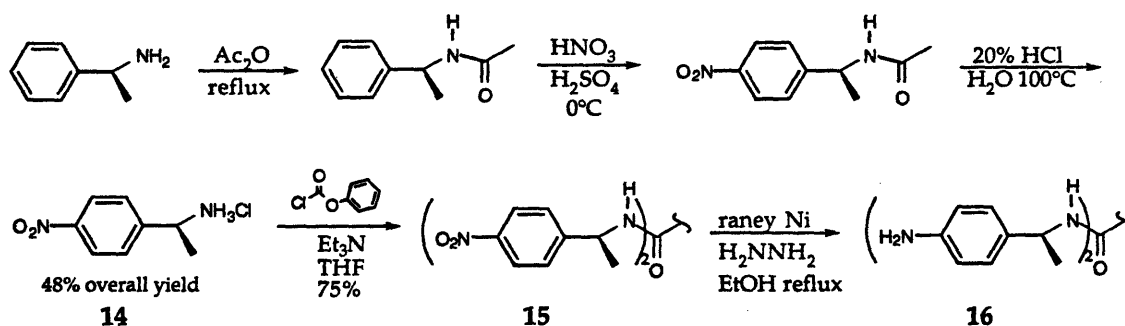
Scheme I-2. *Synthesis of optically active diamino urea spacer 16.*

---

[17] Nowick, J. S.; Ballester, P.; Ebmeyer, F.; Rebek, J., Jr. *J. Am. Chem. Soc.* **1990,** *112,* 8902. Park, T. K.; Schroeder, J.; Rebek, J., Jr. . *Am. Chem. Soc.* **1991,** *113,* 5125.

[18] Perry, C. W.; Brossi, A.; Deitcher, K. H.; Tautz, W.; Teited, S. *Synthesis* **1977,** 492.

[19] Fletcher, T. L.; NamKung, M. J. *J. Org. Chem.* **1958,** *23,* 680.

Xanthene acid **13** was converted to its acid chloride with thionyl chloride and coupled to diamine **16** in the presence of triethyl amine in methylene chloride. The benzyl esters were converted to free acids by treatment with 10% palladium on carbon in ethanol under a hydrogen atmosphere (scheme I-3).[20]
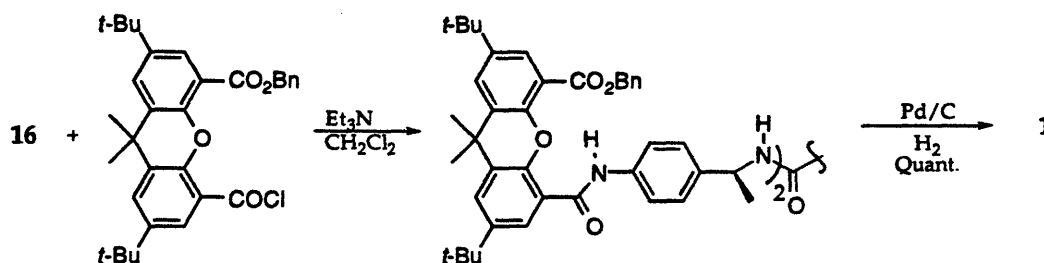
Scheme I-3. *Coupling of the xanthene U-turn to the diamino spacer followed by deprotection.*

Complexation Studies

Binding properties of the asymmetric cleft **1** were investigated by titration with a variety of guests that contained either one or two hydrogen bond acceptor sites. The studies were conducted with the use of ^{1}H NMR to measure changes in proton resonances of the host upon addition of a guest. A solution of host of known concentration was placed in a NMR tube and incremental additions of guest were mixed in the NMR tube and the spectrum recorded. The addition of guest was complete when the host appeared saturated, that is when host peaks do not shift upon continued addition of the guest.

Although it is preferable to monitor a proton that is involved in the binding process, it is not always practical nor necessary. Any resonance that is well-behaved throughout the titration will give reliable binding data. A desirable goal of monitoring a titration is to find a proton whose resonances in the free and bound states are separated by a great distance, which increases the precision of the measurement. It is also important to follow a peak that

[20] Hartung, W. H.; Simonoff, R. *Org. React.* **1953**, *7*, 263.

moves through a clean region of the spectrum and does not broaden significantly. The protons involved in binding are typically ones that undergo the greatest spectral shifts. Unfortunately, they are also the peaks that broaden, sometime disappearing altogether into the baseline. Since they move through a large part of the spectrum they will often overlap with other peaks or become 'lost' in the aromatic region. In either case, some of the most important data points needed for the determination of an association constant are lost. Therefore one should consider all three factors when choosing which peak or peaks to observe.

All binding processes discussed in this thesis (with the exception of the encapsulation studies with calixarenes, chapter 3) are rapid on the NMR time scale. Therefore resonances in the ^{1}H NMR appear as a time averaged mixture of free and bound species. When the exchange rate between free and bound species is slower than the NMR time scale one can simply integrate to determine the relative ratio of the free and bound host. This ratio combined with the known concentrations of total host and guest present will give the association constant for that binding process.[21]

Pyridine was among the first guests used to probe the properties of cleft 1. In deuterochloroform, host 1 was found to bind two pyridines with an association constant of K_{a1}=140 M^{-1}, K_{a2}=5 M^{-1}. 4,4'-Dipyridyl was modeled with cleft 1 and found to be a excellent guest which is capable of forming a 1:1 complex (figure I–8). Experimental evidence supports this conclusion. A ^{1}H NMR titration found that the lower limit of the association constant with dipyridyl is 1 x 10^5 M^{-1}.
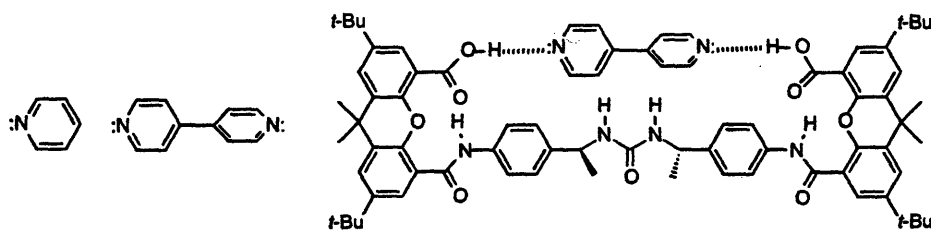
Figure I–8. *Proposed binding complex of dipyridyl and diacid cleft 1.*

21 Connors, K. A. *Binding Constants The Measurement of Molecular Complex Stability*, Wiley-Interscience, New York, 1987.

The large increase in the binding affinity for 4,4'-dipyridyl over pyridine is due to chelation. The two point binding of the 4,4'-dipyridyl can only occur when the guest resides over the asymmetric centers which flank the urea. A qualitative observation in support of a 1:1 complex is the fact that the titration curve is near saturation when only one equivalent of guest is present (figure I–9).
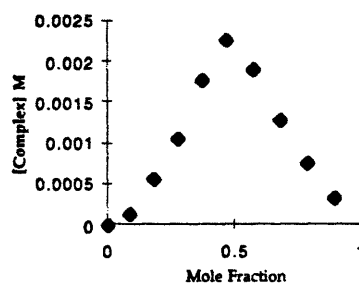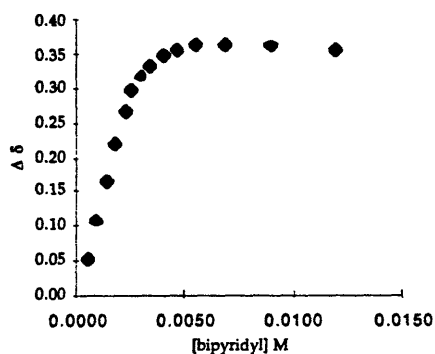
Figure I–9. *Titration data of cleft 1 (0.00512 M) with 4,4'-dipyridyl in CDCl3.*

Figure I–10. *Job plot of cleft 1 with 4,4'-dipyridyl in CDCl3.*

Additional qualitative evidence is shown in the Job plot (figure I–10).[21] Data for a Job plot is obtained from a number of different mixtures of the host and guest. The combined concentration of host and guest is held constant while the ratio between the two species is varied. The concentration of complexed species is plotted against the mole fraction of host. A 1:1 complex will show a maximum at 0.5. A 1:2 complex (one host and two guests) will show a maximum at 0.33 and a 2:1 complex at 0.67. The results of the pyridine/dipyridyl studies indicate that the requirements for enantioselective binding could be met; there is two point contact and complexation may place the chiral centers of the host and guest in close proximity for a third contact.
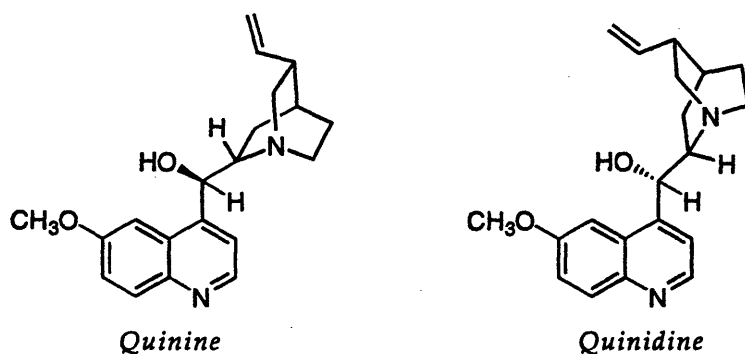
Quinine   *Quinidine*

Two opitcally active compounds were used in asymmetric complexation studies, quinine and quinidine. Each of these guests are equiped with two hydrogen bond acceptors and can be chelated by host **1**. Both guests were titrated against the R,R and the S,S enantiomers of host **1**. These studies did not show the clean titration curves normally seen in 1:1 or 1:2 binding schemes. Instead the observed data reveal a complicated binding scheme that is composed of a 1:1 complex and several different 1:2 complexes (figure I–11).
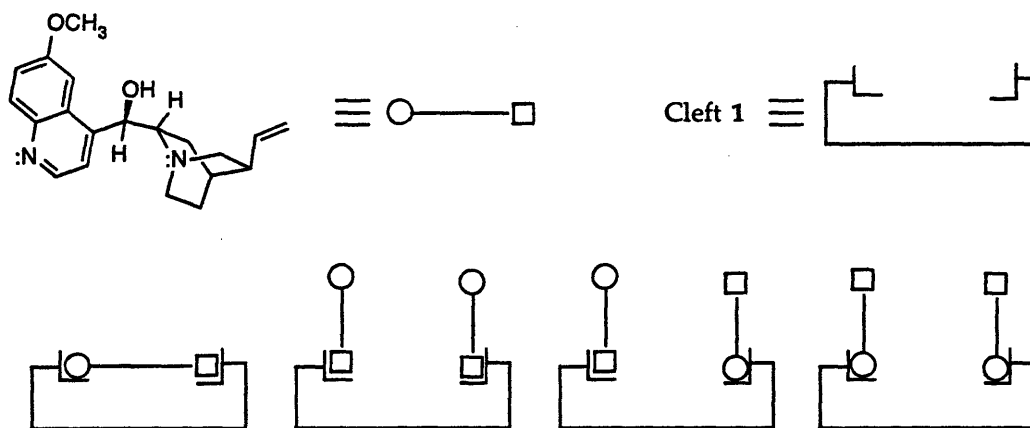
Cleft 1

Figure I–11. *Schematic representing the two non-equivalent bases of quinine and its four possible complexes with cleft 1.*

Due to the multiple binding modes, association constants for these guests could not be determined. Despite this drawback, an obvious distinction is demonstrated in the titration curves of the different host enantiomers with each guest. The maximum downfield shift for a complexed host species is

different for R,R-1 and S,S-1. The slope of the 'decay' portion of the curve also differs for R,R-1 compared to S,S-1 (figures I–12, I–13).
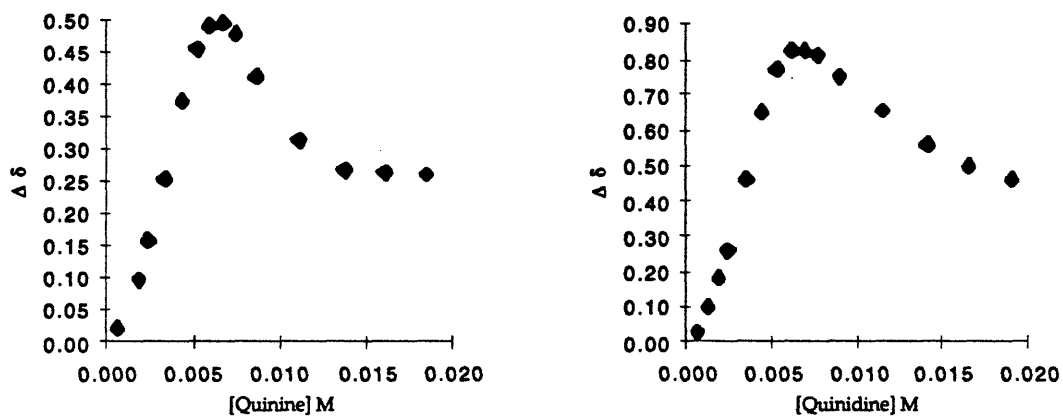
Figure I–12. *Titration data of R,R-1 (0.00964 M) and quinine in CDCl₃.*
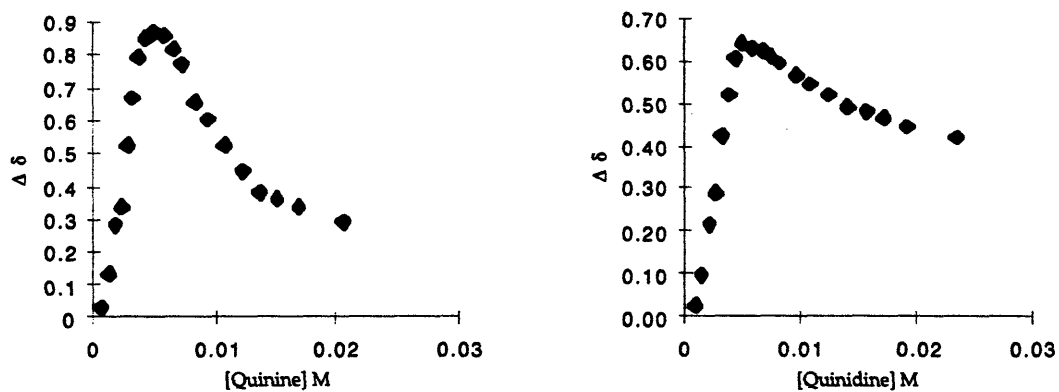
Figure I-13. *Titration data of S,S-1 (0.0055 M) and quinidine in CDCl₃.*
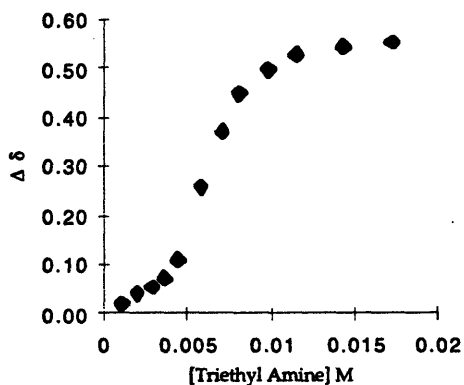
Figure I-14. *Titration data of cleft 1 with*
Et₃N in CDCl₃.

A study with a tertiary alkylamine (triethylamine) similar to that found in quinine and quinidine showed a sigmoidal curve (figure I-14). Triethylamine, being a stronger base than pyridine, was able to deprotonate the carboxylic acids of the host. The observed data shows that the first equivalent of base reacts with only one of the acids of the host. It is not until more than one equivalent of the base is added before the second acid is utilized.

a)   b)
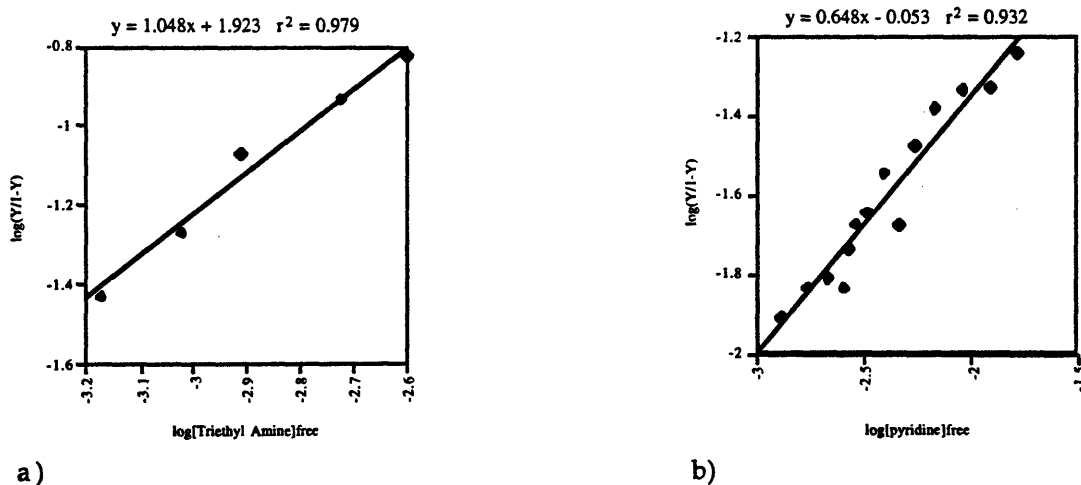
Figure I-15. *Hill plot of cleft 1 and a) triethylamine, b) pyridine.*

Negative cooperativity is typically seen in complexation studies of hosts with two or more binding sites, which usually holds true even when the binding sites seem isolated from one another. This is indeed the case in the pyridine titration with cleft 1 (figure I–15b). A Hill plot gives a slope of 0.7 indicating negative cooperativity. However the results of the Hill plot for the triethylamine titration show no cooperativity. This result seems strange since one would expect the second deprotonation of a diacid to require more energy than the first. A significant conformational change upon complexation with the second equivalent of guest could give the appearance of a non-cooperative 1:2 system. It is probable that the urea serves to stabilize one of the ammonium ion pairs (a favorable interaction which will be discussed in chapter 2). Modeling studies show the urea may make contact with one of the carboxylates, producing a large conformational change in the molecule. Unfortunately such changes destroy the convergence of the diacids.

Experimental

General

Reagent grade solvents were used except where noted. Tetrahydrofuran was distilled from Na/benzophenone ketyl and CH_2Cl_2 was distilled from P_2O_5. Melting points were measured on an Electrothermal 9100 melting point apparatus. NMR spectra were taken on a Varian XL-300 (300 MHz) and a Bruker AC-250 (250 MHz) spectrometers. IR spectra were obtained on a Mattson Sygus 100 FT IR spectrometer. High resolution mass spectra were obtained on a Finnegan Mat 8200 instrument. Flash chromatography was performed using Silica Gel 60 (EM Science, 230–400 mesh). Molecular modeling experiments were performed on a Silicon Graphics Personal Iris using Macromodel 3.5X program with Amber force field.

Titrations

All titrations were performed on a Bruker AC-250 (250 MHz) spectrometer. The deuterated solvents were dried over 4Å molecular sieves.

Analytical grade A volumetric flasks and syringes were used throughout the preparation of the solutions. The titrations were typically carried out at 5–10 mM concentration of host and 25–50 mM concentration guest. Aliquots of the guest solution were added via syringe and the spectrum recorded after each addition until the host was fully saturated. The data was fit to the appropriate binding equation using Systat 5.2 for the Macintosh.

The titration of 4,4'-dipyridyl with diacid cleft 1 (figure I–9) was conducted as follows. A 5.122 mM solution of 1 was prepared by dissolving 27.71 mg of 1 in $CDCl_3$ in a 5 mL volumetric flask and diluting to the mark with $CDCl_3$. A 23.689 mM solution of 4,4'-dipyridyl was prepared by placing 3.70 mg in a 1 mL volumetric flask and dissolving in $CDCl_3$. The solution was then diluted to the mark to give a 1 mL total volume. 500 µL of this host 1 solution was placed in an ^1H NMR tube and the spectrum recorded. Eight 10 µL, two 20 µL, one 30 µL, two 50 µL, one 100 µL, and one 200 µL additions of the guest solution were added and the spectrum recorded after each addition. The changes in the amide protons (δ, ppm) were used to calculate the association constant (Ka, M^{-1}).

A plot of the total concentration of guest in the ^1H NMR tube versus (δ, ppm) gave a curve which was fit, using systat 5.2, to equation I–1. Equation I–2 is derived from equations I–2, I–3 and I–4.

$$\delta = \delta_f - (\delta_b - \delta_f)\left(([H]_T + [G]_T + 1/K_a) - \frac{\sqrt{([H]_T + [G]_T + 1/K_a)^2 - 4[H]_T[G]_T}}{2[H]_T} \right) \qquad \text{eq. 1}$$

$$K_a = \frac{[HG]}{[H]_f[G]_f} \qquad \text{eq. 2}$$

$$[H]_T = [H]_f + [HG] \qquad \text{eq. 3}$$

$$\delta = \frac{\delta_f[H]_f + \delta_b[HG]}{[H]_T} \qquad \text{eq. 3}$$

Where δ is the measured signal (ppm) for the observed proton after each addition. δ_f and δ_b are the signals (ppm) for the free host and complexed host respectively. $[H]_T$, $[H]_f$ and $[HG]$ are concentrations (M) of host (total amount present), free host (uncomplexed) and complexed host respectively. Likewise $[G]_T$ and $[G]_f$ represent the total concentration (M) of guest present and the concentration (M) of free (uncomplexed) guest. K_a is the association constant.

Synthesis & Characterization

(S)-(-)-N-(α-Methylbenzyl) acetamide: (S)-(-)-(α)-Methylbenzylamine (5.1547 g, 42.54 mmol) was dissolved in acetic anhydride and allowed to reflux for 2 hours. The reaction was poured into 200 g of ice and stirred for 1 hour. The precipitate was collected and washed with cold water (100 ml). The damp solid was carried on without further purification. ^{1}H NMR (CDCl$_3$) δ 7.33 (m, 5H), 5.73 (bs, 1H), 5.13 (qt, 1H), 2.28 (s, 3H), 1.49 (d, J=6.9 Hz, 3H).

(S)-(-)-N-(α-Methyl-4-nitrobenzyl) acetamide: (S)-(-)-N-(α-Methylbenzyl) acetamide was slowly added to a solution of HNO$_3$ (10 ml) and H$_2$SO$_4$ (12 ml) at -10°C. After 1 hour the reaction was poured into 200 g of ice. While stirring in an ice bath the solution was brought to a pH 2 with 50% NaOH. The solution was then extracted with methylene chloride (2x, 50 ml). The organic layer was dried over MgSO$_4$ and concentrated *in vacuo*. The product was used without further purification. ^{1}H NMR (CDCl$_3$) δ 8.70 (d, J=8.8Hz, 1H), 7.47 (d, J=8.6Hz, 1H), 6.13 (bs, 1H), 5.16 (qt, 1H), 2.02 (s, 3H), 1.48 (d, J=4.1Hz, 3H).

(S)-(-)-(α)-Methyl-4-nitrobenzylamine hydochloride: (S)-(-)-N-(α-Methyl-4-nitrobenzyl) acetamide was heated in refluxing in 20% aq. HCl (100 ml). After 9 hours the water removed *in vacuo*. Ethanol (3x, 30 ml) was used to form an azeotrope with the water for its removal *in vacuo*. The *p*-nitrobenzylamine was obtained in 48% overall yield from the unsubstituted benzylamine. This product is available from Aldrich.

(S)-N,N'-(α-Methyl-4-nitrobenzyl) urea: (S)-(-)-(α)-Methyl-4-nitrobenzylamine hydochloride (1.0359 g, 5.11 mmol) was dissolved in anhydrous THF (20 ml) and triethyl amine (5 ml) under an argon atmosphere. Phenylchloroformate (0.32 ml, 2.56 mmol) was added to the reaction at room temperature. The reaction refluxed for 12 hours. After cooling ethyl acetate (50 ml) added and the solution was extracted with 2M HCl (2x, 50 ml) then sat. NaCl (2x, 50 ml). The organic layer was dried over

MgSO$_4$ and concentrated *in vacuo*. The white solid was washed with cold ether to give the product in 75.5% yield (0.6907 g, 1.93 mmol). ^{1}H NMR (CDCl$_3$) δ 7.01 (d, J=8.4Hz, 4H), 6.67 (d, J=8.6Hz, 4H), 6.05 (d, J=7.8Hz, 2H), 4.67 (m, 2H), 1.32(d, J=6.9Hz, 6H); ^{13}C NMR (CDCl$_3$) δ 157.3, 153.7, 146.4, 126.8, 123.5, 49.3, 22.8; HRMS m/z for C$_{17}$H$_{18}$N$_4$O$_5$ (M$^+$) calc. 358.1277, found 358.1275.

(S)-N,N'-(α-Methyl-4-aminobenzyl) urea: (S)-N,N'-(α-Methyl-4-nitrobenzyl)-urea (0.1.0173 g, 2.84 mmol) was heated in refluxing ethanol (25 ml) with Raney nickel in ethanol (3 ml, ~50% by weight). Hydrazine (0.89 ml, 28.41mmol) was slowly added over a 5 min. period. The reaction was filtered while hot through celite 10 min. after the addition of hydrazine. The filtrate was concentrated *in vacuo* to give the pure product in 91% yield. mp 205 °C (decomp.); ^{1}H NMR (CD$_3$OD) δ 7.01 (d, J=8.6Hz, 4H), 7.43 (d, J=8.6Hz, 4H), 4.92 (q, J=7.0Hz, 2H), 1.44 (d, J=7.0Hz, 6H); ^{13}C NMR (CDCl$_3$) δ 156.0, 146.5, 132.2, 125.9, 113.2, 47.3, 22.9; HRMS m/z for C$_{17}$H$_{22}$N$_4$O (M$^+$) calc. 298.1793, found 298.1795; [α]$_D^{20}$=-11.7° (c=0.9,methanol).

Chiral Urea Dibenzylester: In an argon filled flask 5-carbobenzoxy-2,7-di-t-butyl-9,9-dimethyl-4-xanthenoic acid (0.0891 g, 0.2989 mmol) was heated in refluxing CH$_2$Cl$_2$ (25 ml) with SOCl$_2$ (2 ml) for 2 hours. The reaction was concentrated, CH$_2$Cl$_2$ (10 ml) was added, and the solvent was stripped. The remaining solids were put under an argon atmosphere with CH$_2$Cl$_2$ (25 ml), triethyl amine (0.5 ml), and (S)-N,N'-(α-Methyl-4-aminobenzyl) urea (0.2989 g, 0.5987 mmol). The reaction stirred at 0°C for 2 hours. The reaction was then extracted with 1M HCl (2x, 50 ml) and H$_2$O (2x, 50 ml). The acidic layer was washed with CHCl$_3$ (30 ml). The organic layers were combined, dried over Na$_2$SO$_4$, and concentrated *in vacuo* to give 0.3445 g of crude material. The product was purified by flash column chromatography using 1:1 ethyl acetate/hexane to give 55% yield (0.2080 g, 0.1648 mmol). ^{1}H NMR (CDCl$_3$) δ 10.58 (s, 2H), 8.34 (d, J=2.5Hz, 2H), 7.86 (d, J=2.5Hz, 2H), 7.76 (d, J=8.4Hz, 4H), 7.66 (d, J=2.5Hz, 2H), 7.58 (d, J=2.5Hz, 2H), 7.27 (m, 14H), 5.19 (s, 4H), 4.90 (bs, 2H), 4.44 (bs, 2H), 1.67 (s, 12H), 1.43 (d, J=6.7 Hz, 6H), 1.35 (s, 18H), 1.34 (s, 18H); ^{13}C NMR (CDCl$_3$) δ 165.1, 163.2, 157.0, 147.8, 146.1, 145.7, 140.7, 137.2, 135.7, 130.9, 129.5, 128.4, 128.1, 127.6, 126.5, 126.2, 125.8, 124.0, 120.7, 117.2, 66.7, 34.5,

34.5, 32.2, 31.2, 30.3; Mass spectra (FAB) was obtained in a matrix with 3-nitrobenzylalcohol, HRMS m/z for $C_{81}H_{91}N_4O_9$ (M^+) calc. 1263.6786, found 1263.6780.

Chiral Urea Diacid: The dibenzylester (0.200 g) was stirred at room temperature in ethanol (10 ml) with 10% Pd/C (0.050 mg) under a hydrogen atmosphere for 23 hours. The reaction was then filtered and concentrated to give the desired product in 95% yield. ^{1}H NMR (CDCl$_3$) δ 10.88 (s, 2H), 8.31 (d, J=2.2Hz, 2H), 7.99 (d, J=2.1Hz, 2H), 7.69 (d, J=8.2Hz, 4H), 7.65 (d, J=2.3Hz, 2H), 7.60 (d, J=2.3Hz, 2H), 7.10 (d, J=7.9Hz, 4H), 5.64 (bs, 2H), 4.60 (bs, 2H), 1.68 (s, 12H), 1.35 (s, 36H); ^{13}C NMR (CDCl$_3$) δ 167.7, 164.0, 147.6, 146.5, 146.0, 145.8, 130.6, 129.8, 128.2, 127.3, 126.4, 125.9, 124.3, 58.3, 34.5, 32.5, 32.3, 31.3, 22.9, 18.2.

Chapter II

Bis Ureas & Anionic Complexation

Introduction

Bis urea **34** is shown to have an excellent geometry for complexation of carboxylates and phosphates. Data is presented which shows the four highly preorganized hydrogen bond donors are able to utilize both syn-anti lone-pairs of electrons of the carboxylate in forming a strong complex. The host is readily prepared in multigram quantities and functional groups on the periphery are easily changed. The oxy-anion hole is exploited in asymmetric complexation studies and as a receptor for phosphate transesterification. In both studies the oxy-anion hole serves to direct the guests into the binding pocket in such a way that the peripheral functionality can exert its influence. A solid state structure is presented which supports the conclusions of the experimental evidence for catalysts.

34
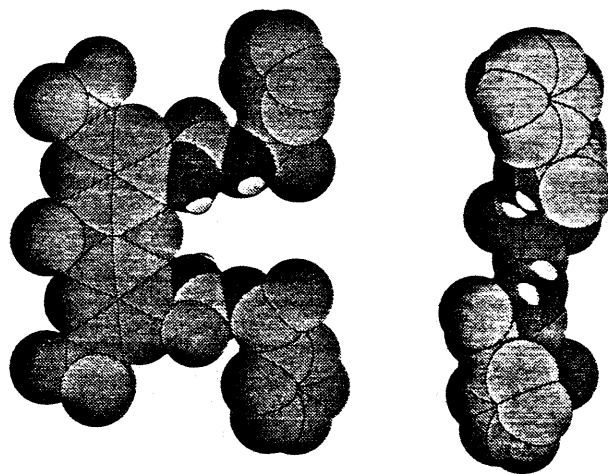
Background

Molecular recognition of anionic guests, such as carboxylates and phosphates, has been explored recently through the use of cationic receptors and, to a lesser extent, neutral receptors. Many of the anion receptors first reported were protonated aza macrocycles (figure II-1).[1] They were used to bind spherically shaped anions (halides),[2] linearly shaped anions (the azide)[3] and the tetrahedrally shaped phosphate.[4] Receptor 20 has been used extensively in the recognition of adenosine triphosphate, diphosphate and acetylphosphate.[5] Lehn linked an acridine fragment to the tetraprotonated macrocycle 20 to achieve both phosphate recognition as well as π–π stacking with the adenosine.[6] Some of the drawbacks of this type of system are due to the lack of a structurally well-defined species. Flexibility and pH dependence of these hosts gives rise to a variety of shapes and sizes in the binding pocket.

1   Dietrich, B. *Pure Appl. Chem.* 1993, *65*, 1457.

2   Park, C. H.; Simmons, H. E. *J. Am. Chem. Soc.* 1968, *90*, 2431. Graf, E.; Lehn J.-M. *J. Am. Chem. Soc.* 1976, *98*, 6403.

3   Lehn, J.-M.; Sonveaux, E.; Willard, A. K. *J. Am. Chem. Soc.* 1978, *100*, 4914.

4   Tabushi, I.; Imuta, J.-I.; Seto N.; Kobuke, Y. *J. Am. Chem. Soc.* 1978, *100*, 6287.

5   Hosseini, M. W.; Lehn, J.-M.; Maggiora, L.; Mertes, K. B.; Mertes, M. P. *J. Am. Chem. Soc.* 1987, *109*, 537. Hosseini, M. W.; Lehn, J.-M.; Jones, K. C.; Plute, K. E.; Mertes, K. B.; Mertes, M. P. *J. Am. Chem. Soc.* 1987, *111*, 6330. Hosseini, M. W.; Lehn, J.-M. *J. Am. Chem. Soc.* 1987, *109*, 7047.

6   Hosseini, M. W.; Blacker, A. J.; Lehn, J.-M. *J. Am. Chem. Soc.* 1990, *112*, 3896.
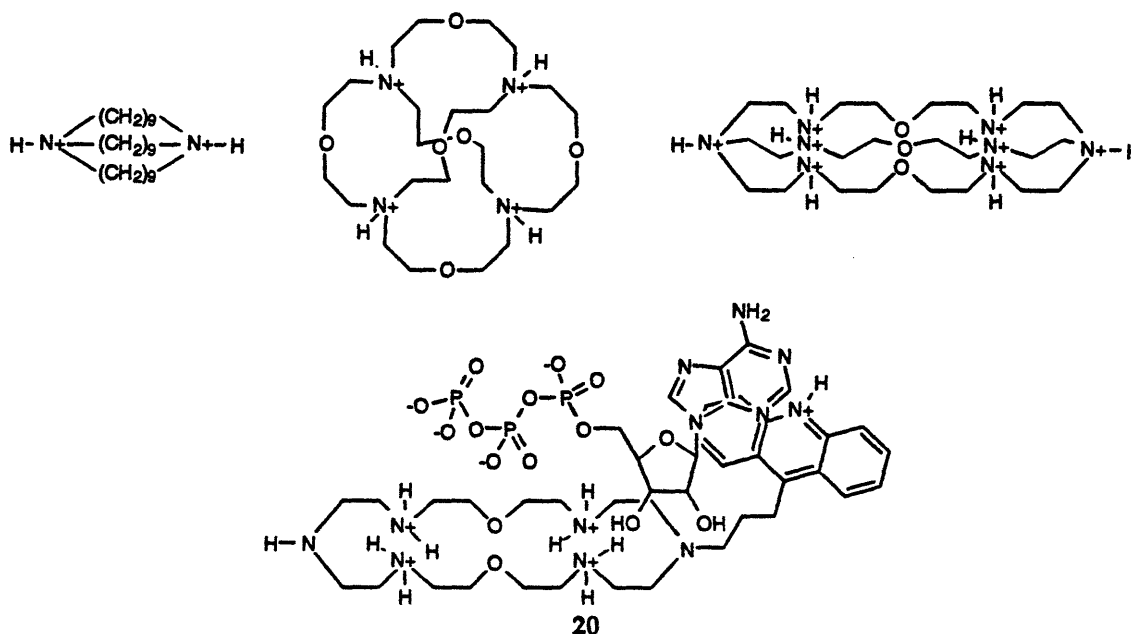
Figure II-1. *Representative structures of protonated aza macrocycles used in anionic complexation.*

Another strategy involving charged receptors uses non-macrocyclic, rigid structures. Hamilton made use of an amido pyridine unit to complex carboxylic acids (figure II-2).[7] The neutral host and guest come together to form an ionic complex. Hamilton used these diacid binders (figure II-2) to form molecular sheets,[8] helices[9] and to shift the cis/trans equilibrium in a proline amide.[10] Diederich used a similar recognition surface in the selective complexation of an α,ω-dicarboxylic acid (figure II-3).[11]

7   Garcia-Tellado, F.; Goswami, S.; Chang, S. K.; Geib, S.; Hamilton, A. D. *J. Am. Chem. Soc.* **1990,** *112,* 7393.

8   Geib, S. J.; Vincent C.; Fan, E.; Hamilton, A. D. *Angew. Chem. Int. Ed.* **1993,** *32,* 119-121.

9   Garcia-Tellado, F.; Geib, S. J.; Goswami, S.; Hamilton, A. D. *J. Am. Chem. Soc.* **1991,** *113,* 9265-9269.

10   Vicent,C.; Hirst, S. C.; Garcia-Tellado, F.; Hamilton, A. D. *J. Am. Chem. Soc.* **1991,** *113,* 5466-5467.

11   Montero, V. A.; Tomlinson, L.; Houk, K. N.; Diederich, F. *Tetrahedron Lett.* **1991,** *32,* 5309-5312.
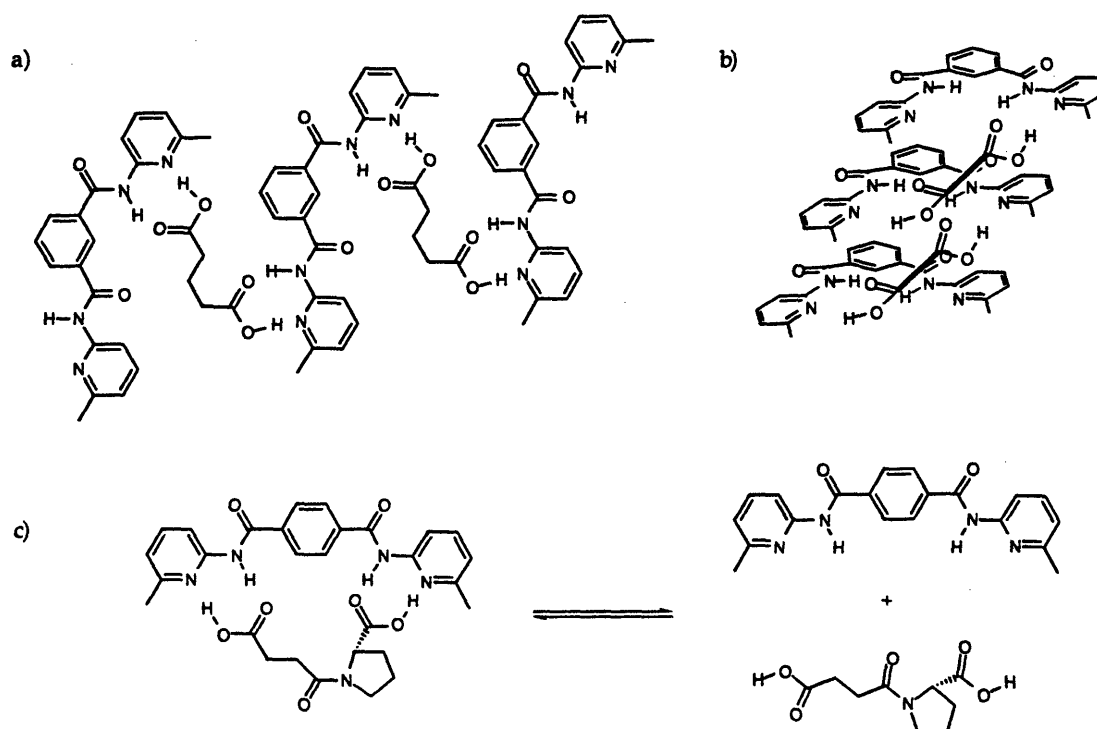
Figure II–2. *Aminopyridine moiety used in the formation of a) molecular sheets, b) helices and c) as a cis/trans isomerization catalyst.*
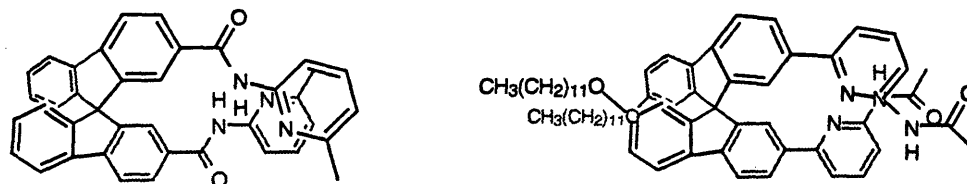
Figure II–3. *Aminopyridines used for selective binding of α,ω-dicarboxylic acids.*

Hamilton attempted to use the pyridinium salt to complex carboxylates or phosphates. However the host preferred to collapse in on itself as revealed in a solid state structure (figure II–4).[12] But the behavior shown by **21** was used to design a new anionic receptor. Two acyl-guanidiniums were positioned *meta* to one another. An intramolecular hydrogen bond forms between the carbonyl oxygen and an N–H of the guanidinium. This helps to preorganize the oxy-anion hole leaving only the aryl–acyl carbon bonds free

---

[12] Dixon, R. P.; Geib, S. J.; Hamilton, A. D. *J. Am. Chem. Soc.* **1992,** *114,* 365-366.

to rotate (figure II–4). One of the disadvantages of using charged hosts like **22** and **23** is that they are prone to complexing multiple guests. UV titrations in acetonitrile show that a 1:1 complex dominates at low phosphate concentration ($Ka=4.6 \times 10^4$ M^{-1}) yet 1:2 and 1:3 complexes are readily formed as the phosphate concentration increases.
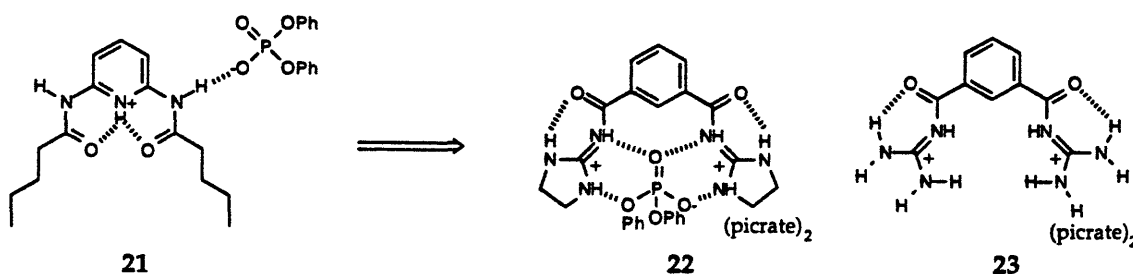
Figure II–4. *Collapsed cleft inspired acylguanidiniums where intramolecular hydrogen bonds help to define the binding pocket.*

The guanidinium functionality is used extensively in phosphate and carboxylate recognition studies.[13] Anslyn reported a highly preorganized bis guanidinium cleft that was able to bind phosphodiesters ($Ka\sim100$–800 M^{-1}) in DMSO/H$_2$O mixtures (figure II–5).[14] The two guanidiniums form a V-shaped cavity very similar to Hamilton's acyl guanidiniums. In fact, many bifunctional anion receptors have this general configuration (figure II–6); two sets of hydrogen bond donors separated by a rigid platform about the length of an anthracene.

13 Kato, Y.; Conn, M. M.; Rebek, J. Jr. *J. Am. Chem. Soc.* **1994**, *114*, 3279-3284. Deslongchamps, G.; Galán, A.; de Mendoza, J.; Rebek, J. *Angew. Chem. Int. Ed. Engl.* **1992**, *31*, 61-63. Galán, A.; de Mendoza, J.; Toiron, C.; Bruix, M.; Deslongchamps, G.; Rebek, J. *J. Am. Chem. Soc.* **1991**, *113*, 9424-9425. Galán, A.; Pueyo, E.; Salmerón, A.; de Mendoza, J. *Tetrahedron Lett.* **1991**, *132*, 1827-1830. Thornton, J. S. J. M.; Snarey, M.; Campbell, S. F. *FEBS Letters* **1987**, *224*, 161-171. Echavarren, A.; Galán, A.; Lehn, J.-M.; de Mendoza, J. *J. Am. Chem. Soc.* **1989**, *111*, 4994-4995. Müller, G.; Riede, J.; Schmidtchen, F. P. *Angew. Chem. Int. Ed. Engl.* **1988**, *27*, 1516-1518. Schmidtchen, F. P.; Schießl, P. *Tetrahedron Lett.* **1993**, *34*, 2449-2452.Schmidtchen, F. P. *Tetrahedron Lett.* **1989**, *30*, 4493-4496. Göbel, M. W.; Bats, J. W.; Dürner, G. *Angew. Chem. Int. Ed. Engl.* **1992**, *31*, 207-209. Russell, V. A.; Etter, M. C.; Ward, M. D. *J. Am. Chem. Soc.* **1994**, *116*, 1941-1952. Schiessl, P.; Schmidtchen, F. P. *J. Org. Chem.* **1994**, *59*, 509-511. Perreault, D. M.; Chen, X.; Anslyn, E. V. *Tetrahedron* **1995**, *51*, 353-362. Peschke, W.; Schiessl, P.; Schmidtchen, F. P.; Bissinger, P.; Schier, A. *J. Org. Chem.* **1995**, *60*, 1039-1043.

14 Ariga, K.; Anslyn, E. V. *J. Org. Chem.* **1992**, *57*, 417-419.
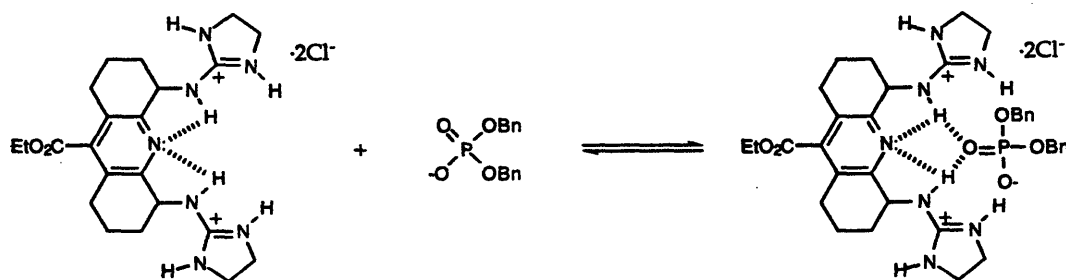
Figure II-5. *Anslyn's high affinity phosphodiester receptor.*
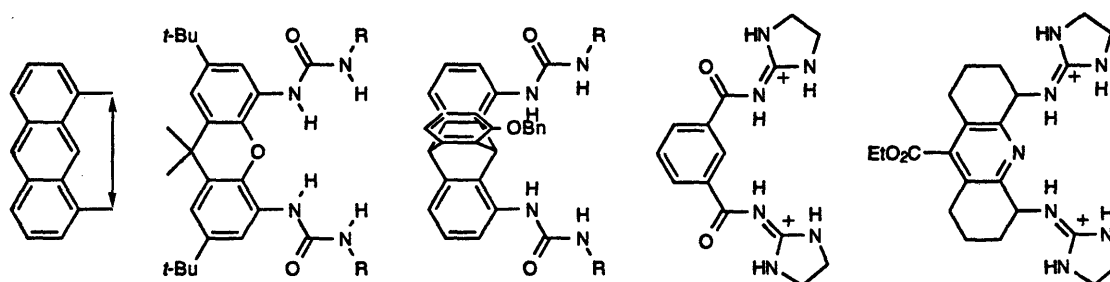
Figure II-6. *Shape comparison of effective receptors for carboxylates and phosphates.*

Anslyn developed a neutral polyaza cleft that was quite similar to bis guanidinium **22**. Because there are no bond rotations in the cleft which destroy the binding pocket, polyaza cleft **24** is completely preorganized (figure II-7). However, the binding pocket is opened up by a doubly covalent-linked recognition surface and is now able to accommodate larger anionic guests. Cleft **24** was found to be an excellent match for the anions of 1,3-dicarbonyl compounds (Ka=7.1x10³ M⁻¹) in acetonitrile.[15]

---

[15] Kelly-Rowley, A. M.; Cambell, L. A.; Anslyn, E. V. *J. Am. Chem. Soc.* **1991**, *113*, 9687-9688. Kelly-Rowley, A. M.; Lynch, V. M.; Anslyn, E. V. *J. Am. Chem. Soc.* **1995**, *117*, 3438-3447.

24
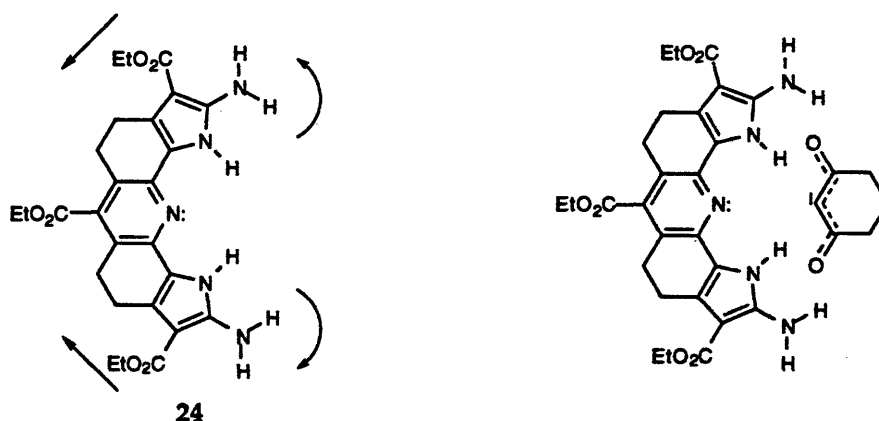
Figure II-7. *Splayed structure of the neutral 1,3-dicarbonyl anionic receptor.*

Hamilton[16] and Kelly[17] reported two other neutral hosts with larger binding pockets. Hamilton uses the multidentate recognition strategy of the natural product ristocentin to design a synthetic receptor for carboxylates. Two N-Cbz serines are connected to 1,2-diaminocyclohexane. The receptor **25** appears to be quite flexible yet high affinities for carboxylates are observed in acetonitrile ($Ka=2.7\times10^5$ M^{-1}). The carboxylates are believed to interact with the carbamate N–H and the hydroxyl groups of the serine side chain. Kelly uses the mono and ditopic receptors **26** and **27** to measure the relative affinities of different guests of similar size (figure II-8). He found the order, in decreasing affinity, to correlate with the pK_b of these guests $ArOPO_3^{-2} \geq ArPO_3^{-2} > ArCO_2^- \geq ArP(OH)O_2^- > ArSO_3^- > \delta$ lactone $> ArNO_2$.

25   **26**   **27**
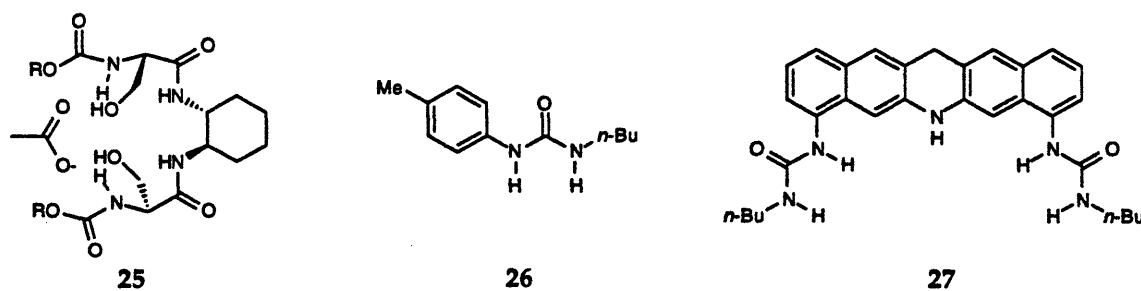
Figure II-8. *Neutral receptors used in oxy-anion complexation studies.*

---

16   Albert, J. S.; Hamilton, A. D. *Tetrahedron Lett.* **1993,** *34,* 7363-7366.

17   Kelly, T. R.; Kim, M. H. *J. Am. Chem. Soc.* **1994,** *116,* 7072.

Urea functionality is a useful tool in anion recognition. Ureas are easily synthesized from amines via isocyanates. Each urea offers two point contacts to a hydrogen bond acceptor, and their neutral attributes make them ideal for recognition studies in a hydrophobic environment. Hamilton[16] (28), Kelly[17] (27) and Wilcox (29, figure II-9) report some examples of urea based anion recognition. Wilcox's receptors have a similar flat '2-dimensional' structure and are effective anion binders in non-polar solvents. Wilcox used 29 to bind sulfonates, phosphates and carboxylates.[18] They used the binding event to properly orient substrates in such a way that the addition of amines to alkynes is catalyzed by having a nearby charged species.[19] This is an excellent example of the advantages offered by the use of hydrogen bonds over ion/ion interactions in molecular recognition. The hydrogen bond has directionality and is able to specifically position a guest in the desired manner. The concept of properly orienting the guests is vital when designing a receptor for catalysts or chiral selection.
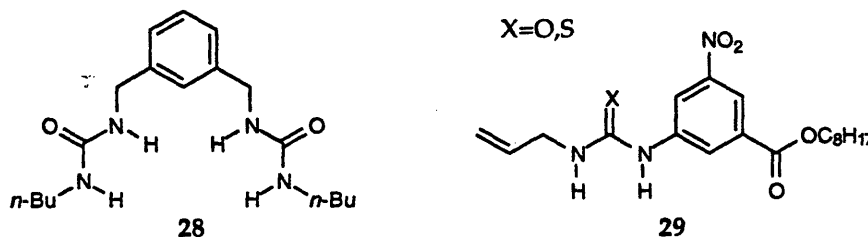
Figure II-9. *Neutral urea based receptors used for the complexation of sulfonates and phosphates.*

Ureas have also been incorporated into '3-dimensional' designs. Feng[20] uses a tryptocene platform to attach a pyridine flanked by two ureas (30) to achieve multipoint recognition of phosphoric acid diesters in DMSO-d_6. Hamilton exploited a diterpyridine–ruthenium complex (31) in order to position two thioureas for the selective recognition of glutarate dianions in

[18] Wilcox, C.; Kim, E.; Romano, D.; Kuo, L. H.; Burt, A. L.; Curran, D. P. *Tetrahedron* **1995**, *51*, 621-634. Smith, P. J.; Reddington, M. V.; Wilcox, C. S. *Tetrahedron Lett.* **1992**, *33*, 6085.

[19] Smith, P. J.; Kim, E.-I.; Wilcox, C. S. *Angew. Chem. Int. Ed. Engl.* **1993**, *32*, 1648.

[20] Feng, Q. Ph.D. Thesis, Massachusetts Institute of Technology, **1994**.

D_2O/DMSO-d_6 mixtures (Ka=8.3x10^3 M^{-1}).[21] Reinhoudt showed that calix[4]arenes provide a good '3-dimensional' support for both ureas and thioureas in anion recognition (**32**, figure II-10).[22] The tetraureas were capable of binding spherical guests in CDCl$_3$ with association constants varying from ~300 to 3000 M^{-1} (Cl$^-$>Br$^-$>I$^-$).

30   **31**   **32**
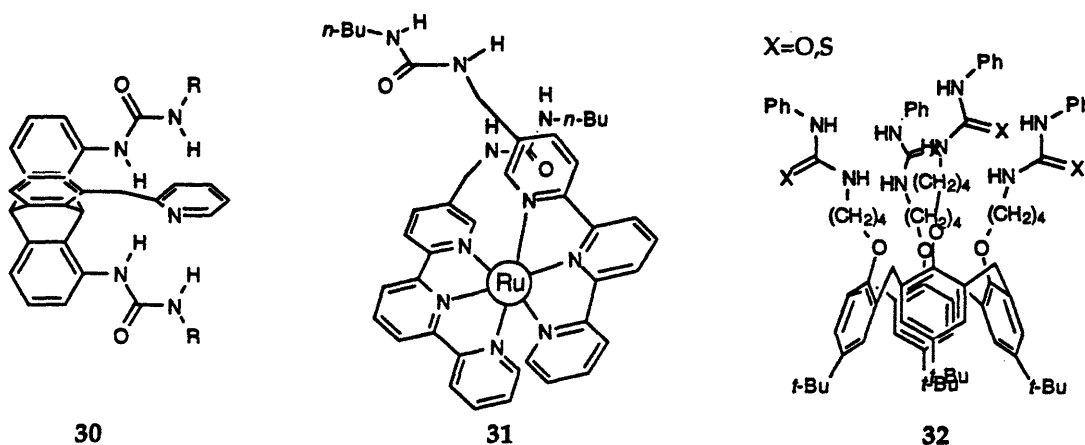
Figure II-10. *Examples of '3-dimensional' urea based anionic receptors.*

Attempts of enantioselective binding of chiral carboxylates have produced little success. The guanidinium based receptor which de Mendoza[23] reports is one of only a few known examples.[24] The chiral selectivity of **33** is limited to aromatic amino acids (figure II-11). The design of receptor **33** combines a crown ether for the ammonium binding of the amino acid while the carboxylate is held in place by the guanidinium. A naphthalene unit provides the third recognition element as π–π stacking interactions with aromatic side chains provide an enantioselective handle. Host **33**, in CH$_2$Cl$_2$,

[21] Goodman, M. S.; Jubian, V.; Hamilton, A. D. *Tetrahedron Lett.* **1994**, *24*, 7363.

[22] Scheerder, J.; Foch, M.; Engbersen, J. F. J.; Reinhoudt, D. N. *J. Org. Chem.* **1994**, *59*, 7815-7820.

[23] Galán, A.; Andreu, D.; Echavarren, A. M.; Prados, P.; de Mendoza, J. *J. Am. Chem. Soc.* **1992**, *114*, 1511-1512

[24] Webb, T. H.; Wilcox, C. S. *Chem. Soc. Rev.* **1993**, 383. Alcázar, V.; Diederich, F. *Angew. Chem. Int. Ed. Engl.* **1992**, *31*, 1503. Garcia Tellado, F.; Albert, J.; Hamilton, A. D. *J. Chem. Soc. Chem. Commun.* **1991**, 1761. Rebek, J. Jr.; Askew, B.; Nemeth, D.; Parris, K. *J. Am. Chem. Soc.* **1987**, *109*, 2432-2434. Owens, L.; Thilgen, C.; Diederich, F.; Knobler, C. B. *Helv. Chem. Acta* **1993**, *76*, 2757-2554.

was able to extract one enantiomer in 90% ee from a racemic mixture of either phenylalanine or tryptophane in H_2O.

33
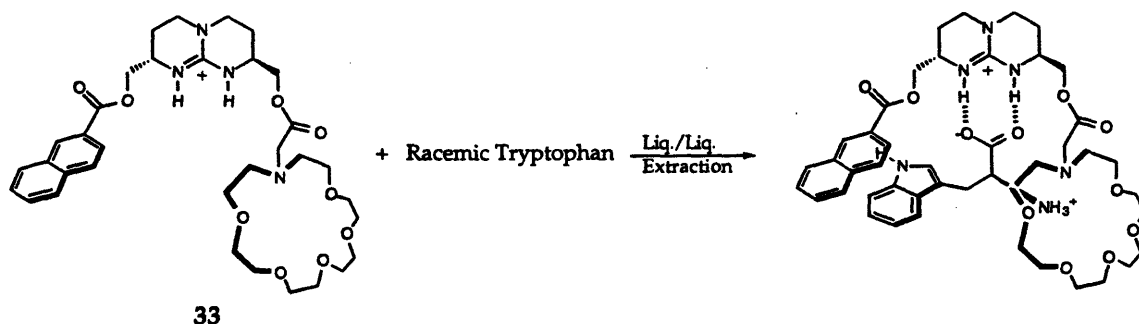
Figure II–11. *Enantioselective recognition of aromatic amino acids by electrostatic and π–π interactions.*

Design

Prompted by the observed affinity of urea for carboxylates in studies of chiral cleft **1** (chapter I), we designed a host for anionic recognition. Host **34** and **35** have several attractive features. They can be rapidly synthesized in multigram quantities. Its modular synthesis provides for easily changed functionality at the periphery of the molecule while maintaining the integrity of the binding site (figure II–12). The design also exploits the demonstrated ability of monoureas to bind carboxylates[25] and provides multipoint hydrogen bonding.

---

25 Erkang, F.; Van Arman, S. A.; Kincaid, S.; Hamilton, A. D. *J. Am. Chem. Soc.* **1993**, *115*, 369. Smith, P. J.; Reddington, M. V.; Wilcox, C. S. *Tetrahedron Lett.* **1992**, *33*, 6085. Etter, M. C.; Urbañczyk-Lipkowska, Z.; Zia-Ebrahimi, M.; Panuto, T. W. *J. Am. Chem. Soc.* **1990**, *112*, 8415.

Ar = Phenyl, 1-Naphthyl

34 **35**
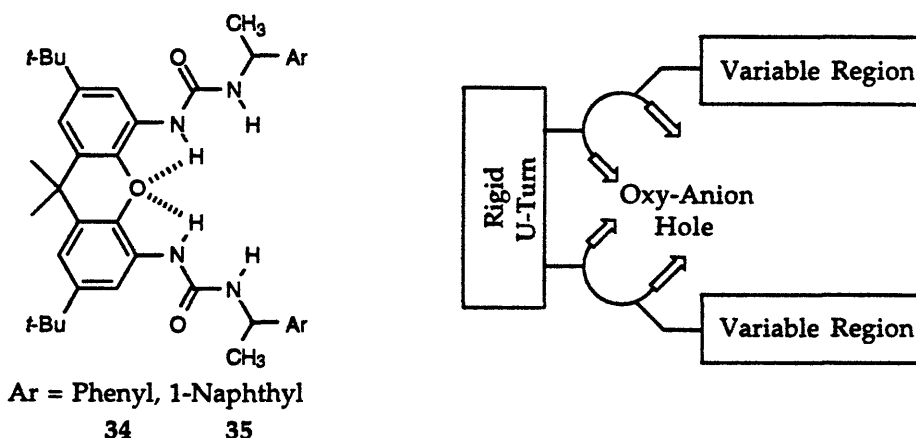
Figure II-12. *Important design features of the bis urea xanthenes.*

The position of the α-carbon of a carboxylate with respect to its usual recognition surfaces (syn lone pairs) represents a unique difficulty in the recognition of chiral carboxylic acids (figure II-13). This challenge is easily met with the use of hosts **34** and **35**. Once again the xanthene provides a rigid U-turn to which ureas are attached. The ureas are held far enough apart so that they do not collapse on one another in a head-to-tail fashion. The xanthene also encourages the ureas to adopt a conformation where all four hydrogen bond donors point 'inward' creating a neutral oxy-anion hole. Another advantage of hosts **34** and **35** is they are able to form hydrogen bonds with the rarely utilized anti lone-pairs of carboxylates as well as the syn lone-pairs. Most importantly the design of hosts **34** and **35** places additional functionality in such a way that allows it to get 'behind' the carboxylate oxygens and interact with other fragments of the guest (figure II-13).

34a
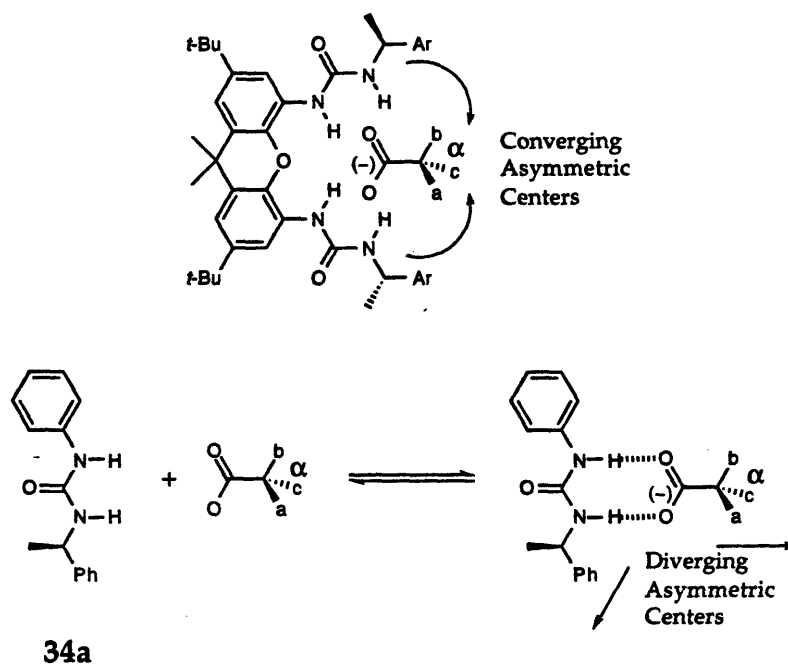
Figure II-13. *Advantages in the bis urea design permits the use of both syn-anti lone-pairs and access of the α-carbon of carboxylates.*

Synthesis

Synthesis of hosts **34** and **35** starts from commercially available 4,5-xanthene dicarboxylic acid **11**. The acids are converted to carbamates via Curtius rearrangements using diphenylphosphorylazide (DPPA) in the presence of benzyl alcohol.[26] Diamine **37** was obtained from hydrogenolysis of the carbamate **36** with 10 % palladium on carbon in ethanol under a hydrogen atmosphere. Diamine **37** can be prepared in gram quantities and stored for months without significant decomposition. Diamine **37** will readily react with most any isocyanate to give a desired bis urea (scheme II-1).

26 Shioiri, T.; Ninomiya, K.; Yamada, S. *J. Am. Chem. Soc.* **1972,** *94,* 6203-6205. Shioiri, T.; Ninomiya, K.; Yamada, S. *Chem. Pharm. Bull.* **1974,** *22,* 1398-1404. Ninomiya, K.; Shioiri, T.; Yamada, S. *Tetrahedron* **1974,** *30,* 2151-2157.
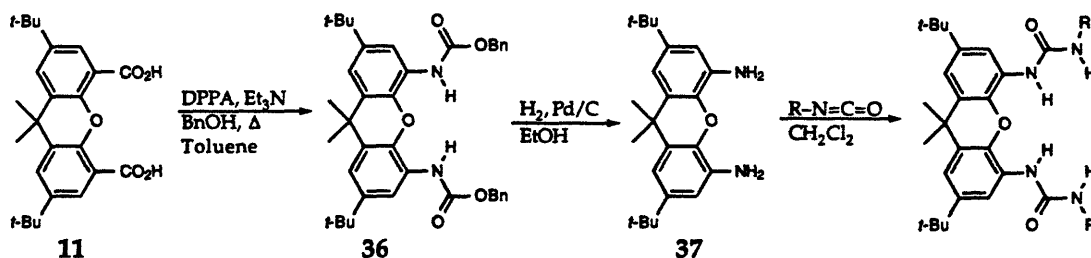
Scheme II–1. *Synthesis of di-tert-butyl xanthene bis ureas.*

The hope for crystalline bis ureas spurred the development of an alternative synthesis for a diamino xanthene that uses ethyl groups as the blocking/solubilizing agents instead of *tert*-butyl groups. Ethyl groups are more robust and are able to withstand the harsh nitration conditions. Attempts at nitrating 2,7 di-*tert*-butyl xanthene, a precursor to the diacid 11, under a variety of conditions always gave products in which *ipso* nitration of the *tert*-butyl groups occurs. Diethyl xanthene 39 is obtained by the Friedel-Crafts diacylation[27] of 9,9-dimethyl xanthene followed by a Wolff-Kishner reduction.[28] This leaves only the 4,5-positions of the xanthene open for nitration by $Cu(NO_3)_2$ to yield dinitroxanthene 41. Diamine 43 is then isolated from the palladium catalyzed reduction of 41 (scheme II–2). Similarly dibenzofuran derivative (42) can be synthesized by this route.

38 n=0
39 n=1

40 n=0
41 n=1

42 n=0
43 n=1
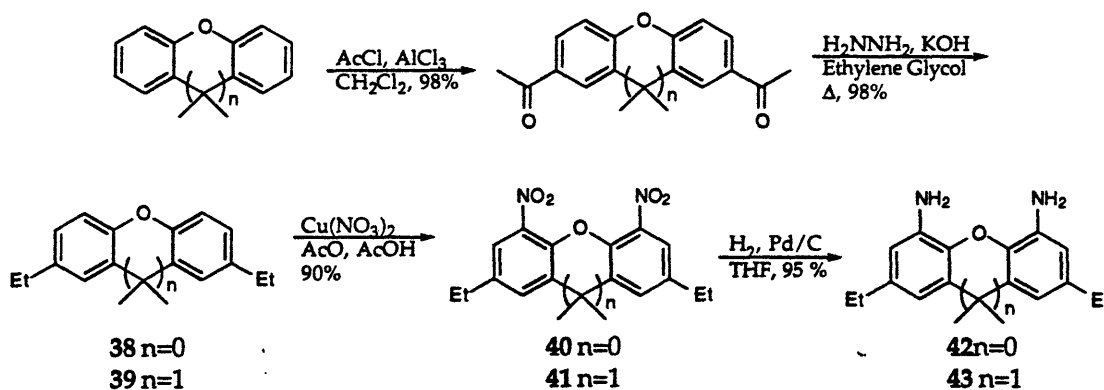
Scheme II–2. *Synthesis of diethyl xanthene and dibenzofuran diamines.*

---

27 For a review see Olah, G. *Friedel-Crafts and Related Reactions*, Wiley-Interscience, New York, 1963.

28 For a review see Todd, S. *Org. React.* 1948, 4, 378.

Diamines **42** and **43** react cleanly with isocyanates to yield bis ureas (scheme II–3).[29]
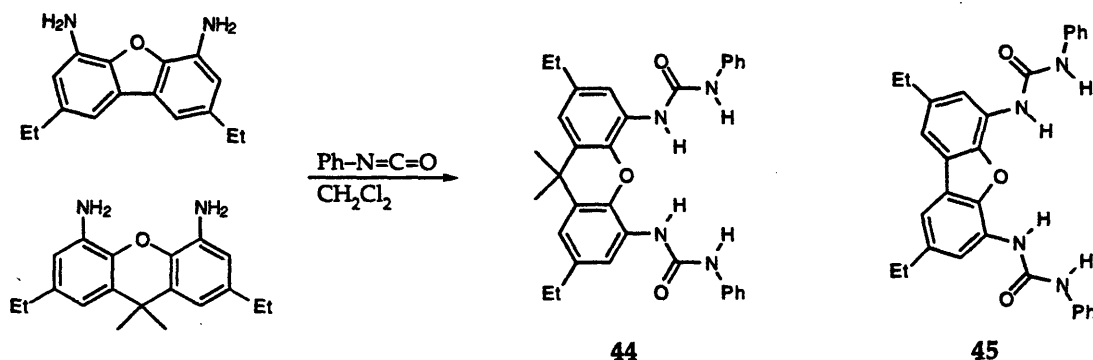
Scheme II–3. *Synthesis of xanthene and dibenzofuran bis ureas.*

While conducting nitrations of xanthene **39** we discovered that selective mononitration and bromination occurs in high yields. It can be desirable to differentiate the two sides of the xanthene, as in xanthene mono acid **13**. Most approaches to desymmetrizing xanthene gave mixtures of products. Scheme II–4 demonstrates the synthesis of three selectively functionalized xanthenes. They are easily prepared on large scale in high yields.
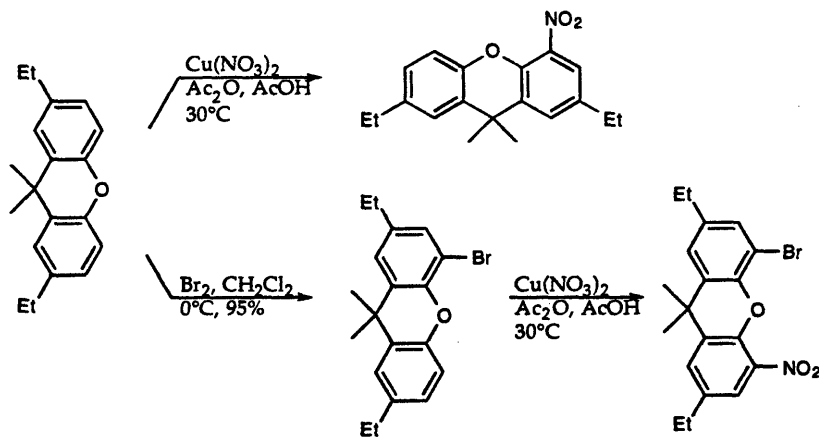
Scheme II–4. *Synthesis of desymmetrized xanthenes.*

29 Ozaki, S. *Chem. Rev.* **1972**, *72*, 475.

A final synthetic procedure for the production of xanthene bis ureas does not use any blocking groups in the 2,7-positions of xanthene. The 9,9-dimethylxanthene can be dilithiated with n-butyl lithium and tetramethyl ethylene diamine (TMEDA) in refluxing heptane.[30] Carbon dioxide is then bubbled through a solution of dilithiated xanthene at low temperature to give dicarboxylic acid **46**. Diisocyanate **47** is then isolated from the reaction of **46** with diphenylphosphoryl azide (DPPA).[31] Diisocyanate **47** is stable for days at 0° C. Diisocyanate **47** reacts cleanly with an excess of primary amine to give xanthene bis urea in high yield. This approach yields gram quantities of crystalline bis ureas. It is advantageous in that amines can be coupled to the xanthene fragment as opposed to isocyanates. This greatly expands the pool of available material which can be coupled to the xanthene (scheme II–5).

46   **47**   **48**
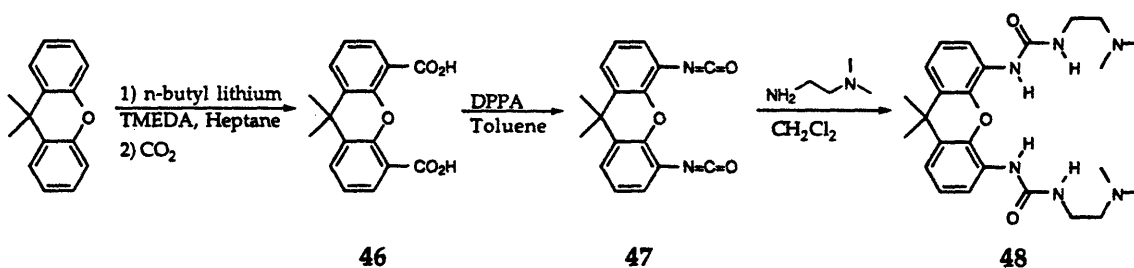
Scheme II–5. *Synthesis of phosphate transesterification catalyst.*

Complexation Studies

Titration experiments were conducted using ^{1}H NMR as discussed in chapter I. Benzoic acid was first used to probe the properties of the bis urea binding pocket. The triethylamine salt of benzoic acid was formed and isolated as an anhydrous white solid. This salt was titrated against bis urea R,R-**34** in deuterochloroform. A modest association constant of 150 M^{-1} is observed. A similar experiment was conducted with the tetraethylammonium salt of benzoic acid (K_a=2 x 10^5 M^{-1}). The binding energy of this guest increased roughly four fold over the triethylamine salt.

[30] Hillebrand, S.; Bruckmann, J.; Krüger, C.; Haenel, M. W. *Tetrathedron Lett.* **1995**, *36*, 75.

[31] Dunayevskiy, Y. M.; Vouros, P.; Wintner, E. A.; Shipps, G. W.; Carell, T.; Rebek, J. Jr. *Proc. Natl. Acad. Sci.* **1996**, in press.

The increased affinity is best explained by the fact that the triethylamine salt is in equilibrium with the free acid and base. In non-polar solvents, like deuterochloroform, a significant amount of free acid is present, which lowers the effective concentration of the carboxylate and in turn gives a smaller observed association constant. Also tetraalkylammonium salts produce more 'naked' anions since there is no on/off equilibrium and they offer only a positive charge to stabilize an anion. The tetraalkylammonium species does not contain any low lying empty orbitals that can accept the excess electron density of the carboxylate. The alkyl groups shield the ammonium and keep the ion pairs separated, thus producing a 'naked' high energy anion. The bis ureas help to stabilize these anions. In more polar solvents, such as deuteromethanol, the charges of the ammonium salts are more solvent stabilized and a decrease in their affinity for bis urea **34** is seen (table II–2).

Bis ureas **34** and **35** were found to cleanly complex carboxylates through chelation. Exclusive formation of a 1:1 complex is significant since most species with multiple binding sites form mixtures of complexes (such as those seen in cleft **1** with quinine and quinidine, chapter I). Experimental evidence supports the proposed 1:1 complex (figure II–14). A Job plot[32] of bis urea **34** with tetraethylammonium benzoate shows a maximum at 0.5 mole fraction, an indication of a 1:1 complex. A control study with mono urea **34a** shows an association constant of K_a=540 M^{-1} when titrated with tetraethylammonium benzoate. The 400 fold decrease in association constant can only be explained by the chelation effect of the bis ureas. Spectroscopic evidence also supports the proposed complex **49**. Changes in the ^{1}H NMR occur upon addition of benzoate to a solution of bis urea **34**. Both urea N–H resonances shift downfield over 3 ppm, suggesting the ureas are actively involved in binding. The xanthene proton, which is *ortho* to the urea, also undergoes a downfield shift. This is consistent with the idea of carboxylate holding the urea in a conformation which orientates the carbonyl oxygen near the *ortho*-xanthene-proton, desheilding it and resulting in its downfield shift (figure II–14).

---

32 Connors, K. A. *Binding Constants The Measurement of Molecular Complex Stability*, Wiley-Interscience, New York, **1987;** p. 24.
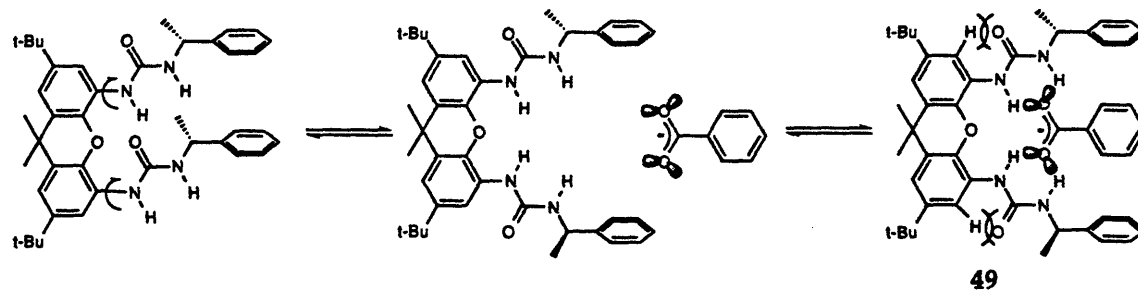
Figure II–14. *Complexation of benzoate by R,R-34.*

Confident that bis ureas are capable of strong, multipoint, 1:1 binding of carboxylates, we wanted to explore the effects of the urea's auxiliaries on guests. Bis ureas 34 and 35 were designed to place chiral centers near the α-carbon of carboxylate guests. Initial complexation studies focused on betaine (57) and ferrocene carboxylate (56). Betaine is insoluble in deuterochloroform. However a 6.24 mM solution of bis urea 34 in deuterocholoroform is able to solubilize 1.3 equivalents of betaine. Not only is bis urea 34 able to solubilize betaine it also transfers information carried in its asymmetric centers to the α-carbon of betaine. The ^{1}H NMR spectrum shows the enantiotopic α-protons of betaine become non-equivalent in the complex and coupling occurs. A similar control experiment was performed with mono urea 34a. This host is only able to solubilize 0.3 equivalents of betaine and no differentiation of the methylene protons is seen. A similar effect is observed in a 1:1 mixture of ferrocene carboxylate (56) with bis urea 34. The proximal cyclopentadiene ring loses its symmetry upon complexation (figure II–15).
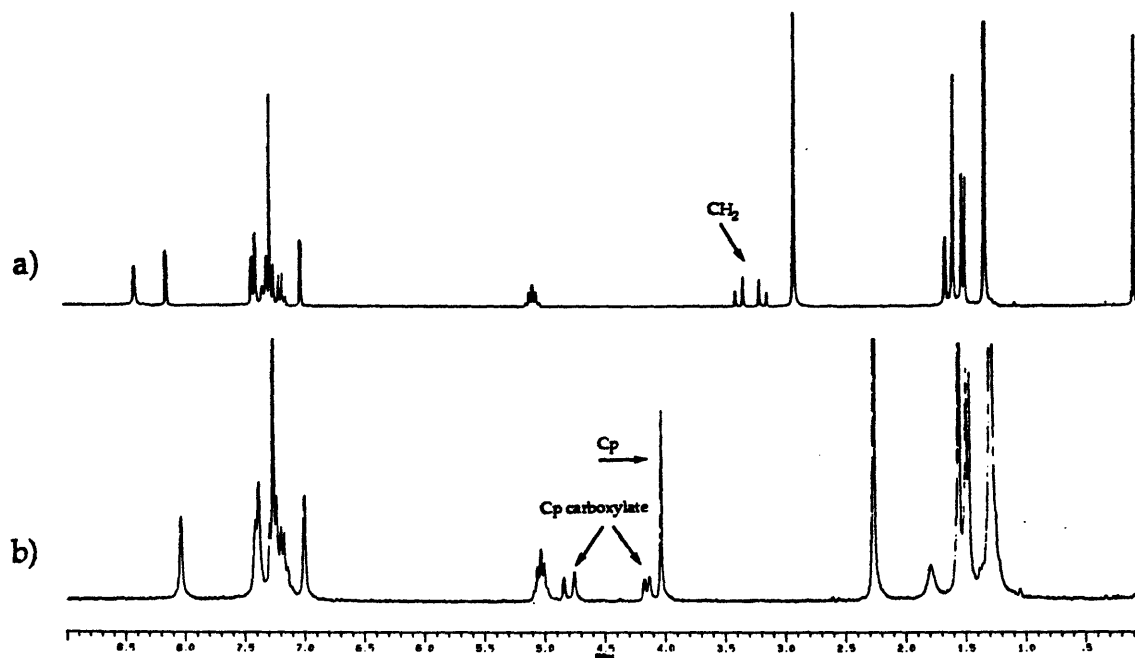
Figure II–15. *^1H NMR spectra of desymmetrized a) betaine and b) ferrocene carboxylate due to complexation with bis urea R,R-34.*

A solution of bis urea **34** was formed in deuteromethylene chloride with betaine and Dr. M. Conn conducted nOe studies. Results show that there is close contact in the complexes between host and guests (figure II–16).
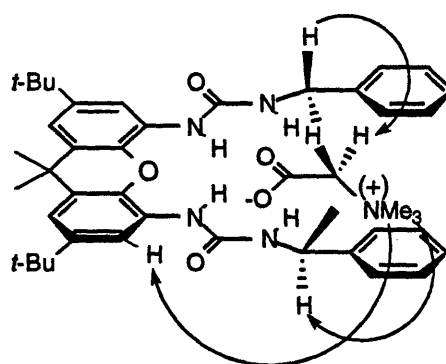
Figure II–16. *Betaine complexed with bis urea **34** shows close contact as revealed in nOe studies.*

Chiral bis urea hosts were investigated to determine the influence of the asymmetric centers on the binding of optically active guests. Ammonium salts of Naproxen® **53, 54** were titrated in deuterochloroform and deuteromethanol (table II–1). Though initial studies in deuterochloroform showed differences in the association constants, the values are not very reliable. To obtain accurate binding data the concentration of host should be on the order of the inverse of the association constant (*e.g.* [Host] = $1/K_a$). However the association constants are roughly 1×10^5 M^{-1}, which means that the titration should be conducted at 1×10^{-5} M concentration of host in deuterochloroform. Such a low concentration is below the sensitivity of ^{1}H NMR. This leaves two options, change to a more hydrogen bond competitive NMR solvent or use another spectroscopic technique such as UV–Vis. We chose to use a more competitive solvent, deuteromethanol. This reduced the binding energies and allowed for accurate ^{1}H NMR titrations using 5 to 10 mM host concentrations. Although there appears to be a slight difference between the R,R and S,S-bis ureas they are not statistically significant at the 95% confidence interval.

Bis Urea	Naproxen Salts		
	53 in CDCl$_3$	53 in CD$_3$OD	54 in CD$_3$OD
R,R-34	350,000	71	130
S,S-34	160,000	77	150
R,R-35	—	—	160
S,S-35	—	—	110

Table II–1. *Observed data for the affinity (M^{-1}) of naproxen salts and bis urea in both CDCl$_3$ and CD$_3$OD.*

Chiral centers of the bis ureas exert limited influence on chiral guests. One fatal flaw plagues the design of the xanthene bis urea—degenerate binding conformers. The optimal binding conformation of bis urea **34** is shown in figure II–17. Complexation of the carboxylate in the plane of the xanthene gives the best opportunity for chiral selection. However the carboxylate can readily complex the bis urea when it is not coplanar with the xanthene (figure II–17). This slight change will remove any negative effects of

steric repulsion, as a result of chiral selection, without affecting the urea-carboxylate interactions.

Coplanar Host & Guest   Non-Coplanar, Diverging
                                        Asymmetric Centers
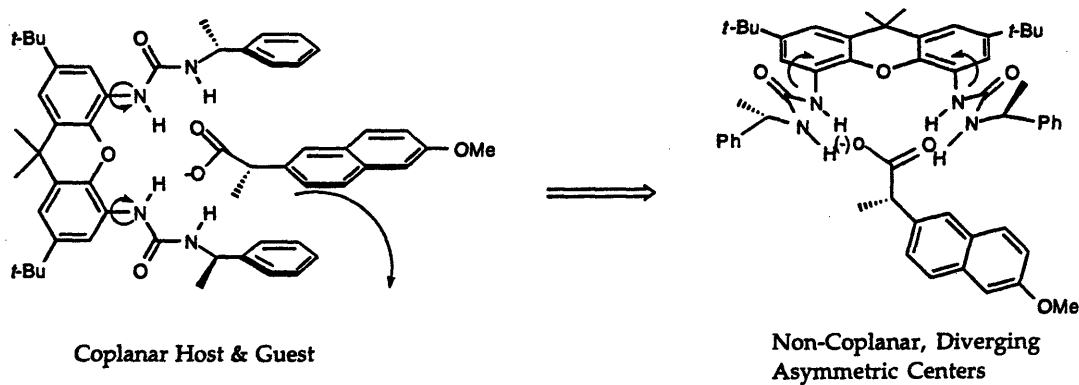
Figure II–17. *Slight conformational changes can cause the asymmetric centers of the host and guest guest to diverge.*

Guest	Hosts			
	R,R-34	S,S-34	**44**	**45**
50	150	—	—	—
51	—	200,000	—	—
52	—	—	6.9×10^6	4.5×10^6
53	353,000	163,000	—	—
55	—	—	3.3×10^6	6.4×10^6
58	105	—	—	—
59	253	—	—	—

Table II–2. *Association constants (M^{-1}) for bis ureas and a variety of guests.*

Anion	Cation		
	Et$_3$NH(+)	Et$_4$N(+)	Me$_4$N(+)
Ph—C(=O)—O(-)	50	51	52
2-(6-methoxy)naphthyl—CH—C(=O)—O(-)		53	54
O—P(=O)(OPh)(Ph)—O(-)			55
ferrocenyl—C(=O)—O(-)			56

57

58

59

Figure II–18. *Guests used to investigate the binding properties of bis ureas.*

Bis urea **44** was also found to be an effective host in phosphate diester recognition. Titrations in deuterochloroform showed orderly 1:1 complex formation with chelation of phosphate **55** and, as seen with carboxylates, large binding affinities were observed for the tetramethylammonium salt of phosphate diester **55** (table II–2). However, the phosphate diester does not bind as strongly as the tetramethylammonium benzoate. Modeling[33] of the complexes indicates that the smaller carboxylate geometry is a better companion for the oxy-anion hole than the larger phosphate. If this modeling prediction were true one would expect a bis urea with a more open binding pocket to form a stronger complex with the phosphates as compared to carboxylates. This is indeed what is observed when dibenzofuran bis urea **45** is titrated against tetramethylammonium salts of phosphate **55** and carboxylate **52** (figure II–19). The binding data reported in table II–2 is from UV titration studies at low concentration (32.1 μM).

---

33 MacroModel V3.5X using the AMBER* force field. Mohamadi, F.; Richards, N. G.; Guida, W. C.; Liskamp, R.; Lipton, M.; Caufield, C.; Chang, G.; Hendrickson, T.; Still, W. C. *J. Comput. Chem.* **1990**, *11*, 440-467.
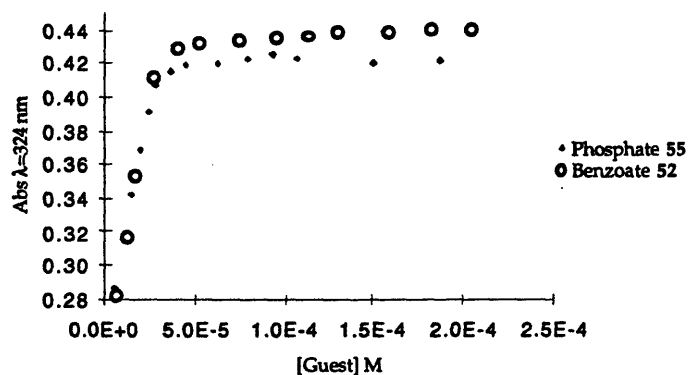
Figure II–19. *Plot of the data for the titration of bis urea 45 (32.114 μM) with tetramethylammonium diphenyl phosphate 55 and benzoate 52.*

Crystal Structure

An X-ray crystal structure was solved for bis urea **48** by Dr. Leticia Toledo. The crystal was obtained from a solution of **48** in acetonitrile by slow evaporation. The crystal contains two different conformations, fragment 1 and fragment 2, of xanthene bis urea **48** (see appendix A). Each structure has the unusual feature of two ureas in close proximity that are not hydrogen bonded to one another in a head-to-tail fashion (figure II–20, appendix A). Instead, the ureas are hydrogen bonded to other xanthene ureas, one above and one below to create a 3-dimensional array. The xanthene is ideal in positioning two self-complementary ureas close enough to form a convergent oxy-anion hole without having them collapse on one another.

Nowick[34] and Gellman[35] have studied 7–10 membered ring formations through intramolecular hydrogen bonds involving ureas and amides. Even with their highly flexible aliphatic systems these investigations showed a significant amount of structural rigidification due to the intramolecular associations. It seems likely that the xanthene is simply too

---

[34] Nowick, J. S.; Abdi, M.; Bellamo, K. A.; Love, J. A.; Martinez, E. J.; Noronha, G.; Smith, E. M.; Ziller, J. W. *J. Am. Chem. Soc.* **1995**, *117*, 89-99.

[35] Liang, G.-B.; Desper, J. M.; Gellman, S. H. *J. Am. Chem Soc.* **1993**, *113*, 925.

rigid to allow the ureas to come in any significant contact. The xanthene's ether oxygen may also provide a small contribution in directing the hydrogen bond donors in a convergent fashion.

'Top' View of 48   'End-on' View of 48
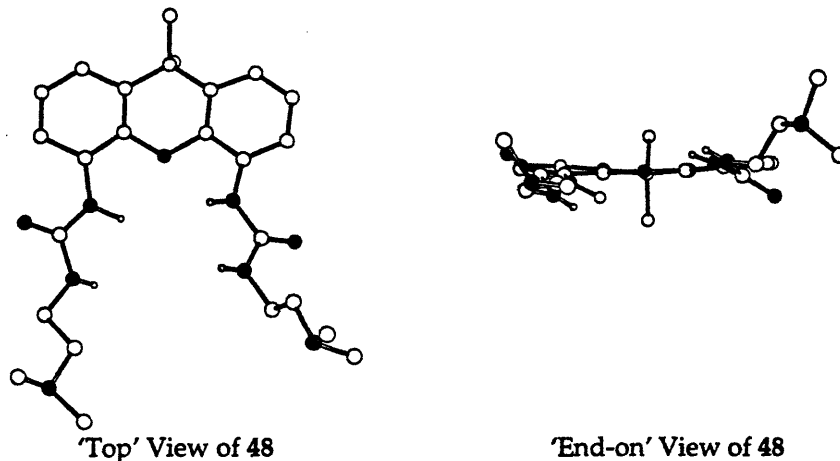
Figure II-20. *Crystal structure of fragment 1 viewed from the 'top' and 'end-on' perspective. The end-on view is down a C₂ axis that bisects the ether oxygen and quantinary carbon of the xanthene.*

Accelerated Phosphate Ester Cleavage

Hamilton developed a molecule for recognition of phosphate diesters. This host (60) is equipped with tertiary amines. The amines provide general base catalysis in the transesterification of phosphate 61 (figure II-21). But, host 60 has a serious design flaw. It has two extra degrees of rotational freedom about the aryl-carbonyl carbon bond preventing the existence of a discrete, well defined binding pocket. As a result, they do not see clean 1:1 binding but a mixture of 1:1 and 1:2 complexes (figure II-21).
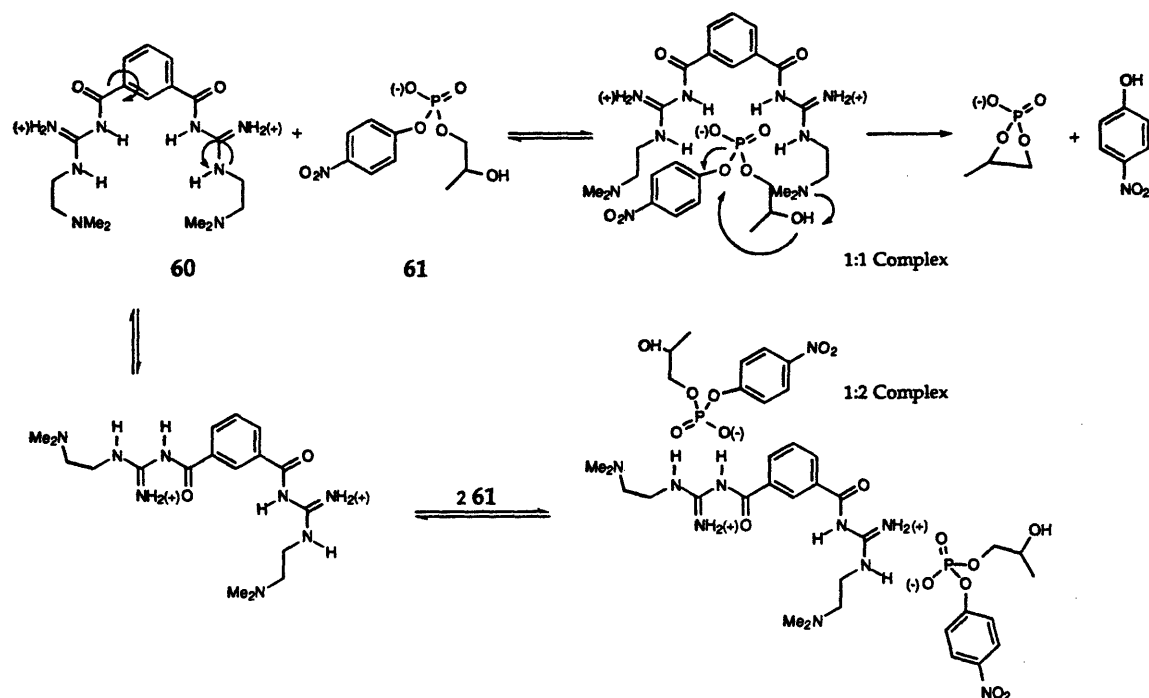
Figure II–21. *The different possible binding conformers of Hamilton's phosphate transesterification receptor.*

Bis urea **48** was shown, by spectroscopic and X-ray data, to have a well defined binding pocket for phosphates. Docking[33] of the substrate, phosphate **61**, with fragment 1 of the crystal structure of receptor **48** (see appendix A), shows the tertiary amines to be properly placed for general base catalysis in the intramolecular transesterification reaction (figure II–22). Similar arguments cannot be made for the dibenzofuran bis urea. Although **45** has stronger binding affinity for phosphates, its splayed geometry removes the amines from bound guests (figure II–23). Therefore, bis urea **48** was employed in transesterification studies with **61** despite its somewhat lower binding affinity.
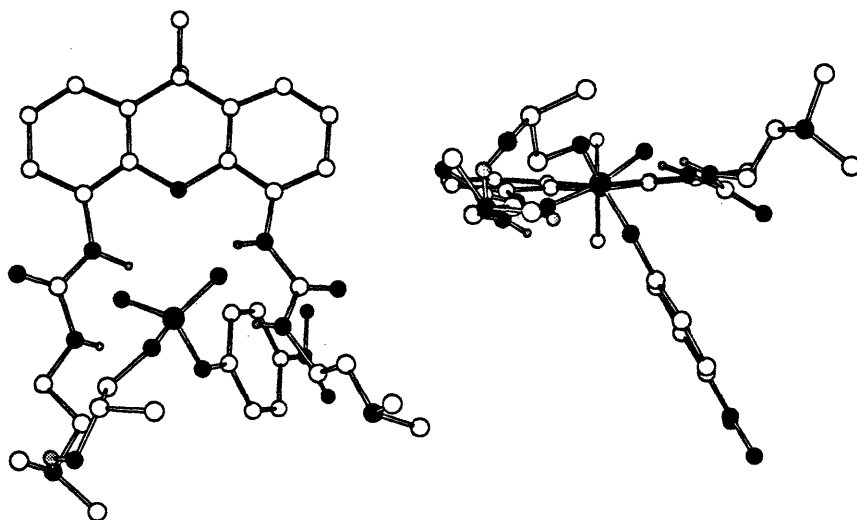
Figure II–22. *MacroModel minimized phosphodiester 61 docked with the crystal structure of 48, fragment 1.*
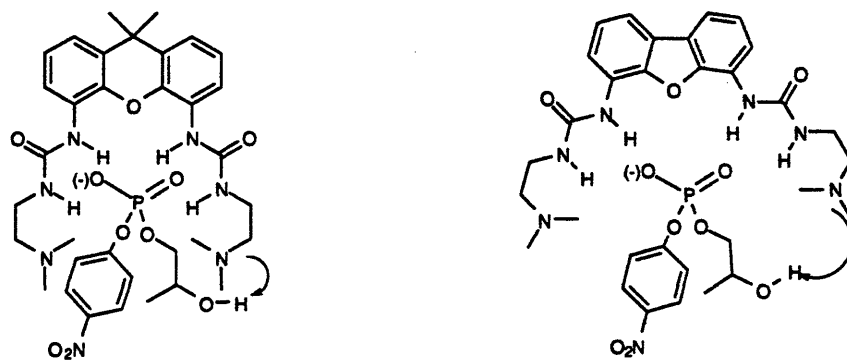
Figure II–23. *Phosphodiester 61 bound with xanthene and dibenzofuran bis ureas.*

The protocol that Hamilton developed was employed in the phosphoryl transfer reaction of 2-hydroxypropyl-*p*-nitrophenyl phosphate (HPNPP).[36] The receptor is added in excess and the appearance of the free *p*-nitrophenol and the disappearance of the phosphate ester **61** is monitored by UV spectroscopy. The reaction is conducted under pseudo first-order conditions. The k_{obs} was determined from equation II–1 (see experimental for

[36] Jubian, V.; Veronese, A.; Dixon, R. P.; Hamilton, A. D. *Angew. Chem. Int. Ed. Engl.* **1995**, *34*, 1237.

its derivation).[37,38] From the plot of k_{obs} versus concentration of receptor **60**, Hamilton obtained a saturation kinetics curve where an effective binding constant (K_a) for the reaction process was determined.

$$\ln\left(\frac{A_o - A_\infty}{A_t - A_\infty}\right) = kt \qquad\qquad\qquad \text{eq. 1}$$

Where A_o is the absorbance of the solution at time=0, A_t is the absorbance measured through out the reaction and A_∞ is the approximation for the finial absorbance reading at time=infinity.

The use of receptor **48** showed a substantial rate acceleration over both the background reaction and the reaction in the presence of Hamilton's receptor (**60**). In acetonitrile, Hamilton reports $k_{obs}/k_{background}$=290 and K_a=625 M^{-1} at 5 mM receptor and 0.1 mM HPNPP concentrations. But bis urea **48** showed $k_{obs}/k_{background}$=1740 and K_a~10,000 M^{-1} at 0.5 mM receptor **48** and 0.01 mM HPNPP concentrations. Even in highly hydrogen bond competitive solvents such as methanol, bis urea **48** was found to have $k_{obs}/k_{background}$=330 and K_a~350 M^{-1} at 5 mM receptor and 0.1 mM phosphate diester **61** concentrations (figure II-24).
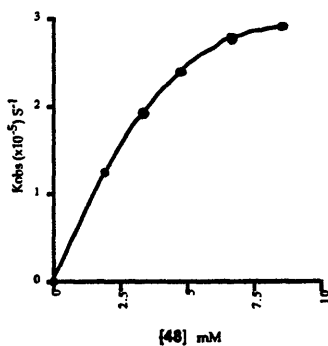
Receptor 48 (mM)	$k_{obs}(\times 10^{-5})S^{-1}$
0.0	0.007
1.90	1.23
3.33	1.92
4.76	2.38
6.66	2.75
8.57	2.88

Figure II-24. *Saturation kinetics of phosphoryl transfer reaction of HPNPP, 61, (0.1 mM) by bis urea 48 in methanol.*

37 Jubian, V.; Dixon, R. P.; Hamilton, A. D. *J. Am. Chem. Soc.* **1992**, *114*, 1120–1121.

38 Connors, K. A. *Chemical Kinetics: The Study of Reactions Rates in Solution* VCH, New York, **1990**.

Experimental

General

Reagent grade solvents were used except where noted. Tetrahydrofuran was distilled from Na/benzophenone ketyl and CH_2Cl_2 was distilled from P_2O_5. Melting points were measured on an Electrothermal 9100 melting point apparatus. NMR spectra were taken on a Varian XL-300 (300 MHz) and a Bruker AC-250 (250 MHz) spectrometers. IR spectra were obtained on a Mattson Sygus 100 FT IR spectrometer. High resolution mass spectra were obtained on a Finnegan Mat 8200 instrument. Flash chromatography was performed using Silica Gel 60 (EM Science, 230–400 mesh). Molecular modeling experiments were performed on a Silicon Graphics Personal Iris using MacroModel3.5X program with Amber force field.

Titrations

All titrations were performed on a Bruker AC-250 (250 MHz) spectrometer. The deuterated solvents were dried over 4Å molecular sieves. Analytical grade A volumetric flasks and syringes were used throughout the preparation of the solutions. The titrations were typically carried out at 5–10 mM concentration of host and 25–50 mM concentration guest. UV titrations were conducted on a Perkin Elmer Lamda 12 UV-Vis spectrophotometer at λ=324 nm. Concentrations for UV titrations ranged around 40 µM for the host and 400 µM for the guests. Aliquots of the guest solution were added via syringe and the spectrum recorded after each addition until the host was fully saturated. The data was fit to a 1:1 complex binding equation (see experimental in chapter I) using Systat 5.2 for the Macintosh.

The titration mono urea 15 with tetraethylammonium benzoate was conducted as follows. A 8.184 mM solution of 15 was prepared by dissolving 2.93 mg of 15 in CDCl₃ in a 1 mL volumetric flask and diluting to the mark with CDCl₃. A 36.46 mM solution of tetraethylammonium benzoate was prepared by placing 45.80 mg in a 5 mL volumetric flask and dissolving in CDCl₃. The solution was then diluted to the mark to give a 1 mL total

volume. 500 µL of the host **15** solution was placed in an ^{1}H NMR tube and the spectrum recorded. Eight 25 µL, two 50 µL, two 100 µL and two 250 µL additions of the guest solution were added to the NMR tube and the spectrum recorded after each addition (figure I-25). The changes in the urea protons (δ, ppm) were used to calculate the association constant (Ka=540 M^{-1}).
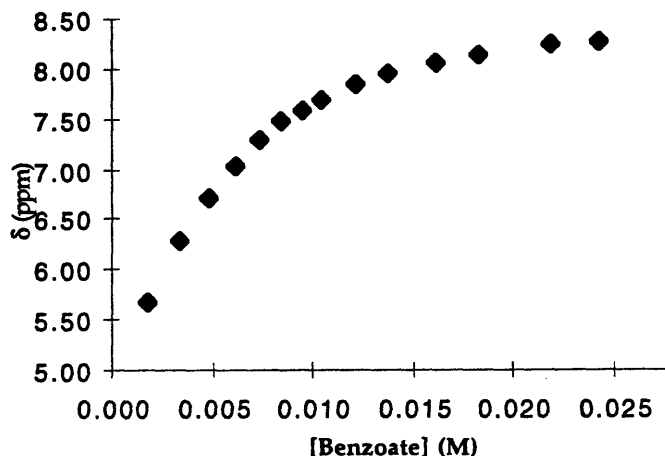
Figure I-25. *Plot of the raw data for the titration of mono urea **15** and Et$_3$N benzoate.*

UV titrations were conducted as follows. 8.60 mg of bis urea **45** was dissolved in CHCl$_3$ in a 1 mL volumetric flask and diluted to the mark with CHCl$_3$. 10 µL of this solution was placed in a 5 mL volumetric flask and diluted to the mark with CHCl$_3$ to give a 32.114 µM solution of **45**. The guest solution was prepared by placing 4.59 mg of phosphate **55** in a 1 mL volumetric flask, dissolving in CHCl$_3$ and diluting to the mark with CHCl$_3$. 50 µL of this solution was placed in a 2 mL volumetric flask and the solvent removed *in vacuo*. The solids were dissolved by the addition of the 32.114 µM host **45** solution and then diluted to the 2 mL mark with this same host solution to give a final solution that was 373.4 µM in phosphate **55** concentration and 32.114 µM in host **45** concentration.

The initial volume of the host solution was 750 µL. It was placed in a quartz cuvette, pathlength of 1 cm, and the spectrum was scanned from 340

nm to 270 nm. $CHCl_3$ (750 μL) was placed in a cuvette and used as the reference cell. Six 10 μL, two 20 μL, four 50 μL, one 200 μL and one 250 μL additions were made to each of the sample and reference cells and the spectrum (340 nm to 270 nm) recorded after each addition (figure II-26). A curve was fit to the plot of the absorbance (λ=324 nm) versus the concentration of the guest (figure II-19) using systat 5.2 for the Macintosh and the 1:1 binding equations presented in the experimental of chapter I.
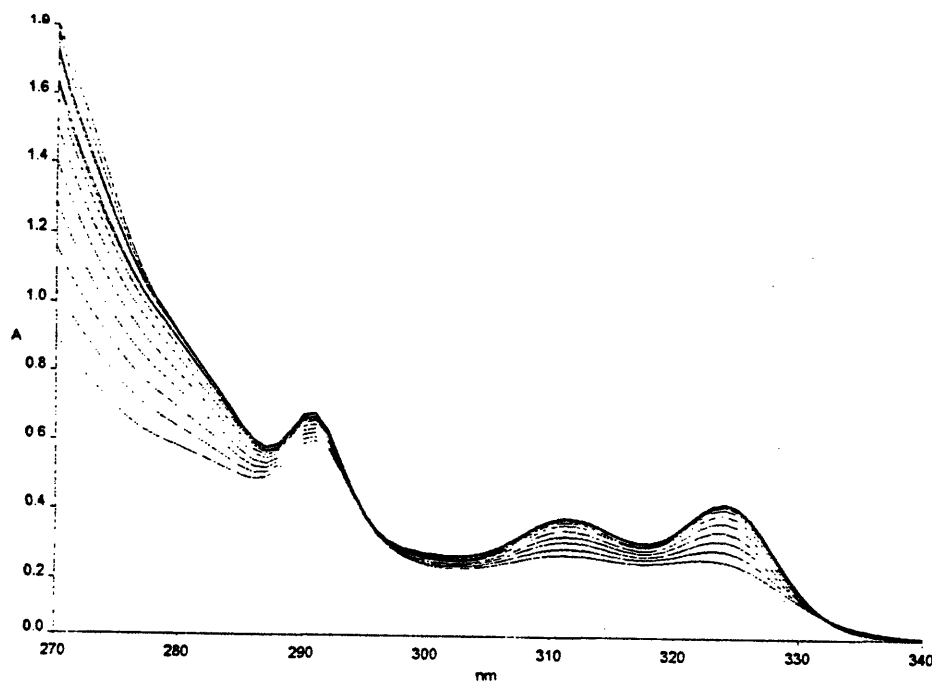
Figure II-26. *UV spectrum data for the titration of bis urea 45 (32.11 μM) with tetramethylammonium diphenyl phosphate.*

Kinetics

A Perkin Elmer Lamda 12 UV-Vis spectrophotometer was used to monitor the formation of *p*-nitrophenol and disappearance of phosphate diester 61 at λ=324 nm. The reactions were run at 25 °C using a Haake D1 constant temperature regulator. The concentration of receptor 48 was varied between 0.1 mM and 3.0 mM in acetonitrile while phosphate 61 was kept at 0.01 mM concentrations. In methanol studies the concentration of receptor 48 was varied between 1 mM and 5 mM while phosphate 61 concentrations were held at 0.1 mM. Conformation of the formation of reaction products was

obtained by comparing with known compounds by HPLC. HPLC grade solvents were used throughout the studies and grade A analytical glassware was used to prepare the solutions. The data was fit to the appropriate kinetic equation using Cricket Graph III for the Macintosh.

A typical set of runs in methanol were carried out as follows. A stock receptor solution (9.52 mM) was prepared by placing 22.31 mg of receptor **48** in a 5 mL volumetric flask and dissolving in methanol before diluting to the mark with methanol. A stock substrate solution (15.20 mM) was prepared by dissolving 5.24 mg of **61** in methanol in a 1 mL volumetric flask. 65.8 µL of the stock substrate solution was transferred to a 1 mL volumetric flask and diluted to the mark with methanol to give a 1.00 mM solution.

Six reactions were prepared by placing 100 µL of the 1.00 mM substrate **61** solution in a quartz cuvette (l=1 cm). Next the appropriate amount of MeOH was added to each cuvette so a final reaction volume of 1 mL would be achieved after the addition of the receptor solution. A reference cell which contained only methanol also was used. At time zero either 0, 200, 350, 500, 700 or 900 µL of the stock receptor **48** solution was added to the cuvettes and the reaction data collected (figure II-27).
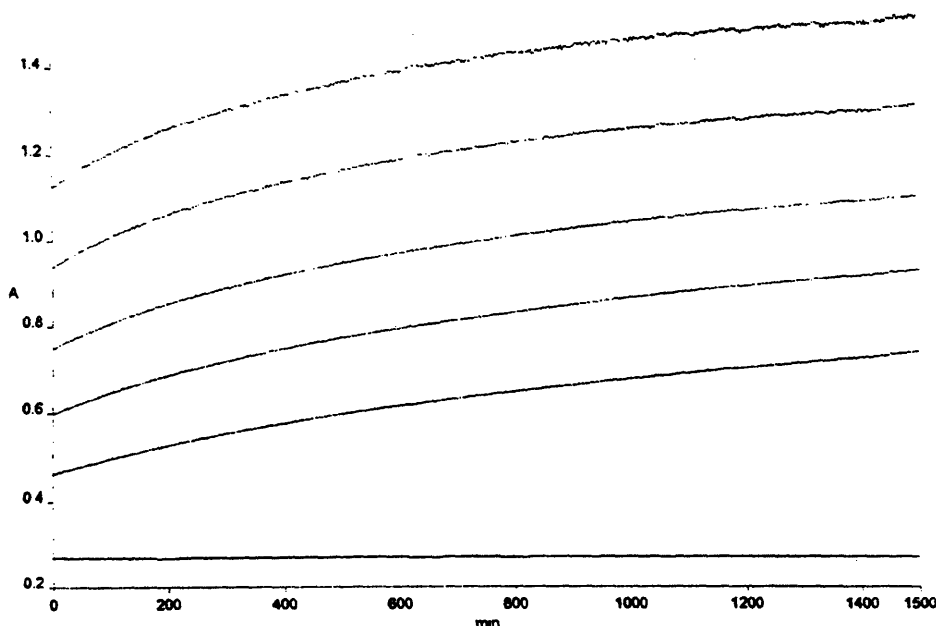
Figure II-27. UV kinetic data for the phosphoryl transesterification of **61** in the presence of receptor **48** in methanol.

A typical set of runs in acetonitrile was carried out as follows. A stock solution of receptor 48 was prepared by placing 16.71 mg in a 5 mL volumetric flask and dissolving in acetonitrile followed dilution to the mark to give a 7.129 mM solution. 1250 µL of this solution was placed in a 5 mL volumetric flask and diluted to the mark with acetonitrile to give a 1.782 mM solution of 48. A substrate stock solution was prepared by placing 5.36 mg of 61 in a 10 mL volumetric flask with 1 eq. (4.11 mg) of 18-crown-6 and 1 µL of H_2O (to help solubilize the phosphate).[37] These compounds were dissolved in acetonitrile and then diluted to the mark to give a solution 1.555 mM in 61. 64.3 µL of this solution were placed in a 1 mL volumetric flask and diluted to the mark with acetonitrile to give a solution 0.100 mM in 61.

Three 100 µL aliquots of the 0.100 mM solution of 61 were placed in three separate cuvettes followed by 750 µL of acetonitrile. At time zero 150 µL of the receptors solution (1.782 mM) was added to each cuvette. A reference cell was employed which contained only acetonitrile.

Reactions in both methanol and acetonitrile were followed at $\lambda=324$ nm, at this wavelength the receptor 48, *p*-nitrophenol and *p*-nitrophenyl phosphate ester have absorptions. The concentration of the receptor does not change during the reaction. The extinction coefficient of 48 is assumed to not significantly change throughout the reaction since the receptor is present in large excess and the total phosphate concentration does not change. Equation II–1 was used to account for the absorptions of both starting material and product to obtain an observed rate for the reaction. It is derived as follows.

$$[R] + [S] \rightleftharpoons [RS] \longrightarrow [RP] \rightleftharpoons [R] + [P]$$

Where R is receptor; S is the substrate, HPNPP; P is the product, *p*-nitrophenol.
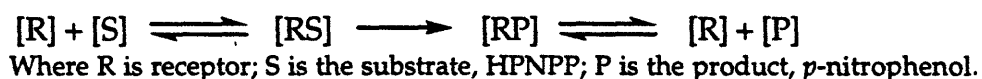
$$A_t = [S]\varepsilon_s + [P]\varepsilon_p \qquad\qquad \text{eq. 2}$$

Where A_t is the absorbance at time t, [S] and [P] are the concentrations of phosphate ester and *p*-nitrophenol at time t, and ε_s and ε_p are the extinction coefficients of phosphate ester and *p*-nitrophenol, respectively, times the pathlength (1 cm) of the cuvette.

$$[S]^0 = [S] + [P] \qquad\qquad \text{eq. 3}$$

Where $[S]^0$ the concentration of phosphate ester at time zero.

$$A_t = [S]\varepsilon_s + \big([S]^o - [S]\big)\varepsilon_p \qquad\qquad\qquad\qquad \text{eq. 4}$$

Combining equations of 2 and 3, followed by rearrangement
gives equation 5.

$$A_t = [S]\big(\varepsilon_s - \varepsilon_p\big) + [S]^o\varepsilon_p \qquad\qquad\qquad\qquad \text{eq. 5}$$

$$[S] = [S]^o e^{-kt} \qquad\qquad\qquad\qquad\qquad\qquad \text{eq. 6}$$

First-order rate equation for the disappearance of phosphate ester.

$$A_t = [S]^o e^{-kt}\big(\varepsilon_s - \varepsilon_p\big) + [S]^o\varepsilon_p \qquad\qquad\qquad \text{eq. 7}$$

Combining equations of 5 and 6, followed by rearrangement
gives equation 8.

$$\frac{A_t - [S]^o\varepsilon_p}{[S]^o\big(\varepsilon_s - \varepsilon_p\big)} = e^{-kt} \qquad\qquad\qquad\qquad \text{eq. 8}$$

$$\ln\big(A_t - [S]^o\varepsilon_p\big) - \ln\big([S]^o\varepsilon_s - [S]^o\varepsilon_p\big) = -kt \qquad \text{eq. 9}$$

Taking the ln of both sides eq. 8, followed by multiplying by -1
gives equation 10.

$$\ln\big([S]^o\varepsilon_s - [S]^o\varepsilon_p\big) - \ln\big(A_t - [S]^o\varepsilon_p\big) = kt \qquad \text{eq. 10}$$

$$A_o = [S]^o\varepsilon_s \qquad\qquad A_\infty = [S]^o\varepsilon_p \qquad\qquad \text{eq. 11, 12}$$

$$\ln\big(A_o - A_\infty\big) - \ln\big(A_t - A_\infty\big) = kt \qquad\qquad \text{eq. 13}$$

Substituting the initial absorbance (A_o) and absorbance at infinite time
(A_∞) into equation 10 gives equation 13 which rearranges to equation 1.

$$\ln\left(\frac{A_o - A_\infty}{A_t - A_\infty}\right) = kt \qquad\qquad\qquad\qquad \text{eq. 1}$$

X-ray Diffraction Studies

A crystal of about 0.4x0.4x0.2mm was mounted on a fiber embedded in
a matrix of Paraton N. Data were collected at 23 °C on a Siemens CCD
diffractometer (equipped with an automated 3 circle goniometer and a solid
state generator) using graphite-monochromatized Mo-Kα radiation (0.710690
Å) by the ω scan method operating under the program SMART.[39] A total of 15

39 SMART, V. 4.0; Siemens Industrial Automation, Inc.; Madison, WI, 1994.

frames at 30 seconds measured at 0.3° increments of ω at three different values of 2θ and ϕ were collected, and after least squares, a preliminary unit cell was obtained. For data collection, three sets of frames of 30 seconds exposure were collected. Data were collected in three distinct shells. For the first shell, 606 frames were collected with values of ϕ = 0° and ω = -26°, for the second shell, 435 were collected with ϕ = 88° and ω = -21° and for the third shell values of ϕ = 180° and ω = -23° were used to collect 230 frames. At the end of data collection the first 50 frames of the first shell were recollected to correct for any crystal decay, but no anomalies were observed. The data were integrated using the program SAINT[40] The integrated intensities of the three shells were merged into one reflection file. The data were filtered to reject outliers based on the agreement of the intensity of the reflection and the average of the symmetry equivalents to which the reflection belongs. Of a total of 18948 reflections which were collected ($2\theta_{max}$=46.6°), 7499 were unique (R_{int} = 0.064); equivalent reflections were merged.

The space group was determined to be monoclinic $P2_1/n$. The unit cell dimensions were a=11.667(5)Å, b=24.22(1)Å, c=18.486(7)Å β=96.86(2)°, V=5186(3) Å^3 with Z=8. The structure was solved using the direct methods program Sir92 of the TeXsan[41] (version 1.7-1) crystallographic package of Molecular Structure Corporation. The non-hydrogen atoms were refined anisotropically. Hydrogen atoms were included but not refined. The final cycle of full-matrix least-squares refinement was based on 2911 reflections ($I>3\sigma(I)$) and 533 variables gave a final R=0.115 ($1/\sigma^2$) and R_w=0.096.

Synthesis

2,7-Diacetyl-9,9-dimethylxanthene: Acetyl chloride (3.66 mL, 51.43 mmol) and 9,9-dimethylxanthene (5.150 g, 24.49 mmol) were dissolved in CH_2Cl_2 (50 mL) and cooled to 0 °C. Solid $AlCl_3$ (8.164 g, 61.23 mmol) was slowly added over a 15 min. period. The reaction was stirred for an additional

[40] SAINT, V. 4.0; Siemens Industrial Automation, Inc.; Madison, WI, 1995.

[41] TeXsan: Single Crystal Analysis Package, V. 1.7-1; Molecular Structure Corporation; Woodlands, TX, 1995.

45 min. before it was poured into ice water (250 mL). The mixture was diluted with CH_2Cl_2 (200 mL) and the layers were separated. The aq. layer was washed with CH_2Cl_2 (100 mL). The organic layers were combined and washed with H_2O (3x's, 100 mL) and brine (2x's, 50 mL). The organic layer was dried with $MgSO_4$ and concentrated to give the product in 98% yield. mp 159 °C; IR (KBr) 3095, 1673, 1617, 1596, 1576, 1482, 1359, 1313, 1267, 1247 cm^{-1}; ^{1}H NMR (CDCl$_3$) δ 8.11 (d, J=2.1Hz, 2H), 7.83 (dd, J=8.5, 2.1Hz, 2H), 7.12 (d, J=8.5Hz, 2H), 2.60 (s, 6H), 1.70 (s, 6H); ^{13}C NMR (CDCl$_3$) δ 196.4, 153.2, 133.1, 129.8, 128.5, 127.1, 116.5, 34.0, 32.7, 26.3.

2,7-Diethyl-9,9-dimethylxanthene: 2,7-Diacetyl-9,9-dimethylxanthene (1.825 g, 6.20 mmol) was suspended in ethylene glycol (25 mL) with KOH (2.435 g, 43.4 mmol) and hydrazine (1.36 mL, 43.4 mmol). The mixture was heated to 180 °C for 24 hrs. After the reaction cooled it was poured into H_2O (100 mL) and acidified with 6N HCl. The mixture was washed with Et$_2$O (2x's, 50 mL). The Et$_2$O were combined and washed with 1M HCl (1x, 50 mL), H_2O (2x's, 50 mL) and brine (1x, 50mL). The Et$_2$O layer was dried with $MgSO_4$ and concentrated to give the product as a yellow oil in 93% yield. IR (KBr) 2964, 2928, 2869, 1484, 1417, 1297, 1261, 1222, 821 cm^{-1}; ^{1}H NMR (CDCl$_3$) δ 7.21 (d, J=1.8Hz, 2H), 7.03 (dd, J=8.3, 1.9Hz, 2H), 6.95 (d, J=8.2Hz, 2H), 2.63 (q, J=6.7Hz, 4H), 1.63 (s, 6H), 1.24 (t, J=7.6Hz, 6H); ^{13}C NMR (CDCl$_3$) δ 148.7, 138.5, 129.8, 126.7, 125.2, 116.1, 34.1, 32.4, 28.5, 15.9.

2,7-Diethyl-9,9-dimethyl-4,5-dinitroxanthene: A 2:1 mixture of acetic anhydride/acetic acid (30 mL) was heated to 30 °C. Cupric nitrate (6.836 g, 34.08 mmol) was added and the suspension stirred for 15 min. before 2,7-diethyl-9,9-dimethylxanthene (3.612 g, 13.63 mmol) was added dropwise over a 10 min. period. The reaction stirred for 12 hrs. at 30 °C before being poured in H_2O (60 mL). The suspension was stirred for 30 min., filtered and washed with H_2O. The product was obtained in 90% yield. mp 154-155 °C; IR (KBr) 3132, 2972, 1534, 1463, 1398, 1336, 1263 cm^{-1}; ^{1}H NMR (CDCl$_3$) δ 7.59 (d, J=1.5Hz, 2H), 7.46 (d, J=1.4Hz, 2H), 2.70 (q, J=7.6Hz, 4H), 1.68 (s, 6H), 1.27 (t, J=7.6Hz, 6H); ^{13}C NMR (CDCl$_3$) δ 140.7, 140.0, 139.0, 132.3, 129.5, 122.7, 35.0, 31.8, 28.1, 15.2; HRMS m/e for $C_{19}H_{20}N_2O_5$ (M$^+$) calcd 356.13722, obsd 356.13766.

4,5-Diamino-2,7-diethyl-9,9-dimethylxanthene: 2,7-Diethyl-9,9-dimethyl-4,5-dinitroxanthene (0.4728 g, 1.326 mmol) was stirred with suspension of 5% Pd/C (250 mg) in THF (25 mL) under a hydrogen atmosphere for 24 hrs. The solution was filtered through celite and concentrated to give the product in 95% yield. mp 112 °C; IR (KBr) 3411, 2966, 2925, 1631, 1482, 1448, 1277, 1215, 1165 cm^{-1}; ^{1}H NMR (CDCl$_3$) δ 6.68 (d, J=1.6Hz, 2H), 6.52 (d, J=1.8Hz, 2H), 3.28 (brs, 4H), 2.57 (q, J=7.6Hz, 4H), 1.62 (s, 6H), 1.23 (t, J=7.6Hz, 6H); ^{13}C NMR (CDCl$_3$) δ 138.6, 136.8, 134.0, 130.2, 114.9, 113.1, 34.3, 31.8, 28.6, 15.7; HRMS m/e for C$_{19}$H$_{24}$N$_2$O (M$^+$) calcd 296.18886, obsd 296.18856.

4-Bromo-2,7-diethyl-9,9-dimethylxanthene: 2,7-diethyl-9,9-dimethylxanthene (1.470 g, 5.52 mmol) was dissolved in CH$_2$Cl$_2$ (25 mL) and cooled in an ice bath. Bromine (0.28 mL, 5.52 mmol) was added and the reaction slowly came to room temperature and stirred for 16 hrs. The reaction was concentrated *in vacuo* to give the product as an oil in 95% yield. IR (KBr) 2965, 2930, 2871, 1566, 1498, 1458, 1420, 1326, 1292, 1273, 1257, 1237, 1210 cm^{-1}; ^{1}H NMR (CDCl$_3$) δ 7.24 (d, J=2.1Hz, 1H), 7.18 (d, J=1.8Hz, 1H), 7.14 (d, J=1.9Hz, 1H), 7.06-7.04 (m, 2H), 2.62 (q, J=7.7Hz, 2H), 2.59 (q, 7.7Hz, 2H), 1.6 (s, 6H), 1.23 (t, J=7.6Hz, 3H), 1.22 (t, J=7.6Hz, 3H); ^{13}C NMR (CDCl$_3$) δ 148.5, 145.6, 139.4, 139.2, 131.8, 130.3, 129.6, 126.8, 124.9, 124.4, 116.5, 110.2, 34.8, 32.0, 28.5, 28.2, 15.8, 15.6.

4-Bromo-2,7-diethyl-9,9-dimethyl-5-nitroxanthene: Acetic anhydride/acetic acid (2:1, 3 mL) were heated to 30 °C before cupric nitrate (0.566 g, 2.82 mmol) was added. After 15 min. 2,7-diethyl-9,9-dimethylxanthene (0.814 g, 2.57 mmol) was added. After 4 hrs. the reaction was poured into H$_2$O (40 mL). The mixture stirred for 10 min. before being washed with Et$_2$O (50 mL). The organic layer was separated and washed with H$_2$O (2x's, 25 mL) followed by brine. The Et$_2$O solution was dried with MgSO$_4$ and concentrated *in vacuo* to give the crude product. A white solid was obtained after a flash silica column using 100% hexane. IR (KBr) 2965, 2931, 2873, 1532, 1453, 1351, 1328, 1298, 1262, 1213 cm^{-1}; ^{1}H NMR (CDCl$_3$) δ 7.61 (d, J=1.8Hz, 1H), 7.44 (d, J=2.1Hz, 1H), 7.32 (d, J=1.9Hz, 1H), 7.15 (d, J=1.8Hz, 1H),

2.70 (q, J=7.6Hz, 2H), 2.62 (q, J=7.6Hz, 2H), 1.64 (s, 6H), 1.27 (t, J=7.6Hz, 3H), 1.23
(t, J=7.6Hz, 3H); ^{13}C NMR (CDCl$_3$) δ 144.4, 141.8, 140.9, 138.9, 138.4, 132.8, 130.8,
130.7, 129.7, 124.0, 122.2, 110.4, 35.0, 31.6, 28.0, 27.9, 15.3, 15.0.

2,7-Diethyl-9,9-dimethyl-4-nitroxanthene: Acetic anhydride/acetic acid
(2:1, 8 mL) were heated to 30 °C before cupric nitrate (1.427 g, 7.12 mmol) was
added. After 15 min. 2,7-diethyl-9,9-dimethylxanthene (1.723 g, 6.47 mmol)
was added. The reaction stirred for 90 min. before being poured into H$_2$O (50
mL). The H$_2$O was decanted and the oily solid was washed with H$_2$O. The
residue was taken-up in Et$_2$O, dried with Na$_2$SO$_4$ and concentrated *in vacuo*.
The product was isolated as an oil via flash silica column using 100% hexane.
IR (KBr) 2966, 2931, 2873, 1532, 1498, 1469, 1418, 1355, 1278, 1258, 1239, 1209 cm$^-$
^{1}; ^{1}H NMR (CDCl$_3$) δ 7.57 (d, J=2.1Hz, 1H), 7.45 (d, J=2.1Hz, 1H), 7.21 (brs, 1H),
7.06 (brs, 2H), 2.69 (q, J=7.7Hz, 2H), 2.65 (q, J=7.5Hz, 2H), 1.65 (s,6H), 1.27 (t,
J=7.5Hz, 3H), 1.25 (t, J=7.8Hz, 3H); ^{13}C NMR (CDCl$_3$) δ 147.5, 142.4, 140.1, 138.5,
138.1, 133.3, 129.9, 128.9, 127.1, 124.7, 122.2, 116.7, 34.6, 31.9, 28.4, 28.1, 15.7, 15.2;
MS m/e for C$_{19}$H$_{21}$NO$_3$ (M$^+$) calcd 311.15, obsd 311.2.

4,5-N,N'-diphenylureido-2,7-diethyl-9,9-dimethylxanthene: Diamino
xanthene **43** (1.0615 g, 3.58 mmol) was dissolved in CH$_2$Cl$_2$ (25 mL) with
phenyl isocyanate (817 μL, 7.52 mL) and 1 drop of pyridine at 0 °C. After 2
min. the reaction turned to a white solid mass. After 20 min. hexane was
added and the solids were filtered and washed with hexane to give the
product as a white solid in quantitative yield. mp 234 °C; ^{1}H NMR (DMSO) δ
9.00 (s, 2H), 8.46(s, 2H), 7.98(s, 2H), 7.52(d, J=6.0 Hz, 4H), 7.31(dd, J=6.4 Hz, 4H),
6.98(m, 4H), 2.60(q, J=6.0, 0.5 Hz, 4H), 1.58(s, 4H), 1.20(t, 6.2 Hz, 6H), ^{13}C NMR δ
152.2, 139.7, 138.2, 136.4, 129.5, 128.8, 126.9, 121.7, 118.0, 117.7, 116.6, 34.0, 31.7,
28.2, 15.6.

4,5-N,N'-Bis-(dimethylamino ethylene)-ureido-9,9-dimethylxanthene:
Xanthene diacid (**46**) was dissolved/suspended in CH$_2$Cl$_2$ with a drop of 5%
DMF/CH$_2$Cl$_2$ with oxalyl chloride (801 μL, 6.31 mmol). After 3.5 hours the
solids were filtered and the filtrate was concentrated *in vacuo*. The dried
solids were dissolved in acetone and NaN$_3$ (0.215 g, 3.31 mmol) in 1 mL H$_2$O

was added and a precipitate was formed. Toluene (50 mL) was added and the layers separated. The organic layer washed with H_2O (2xs) and then dried over $MgSO_4$. The dried solution was filtered and concentrated under vacuum to a volume of ~45 mL. The solution was then heated to 70 °C under Ar. After 30 min. the reaction was cooled to 0 °C, Et_3N (880 μL, 6.31 mmol) and N,N-dimethylethylene diamine (363 μL, 3.31 mmol) were added. After 30 min. the reaction was concentrated *in vacuo* to give the product as a white solid. ^1H NMR (DMSO) δ 7.79(dd, J=8.1, 1.5 Hz, 2H), 7.14(dd, J=7.8, 1.5 Hz, 2H), 7.03(t, J=8.1 Hz, 2H), 3.37(t, J=6.5 Hz, 4H), 2.50(t, J=6.5 Hz, 4H), 2.28(s, 12H), 1.58(s, 6H). See appendix A for the crystal structure.

Bis-Urea Chiral Clefts: 4,5-diamino-2,7-di-t-butyl-9,9-dimethyl-4-xanthene (0.226 g, 0.642 mmol) was stirred in CH_2Cl_2 (20 ml) under an Ar atmosphere at room temperature with S-(-)-1-(1-napthyl) ethylisocyanate (0.23 ml, 1.28 mmol) for 21 hours. The CH_2Cl_2 was removed and the residue was dissolved in Et_2O (75 ml). The Et_2O was washed with 1M HCl, sat. $NaHCO_3$ and brine. The organic layer was dried over $MgSO_4$, filtered and concentrated *in vacuo* to give the crude product. The product was obtained in 88% yield after a silica flash column using CH_2Cl_2 (500 ml) followed by 10% ethyl acetate in CH_2Cl_2 as the eluent.

Characterization

(R) phenyl bis urea: $[\alpha]^{22}_D$ -81.8° (c=3.3, $CHCL_3$); mp 160-162 °C; FTIR (KBr) 3323, 2965, 2905, 2870, 1648, 1554, 1433, 1227, 860, 750, 698, 605 cm^{-1}; ^1H NMR (DMSO) δ 8.15 (s, 2H), 8.11 (d, J=1.1Hz, 2H), 7.30 (m, 10H), 7.05 (s, 2H), 6.88 (d, J=6.9Hz, 2H), 4.86 (dq, 2H), 1.56 (s, 6H), 1.39 (d, J=6.8Hz, 6H), 1.25 (s, 2H); ^{13}C NMR ($CDCl_3$) δ 156.8, 146.1, 143.9, 138.9, 129.4, 128.4, 126.9, 126.5, 125.9, 117.7, 117.4, 49.9, 34.9, 34.7, 32.3, 31.5, 23.3; HRMS m/e for $C_{41}H_{50}N_4O_3$ (M^+) calcd 646.3883, obsd 646.3878.

(S) phenyl bis urea: $[\alpha]^{22}_D$ +56.9° (c=1.7, $CHCL_3$)

(S)-1-napthyl bis urea: $[\alpha]^{22}_D$ +122.1° (c=1.3, $CHCL_3$); FTIR (KBr) 3374, 2963, 1654, 1543, 1429, 1226, 776 cm^{-1}; ^1H NMR ($CDCl_3$) δ 8.02 (bs, 2H), 7.99 (bs,

2H), 7.67 (d, J=7.9Hz, 2H), 7.56 (s, 2H), 7.53 (s, 2H), 7.38 (d, J=7.0Hz, 2H), 7.27 (d, J=13.1Hz, 2H), 7.17 (dd, J=7.8, 7.5Hz, 4H), 7.10 (d, J=2.1, 2H), 5.79 (bs, 2H), 5.56 (dq, 2H), 1.59 (s, 6H), 1.24 (s, 18H); ^{13}C NMR (CDCl$_3$) δ 156.6, 146.0, 139.3, 138.7, 133.8, 130.7, 129.3, 128.5, 127.7, 126.4, 126.3, 125.5, 125.1, 123.3, 122.4, 117.4, 45.8, 34.8, 34.7, 32.4, 31.4; HRMS m/e for C$_{49}$H$_{54}$N$_4$O$_3$ (M$^+$) calcd 746,4195 obsd.

(R)-1-napthyl bis urea: [α]$^{22}_D$ -130.4° (c=0.9, CHCL$_3$)

Chapter III

Self-Assembly & Encapsulation

Introduction

Tetraureido calix[4]arene **70** was previously reported from our group[1] by Ken Shimizu and evidence for its reversible assembly and encapsulation of aromatic guests was presented. Since then conclusive evidence was obtained and is presented here showing dimer **71·71** to be an excellent molecular container for species about the size of cyclohexane (101.6 Å^3).[2] Dimer **71·71** is soluble in non-polar aromatic and chlorinated solvents. The dimer's cavity is very size selective. Large solvents like *p*-xylene and toluene are readily displaced from the cavity by better matched guests such as benzene. Data were obtained that suggest guests are able to hydrogen bond in the interior of the cavity to the ureas. Finally, results show the dimer to be an effective cage for the catalysis of the Claisen rearrangement of allyl vinyl ether.

70 R = H
71 R = F

70·70 Ar = C$_6$H$_5$
71·71 Ar = C$_6$H$_4$,*p*-F
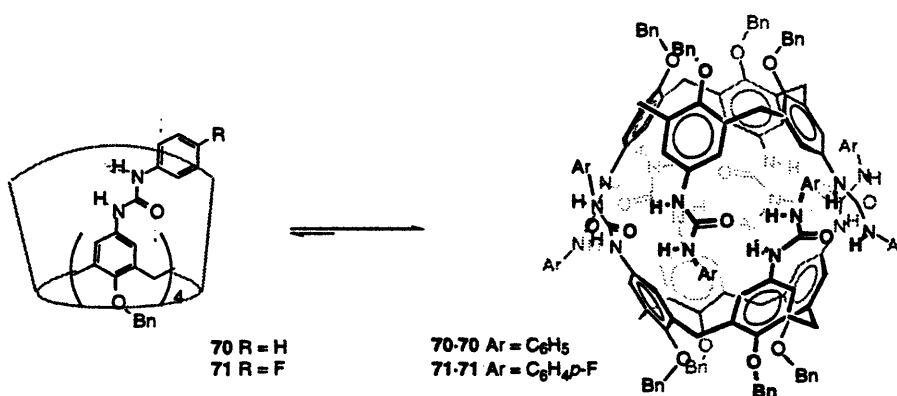
[1] Shimizu, K.; Rebek, J. Jr. *Proc. Natl. Acad. Sci. USA* **1995**, *92*, 12403. Shimizu, K. PhD Thesis, Massachusetts Institute of Technology, **1995**.

[2] Calculated by MacroModel (see reference 33 chapter II)

Background

Molecular capsules[3] and self-organizing molecular assemblies[4] have been the subject of numerous studies (figure III-1). It has only been in recent years that these two concepts were merged giving molecules that self-assemble forming cavities suitable for encapsulation of select molecular targets.[5-16] Assembly through non-covalent interactions offers a promising approach for the rapid formation of large molecular structures by directing a collection of smaller synthetically accessible units to come together.

a)   b)

X = $\{CH_2\text{-}S\text{-}CH_2\}$

        $\{O\text{-}CH_2\text{-}O\}$
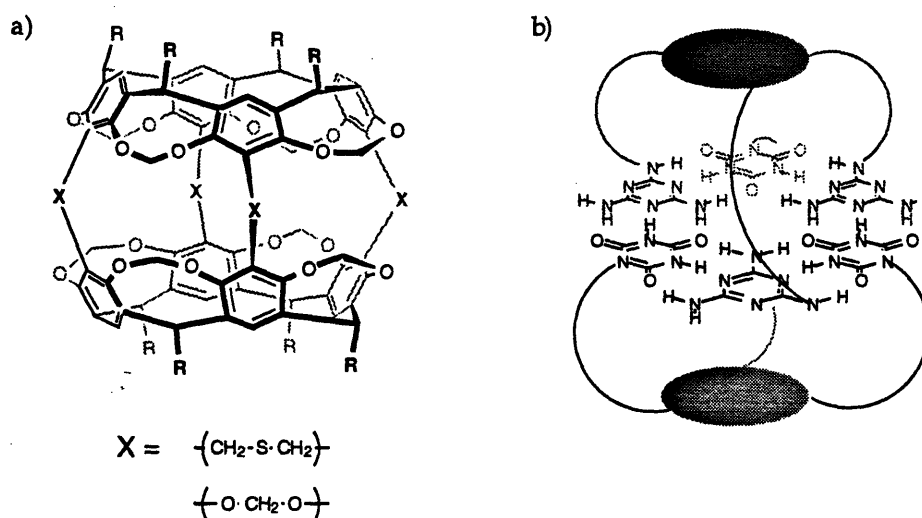
Figure III-1. *Examples of a) covalently linked capsules (Cram) and b) non-covlent molecular assemblies (Whitesides).*

One of the earliest examples of this strategy was reported by Rebek and coworkers.[5] The self-assembling 'Tennis Ball' uses two glycoluril units fused to a durene spacer to form a spherical structure which has self-

---

3   For examples of encapsulation in covalently linked capsules see: Robbins, T. A.; Knobler, C. B.; Bellow, D. R.; Cram, D. J. *J. Am. Chem. Soc.* **1994**, *116*, 111-122. Ikeda, A.; Shinkai, S. *J. Chem. Soc., Perkin Trans. 1* **1993**, 2671-2673. Garel, L.; Dutasta, J. P.; Collet, A. *Angew. Chem., Int. Ed. Engl.* **1993**, *32*, 1169-1171.

4   For reviews see: Lindsey, J. S. *New. J. Chem.* **1991**, *15*, 153-180. Lehn, J. M. *Angew. Chem., Int. Ed. Engl.* **1990**, *29*, 1304-1319. Whitesides, G. M.; Mathias, J. P. *Science* **1991**, *254*, 1312-1319. Philp, D; Stoddart, J. F. *Syn. Lett.* **1991**, 445-448.

5   Wyler, R.; de Mendoza, J.; Rebek, J., Jr. *Angew. Chem., Int. Ed.Engl.* **1993**, *32*, 1699-1701.

complementary, interlocking units much like the seams of a tennis ball (72, figure III–2). Dimer 72·72 was found to encapsulate small organic molecules such as CH_4, $CH_2=CH_2$ and $CHCl_3$.[6] Encapsulation of such guests was observed by ^{1}H NMR where bound species like CH_4 show a signal at -0.91 ppm in $CDCl_3$.

R=Ph, 4-Me₂N-Ph

72   72a
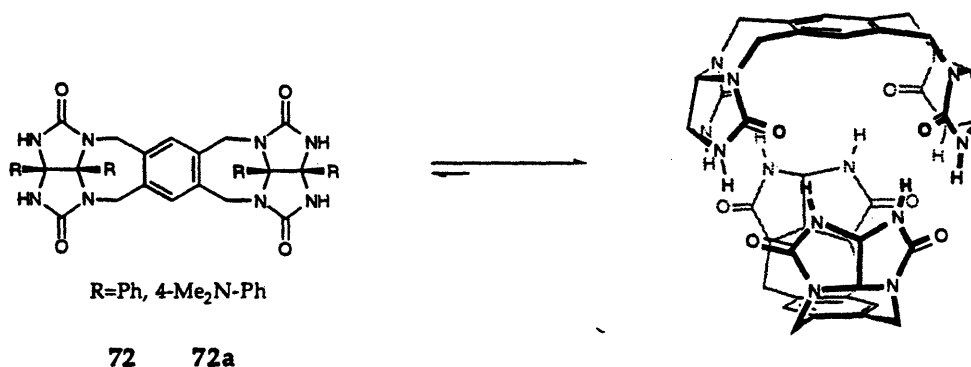
Figure III–2. *The concave surface forms a self-complementary assembly resembling a tennis ball.*

Rebek and coworkers used both acid-base[7] and reduction-oxidation[8] chemistry to control these glycoluril based assemblies. In the first case, 72 is synthesized where R= 4-Me₂N-Ph (72a). Xenon is encapsulated by 72a·72a in DMF-d_7. The dimer begins to disassemble, releasing encapsulated xenon, when p-toluene sulfonic acid is added to the solution. There is an inverse relation between the disappearance of the dimer with the appearance of protonated dimethyl amine. The authors attribute break-up of the dimer to the repulsive forces of a multi-protonated periphery of the assembly.

6   Branda, N.; Wyler, R.; Rebek, J. Jr. *Science* **1994**, *263*, 1267-1268.

7   Branda, N.; Grotzfeld, R. M.; Valdés, C.; Rebek, J. Jr. *J. Am. Chem. Soc.* **1995**, *117*, 85-88.

8   Garcías, X.; Rebek, J. Jr. *Angew. Chem. Int. Ed. Engl.* in press.

R=CO$_2$n-Bu   R=CO$_2$n-Bu
73   **74**
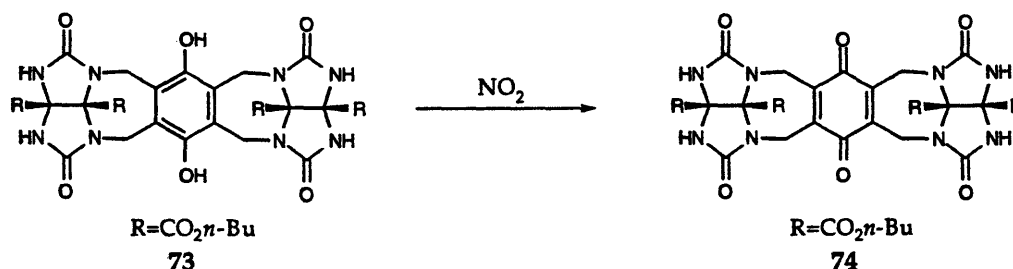
Figure III-3. *Control of the oxidation state of the spacer provides a mechanism for the control of encapsulation.*

Using Dimers **73·73** and **74·74** they found that the electronics of the aromatic spacer influence the binding affinity of the guests.[8] Electron rich **73·73** shows a significant increase in affinity over the electron poor **74·74** for species such as CH_4, C_2H_6 and CH_3F. They also discovered that dimer **73·73** is converted to **74·74** in the presence of NO_2, thereby, providing a mechanism in which the amount of encapsulated guest can be controlled through the oxidation state of the dimer (figure III-3, table III-1).

	Ka (M^{-1})	
Guest	73·73	74·74
CH_4	70	10
C_2H_6	51	13
CH_3F	17	<0.3

Table III-1. *Association constants for the electron rich (73·73) and electron poor (74·74) tennis balls.*

While this first generation of self-assembling dimers provided excellent models in which to unravel the physical behaviors of such novel structures, their 'minimalist' topology limited their applications and the type of guests that could be used. A second generation of glycoluril based assemblies has involved the exploration of larger spacers.[9] Dimer **75·75** (figure

9   Valdés, C.; Spitz, U. P.; Kubik, S. K.; Rebek, J. Jr. *Angew. Chem. Int. Ed. Engl.* **1995**, *34*, 1885-1887. Valdés, C.; Spitz, U. P.;Toledo, L. M.; Kubik, S. K.; Rebek, J. Jr. *J. Am. Chem. Soc.* **1995**, *117*, 12733-12745. Garcías, X.; Toledo, L. M.; Rebek, J. Jr. *Tetrahedron Lett.* **1995**, *36*, 8535-8538.

III–4) is still a concave assembly with roughly a spherical cavity but the spacer between the glycoluril recognition surfaces is extended by six fused 6-membered rings. The dimeric species is so large that it readily accepts 1,3,5,7-tetramethyladamantane and ferrocenecarboxylic acid into its cavity.[10] In small solvents like $CDCl_3$ the ^{1}H NMR shows what appears to be ill-defined aggregates. Only after seeding with larger more suitable guests does dimer **75·75** form as a distinct assembly.

R=Ph, CO_2isopentyl

75
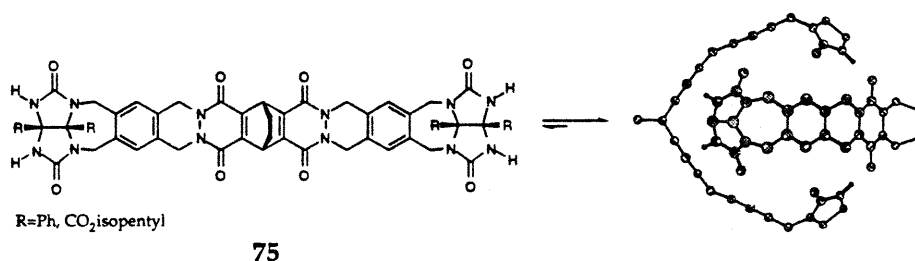
Figure III–4. *Self-assembly of the larger 'soft ball'.*

The production of **76** provides a system that offers eight additional hydrogen bonds in the dimer as compared to **75·75** (figure III–5).[11] The effect of doubling the number of hydrogen bonds is quickly seen in the ^{1}H NMR of **76**. It appears as a discrete dimeric assembly. Kang determined dimer **76·76** has two $CDCl_3$ solvent molecules present in its cavity. The addition of adamantane or several of its derivatives causes the expulsion of the two $CDCl_3$ molecules as the up-take of the new guests proceeds. Heating the mixture causes the equilibrium to favor the removal of the $CDCl_3$ from the interior cavity. This entropically driven behavior, though common in aqueous environments, is rarely seen in apolar solvents like $CDCl_3$. Preliminary results with this dimeric species suggest that it is quite efficient in catalyzing the Diels-Alder reaction of cyclohexadiene and *p*-quinone.[12]

---

[10] Meissner, R. S.; de Mendoza, J.; Rebek, J. Jr. *Science* **1995,** *270,* 1485-1488.

[11] Kang, J.; Rebek, J. Jr. *Nature* in press.

[12] Kang, J.; Rebek, J. Jr. *Science* in press.
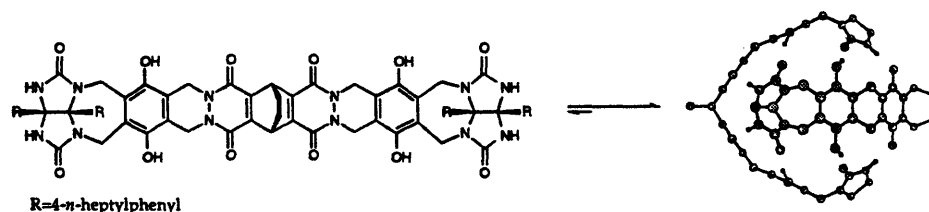
R=4-*n*-heptylphenyl

76

Figure III–5. *Phenolic groups provide eight additional hydrogen bonds to help form a discrete dimer in the 'soft ball' molecule.*

Another enlarged glycoluril derivative makes use of a novel C₃ triphenylene spacer (77, figure III–6).[13] The dimeric topology resembles that of a disc-shaped 'Jelly-Doughnut'. Flat disc-shaped guests such as benzene and cyclohexane are good complements to the cavities interior. The spherical solvent CDCl₃ is displaced rapidly by the addition of benzene, suggesting CDCl₃ is a poor match for the cavity. However when a disc-like solvent, *p*-xylene-d_{10}, is used it takes hours, after the addition of a favorable guest like cyclohexane, for the system to reach equilibrium. The prediction of such trends is difficult due to the novel behavior exhibited by these assemblies. Each cavity needs to be explored to determine its unique assembly and encapsulation properties.
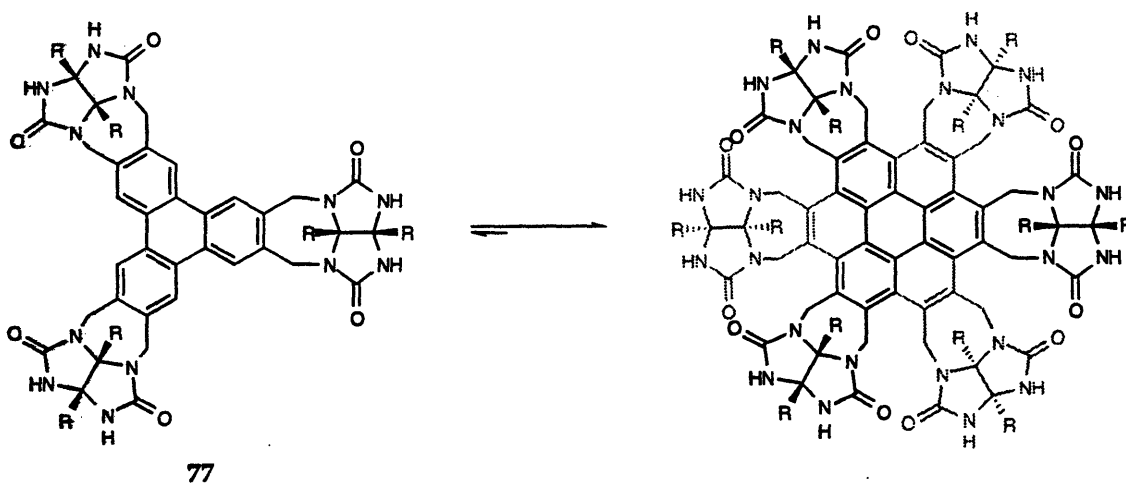
77

Figure III–6. *Self-assembling of the C₃ triphenylene 'Jelly Doughnut'.*

13 Grotzfeld, R. M.; Branda, N. Rebek, J. Jr. *Science* **1996**, *271*, 487–489.

Shinkai was first to report a self-assembling dimeric capsule using a calix[4]arene.[14] The system is a hetero-dimer that uses the strong interactions between a pyridine and a carboxylic acid to bring two 'upper' rim edges of the bowl-like calix[4]arenes together to form a football shaped cavity (figure III-7). While it is an elegant example of controlled assembly, the large holes in the central belt of the dimer mostly likely allow guests to move freely in-and-out of the cavity. Encapsulation with hetero dimer 78·79 has not been reported to date.

78   79
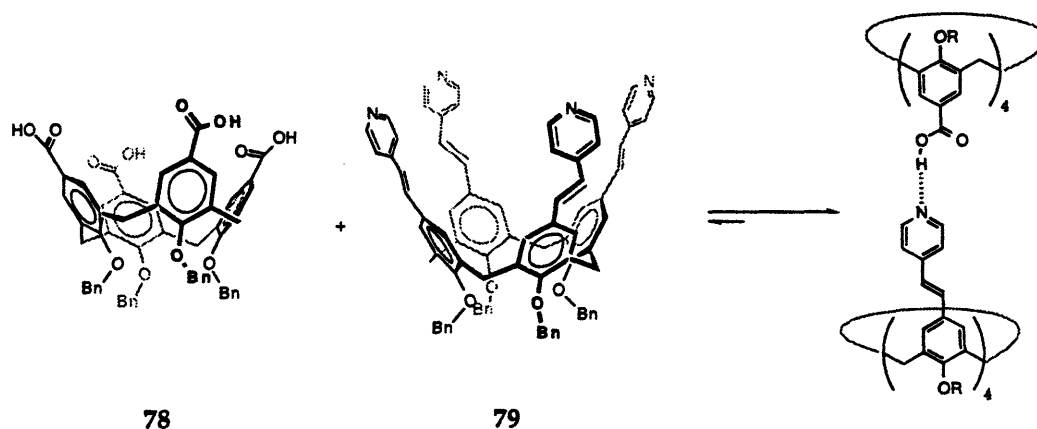
Figure III-7. *Self-assembly of a two component calix[4]arene.*

The first reported dimeric calix[4]arene (70·70) capable of encapsulation[1] inspired the reinvestigation of very similar tetraureido calix[4]arenes.[15,16] These compounds exhibit similar characteristics. The ^{1}H NMRs show all the attributes of a dimeric calix[4]arene species (details to be discussed in the following sections). Scheerder and Reinhoudt's studies of 80 revealed an intriguing allosteric effect.[16] If dimer 80·80 is subjected to $Na^+ClO_4^-$, the tetraester arrangement complexes the Na^+ ion and the dimer falls apart to give a monomeric species. Scheerder attributes the dissociation to the repulsive force between the two Na^+ ions, though they are separated by over 12 Å. Molecular modeling shows that complexation of the Na^+ ion in the

14 Koh, K.; Araki, K. Shinkia, S. *Tetrahedron lett.* 1994, *35*, 8255-8258.

15 Jakobi, R. A.; Böhmer, V.; Grüttner, C.; Kraft, D.; Vogt, W. *New J. Chem.* 1996, *20*, 493-501.

16 Scheerder, J. PhD Thesis, University Twente, 1995.

dimer causes the ether oxygens on the 'lower' rim to move apart to accommodate the Na^+ ion. This in turn produces a near cylindrical calix[4]arene and causes the R groups of the urea to crash into the complimentary calix[4]arene (figure III–8). It seems that this steric collision should be a significant contributor to the break-up of the dimer.
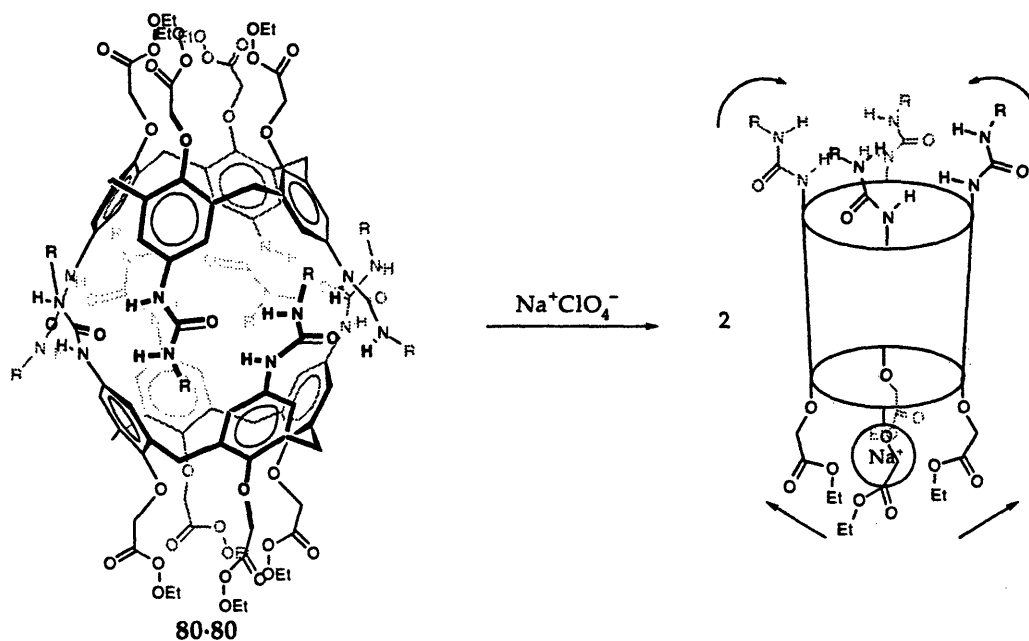
Figure III–8. *Disassembly of a tetraureido calix[4]arene due to complexation of a Na^+ ion.*

Design & Shape

Calixarenes[17] are synthesized from the condensation of *p*-alkyl phenol and formaldehyde.[18] Conditions can be adjusted to favor the formation of different sized species.[17] The product containing four units is most readily formed (figure III–9). The calixarene can access a variety of conformations and at room temperature the conversion between conformers is rapid. The

[17] For recent reviews see: *Calixarenes; Monographs in Supramolecular Chemistry*; Gutsche, C. D., Ed.; The Royal Society of Chemistry: Cambridge, 1989. Böhmer, V. *Angew. Chem., Int. Ed. Engl.* **1995**, *34*, 713-745. Böhmer, V. *Angew. Chem., Int. Ed. Engl.* **1995**, *34*, 713-745. Gutsche, C. D. *Aldrichimica Acta* **1995**, *28*, 3-9. Linnane, P.; Shinkai, S. *Chem. Ind.* **1994**, 811-814. *New J. Chem.* **1996**, *20*, (issue dedicated to calixarene chemistry).

[18] Gutsche C. D.; Iqbal, M. *Org. Syn.* **1990**, *68*, 234-237.

conversion of the cone conformer to the opposite cone conformer involves the hydroxyl groups passing through the annulus of the calixarene (figure III–9). The energy barrier for this conversion is about 14 Kcal/mol.[19]
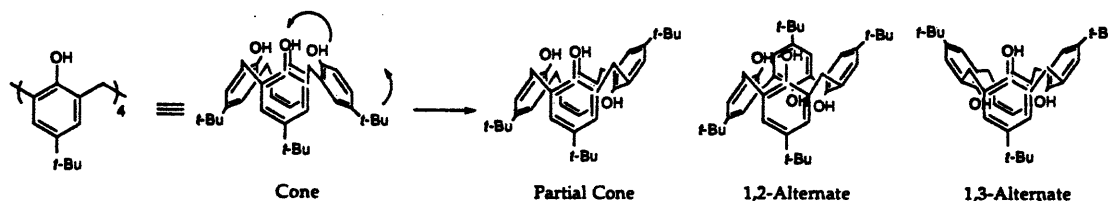
Figure III–9. *Calix[4]arene exist in four different conformations. Alkylation of the phenols can be used to isolate any of these conformers.*

Alkylations of the phenolic groups can freeze out the conformational exchanges. The desired conformer is obtained as a stable product simply by selecting the appropiate reaction conditions.[17] Synthesis and isolation of the cone conformer of a large number of calix[4]arene derivatives have been reported.[17] The combination of the calix[4]arenes rigid bowl-like cavity and its extensively explored functionalization chemistry make it an attractive tool for self-assembly studies.

Another useful tool in self-assembly is the urea. Ureas are easily prepared and their self-complementary structure is a necessary feature in the formation of homodimers. Solid state studies show ureas in head-to-tail hydrogen bonding in the formation of molecular sheets.[20] More importantly, in the history of encapsulation, ureas form helical structures that encapsulated aliphatic hydrocarbons.[21] A liquid hydrocarbon can be added to a saturated solution of urea in H_2O at room temperature. Crystals of the self-assembled ureas with the inclusion of the alkane soon form. The size of the helix can be controlled by the hydrocarbon being employed. Accordingly, a

---

[19] Gutsche C. D. *Calixarenes*, The Royal Society of Chemistry, Cambridge, England, 1989.

[20] Etter, M.; Urbañczyk-Lipkowska, Z.; Zia-Ebrahimi, M.; Panunto, T. W. *J. Am. Chem. Soc.* 1990, 112, 8415-8426. Etter, M. C. *Acc. Chem. Res.* 1990, 23, 120. Etter, M. C.; Panunto, T. W. *J. Am. Chem. Soc.* 1988, 110, 5896-5897.

[21] Schlenk, W. Jr.; *Ann. Chem.* 1949, 565, 204. Schlenk, W. Jr.; *Ann. Chem.* 1951, 573, 142. Schiessler, R. W.; Flitter, D. *J. Am. Chem. Soc.* 1952, 74, 1720. Smith, A. E. *J. Chem. Phys.* 1952, 18, 150.

small change in the angle of the urea hydrogen bonds can take the structure from a helix to a cylinder (figure III–10).
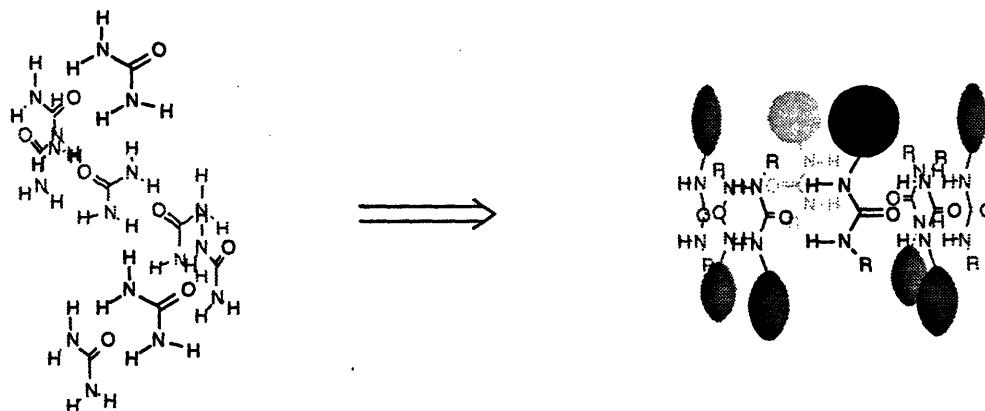
Figure III–10. *Ureas area known to assemble in helical and circular patterns.*

Design of molecular containers **70, 71** combines the structurally rigid bowl-shaped calix[4]arene with the self-complementary urea. Placing four ureas on the 'upper' rim of a calix[4]arene ideally spaces the ureas so that they do not interact intramolecularly. In fact they are exactly spaced to fit another urea between any two (figure III–11). This is the perfect setup for the self-assembly of a dimeric system, two halves each with four highly preorganized ureas on the upper rim of a rigid calix[4]arene bowl. The calix[4]arene dimeric species has certain advantages over other encapsulating hosts: 1) encapsulation is reversible, 2) the size of the guests are only limited by the size of the cavity 3) There are no 'holes' in the dimer that allow guests to filter in-and-out of the cavity and 4) it has good solubility properties and can be studied in a variety of solvents.
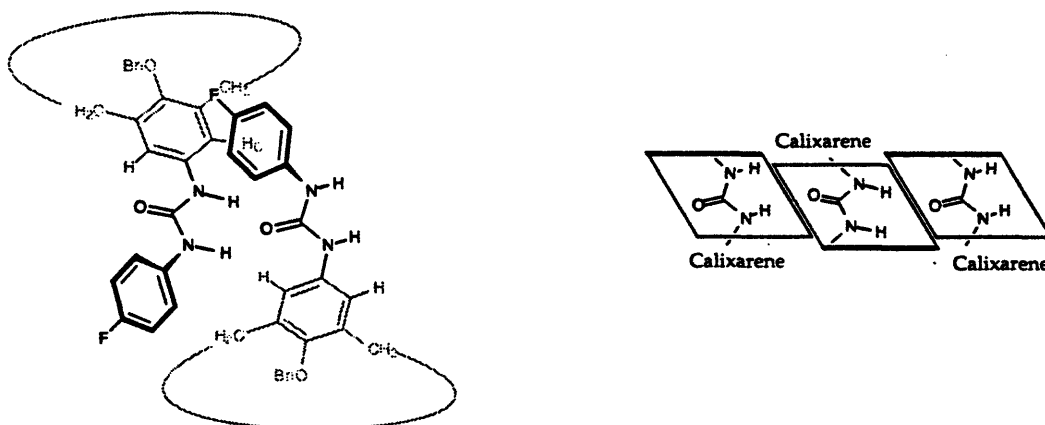
Figure III–11. *Head-to-tail arrangment of the ureas in the calix[4]arene dimer* **71·71**.

Synthesis

Functionalization of calix[4]arenes has been investigated extensively.[17] Using these well developed procedures, Shimizu developed a synthetic route to tetraurea calix[4]arene **70** (scheme III–1).[1] Ullman coupling of tetraiodo **82** with phthalimide will proceed in high yield if the reaction is heated in vigorously refluxing N-methylpyrolidinone (NMP B.P.=202.0 °C). It was found that yields dropped if the reflux was meek. It is also important not to purify products **83** and **84** via chromatography. A substantially greater amount of final product is obtained if purification is delayed until after tetraurea formation.
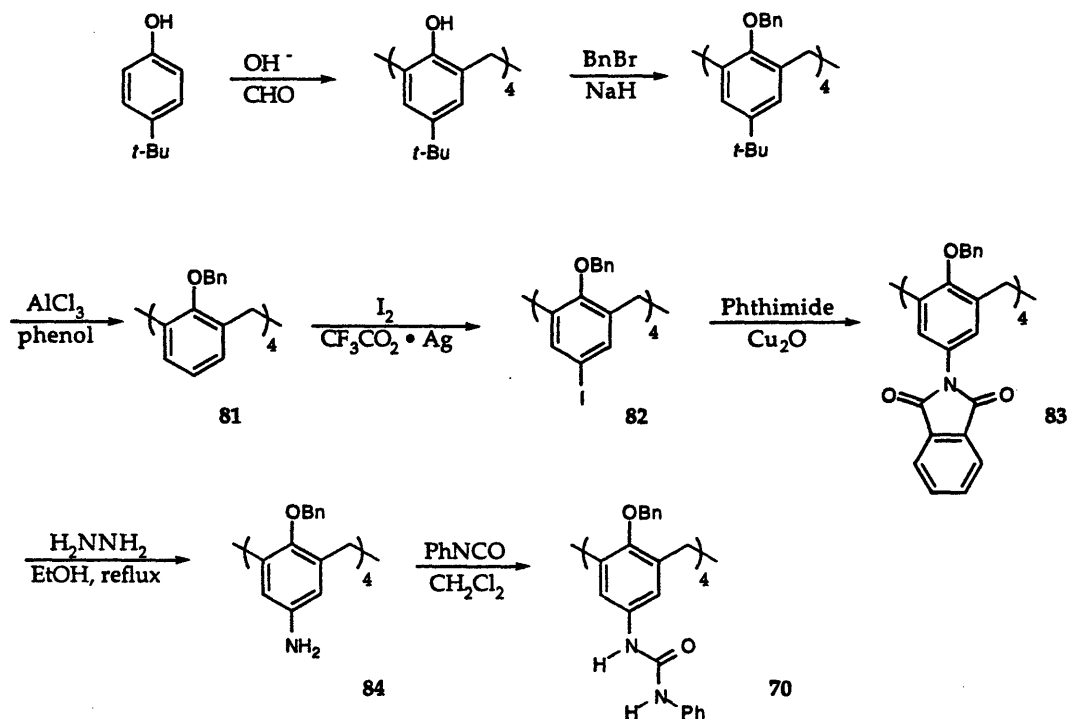
Scheme III-1. *Synthesis of tetraureido calix[4]arene via a phthalimide.*

An alternative synthesis was developed that is one step shorter and avoids formation of products that are difficult to purify. This procedure involves selective tetranitration of calix[4]arene 81.[15] A reduction to the tetraamine 84 is carried out with Raney nickel and hydrazine in refluxing ethanol. As before, reaction with an isocyanate gives the tetraurea (scheme III-2).
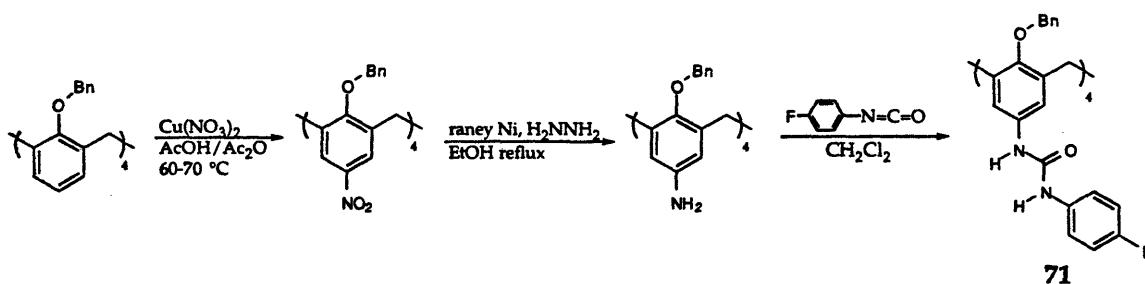
Scheme III-2. *Synthesis of tetraureido calix[4]arene via a nitro group.*

Assembly

Tetraurea calix[4]arene **71** is soluble in DMSO-d_6 and has a [^1]H NMR spectrum typical of most organic species: aromatics between 6.6 and 7.5 ppm, urea protons at 8.39 and 8.12 ppm, a singlet benzyl peak at 4.88 ppm and two different methylene protons at 4.14 and 2.84 ppm (figure III–12a). However if this same compound is dissolved in benzene-d_6, its [^1]H NMR shows two different aryl protons in the calix[4]arene (H_a and H_b). Another striking change is seen in the benzyl hydrogens on the 'lower' rim of the calix[4]arene. They have become non-equivalent and are coupled to one another (figure III–12b).[22] This is exactly the expected spectrum if there is a strongly bound dimer. In the dimer the rotation of the aryl–urea bond is frozen out. This places either H_a or H_b near the carbonyl of the urea and the other aryl proton next to the N–H. The ureas must all be pointing in the same direction. Any other arrangement will produce a more complicated spectrum.[1] Each half of the dimer is chiral and is bound to its mirror image. The dimer is mesomeric with S_8 symmetry. Additional evidence is found in the proton spectrum to support this conclusion. The eight sets of bridging methylene protons in the calix[4]arene remain as a simple AX quartet. Varying the concentration of the dimer **71·71** has no effect on the position of the urea proton resonances, unlike most ureas which are highly concentration dependent. The sharp peaks in the [^1]H NMR indicate a well defined dimeric species involving up to eight hydrogen bonded ureas.

---

[22] This behavior has been observed in similar systems, see ref. 1 & 16.
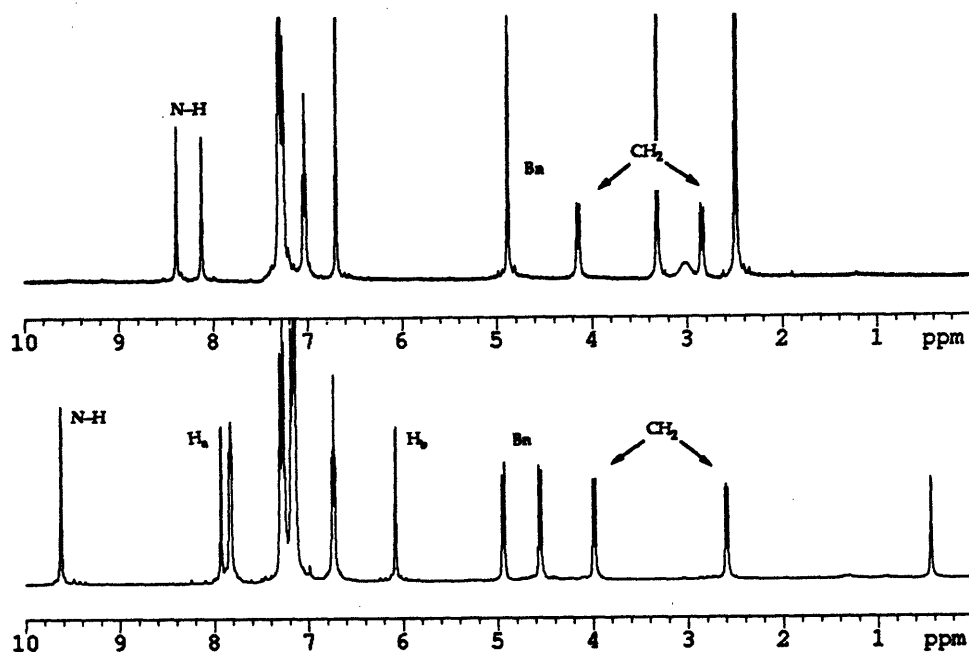
Figure III–12. ^1H *NMR of* **71** *in a) DMSO-d_6 and b) benzene-d_6.*

The dimer was exposed to an excess of a phenyl-α-phenyl ethyl urea derivative. This urea was able to 'denature' the assembly and give a ^1H NMR spectrum reminiscent of **71** in DMSO-d_6 (figure III–13). In addition to ^1H NMR, mass spectrometry also supports the presence of a self-assembled dimeric species.[1] However the most convincing evidence for the formation of a molecular container is found in encapsulation studies.
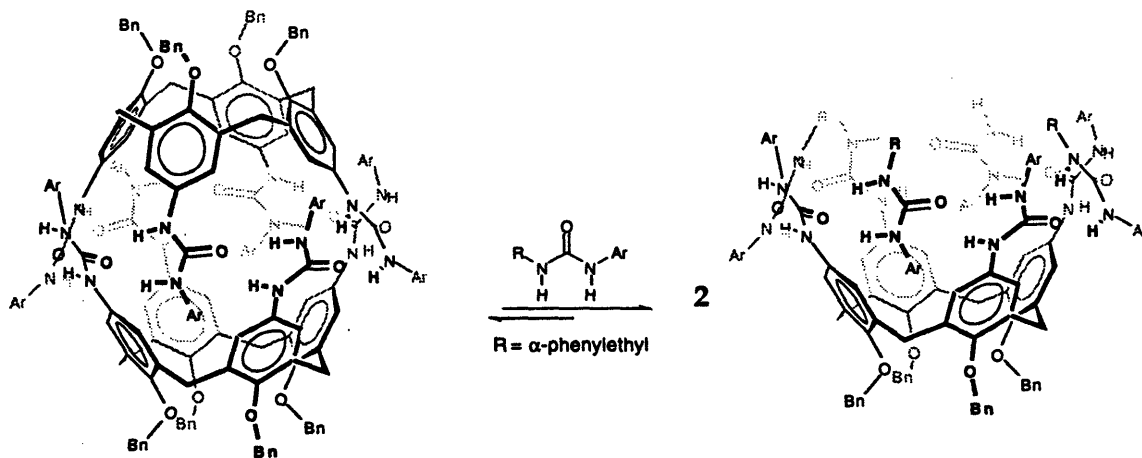
Figure III–13. *The 'denaturing' of the dimeric assembly by a urea.*

Encapsulation

The main force driving encapsulation is based on size complementarity. Therefore the solvent in which to conduct encapsulation studies is one that is non-polar enough to permit dimerization and is a poor fit in the newly created cavity. Just as recognition studies of hydrogen bond formation depend on solvent polarity, encapsulation studies depend on the size of the solvent. Ethylbenzene and *p*-xylene were determined to be excellent solvents to conduct encapsulation studies with calix[4]arene dimer **71·71**.

A convenient method was devised for estimating the volume of a cavity using MacroModel.[23] It involves calculating the volume, using MacroModel, of the dimer both empty and completely filled with arbitrary stuffing. MacroModel does not count empty space or overlap of Van der Waals volumes. Therefore the difference between the empty and filled volumes is the volume of the cavity.

Extending this approach, we compared the percent of the cavity filled by 'good' guests to the percent of space that solvent molecules actually 'fill' in a given volume of solvent as calculated by MacroModel. First, a number of solvents were chosen and their Van der Waals (VDW) volumes calculated by MacroModel. The VDW volumes were then multiplied by the total number of molecules in a given volume of solvent (1 cm^3). This filled volume was divided by the original solvent volume (1 cm^3) to obtain the calculated fraction of filled space in a 1 cm^3 volume of solvent (table III–2). About 57% of the actual space in a given volume of solvent is occupied by the VDW volume. This number seems reasonable since the volume occupied by the average organic molecule in the solid state is about 65% as shown from X-ray crystallography.[24] A 'good' fitting guest seems to occupy ~40% of the cavity as calculated by MacroModel. This is not to imply that these numbers are meant to necessarily have real physical meaning. This is only a convention used in

---

[23] Hamann, B. C.; Shimizu, K. D.; Rebek, J. *Angew. Chem.* **1996**, in press.

[24] Kataigorodskii, V.I. *Molecular Crystals and Molecules* (New York: Academic press, 1973).

conjunction with MacroModel to help predict what molecules may be suitable guests for encapsulation studies.

Solvent	% Filled	vdw Vol. ($\mathring{A}^3$)	Total Vol. ($\mathring{A}^3$)	Mol. Wt. (g/mol)	Density (g/mL)
Chloroform	57.0	75.7	5.698×10^{23}	119.38	1.492
p-Xylene	57.3	116.6	5.726×10^{23}	106.17	0.866
Toluene	56.4	99.6	5.645×10^{23}	92.14	0.867
Benzene	56.2	83.4	5.601×10^{23}	78.11	0.874
Methanol	56.1	37.7	5.606×10^{23}	32.04	0.791
Cyclohexane	56.6	101.6	5.664×10^{23}	84.16	0.779

Table III-2. *Calculated values for the MacroModel estimation for the VDW occupied volume of selected solvents in the liquid phase.*

The first sign of an encapsulated guest came when Shimizu observed two distinct dimeric assembles in toluene-d_8 and benzene-d_6 solvent mixtures.[1] He also detected direct evidence in the ^{19}F NMR of encapsulated monofluorobezene. The appearance of a new peak in the presence of dimer 70·70 suggested that the guest was inside.[1] Since then similar experiments were carried out with fluorinated calix[4]arene dimer 71·71. Once again a new encapsulated fluorobenzene peak appeared next to the free species and integrated as a 1:1 complex with the host (figure III-14). The host peak remained unchanged in the ^{19}F NMR but a number of changes were seen in the ^1H NMR. This is not surprising since the fluorines in dimer 71·71 are shielded from the interior of the cavity.
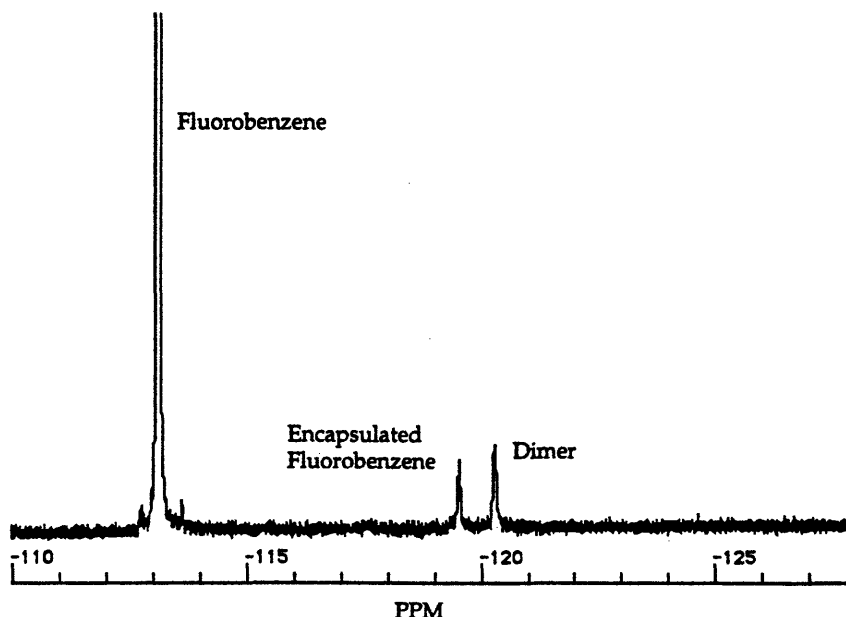
Figure III–14. ^{19}F *NMR showing separate signals for encapsulated and free fluoro benzene.*

Most importantly for the first time we could see the encapsulated guest in the ^1H NMR. There were three new resonances for the encapsulated fluorobenzene, one for each the *ortho, meta* and *para* positions. All of the peaks move upfield upon encapsulation. The resonance for the *para* proton is not shifted upfield nearly as much as the resonances for the *ortho* and *meta* positions. This strongly suggests a particular orientation of the guest is favored within the cavity. We predict an orientation where the fluorine is in the plane of the urea 'zipper'. This places the *ortho* and *meta* protons in the face of the π surface of the calix[4]arene aromatics and the *para* proton in the less deshielding urea surface (figure III–15).
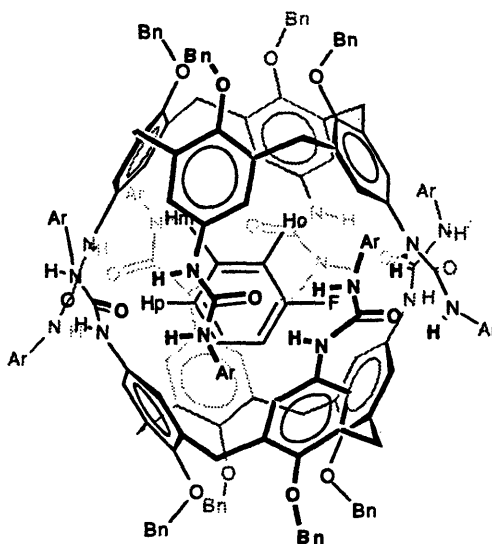
Figure III–15. *The preferred orientation of* **71·71**
encapsulated fluorobenzene.
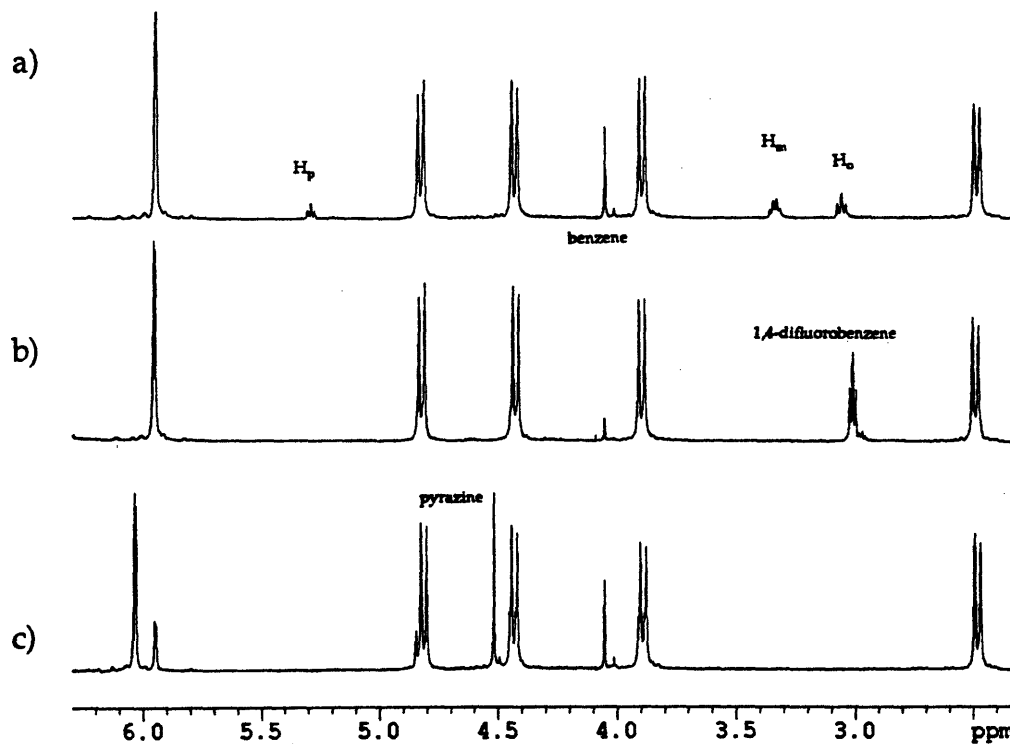
Figure III–16. *¹H NMR of dimer* **71·71** *with encapsulated benzene and*
a) fluorobenzene, b) pyrazine and c) pyrizine.

Free and encapsulated guests appear as distinct species since encapsulation by the tetraurea calix[4]arene is slow on the NMR time scale. In fact, it may take several days for equilibrium to be reached depending on the nature of the solvent and guest being studied. Benzene was added in excess to a solution of calix[4]arene 71 in p-xylene-d_{10}. Using ^{1}H NMR, the appearance of encapsulated benzene was monitored over the course of 40 minutes. The rate of benzene up-take is found from the equation for first order reversible reaction (equation 1). The half-life was determined to be about 8 minutes. Benzene-d_6 was added, equal to the amount of proteo species. Again the rate of exchange is calculated from equation 1 and the half-life found to be approximately 100 minutes. Two assumptions were made for the determination of the rates of benzene up-take and release from calix[4]arene 71·71. First, there is no significant encapsulation selectivity between the proteo and deutero benzenes. This assumption seems valid since at equilibrium, half of the encapsulated proteo-benzene disappeared. Secondly, it was assumed that dimer 71·71 was always saturated with benzene, either proteo or deutero, and p-xylene-d_{10} encapsulated 71·71 was not present in any significant quantity.

$$A \; \underset{k_{-1}}{\overset{k_1}{\rightleftharpoons}} \; B$$
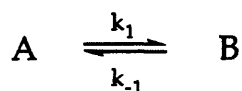
$$\ln \frac{[A]_0 - [A]_e}{[A]_t - [A]_e} = kt \qquad\qquad\qquad \text{eq. 1}$$

Where $[A]_0$ is the initial dimer concentration, $[A]_e$ is benzene($-d_6$) encapsualted dimer concentration at equilibrium and $[A]_t$ is the encapsulated dimer concentration at time t.

An association constant was obtained for benzene and dimer 71·71 simply by mixing 5.989 mM of 71 with 21.94 mM benzene in p-xylene-d_{10}. Integration of the ^{1}H NMR gave the ratio of p-xylene-d_{10} to benzene encapsulated 71·71. An association constant of 230 M^{-1} was calculated from this data using equations 2–5.

$$K_a = \frac{[HG]}{[H]_f[G]_f} \qquad \text{eq. 2}$$

$$[G]_f = [G]_T - [HG] \qquad \text{eq. 3}$$

$$[HG] = X[H]_T \qquad \text{eq. 4}$$

$$[H]_f = (100 - X)[H]_T \qquad \text{eq. 5}$$

Where $[H]_f$ and $[G]_f$ are the free host and guest concentrations and $[HG]$ is the concentration of the encapsulated complex at equilibrium. X is the % of encapsulated complex present as determined by ^1H NMR integration.

The data from the benzene studies provides a good reference point from which other aromatic guests can be compared. Therefore a series of competition studies were undertaken where equal molar quantities of benzene and another guest were added to a solution of dimer 71·71 in *p*-xylene-d_{10}. The benzene/guests mixtures were in excess relative to the host. The results are listed in table III-3.

Guest	Affinity		Guest	Affinity	
	25°C	50°C		25°C	50°C
C_6H_6	1.0	0.82	$C_6H_5CH_3$	<0.1	<0.1
C_6H_5F	2.6	2.5	C_6H_5OH	0.83	1.2[a]
p-$C_6H_4F_2$	5.8	6.9	$C_6H_5NH_2$	0.32	0.39
C_6H_5Cl	0.30	0.55	pyrazine	3.2	3.0
C_6H_5Br	0	0	pyridine	1.2	1.1

Table III-3. *Relative affinities of dimer (2.94x10⁻³M) for guests (21.9x10⁻³M) in competition experiments with benzene (21.9x10⁻³M). a) A precipitate formed after several hours.*

The cavity is quite size selective. Fluorobenzene is an excellent guest but chlorobenzene is barely bound and bromobenzene was completely unchanged. Toluene is a poor guest relative to benzene yet the similarly shaped aniline and phenol are quite competitive. This suggests there is some additional favorable interactions between the guests and the interior of the cavity. Strong affinity is also seen with pyridine and pyrazine, again implying

additional hydrogen bonded stabilizing interactions. As mentioned earlier guests seem to favor a particular orientation within the cavity. Typically hydrogen bond donor or acceptor sites prefer to lie in the plane of the urea belt, directing the *ortho* and *meta* positioned protons of the guests into the π faces of the calix[4]arene. This is supported by the large upfield shifts of these protons relative to the *para* positioned proton.

A number of potential guests, capable of forming hydrogen bonds, were mixed with 71·71 in *p*-xylene-d_{10} (figure III–17). Unfortunately, upon doing so the host precipitated from solution. It is likely that the guests disrupt the dimer's ability to self-assemble. Formation monomeric 71 exposes the highly polar tetraurea surface, ill-defined aggregates form and the species falls out of solution.

formamide formic acid imidazole L-Ascorbic Acid Squaric Acid $Bu_4N^{(+)}PF_6^{(-)}$
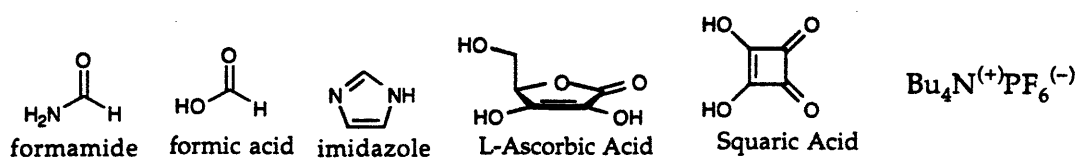
Figure III–17. *Guests that caused dimer 71·71 to precipitate from solution (p-Xylene-d_{10}) upon mixing.*

Hydrocarbon guests with more of a '3-dimensional' shape were used to investigate the cavity of dimer 71·71.[25] Cubane, cyclohexane and *n*-pentane were all found to be suitable guests. *n*-Hexane and norbornylene were only moderately attracted to the interior while no inclusion of *o*-carborane was seen. The cavity not only restricts the translational motion of the guests but the rotational freedom of some guests seems to be limited as well. Cubane with its highly organized, rigid *eight* carbon frame is easily accomodated by calix[4]arene 71·71, yet the floppy *six* carbon structure of *n*-hexane is only reluctantly accepted. As expected, the more preorganized cyclohexane was found to have a greater affinity for the interior of 71·71 than did *n*-hexane. Encapsulated cubane and cyclohexane show a sharp singlet at 1.59 ppm and –1.1 ppm, respectively in the ^{1}H NMR. Therefore, these guests must be rotating rapidly within the cavity relative to the NMR time scale.

---

[25] ^{1}H NMR spectra of encapsulated guests can be found in appendix B.

Low temperature studies show that certain guest conformations may be stabilized within the cavity. Three separate studies were conducted with 71·71 and cyclohexane, tetrahydropyran or 1,4-dioxane in toluene-d_8. Calix[4]arene 71·71 was saturated with guest and the sample cooled. Using ^{1}H NMR the coalescent temperatures for the free and encapsulated guests were determined. In each study, the axial and equatorial protons could be clearly seen and the final distance between these two peaks determined (Δv).[27] This data combined with equations 7–8 gave a $\Delta G^{\ddagger}$ value for the chair-chair inversion (table III–4).[26] Although there seems to be an increase in the energy required for a chair-chair inversion for bound species, the differences are small and are near or within experimental error.[26] Guests, such as 1,4 cyclohexanediol or piperazine, capable of forming stronger hydrogen bonds than 1,4-dioxane with the interior of the cavity may be required to see energy differences outside the range of experimental error.

26 Friebolin, H. *Basic One- and Two-Dimensional NMR Spectroscopy* VCH, Weinheim, Germany, 2nd Ed., 1993. Errors in $\Delta G^{\ddagger}$ have been estimated at ±0.4 Kcal/mol.

	Guests		
	Cyclohexane	Tetrahydropyran	1,4-Dioxane
Δv (Hz) Bound	49.81	203.3	339.4
T_c (°K) Bound	223	229	237
$\Delta G^{\ddagger}$ Bound[26] (Kcal/mol)	10.8	10.4	10.7
Δv (Hz) Free	250.0	203.6	—[27]
T_c (°K) Free	231	214	—
$\Delta G^{\ddagger}$ Free[26] (Kcal/mol)	10.5	9.8	9.4
$\Delta G^{\ddagger}$ Lit. Value (Kcal/mol)	10.3[28]	9.4[29]	9.4[30]
Volume VDW (Å^3)[31]	101.6	94.0	87.0

Table III–4. *Measured data for the energy barrier of chair-chair inversions of free and bound six membered ring guests.*

$$k = X\frac{k_BT}{h}e^{-\Delta G_c^{\ddagger}/RT}$$

eq. 6

Where k_B = Boltzmann constant = 3.2995×10^{24} cal·K^{-1}
X = transmission coefficient = 1
h = Planck constant = 1.5836×10^{-34}

Equation 6 simplfies to

$$\Delta G_c^{\ddagger} = 4.58T_c\left(10.32 + \log\frac{T_c}{k_c}\right)\text{cal} \bullet \text{mol}^{-1}$$

eq. 7

Where T_c is the coalesance temperature and k_c is the rate constant at this temperature and is determined from equation 8.

---

[27] In the case of free 1,4-dioxane the final peak separation (Δv) could not be obtained due to the need for extremely low temperatures.

[28] Anet, F.A. L.; Bourn, A. J. R. *J. Am. Chem. Soc.* **1967**, *89*, 760.

[29] Lambert, J. B.; Keske, R. G.; Weary, D. K. *J. Am. Chem. Soc.* **1967**, *89*, 5921.

[30] Anet, F.A. L.; Sandstrom, J. *Chem Comm.* **1971**, 1558.

[31] See ref. 33, chapter II.

$$k_c = \frac{\pi \Delta v}{\sqrt{2}} = 2.22 \Delta v \qquad\qquad\qquad\qquad \text{eq. 8}$$

Where Δv is the is the separation (Hz) of two signals in the absence of exchange.

Catalysis

The apparent conformational preferences displayed by guests lead us to believe that dimer 71·71 would be useful in catalyzing reactions in which the transition state was similar to that of the cyclohexane chair conformation. The Claisen rearrangement of allyl vinyl ether was chosen since the starting material was similar in size to n-hexane and the interior of the cavity will help to preorganize the substrate into a cyclic conformer (figure III-18).

Bound
Product
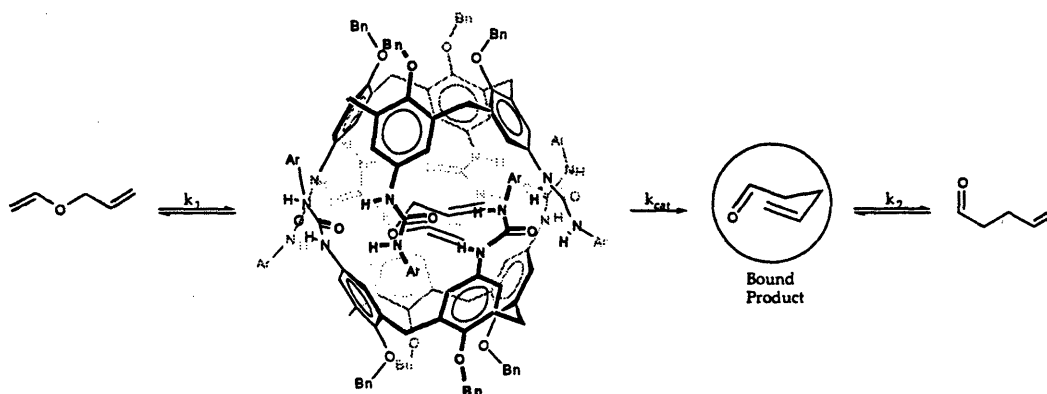
Figure III-18. *The proposed three step process for the 71·71 catalysis of a Claisen rearrangement.*

Allyl vinyl ether was first mixed with a solution of 71 in ethylbenzene d_{10}. The ^{1}H NMR showed that dimer 71·71 was capable of encapsulating the starting material (figure III-19). Next 4-pentenal, the rearrangement product, was mixed with the dimer in ethylbenzene-d_{10}. This time the ^{1}H NMR showed no evidence of encapsulated guest. Finally two solutions of the allyl vinyl ether were prepared in ethylbenzene-d_{10}, one of these solutions contained about 5% (mol/mol) of 71·71. The solutions were heated to 90 °C and the ^{1}H NMRs recorded over the course of several days. Both reactions showed clean conversion of the ether to the aldehyde and, by

integration, the reaction with catalyst present showed a marked increase in the rate of product formation. These results indicated that there is turnover of the catalyst and that product inhibition is not a significant factor.
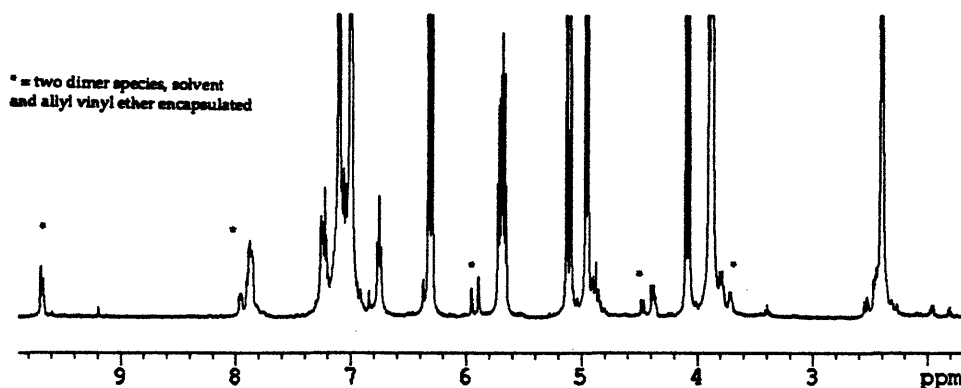
Figure III–19. ^1H *NMR spectra of encapsulated allyl vinyl ether.*

Kinetic measurements were made by following the disappearance of allyl vinyl ether using gas chromatography (GC). Solutions of allyl vinyl ether in ethylbenzene were prepared. Four trials contained varying amounts of dimer **71·71**, one control trial contained dimer **71·71** and excess benzene (a competitive inhibitor) and five control samples were of the background reaction. Each sample contained propylbenzene as internal standard for GC analysis. The reactions were heated to 90 °C and monitored though at least three half-lives. At this temperature it is likely that the rate of uptake of allyl vinyl ether (k_1) and product release (k_2) by the dimer would be much faster than rate of rearrangement (k_{cat}). However the rates of k_1 and k_2 have not been determined experimentally. Therefore only k_{obs} ($k_{obs}=k_1+k_{cat}+k_2$) will be reported here (figure III–20) although it is likely $k_{obs} \approx k_{cat}$.

K_{obs} (min^{-1})	mol % cata
3.65×10^{-4}	0.0
3.73×10^{-4}	0.25
4.66×10^{-4}	2.4
4.96×10^{-4}	3.6
5.20×10^{-4}	4.8
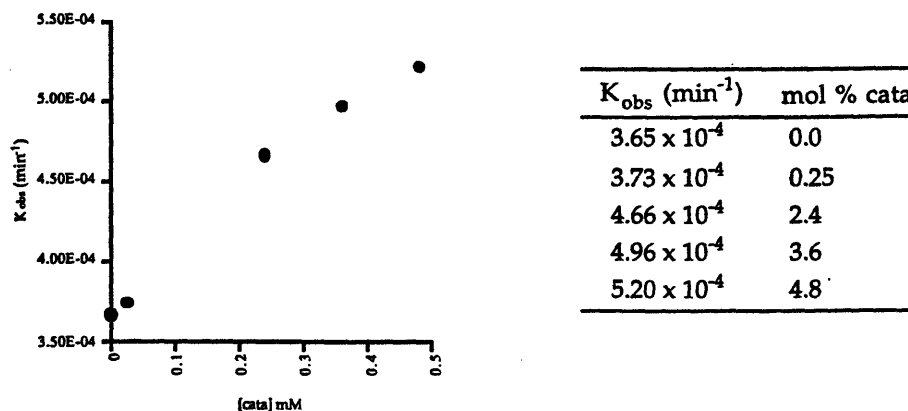
Figure III-20. *Data of the observed reaction rate (k_{obs}) as it relates to the mol % catalyst present.*

The control experiment in which benzene, with its higher binding affinity, was used as a competitive inhibitor showed a k_{obs}=3.1 x 10^{-4} min^{-1}. This is the same rate compared to the reaction without catalyst present, within experimental error.[32] Filling the cavity with benzene removes the availability of the dimer's interior and reveals that the reaction is catalyzed in the interior of the cavity and not simply by external contact with the tetraureido calix[4]arene. Current data show that **71·71** is an effective cage for the catalysis of the Claisen rearrangement of allyl vinyl ether.

Outlook

Additional kinetic and binding studies of allyl vinyl ether are needed to determine true rate of uptake (k_1) and product release (k_2). A saturation kinetics curve will also be necessary to unravel a complete picture of this catalyst.

Further investigations to probe the interior surface of the dimer would benefit from the use of guests capable of forming stronger hydrogen bonds. A series of low temperature ^{1}H NMR studies using cyclohexanol, cyclohexanediols and cyclohexanetriols may provide interesting answers to this question.

---

[32] Experimental error was estimated at ±10%.

One puzzling question still remains—why do moderately hydrogen bonding competitive solvents cause the dimer to break apart to monomer? Other dimeric self-assembling systems remain as the dimer despite the presence of DMF or DMSO in chloroform solutions.[7] These systems contain a healthy 12 hydrogen bonds in the dimeric assembly. The calix[4]arene **71** seems capable of forming 16 hydrogen bonds in the dimer. The rapid change from dimer to monomer with **71** implies that the hydrogen bonds are highly cooperative and disrupting a small portion of the assembly cause the collapse of the entire structure. Structural modifications at the 'lower' rim of the calix[4]arene may be key in forming a highly stable in dimer. Changes in the ether linkages on the 'lower' rim will change the shape of the calix[4]arene bowl, causing it to be either more cylindrical or diamond-shaped. This in turn will provide a different head-to-tail binding geometry for the ureas.

This basic calix[4]arene design will provide an interesting launching pad for further encapsulation and catalysis studies. Variations on the 'upper' and 'lower' rims will likely change the shape and selectivity of the cavity. A change in the number of calix[#]arene units can enlarge the cavity making possible the catalysis of bimolecular reactions.

Experimental

General

Reagent grade solvents were used except where noted. Methylene chloride was distilled from P_2O_5. Melting points were measured on an Electrothermal 9100 melting point apparatus. NMR spectra were taken on a Varian XL-300 (300 MHz) and a Bruker AC-250 (250 MHz) spectrometers. IR spectra were obtained on a Mattson Sygus 100 FT IR spectrometer. High resolution mass spectra were obtained on a Finnegan Mat 8200 instrument. Flash chromatography was performed using Silica Gel 60 (EM Science, 230–400 mesh). Molecular modeling experiments were performed on a Silicon Graphics Personal Iris using the MacroModel 3.5X program with Amber force field.

Encapsulation Studies

All encapsulation studies were performed on a Varian VXR (500 MHz) spectrometer equipped with Oxford VTC-4 temperature controllers. The deuterated solvents were dried over 4Å molecular sieves. Analytical grade A volumetric flasks and syringes were used throughout the preparation of the solutions. Solutions in which equilibrium values were determined were always re-checked after standing at room temperature for ~24 hours.

Competition studies were conducted by preparing a 5.989 mM solution of 71 (monomeric) in p-xylene-d_{10}. Benzene (500 µL) was mixed with equal molar quantities of competing guests, 10 µL of this mixture was diluted with 90 µL of p-xylene-d_{10}. Next, 10 µL of the p-xylene-d_{10} diluted solutions were mixed with 500 µL of the calix[4]arene (71·71) solution in an NMR tube to give a final sample that contained 2.936 mM 71·71, and 10.97 equivalents of benzene and the competing guests. The NMR tubes were capped and heated to 60 °C for six hour to equilibrate the samples. The samples were re-checked 24 hours latter to ensure equilibrium had been reached.

Low temperature ^{1}H NMR studies were conducted using 1–3 mM dimer concentrations and 5 µL of the encapsulated species. The samples were heated overnight at 60 °C to ensure equilibrium—the dimer 71·71 was not necessarily saturated with guest. The solutions were then cooled in a Varian VXR (500 MHz) spectrometer equipped with Oxford VTC-4 temperature controller. The temperature was lowered by 10 °C increments and equilibrated for 10 minutes before another temperature change was made. One degree temperature changes were made near the coalescence temperatures.

Kinetics

A Hewlett Packard 5890 Gas Chromatograph was used to monitor the formation of 4-pentenal and disappearance of allyl vinyl ether. One each of the catalyzed and background reactions were monitored using a Varian VXR (500 MHz) spectrometer equipped with Oxford VTC-4 temperature controller. Both ^{1}H NMR and GC peak were matched to known samples of both starting material and product. Peak areas were calculated using a Hewlett Packard

3396A integrator. Propyl benzene (7.17 mM) was used as the internal standard. The reactions were run at 90 °C in a 14 L constant temperature oil bath. Initial concentrations of allyl vinyl ether were 9.57 mM while the concentration of monomeric catalyst was varied between 0.05 mM and 1.0 mM. Reagent grade ethylbenzene was purified according the literature procedures.[33] Grade A analytical glassware was used to prepare solutions. The data was fit to the appropriate kinetic equation using Cricket Graph for the Macintosh.

A typical kinetic run was conducted as follows. Allyl vinyl ether (10 µL) was placed in a 1 mL volumetric flask with 10 µL of propylbenzene and diluted to the mark with ethylbenzene to give a solution 0.957 M in allyl vinyl ether and 0.0717 M in propylbenzene. The dimer **71·71** stock solution was prepared by placing 13.33 mg of **71** in 2 mL volumetric flask and diluted with ethylbenzene. 100 µL of the ether stock solution was added to a 1 mL volumetric flask with 150 µL of dimer **71·71** solution and diluted to the mark with ethylbenzene to give a final solution that is 7.17 mM in propylbenzene (internal standard), 9.57 mM in substrate (allyl vinyl ether), and 0.359 mM in catalysts (dimer **71·71**). The reaction was quickly transferred to a Waters 1 1/2 dram sample vial (part no. 72710) fitted with a Waters self sealing septum (part no. 22861) and placed in a 14 L constant temperature oil bath. Aliquots (1 µL) were withdraw via 10 µL microsyringe and injected into a Hewlett Packard 5890 G.C. to monitor the disappearance for allyl vinyl ether (figure III-20).

---

[33] Perrin, D. D.; Armarego, W. L. F.; Perrin, D. R. *Purification of Laboratory Chemicals* 2 Ed., Pergamon Press, 1980.
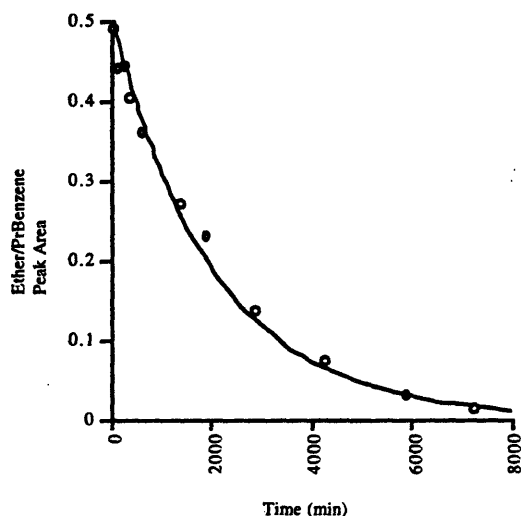
Figure III–20. *Plot of the ratio of allyl vinyl ether/propyl benzene peak areas versus concentration of dimer* **71·71.**

Synthesis & Characterization

Cone-conformer of 4,4',4'',4'''-tetranitro-O,O',O'',O'''-tetrabenzylcalix[4]arene: The cone-conformer of O,O',O'',O'''-tetraoctylcalix[4]arene (1.7103 g, 2.179 mmol) was heated to 60 °C in acetic acid (5 mL)/acetic anhydride (10 mL) with $Cu(NO_3)_2 \cdot 3H_2O$ (2.632 g, 10.89 mmol) for 3 hours. The crude reaction was poured into H_2O (200 mL) and the precipitate filtered. The solids were washed with water, dilute NH_4OH and more H_2O. They were then dried and purified by column chromatography using 100% CH_2Cl_2 as the eluent. Yield=80%; mp 219.5 °C; ^1H NMR ($CDCl_3$) δ 7.48-7.19(Ar, 28H), 5.04(s, 8H), 4.13(d, J=14.1Hz, 4H), 2.99(d, J=14.2Hz, 4H); HRMS (FAB, 3-nitrobenzyl alcohol) calcd for $C_{84}H_{68}F_4N_8O_8$ (M + H), 965.30337; found, 965.30356.

Cone-conformer of 4,4',4'',4'''-tetraamino-O,O',O'',O'''-tetrabenzylcalix[4]arene: The cone-conformer of 4,4',4'',4'''-tetranitro-O,O',O'',O'''-tetrabenzylcalix[4]arene (0.912 g, 0.945 mmol) was suspended in

EtOH (30 mL) with an excess of Raney nickel. The reaction was heated to reflux and excess hydrazine (~1 mL) was added in portions via pipet. After two hours the starting material had disappeared (by TLC). The reaction was cooled, filtered through celite and the celite washed with THF. The filtrate was concentrated to give a crude product that corresponded (TLC and ^{1}H NMR) to the previously reported desired product.[1] The tetraamine was carried on without further purification.

Cone-conformer of 4,4',4'',4'''-tetrakis(*p*-fluorophenyl urea)-O,O',O'',O'''-tetrabenzylcalix[4]arene : The crude cone-conformer of 4,4',4'',4'''-tetraamino-O,O',O'',O'''-tetrabenzylcalix[4]arene was dissolved in CH_2Cl_2 with *p*-flourophenyl isocyanate (0.54 mL, 4.73 mmol) at room temperature under Ar. After 12 hours MeOH (50 mL) was added and the reaction stirred for an additional hour. The product was purified by column chromatography using 13% EtOAc/CH_2Cl_2→15% EtOAc/CH_2Cl_2 as the eluent. mp 190 °C dec; ^{1}H NMR (CDCl$_3$) δ 9.23(s, 4H), 7.73-7.02(Ar, 24H), 5.70(s, 4H), 4.81(d, J=11.7Hz, 4H), 4.37(d, J=11.7Hz, 4H), 3.60(d, J=12.3Hz, 4H), 2.20(d, J=12.6Hz, 4H); ^{13}C NMR (CDCl$_3$) δ 154.2, 149.6, 137.4, 136.6, 135.1, 133.2, 129.4, 127.9, 119.4, 119.3, 119.2, 116.7, 116.5, 116.2, 116.0; HRMS (FAB, 3-nitrobenzyl alcohol) calcd for $C_{84}H_{68}F_4N_8O_8$ (M + H), 1393.5174; found, 1393.5172.

Chapter IV

Studies Toward the Pre-biotic Origins of the Translational Code

Introduction

The pre-biotic origins of the translational code were investigated using simple monomeric units of both amino acids and ribonucleosides. The stability of these 2'O-ribonucleosides towards solvolysis was measured through the use of HPLC. The rates of solvolysis of many different amino acid–ribonucleoside pairs were compared to determine if any possible coding scheme was present. The current data suggest no such pattern.
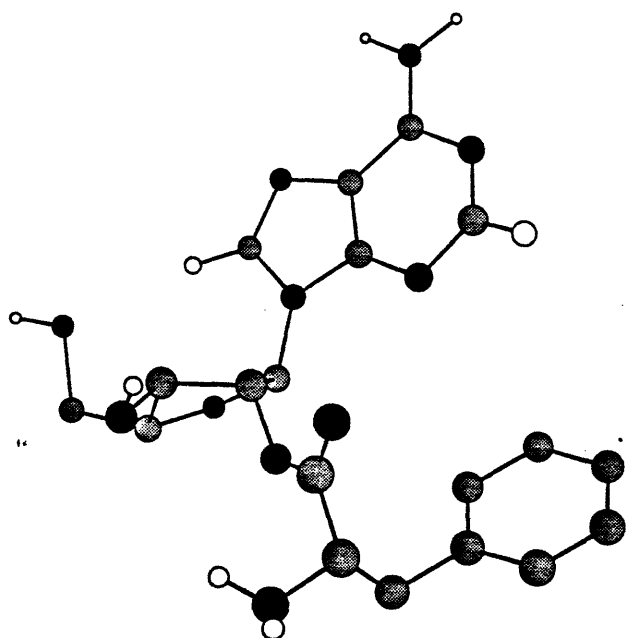
2'O-phenylalanine adenosine

Background

Attempts to develop an understanding of the origins of life are necessarily focused on one chemical aspect which makes life possible—catalysis. These catalytic processes can be divided into two main functions essential for life, replication of genetic information and all enzymatic processes that support replication, directly or indirectly. Modern DNA replication relies completely on the work of proteins not only for their supporting role in building and maintaining the local environment (the cell) but also in the replication process itself. Of course the information preserved in replicating (ribo)nucleosides is in turn responsible for the coding of these very same enzymes. This synergetic relationship begs the question how did it develop? Four probable theories are summarized by Orgel.[1]

1. Early functional proteins replicated directly. They 'invented' nucleic acids and were ultimately enslaved by them.

2. Early nucleic acids or related molecules replicated directly. They 'invented' protein synthesis. Unencoded polypeptides may or may not have been involved in the earliest precoding replication mechanism.

3. Nucleic acid replication and genetic coding of proteins coevolved.

4. The first form of life on the earth was based on some inorganic or organic system unrelated to proteins or nucleic acids...The early system 'invented' the nucleic acid/protein system, or a precursor of it.

---

1   Orgel, L. E. "Evolution of the genetic Apparatus: A Review" *Cold Spring Harbor Symposia on Quantitative Biology,* 1987, 52, 9–16.

Whatever scenario one considers, the question of coding must still be addressed. How did the current system of mRNA providing a coded template—where tRNA binds and delivers a specific amino acid for peptide bond formation—develop? In order to answer this question we first need to assume that current living systems evolved from simpler ones (*e.g.* small oligomers as opposed to the current large biopolymers of ribonuleosides and amino acids). It also follows that these systems should be composed of simple monomeric units that were available in the 'primordial soup'. In the 1950's Miller demonstrated that an environment similar to that believed to be present on the pre-biotic earth could give rise to the building blocks of modern life. Prolonged exposure of NH_3, HCN, H_2O and formaldehyde to heat and electrical discharge produced amino acids and nucleotides.[2] Subsequent investigations have also demonstrated the possible pre-biotic synthesis of ribose.[3] Since these monomeric building blocks of life are used today in living systems and were shown to likely exist in the 'primordial soup', it is reasonable to suppose an early coding system developed directly from ribonucleosides and aminoacids.

Ribonucleosides and amino acids have two features in common, a variable region and a non-varied backbone (figure IV–1). The variable region in a ribonucleoside is a purine or pyrimidine base. It is this fragment which contains the unique piece of information in that monomeric unit. Likewise the variable units in amino acids (the side chains) give rise to their different monomers.

[2] Miller, S. L.; Orgel L. E. *The Origins of Life on the Earth*, 1974; Prentice Hall, Engelwood Cliffs, New Jersey.

[3] Echenmoser, A. *Origins Life*, 1994, 24, 389.

Non-Variable Backbones   Variable Regions
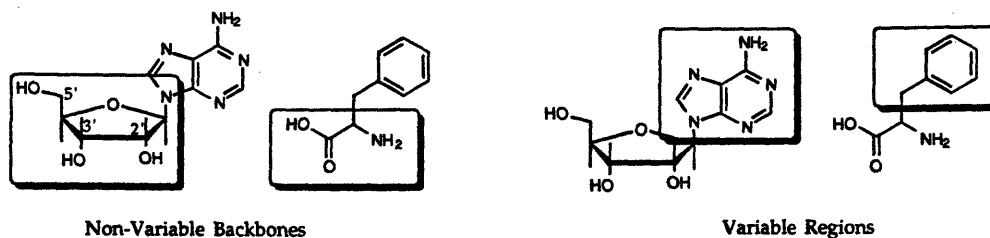
Figure IV-1. *Comparison of the conserved and varible regions in amino acids and ribonucleosides.*

Successful information transfer, a form of molecular recognition, between a ribonucleoside base and amino acid side chain requires that they be spatially close to one another. An obvious means to bring these units together is to link them covalently. The ribose provides three possible points of attachment, the 2', 3' and 5' hydroxyl groups. The amino acid has one point of attachment to offer, the carboxylic acid. Modeling the possible ester linkages between the amino acid and ribonucleoside show that only the 2' and 5' hydroxy esters bring the side chain near the purine or the pyrimidine base. If we further consider a small oligo-ribonucleoside linked together through 3'-5' phosphate esters it becomes clear that the only remaining point of attachment for amino acids is the 2'-hydroxyl group of the ribose (figure IV-2).
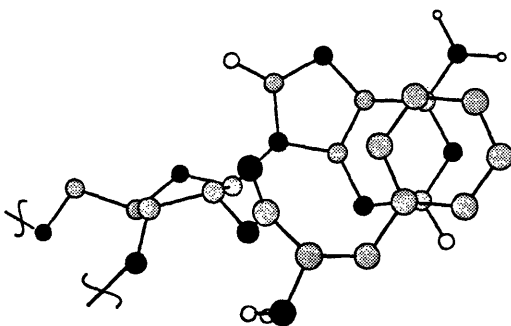
Figure IV-2. *2'O-phenylalanine adenosine*

Studies by Usher[4] and Lacey[5] show stereoselective aminoacylation of activated amino acids occurs at the 2'-hydroxyl position of a ribonucleoside. Conversely we were interested in comparing the relative stabilities of the ester linkage in amino esters of ribonucleosides. Differences in ester bond stabilities (either as more or less stable) due to specific side chain pairing with a particular base may provide a foundation on which the genetic code could be built.

Investigation of this hypothesis involved simple ester adducts of monomeric amino acids and nucleosides. Ester linkages through the 2' hydroxyl of the ribose allowed for close contact of the side chains with the purine and pyrimidine bases. The 3' and 5' hydroxyl groups have been blocked to prevent intramolecular aminoacyl migrations.

Synthesis

2'O-aminoacylated ribonucleosides are prepared by first blocking the 3' and 5' hydroxyls of the ribose. This prevents aminoacyl migration of the 2' ester and helps solubilize the molecules in apolar solvents. This is accomplished by the use of 1,3-dichloro-1,1,3,3-tetraisopropyldisiloxane (scheme IV-1).[6] Protection of the exocyclic nitrogen of adenosine can be carried out with o-nitrophenyl sulfenyl chloride (NPS-Cl).[7] This approach was tried with cytidine, but gave disappointing results, as did attempts to protect cytidine with BOC-ON in CH_2Cl_2. In the case of adenosine coupling conditions were found such that there is no need for this protection. The protection of the exocyclic nitrogen of cytidine can be carried out with 9-fluorenylmethyl chloroformate (Fmoc-Cl) in pyridine (scheme IV-2).

4   Profy, A. T.; Usher D. A. *J. Am. Chem. Soc.* **1984**, *106*, 5030. Profy, A. T.; Usher T. A. *J. Mol. Evol.* **1984**, *20*, 147. Usher, D. A.; Needels, M. C. *Adv. Space Res.* **1984**, *4*, 163. Usher D. A.; Profy, A. T.; Walstrum S. A.; Needels, M. C.; Bulack, S. C.; Lo K. M. *Origins of Life* **1984**, *14*, 621.

5   Lacey, J. C. Jr.; Staves, M. P.; Thomas, R. D. *J. Mol. Evol.* **1990**, *31*, 244.

6   Markiewicz, W. T.; Nowakowska, B.; Adrych, K. *Tetrahedron Lett.* **1988**, *29*, 1561.

7   Craine, L.; Raban, M. *Chem. Rev.* **1989**, *89*, 689.

B = Adenosine, Cytidine, Uridine
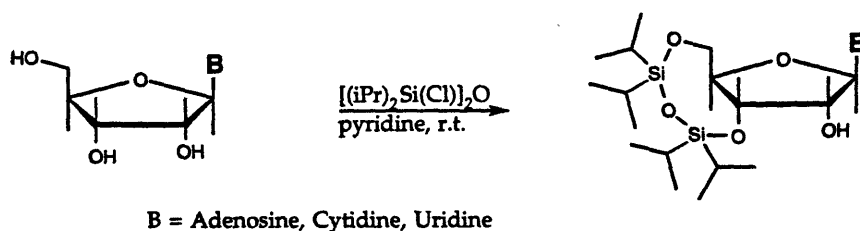
Scheme IV-1. *Synthesis of 3',5' silylated ribonucleosides.*
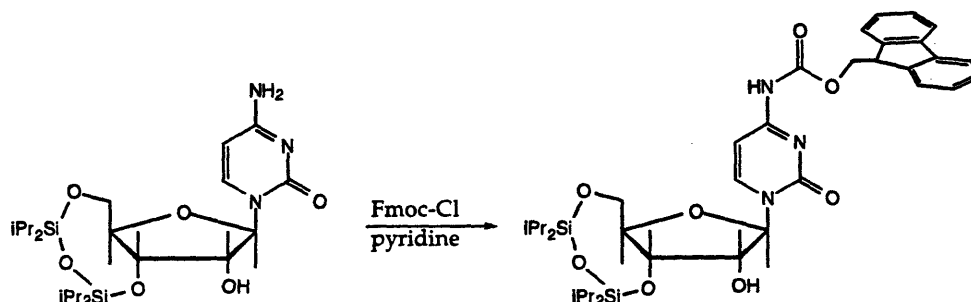
Scheme IV-2. *Protection of the exocyclic nitrogen of cytidine.*

Coupling of amino acids and nucleosides utilized several different approaches involving activation of N-protected amino acids. Successful approaches are with 1-(3-dimethylaminopropyl)-3-ethylcarbodiimide hydrochloride (EDC) or by conversion to an acid chloride with oxalyl chloride. The EDC couplings work for both Fmoc and NPS protected amino acids (scheme IV-3).
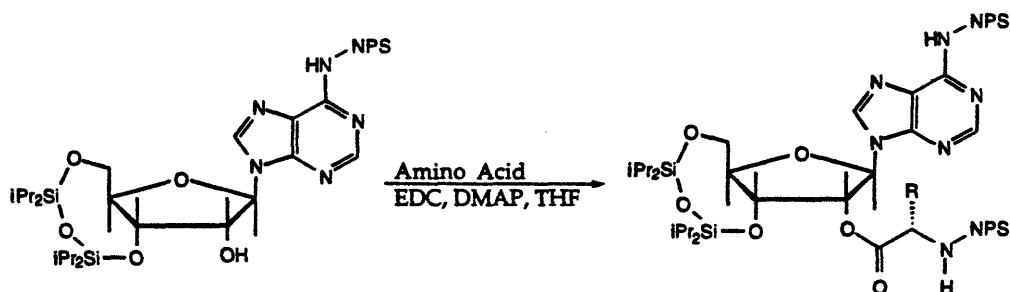
Amino Acid = NPS-Val, NPS-Asn, NPS-Phe, NPS-Met,
NPS-Trp, NPS-Gly, Fmoc-Ala, Fmoc-Gln-Trt
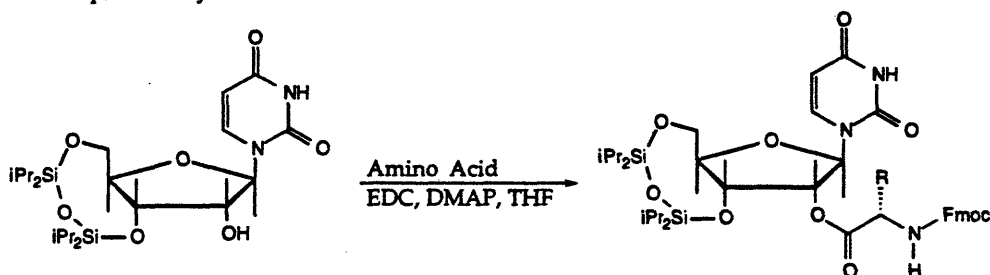
Amino Acid = NPS-Val, NPS-Asn, NPS-Phe, NPS-Met,
NPS-Trp, NPS-Gly, Fmoc-Ala, Fmoc-Gln-Trt

Scheme IV-3. *Amino acid couplings with ribonucleosides using EDC.*

Adenosine	Uridine	Cytidine
NPS-Pro	Fmoc-Gln	Fmoc-Gln
	Cbz-His	Fmoc-Trp
		Fmoc-Pro

Table IV-1. *Failed couplings of amino acids with ribonucleosides using EDC.*

The acid chloride approach initially met with little success, but it was found that the addition of a catalytic amount of dimethylamino pyridine (DMAP) was necessary to give the desired products (scheme IV-4, table IV-2).
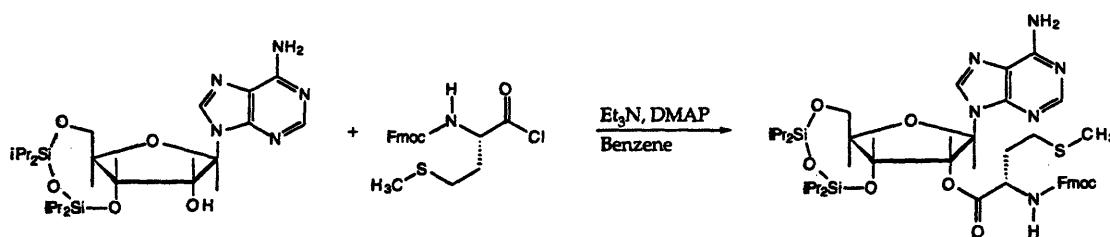
Scheme IV–4. *Ester formation through acid chloride activation using DMAP.*

Adenosine	Uridine	Cytidine
Fmoc-Ile	Fmoc-Val	Fmoc-Phe
Fmoc-Met	Fmoc-Phe	Fmoc-Met
Fmoc-Trp	Fmoc-Met	
Fmoc-Pro	Fmoc-Glu-γ-*t*-Butyl	
Fmoc-*t*-Bu-Ser	Fmoc-Lys-tBoc	
Fmoc-Trt-Cys	Arg(MTr)	
Fmoc-Ala	Fmoc-*t*-Bu-Ser	

Table IV–2. *Successfully coupled amino acyl chlorides with ribonucleosides using DMAP.*

The deprotection of the NPS group[8] is generally sluggish and yields are low (scheme IV–5). However, the deprotection of the NPS protected cytidine is rapid and efficient.
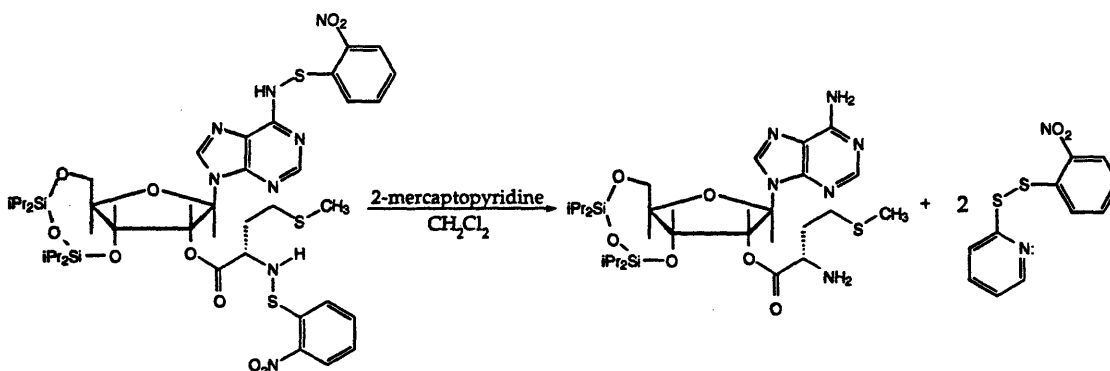
Scheme IV–5. *Deprotection of the NPS group using 2-mercaptopyridine.*

---

8 Stern, M.; Warshawsky, A.; Fridkin, M. *Int. J. Pept. Protein Res.* **1979**, *13*, 315.

Deprotection of the Fmoc derivatives is carried out with either piperidine or diethyl amine (scheme IV–6).[9]
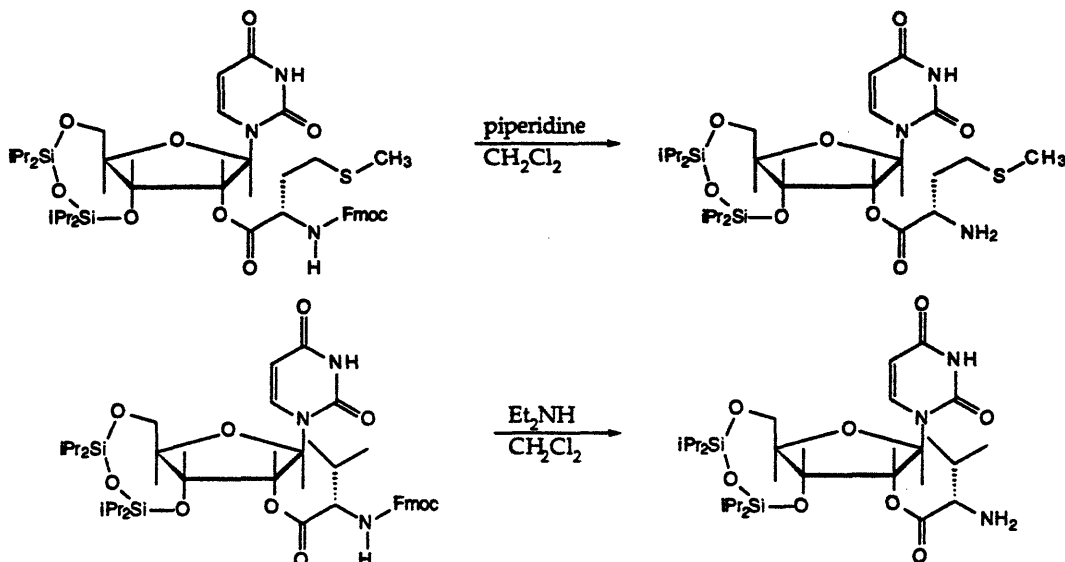
Scheme IV–6. *Deprotection of the Fmoc group using base.*

Both methods are fast but each suffers from the problem of competing aminolysis of the ester bond. It is somewhat easier to reduce this side reaction using the more volatile diethyl amine. The reaction can be quickly stopped by dilution with toluene and removal of solvents under vacuum.
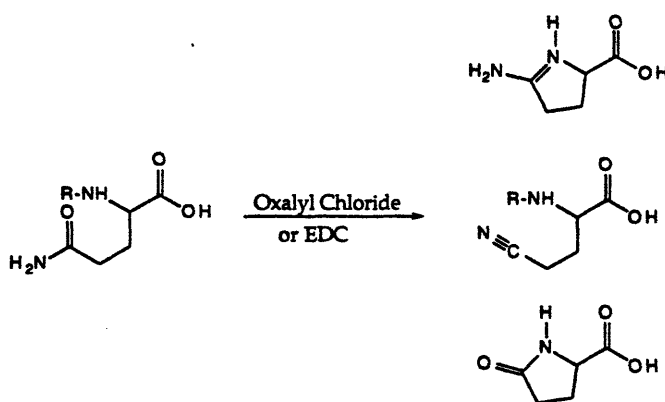
Figure IV–3. *Possible side reactions of the primary amide of glutamine.*

9 Atherton, E.; Sheppard, R. C. "The Fluorenylmethoxycarbonyl Amino Protecting Group" *The Peptides* 1987, *9*, 1-38, Academic Press, Orlando, Florida.

A number of attempts were made in preparing glutamine derivatives. Glutamine readily undergoes a number of side reactions upon activation (figure IV-3).[10] It was also found that once the desired product is made it quickly decomposes in solution to other materials. One of the predominant products is the cyclic pyroglutamic acid (scheme IV-7). The only product isolated from the deprotection of uridyl glutamine ester was pyroglutamic acid 90. Deprotection of Fmoc-glutamine-adenosine gave both pyroglutamic acid and glutamine esters as separate isolated products. However, the adenosine-glutamine product decomposed in CD_3OD over the course of several hours to give mainly the pyroglutamic acid species.
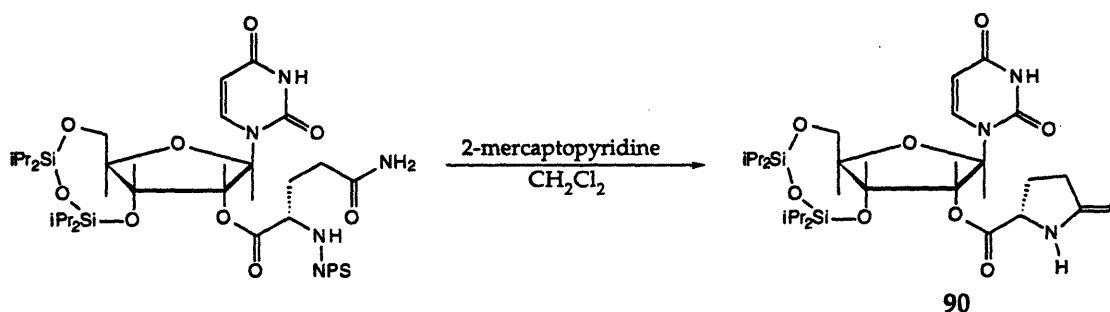
Scheme IV-7. *NPS deprotection followed by intramolecular cyclization to form the pyroglutamate ester of uridine.*

Accepting Nature's tendency to form **90**, the adenosine, cytidine and uridine esters of pyroglutamic acid were prepared. Originally the adenosine and uridine derivatives were serendipitously prepared in an attempt to obtain the glutamine species. Since then the adenosine and cytidine derivatives were prepared in one step by directly coupling the nucleoside with the lactam acid (scheme IV-8).

---

10 Bodanszky, M.; Bodanszky, A. *The Practice of Peptide Synthesis* **1984**, Springer-Verlag, Berlin, Heidelberg.
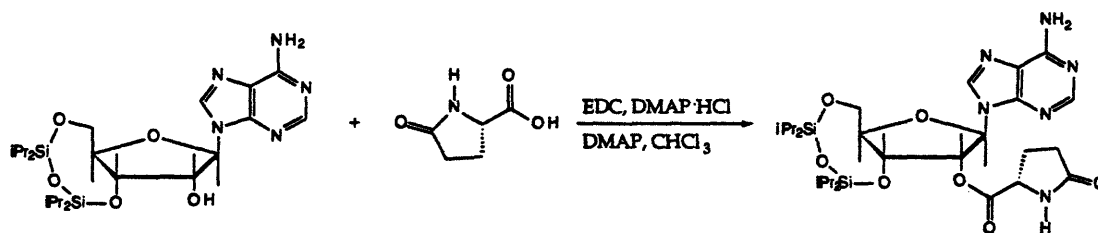
Scheme IV–8. *Carbodiimide coupling of pyroglutamic acid to a ribonucleoside.*

Kinetics of solvolysis

The relative stabilities of a number of 2'O-aminoacylated ribonucleosides, in an aqueous environment, were determined. The kinetics of solvolysis[11] were studied by monoriting both the appearance of cleaved ribonucleoside and disappearance of starting material via HPLC (figure IV–4).
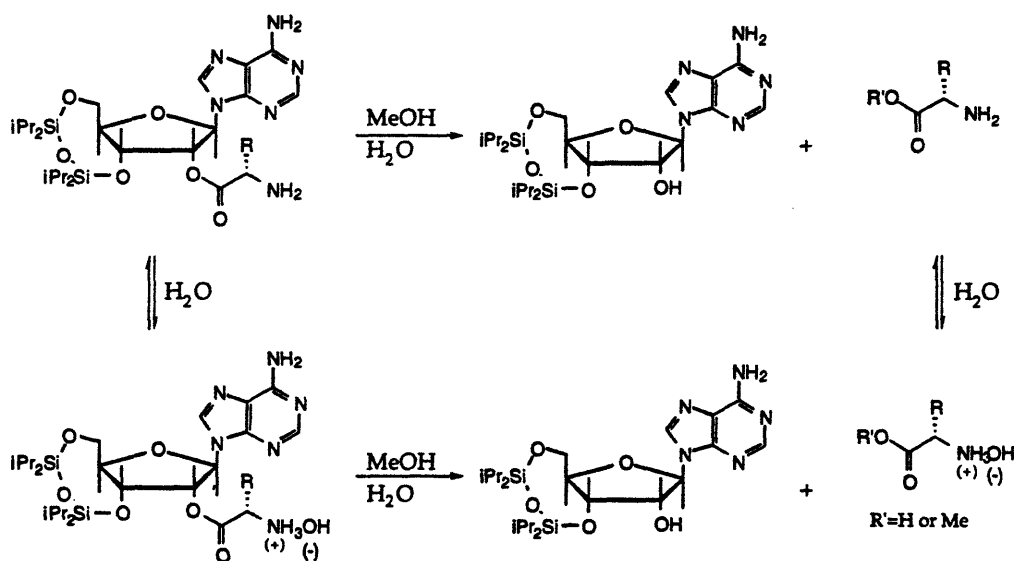
Figure IV–4. *Hydrolysis pathways for 2'O-aminoacylated ribonucleosides.*

Data show the rates of product appearance and starting material disappearance agree, within experimental error, with the exception of the

---

11   25% THF, 25% MeOH and 50% aqueous hepes buffer pH 7.7, I=0.2 M.

uridine-methionine derivative (table IV–3). The origin of this discrepancy is not known.

	$t_{1/2}$ of Ester Cleavage (min)		$t_{1/2}$ of Prod. Formation (min)	
	Uridine	Adenosine	Uridine	Adenosine
Val	7590	5363	10176	5038
pyro-Glu	4038	3194	4300	2284
Phe	1490	1080	2119	1270
Met	681	781	1800	1043
Trp	1369	902	1317	990
Pro	205	157	210	137

Table IV–3. *Comparison of the rates of solvolysis of aminoacylated ribonucleosides by observing both the disappearance of starting material and the appearance of product.*

Solvolysis rates vary greatly throughout a series of different amino acids attached to a particular nucleoside. Unfortunately this variability has been similar for both the adenosine and uridine series (table IV–3).

Discussion

None of the data suggests a mechanism for a selection process. The widely varying rates for uridine aminoacyl esters are mirrored in the adenosine series. Two main factors contribute to the rate of ester hydrolysis, the nature of the side chain and the pKa of the α-NH$_2$ group. The influence of the side chain comes mainly from steric factors, the valine derivative being the one most slowly hydrolyzed. However the phenylalanine derivative is slower to react than the more sterically hindered tryptophane species. This can be accounted for by the fact that protonation of the α-NH$_2$ will greatly enhance the hydrolysis rate (the pKa values and relative rates of hydrolysis for amino acid methyl esters are given in table IV–4). It is possible that a nucleoside base could interact selectively with the α-NH$_2$ producing subtle changes in the pKa's, which in turn would produce large differences in the stability of the ester linkage and a source for translational coding.

Methyl ester	pKa	$t_{1/2}$(rel.)
Valine	7.49	10.2
Phenylalanine	7.05	1.4
Methionine	7.09	1.0
Tryptophane	7.29	2.6

Table IV–4. *Comparison of the effect of the α-NH2 basicity on rates of ester hydrolysis.*

These experiments have not uncovered selective interactions between the nucleosides and amino acids. Close contact between H2 of adenosine and the side chain of methionine has not been seen in nOe studies of the adenosine-methionine derivatives. Other ^{1}H NMR data show the coupling constants for the methine protons of the ribose in the adenosine-proline species match the ones predicted by a macromodel minimized structure in the 3'endo conformation (table IV–5).[12] While the 3'endo conformer is one favored by ribonucleosides, the also favored 2'endo would provide more intimate contact (figure IV–5). The 2'endo conformer is not accessible due to the 3',5'O-tetraisopropyldisilyloxane blocking group.

Coupling (Hz)	Experimental	Calc. 2'endo	Calc. 3'endo
$H_1'–H_2'$	none observed	8.0	1.1
$H_2'–H_3'$	5.1	5.6	4.4
$H_3'–H_4'$	9.2	1.1	9.3

Table IV–5. *Comparison of experimentally determined coupling constants with predicted coupling constants for the 2'endo and 3'endo conformers.*

---

[12] Strutures minimized using MacroModel, Amber, PRCG, in $CHCl_3$.

3' endo   2'endo
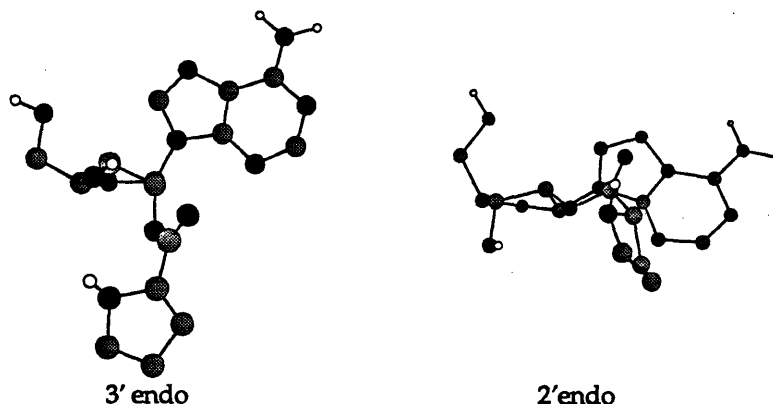
Figure IV-5. *2' and 3'endo conformations of 2'O-proline adenosine.*

The eight membered disilyloxane ring prevents the usual pseudo
rotations of the ribose ring. It was hoped that changing this protecting group
to *tert*-butyl dimethyl silyl groups (TBDMSi) would free the ribose and allow
the psuedo rotations and access to the 2'endo conformation. However the [1]H
NMR of these derivatives suggest that they adopt the 3'endo conformation
and the kinetic data closely follows that of the previous disilyloxane (table
IV–6).

	t₁/₂ (min)	
	Adenosine	Uridine
Phe	2006	4608
Met	1577	2810
Trp	2670	3758

Table IV-6. *Rate of solvolysis of TBDMSi ribonucleoside
derivatives.*

A possible method to overcome conformational flexibility of these
systems is to use dinucleotides. This will force the amino acid side chain
between two nucleosides no matter what conformation they adopt. In fact a
dinucleotide may very well be a necessary requirement in developing a
coding scheme.

Experimental

General

Reagent grade solvents were used except where noted. Tetrahydrofuran was distilled from Na/benzophenone ketyl and CH_2Cl_2 was distilled from P_2O_5. Melting points were measured on an Electrothermal 9100 melting point apparatus. NMR spectra were taken on a Varian XL-300 (300 MHz) and a Bruker AC-250 (250 MHz) spectrometers. IR spectra were obtained on a Mattson Sygus 100 FT IR spectrometer. High resolution mass spectra were obtained on a Finnegan Mat 8200 instrument. Molecular modeling experiments were performed on the Macromodel program with Amber force field.

Kinetics

HPLC grade solvents were used throughout the experiments. A typical solvolysis run consisted of preparing a stock solution of the amino acylated ribonucleoside in THF, 14.93 mg a 1 mL volumetric flask diluted to the mark to give a 22.9815 mM solution. A 50 µL aliquot of this solution was placed in a 5 mL volumetric flask with 1200 µL THF, 1250 µL MeOH and diluted to the mark with Hepes Buffer solution (pH=7.7, I=0.2 M NaCl) at time zero. The ratio of THF/MeOH/Buffer was always 1:1:2. The starting concentration of each amino acylated ribonucleoside was between 100 and 200 µM. The temperature was kept constant at 25 °C using a Waters 717 auto sampler. 5 µL injections were made with this auto sampler. It was connected to the Waters 600E system controller. The products were monitored using a Waters 490E Multiwavlength Detector, λ=260 nm. The data was worked-up using Maxima Chromatography software. The reaction materials were eluted through a Ranin Microsorb-MV (C_{18}, 5µ, 4.6 X 250 mm) column with 85% (1% TEA/MeOH) and 15% H_2O at 1 mL/min. The rates of reaction were calculated using pseudo first-order kinetics model (equations IV–1,2) with the GraphIt program for PC's.

$$[S] = [S]^\circ e^{-kt}$$ eq. 1

$$[P] = [S]^\circ\left(1 - e^{-kt}\right)$$ eq. 2

Where $[S]^\circ$ is the initial starting material concentration;
$[S]$ is the starting material concentration at time t;
$[P]$ is the product concentration at time t; k is the rate constant.

Synthesis

N-2-nitrophenylsulfenyl 3',5'-O-[1,1,3,3-tetrakis(1-methylethyl)disiloxanyl]-adenosine: 3',5'-O-Tetraisopropyldisilyloxane adenosine (5.6682 g, 11.12 mmol) was dried by dissolving in anhydrous benzene and evaporating (3x's). It was then dissolved in anhydrous CH_2Cl_2 (100 mL) with chlorotrimethylsilane (2.8 mL, 22.24 mmol), Et_3N (3.1 mL, 22.24 mmol) and a catalytic amount of imidazole. After 60 min. the reaction was washed with H_2O (1x), Brine (1x) and dried over $MgSO_4$. The CH_2Cl_2 was removed and the residue dissolved in $CHCl_3$ (100 mL). Et_3N (3.1 mL, 22.24 mmol) was added and the reaction heated to reflux. After 20 hrs. the reaction was cooled, evaporated and the residue dissolved in THF (75 mL). 1M HCl (aq., 75 mL) and *o*-nitrophenylsulfenyl chloride (0.3946 g, 2.08 mmol) were added and the reaction was stirred vigorously for 10 min. The reaction was then diluted with toluene (150 mL) and the layers separated. The aq. layer was washed with toluene. The organic layers were combined and washed with H_2O (2x's) and brine (1x). The organic layer was dried over $MgSO_4$ and the solvent evaporated. The purified product was obtained via flash chromatography ($CH_2Cl_2 \rightarrow$ 4% MeOH/CH_2Cl_2). See characterization in the next section.

N-(9-fluorenylmethoxycarbonyl)-3',5'-O-[1,1,3,3-tetrakis(1-methylethyl)disiloxanyl]-cytidine: 3',5'-O-Tetraisopropyldisilyloxane cytidine (5.0321 g, 10.36 mmol) was dried by dissolving in anhydrous benzene and evaporating (3x's). It was then dissolved in anhydrous pyridine (15 mL) with 9-fluorenylmethyl chloroformate (2.9480, 11.40 mmol) under Ar at room temperature. After 2 hrs. the reaction was poured into 1M HCl (aq., 100 mL). Et_2O (250 mL) was added and the layers separated. The Et_2O layer was washed

with 1M HCl (aq.) until the aqueous layer remained acidic. The Et$_2$O was washed with brine (3x's), dried over MgSO$_4$ and the solvent evaporated to give the crude product. The desired product was obtained via flash chromatography (50% Hexane/CH$_2$Cl$_2$ → CH$_2$Cl$_2$ → 3% MeOH/CH$_2$Cl$_2$). See characterization in the next section.

2'-O-[N-(9-fluorenylmethoxycarbonyl)-L-valine] 3',5'-O-[1,1,3,3-tetrakis(1-methylethyl)disiloxanyl]-uridine: N-Fmoc-Valine (68.0 mg, 0.201 mmol) and oxalyl chloride (53 µL, 0.603 mmol) were dissolved in CH$_2$Cl$_2$ (5 mL). A drop of 5% DMF in CH$_2$Cl$_2$ was added and the reaction stirred at room temperature under Ar for 30 min. The reaction was diluted with CCl$_4$ (10 mL) and the solvents evaporated. 3',5'-O-Tetraisopropyldisilyloxy uridine (97.6 mg, 0.201 mmol) was dried by dissolving in anhydrous benzene and evaporating (3x's). It was then dissolved in anhydrous benzene (3 mL) and stirred over 4Å molecular sieves for 2 hrs. The uridine solution was transferred to the dry acid chloride. The sieves were washed with anhydrous benzene (2 mL) and this was also added to the reaction followed by Et$_3$N (56 µL, 0.402 mmol) and a catalytic amount of DMAP. The reaction stirred at room temperature for 50 min. and then the solvent was evaporated. The purified product was obtained via flash chromatography (CH$_2$Cl$_2$ → 2% MeOH/CH$_2$Cl$_2$) in 91% yield (0.1474 g). See characterization in the next section.

2'-O-L-methionine 3',5'-O-[1,1,3,3-tetrakis(1-methylethyl)disiloxanyl]-uridine: N-Fmoc-Methioninyl-uridine (0.9123 g, 1.0859 mmol) was dissolved in anhydrous CH$_2$Cl$_2$ (4 mL) with piperidine (1 mL) at room temperature. After 1 hr. the reaction was diluted with toluene (20 mL) and the solvents evaporated. The purified was obtained via flash chromatography (CH$_2$Cl$_2$ → 4% MeOH/CH$_2$Cl$_2$). See characterization in the next section.

2'-O-L-tryptophan 3',5'-O-[1,1,3,3-tetrakis(1-methylethyl)disiloxanyl]-adenosine: N-Fmoc-Tryptophanyl-adenosine (98.8 mg, 0.1076 mmol) was dissolved in anhydrous CH$_2$Cl$_2$ (3 mL) with diethylamine (1 mL) at room temperature. After 1 hr. the reaction was diluted with toluene (20 mL) and

the solvents evaporated. The purified was obtained via flash chromatography ($CH_2Cl_2 \rightarrow$ 5% $MeOH/CH_2Cl_2$). See characterization in the next section.

2'-O-[N-(2-nitrophenylsulfenyl)-L-phenylalanine] 3',5'-O-[1,1,3,3-tetrakis(1-methylethyl)disiloxanyl]-uridine: 3',5'-O-Tetraisopropyldisilyloxane uridine (0.1118 g, 0.2297 mmol) and NPS-phenylalanine (0.1262 g, 0.2526 mmol) were dried by dissolving in anhydrous benzene and evaporating (3x's). 1-(3-Dimethylaminopropyl)-3-ethylcarbodiimide hydrochloride (0.1317 g, 0.6891 mmol) and a catalytic amount of DMAP were added to the dried starting materials. Anhydrous THF (5 mL) was added and the reaction stirred under Ar at room temperature for 20 hrs. The solvent was then removed by evaporation. The purified product was obtained in 79% yield (0.1348 g) via flash chromatography ($CH_2Cl_2 \rightarrow$ 2% $MeOH/CH_2Cl_2$). See characterization in the next section.

2'-O-L-trptophan 3',5'-O-[1,1,3,3-tetrakis(1-methylethyl)disiloxanyl]-uridine: N-NPS-Tryptophanyl-uridine (0.1796 g, 0.2174 mmol) was mixed with 2-mercaptopyridine (25.3 mg, 0.2282 mmol) in CH_2Cl_2 at room temperature. The reaction stirred for 16 hrs. before the solvent was removed by evaporation. The purified product was obtained via flash chromatography (2% $MeOH/CH_2Cl_2 \rightarrow$ 5% $MeOH/CH_2Cl_2 \rightarrow$ 10% $MeOH/CH_2Cl_2$). See characterization in the next section.

Characterizations

2'-O-[N-(9-fluorenylmethoxycarbonyl)-L-valine] 3',5'-O-[1,1,3,3-tetrakis(1-methylethyl)disiloxanyl]-uridine: [^1]H NMR ($CDCl_3$) δ 9.39 (s, 1H), 7.79 (d, J=8.0Hz, 1H), 7.78 (d, J=7.2Hz, 2H), 7.62 (d, J=7.2Hz, 2H), 7.43-7.28 (Ar, 4H), 5.78 (s, 1H), 5.71 (d, J=8.0Hz, 1H), 5.60 (d, J=2.3Hz, 1H), 5.50 (d, J=4.6Hz, 1H), 4.49 (dd, J=8.9, 4.3Hz, 1H), 4.43-4.38 (m, 2H), 4.28-4.23 (m, 2H), 4.05-3.94 (m, 2H), 2.23 (m, 1H), 1.10-0.98 (m, 34H)

2'-O-[N-(9-fluorenylmethoxycarbonyl)-L-phenylalanine] 3',5'-O-[1,1,3,3-tetrakis(1-methylethyl)disiloxanyl]-uridine: [^1]H NMR ($CDCl_3$) δ 9.72 (s, 1H),

7.78-7.25 (Ar, 14H), 5.75 (s, 1H), 5.72 (s, 1H), 5.60 (d, J=8.7Hz, 1H), 5.51 (d, J=4.6Hz, 1H), 4.88 (dd, J=13.8, 6.9Hz, 2H), 4.47 (dd, J=9.5, 4.8Hz, 1H), 4.44-4.16 (m, 3H), 4.03-3.96 (m, 2H), 3.30 (dd, J=14.1, 5.3Hz, 1H), 3.06 (dd, J=13.9, 7.2Hz, 1H), 1.10-1.00 (m, 28H); ^{13}C NMR (CDCl₃) δ 170.0, 163.4, 155.5, 149.7, 143.7, 141.2, 139.3, 135.8, 129.3, 128.5, 127.5, 126.9, 125.0, 119.8, 102.1, 88.8, 81.9, 76.2, 67.4, 66.9, 59.2, 54.5, 47.0, 38.4, 17.3, 17.2, 17.2, 17.1, 17.0, 16.8, 16.8, 16.7, 13.3, 12.8, 12.8, 12.3

2'-O-[N-(2-nitrophenylsulfenyl)-L-glutamine] 3',5'-O-[1,1,3,3-tetrakis(1-methylethyl)disiloxanyl]-uridine: ^{1}H NMR (CDCl₃) δ 8.21 (d, J=8.2Hz, 1H), 8.01 (d, J=8.2Hz, 1H), 7.76 (d, J=8.1Hz, 1H), 7.64 (dd, J=7.6, 7.6Hz, 1H), 7.22 (m, 1H), 6.43 (bs, 1H), 6.23 (bs, 1H), 5.80 (s, 1H), 5.71 (d, J=8.1Hz, 1H), 5.42 (d, J=4.8Hz, 1H), 4.36 (dd, J=9.3, 4.9Hz, 1H), 4.23 (d, J=13.5Hz, 1H), 4.08 (d, J=9.6Hz, 1H), 3.98 (d, J=12.5Hz, 1H), 3.80-3.71 (m, 2H), 1.13-0.95 (m, 28H)

2'-O-[N-(2-nitrophenylsulfenyl)-L-methionine] 3',5'-O-[1,1,3,3-tetrakis(1-methylethyl)disiloxanyl]-uridine: ^{1}H NMR (CDCl₃) δ 9.28 (bs, 1H), 8.26 (d, J=8.2Hz, 1H), 8.01 (d, J=8.2Hz, 1H), 7.75 (d, J=8.1Hz, 1H), 7.68 (dd, J=7.7, 7.7Hz, 1H), 7.26 (dd, J=7.7, 7.7Hz, 1H), 5.82 (s, 1H), 5.72 (d, J=8.0Hz, 1H), 5.50 (d, J=4.8Hz, 1H), 4.41 (dd, J=9.2, 5.0Hz, 1H), 4.25 (d, J=13.2Hz, 1H), 4.03 (d, J=8.9Hz, 1H), 3.98 (d, J=12.7Hz, 1H), 3.86 (dd, J=12.7, 7.1Hz, 1H), 3.55 (d, J=7.8Hz, 1H), 2.70 (m, 2H), 2.20 (m, 1H), 2.08 (m, 4H), 1.09-0.98 (m, 28H); ^{13}C NMR (CDCl₃) δ 171.6, 163.6, 163.5, 163.3, 149.9, 144.9, 142.6, 138.9, 133.9, 125.6, 124.7, 124.5, 102.2, 88.4, 82.1, 76.2, 67.4, 62.5, 59.2, 32.7, 31.0, 30.1, 17.2, 17.1, 16.9, 16.7, 16.6, 15.1, 13.4, 12.8, 12.3

2'-O-[N-(2-nitrophenylsulfenyl)-L-trptophan] 3',5'-O-[1,1,3,3-tetrakis(1-methylethyl)disiloxanyl]-uridine: ^{1}H NMR (CDCl₃) δ 10.67 (bs, 1H), 9.48 (bs, 1H), 8.22 (d, J=8.2Hz, 1H), 7.89-7.93 (Ar, 2H), 7.72 (d, J=7.4Hz, 1H), 7.50-7.44 (Ar, 3H), 5.83 (d, J=8.0Hz, 1H), 5.74 (s, 1H), 5.55 (d, J=4.2Hz, 1H), 4.41 (dd, J=9.3, 4.2Hz, 1H), 4.30 (d, J=12.4, 1H), 4.08-3.97 (m, 3H), 3.56 (dd, J=14.4, 4.9Hz, 1H), 3.41 (dd, J=14.6, 5.0Hz, 1H), 3.17 (d, J=10.3, 1H), 1.11-0.94 (m, 28H); ^{13}C NMR (CDCl₃) δ 171.3, 163.5, 151.0, 144.9, 142.3, 139.3, 136.3, 133.6, 127.8, 125.4, 124.4,

123.9, 121.8, 119.4, 118.2, 111.7, 108.8, 102.5, 88.0, 82.2, 76.2, 67.4, 65.3, 59.1, 29.4, 17.3, 17.2, 16.8, 16.6, 13.4, 12.9, 12.8, 12.4

2'-O-[N-(2-nitrophenylsulfenyl)-L-phenylalanine] 3',5'-O-[1,1,3,3-tetrakis(1-methylethyl)disiloxanyl]-uridine: ^{1}H NMR (CDCl$_3$) δ 9.87 (bs, 1H), 8.16 (dd, J=8.4, 1.1Hz, 1H), 7.77 (d, J=8.2, 1H), 7.41-7.08 (Ar, 8H), 5.88 (s, 1H), 5.75 (dd, J=8.2, 1.4Hz, 1H), 5.56 (d, J=4.9Hz, 1H), 4.48 (dd, J=9.3, 4.8Hz, 1H), 4.28 (d, J=13.4Hz, 1H), 4.12 (d, J=9.5Hz, 1H), 4.02 (dd, J=13.4, 2.1Hz, 1H), 3.86 (ddd, J=9.5, 9.4, 4.3Hz, 1H), 3.37 (dd, J=14.1, 4.3Hz, 1H), 3.29 (d, J=9.5Hz, 1H), 2.95 (dd, J=14.0, 9.5Hz, 1H), 1.11-0.98 (m, 28H); ^{13}C NMR (CDCl$_3$) δ 171.4, 149.9, 144.7, 142.3, 139.2, 136.9, 133.6, 129.5, 128.6, 127.0, 125.4, 124.5, 102.2, 88.5, 82.1, 76.3, 67.7, 65.7, 59.3, 39.8, 17.3, 17.2, 16.8, 13.4, 12.8, 12.4

2'-O-L-trptophan 3',5'-O-[1,1,3,3-tetrakis(1-methylethyl)disiloxanyl]-uridine: IR (KBr) 3372, 3168, 2946, 2868, 1750, 1697, 1459, 1399, 1272, 1161, 1124, 1038, 885, 698 cm^{-1}; ^{1}H NMR (CDCl$_3$) δ 8.90 (bs, 1H), 7.73 (d, J=8.2Hz, 1H), 7.61 (d, J=7.4Hz, 1H), 7.34 (d, J=7.7Hz, 1H), 7.19-7.07 (Ar, 3H), 5.78 (s, 1H), 5.71 (d, J=8.1Hz, 1H), 5.51 (d, J=4.8Hz, 1H), 4.42 (dd, J=9.1, 4.9Hz, 1H), 4.25 (d, J=13.2Hz, 1H), 4.05-3.93 (m, 3H), 3.38 (dd, J=14.3, 4.4Hz, 1H), 3.00 (dd, J=14.4, 8.1Hz, 1H), 1.17-0.92 (m, 28H); ^{13}C NMR (CDCl$_3$) δ 173.4, 163.5, 163.4, 150.3, 139.1, 136.3, 127.6, 123.3, 121.9, 119.3, 118.5, 111.3, 110.7, 102.4, 88.5, 82.2, 75.5, 67.6, 59.4, 59.4, 55.5, 30.7, 17.3, 17.2, 16.9, 16.8, 13.4, 12.9, 12.5; HRMS calcd for C$_{31}$H$_{50}$N$_6$O$_6$Si$_2$ [M+2H]$^+$ 674.3167, found 674.3144.

2'-O-L-phenylalanine 3',5'-O-[1,1,3,3-tetrakis(1-methylethyl)disiloxanyl]-uridine: IR (KBr) 3163, 2946, 2868, 1701, 1458, 1400, 1270, 1163, 1122, 1038, 993, 885, 701 cm^{-1}; ^{1}H NMR (CDCl$_3$) δ 7.74 (d, J=8.2Hz, 1H), 7.33-7.20 (Ar, 5H), 5.81 (s, 1H), 5.70 (d, J=8.1Hz, 1H), 5.46 (d, J=4.7Hz, 1H), 4.41 (dd, J=9.1, 5.0Hz, 1H), 4.25 (d, J=13.2Hz, 1H), 4.05-3.96 (m, 2H), 3.91 (dd, J=8.7, 4.3Hz, 1H), 3.24 (dd, J=13.8, 4.3Hz, 1H), 2.80 (dd, J=13.8, 8.7Hz, 1H), 1.09-0.97 (m, 28H); ^{13}C NMR (CDCl$_3$) δ 163.5, 150.3, 139.9, 137.1, 129.3, 128.5, 126.8, 102.0, 91.0, 81.9, 75.1, 68.9, 60.3, 55.7, 41.0, 17.2, 16.9, 13.4, 12.9, 12.5; HRMS calcd for C$_{30}$H$_{47}$N$_3$O$_8$Si$_2$ [M+H]$^+$ 634.2980, found 634.2986.

2'-O-L-methionine 3',5'-O-[1,1,3,3-tetrakis(1-methylethyl)disiloxanyl]-uridine: IR (KBr) 3134, 2946, 2878, 1750, 1698, 1465, 1439, 1398, 1274, 1170, 1124, 1038, 885, 856, 704 cm^{-1}; ^{1}H NMR (CDCl$_3$) δ 7.74 (d, J=8.2Hz, 1H), 5.81 (s, 1H), 5.69 (d, 8.2Hz, 1H), 5.42 (d, J=4.7Hz, 1H), 4.34 (dd, J=9.5, 4.8Hz, 1H), 4.24 (d, J=13.4Hz, 1H), 4.00-3.93 (m, 2H), 3.74 (d, J=4.8Hz, 1H), 2.70-2.62 (m, 2H), 2.08-1.99 (m, 4H), 1.79 (m, 1H), 1.07-0.99 (m, 28H); ^{13}C NMR (CDCl$_3$) δ 174.1, 163.2, 149.9, 138.8, 102.2, 88.5, 82.1, 75.7, 67.4, 59.2, 53.2, 30.4, 17.3, 16.9, 16.7, 15.2, 13.4, 12.9, 12.3; HRMS calcd for C$_{26}$H$_{49}$N$_3$O$_8$SSi$_2$ [M+H]$^+$ 618.2701, found 618.2695.

2'-O-L-proline 3',5'-O-[1,1,3,3-tetrakis(1-methylethyl)disiloxanyl]-uridine: IR (KBr) 3126, 2945, 2868, 1750, 1697, 1465, 1444, 1394, 1273, 1180, 1124, 1037, 886, 706 cm^{-1}; ^{1}H NMR (CDCl$_3$) δ 7.73 (d, J=8.2Hz, 1H), 5.83 (s, 1H), 5.68 (d, J=8.4Hz, 1H), 5.43 (d, J=4.8Hz, 1H), 4.37 (dd, J=9.4, 4.8Hz, 1H), 4.25 (d, J=13.5Hz, 1H), 4.02-3.95 (m, 2H), 3.10 (m, 1H), 2.96 (m, 1H), 2.18 (m, 1H), 1.99 (m, 1H), 1.73 (m, 2H), 1.08-0.97 (m, 28H); ^{13}C NMR (CDCl$_3$) δ 173.4, 163.4, 150.0, 139.0, 102.2, 88.5, 82.1, 75.6, 67.6, 59.3, 59.1, 46.5, 30.2, 25.1, 17.2, 16.7, 16.7, 13.4, 12.9, 12.4; HRMS calcd for C$_{26}$H$_{47}$N$_3$O$_8$Si$_2$ [M+H]$^+$ 584.2824, found 584.2808.

2'-O-L-pyroglutamic acid 3',5'-O-[1,1,3,3-tetrakis(1-methylethyl)disiloxanyl]-uridine: IR (KBr) 3198, 2946, 2868, 1759, 1698, 1464, 1398, 1274, 1187, 1124, 1038, 885, 699 cm^{-1}; ^{1}H NMR (CDCl$_3$) δ 11.54 (bs, 1H), 7.95 (bs, 1H), 7.78 (d, J=8.2Hz, 1H), 5.77 (s, 1H), 5.74 (dd, J=8.2, 2.1Hz, 1H), 5.50 (d, J=4.7Hz, 1H), 4.41 (dd, J=1.7Hz, 1H), 3.98 (d, J=14.4Hz, 1H), 2.51 (m, 1H), 2.37 (t, 6.9Hz, 2H), 2.22 (m, 1H), 1.09-0.96 (m, 28H); ^{13}C NMR (CDCl$_3$) δ 179.5, 170.4, 163.6, 163.2, 151.5, 137.7, 102.9, 88.2, 82.3, 75.7, 67.2, 59.0, 55.4, 29.0, 25.0, 17.2, 16.8, 13.4, 12.8, 12.8, 12.4; HRMS calcd for C$_{26}$H$_{43}$N$_3$O$_9$Si$_2$ [M+H]$^+$ 598.2216, found 598.2610.

2'-O-L-valine 3',5'-O-[1,1,3,3-tetrakis(1-methylethyl)disiloxanyl]-uridine: ^{1}H NMR (CDCl$_3$) δ 7.80 (d, J=8.2Hz, 1H), 5.80 (s, 1H), 5.69 (d, J=8.1Hz, 1H), 5.44 (d, J=4.7Hz, 1H), 4.35 (dd, J=9.2, 4.8Hz, 1H), 4.26 (d, J=13.2Hz, 1H), 4.05-3.94 (m, 2H), 3.50 (d, J=4.3Hz, 1H), 2.12 (m, 1H), 1.09-0.91 (m, 34H); ^{13}C NMR (CDCl$_3$) δ 173.8, 163.5, 150.0, 138.9, 102.1, 88.5, 82.0, 75.4, 67.2, 59.5, 59.1, 31.9, 19.0,

17.4, 17.3, 17.1, 16.8, 16.7, 16.5, 13.4, 12.9, 12.8, 12.1; HRMS calcd for
$C_{26}H_{47}N_3O_8Si_2$ 585.2902, found 585.2897.

N-2-nitrophenylsulfenyl 2'-O-[N-(2-nitrophenylsulfenyl)-L-valine] 3',5'-O-[1,1,3,3-tetrakis(1-methylethyl)disiloxanyl]-adenosine:

^{1}H NMR (CDCl$_3$) δ 8.51 (s, 1H), 8.34 (d, J=8.2Hz, 1H), 8.28 (d, 8.1Hz, 1H), 8.20 (s, 1H), 8.13 (d, J=8.2Hz, 1H), 7.70-7.46 (Ar, 3H), 7.35-7.24 (Ar, 2H), 6.02 (s, 1H), 5.96 (d, J=5.4Hz, 1H), 5.21 (dd, J=9.4, 5.3Hz, 1H), 4.20 (d, J=12.8Hz, 1H), 4.11-3.99 (m, 2H), 3.52 (dd, J=9.7, 4.6Hz, 1H), 3.32 (d, J=9.8Hz, 1H), 2.25 (m, 1H), 1.16-1.00 (m, 34H)

N-2-nitrophenylsulfenyl 2'-O-[N-(2-nitrophenylsulfenyl)-L-phenylalanine] 3',5'-O-[1,1,3,3-tetrakis(1-methylethyl)disiloxanyl]-adenosine:

^{1}H NMR (CDCl$_3$) δ 8.49 (s, 1H), 8.34 (d, J=8.1Hz, 1H), 8.26 (bs, 1H), 8.18 (d, J=8.1Hz, 1H), 8.13 (s, 1H), 7.56-7.12 (Ar, 11H), 6.04 (d, J=5.4Hz, 1H), 5.97 (s, 1H), 5.39 (d, J=9.2, 5.4Hz, 1H), 4.17 (d, J=12.4, 1H), 4.11-4.01 (m, 2H), 3.41 (dd, J=13.9, 3.9Hz, 1H), 3.17 (d, J=9.8Hz, 1H), 2.90 (dd, J=13.8, 10.1Hz, 1H), 1.13-0.99 (m, 28H)

N-2-nitrophenylsulfenyl 3',5'-O-[1,1,3,3-tetrakis(1-methylethyl)disiloxanyl]-adenosine:

^{1}H NMR (CDCl$_3$) δ 8.84 (bs, 1H), 8.45 (s, 1H), 8.32 (d, J=7.9Hz, 1H), 8.11 (s1H), 7.49-7.47 (Ar, 2H), 7.29 (ddd, J=5.7, 5.6, 2.7Hz, 1H), 5.93 (s, 1H), 5.20 (dd, J=7.5, 5.6Hz, 1H), 4.65 (d, J=5.5Hz, 1H), 4.13-3.99 (m, 3H), 3.35 (bs, 1H), 1.10-1.03 (m, 28H); ^{13}C NMR (CDCl$_3$) δ 155.0, 153.3, 149.6, 143.1, 142.4, 141.5, 134.2, 125.9, 125.5, 124.1, 122.3, 90.1, 82.4, 74.9, 71.0, 61.9, 17.4, 17.3, 17.1, 16.9, 13.3, 13.0, 12.7

2'-O-L-alanine-N-2-nitrophenylsulfenyl 3',5'-O-[1,1,3,3-tetrakis(1-methylethyl)disiloxanyl]-adenosine:

^{1}H NMR (CDCl$_3$) δ 8.90 (bs, 1H), 8.46 (s, 1H), 8.32 (d, J=8.2Hz, 1H), 8.14 (s, 1H), 7.52-7.42 (Ar, 2H), 7.30 (d, J=8.3Hz, 1H), 5.97 (s, 1H), 5.90 (d, J=5.4Hz, 1H), 5.23 (dd, J=8.6, 5.5Hz, 1H), 4.15 (dd, J=13.5, 2.9Hz, 1H), 4.02-3.98 (m, 2H), 3.70 (q, J=7.0Hz, 1H), 1.65 (bs, 2H), 1.40 (d, J=7.0Hz, 3H), 1.05-0.95 (m, 28H)

2'-O-[N-(9-fluorenylmethoxycarbonyl)-L-tryptophan] 3',5'-O-[1,1,3,3-tetrakis(1-methylethyl)disiloxanyl]-adenosine:

^{1}H NMR (CDCl$_3$) δ 8.33 (s, 1H),

8.23 (s, 1H), 7.81 (s,1H), 7.76-7.08 (Ar, 13H), 6.06 (bs, 2H), 5.86 (d, J=6.3Hz, 1H), 5.74 (s, 1H), 5.42 (d, J=10.2Hz, 1H), 5.24 (dd, J=10.0, 6.5Hz, 1H), 4.9 (m, 1H), 4.42-3.95 (m, 5H), 3.46 (dd, J=17.9, 5.2Hz, 1H) 3.26 (dd, J=17.7, 8.4Hz, 1H), 1.10-0.99 (m, 28H); ^{13}C NMR (CDCl$_3$) δ 171.0, 155.9, 155.3, 152.4, 148.8, 143.7, 143.6, 141.2, 139.7, 136.1, 127.6, 127.5, 127.0, 125.0, 125.0, 123.0, 122.2, 120.0, 119.9, 119.7, 118.3, 111.4, 109.9, 87.5, 81.7, 76.3, 68.8, 67.0, 60.0, 54.8, 47.0, 28.2, 17.3, 17.2, 16.9, 16.8, 13.3, 12.9, 12.7, 12.5

2'-O-[N-(9-fluorenylmethoxycarbonyl)-L-methionine] 3',5'-O-[1,1,3,3-tetrakis(1-methylethyl)disiloxanyl]-adenosine: ^{1}H NMR (CDCl$_3$) δ 8.27 (s, 1H), 7.98 (s, 1H), 7.75 (d, J=7.1Hz, 2H), 7.58 (d, J=7.2Hz, 2H), 7.39 (dd, J=7.3, 7.3Hz, 2H), 7.29 (dd, J=7.2, 7.2Hz, 2H), 6.27 (bs, 2H), 6.02 (s, 1H), 5.98-5.94 (m, 2H), 5.23 (dd, J=8.4, 5.3Hz, 1H), 4.73 (m, 1H), 4.44 (d, J=7.0Hz, 2H), 4.24-4.14 (m, 2H), 4.04-4.00 (m, 2H), 2.65 (dd, J=12.6, 7.3Hz, 2H), 2.26 (m, 1H), 2.12 (s, 3H), 2.02 (m, 1H), 1.09-1.03 (m, 28H); ^{13}C NMR (CDCl$_3$) δ 171.1, 156.0, 155.5, 152.8, 148.9, 143.7, 143.5, 141.2, 139.4, 127.6, 127.0, 124.9, 120.1, 119.9, 87.4, 81.7, 76.3, 68.6, 66.9, 59.8, 59.8, 53.1, 47.0, 32.4, 30.0, 17.3, 17.2, 17.0, 16.8, 16.7, 15.3, 13.2, 12.9, 12.7, 12.3

2'-O-L-phenylalanine 3',5'-O-[1,1,3,3-tetrakis(1-methylethyl)disiloxanyl]-adenosine: ^{1}H NMR (CDCl$_3$) δ 8.28 (s, 1H), 7.99 (s, 1H), 7.31-7.24 (Ar, 5H), 6.14 (bs, 2H), 6.00 (s, 1H), 5.83 (d, J=5.2Hz, 1H), 5.15 (dd, J=9.1, 5.3Hz, 1H), 4.21 (d, J=12.1, 1H), 4.09-4.00 (m, 2H), 3.89 (dd, J=8.8, 4.2Hz, 1H), 3.26 (dd, J=13.7, 4.1Hz, 1H), 2.81 (dd, J=13.7, 8.9Hz, 1H), 2.02 (bs, 2H), 1.10-0.95 (m, 28H); ^{13}C NMR (CDCl$_3$) δ 173.7, 155.5, 153.2, 149.1, 139.1, 137.2, 129.3, 128.6, 126.9, 120.2, 87.5, 81.9, 76.0, 68.8, 60.2, 55.8, 41.2, 17.4, 17.3, 17.3, 17.0, 16.9, 16.9, 13.3, 13.0, 12.8, 12.6; HRMS calcd for C$_{31}$H$_{48}$N$_6$O$_6$Si$_2$ 656.3174, found 656.3168.

2'-O-L-valine 3',5'-O-[1,1,3,3-tetrakis(1-methylethyl)disiloxanyl]-adenosine: ^{1}H NMR (CDCl$_3$) δ 8.29 (s, 1H), 8.06 (s, 1H), 6.04 (s, 1H), 5.78 (d, J=5.0Hz, 1H), 5.70 (bs, 2H), 5.04 (d, J=9.2, 5.2Hz, 1H), 4.22 (d, J=12.0Hz, 1H), 4.08-3.99 (m, 2H), 3.51 (d, J=1.8Hz, 1H), 2.13 (m, 1H), 1.87 (bs, 2H), 1.09-0.95 (m, 34H)

2'-O-L-alanine 3',5'-O-[1,1,3,3-tetrakis(1-methylethyl)disiloxanyl]-adenosine: IR (KBr) 3125, 2946, 2868, 1758, 1698, 1465, 1398, 1273, 1125, 1077, 1038, 994, 886, 859, 766, 701 cm^{-1}; ^{1}H NMR (CDCl$_3$) δ 8.29 (bs, 1H), 8.01 (s, 1H), 6.04 (s, 1H), 5.81 (bs, 2H), 5.80 (d, J=5.2Hz, 1H), 5.06 (dd, J=9.0, 5.2Hz, 1H), 4.20 (d, J=11.6Hz, 1H), 4.05-3.98 (m 2H), 3.70 (q, J=7.1Hz, 1H), 1.82 (bs, 2H), 1.41 (d, J=7.1Hz, 3H), 1.09-0.95 (m, 28H)

2'-O-L-methionine 3',5'-O-[1,1,3,3-tetrakis(1-methylethyl)disiloxanyl]-adenosine: ^{1}H NMR (CDCl$_3$) δ 8.28 (s, 1H), 8.02 (s, 1H), 6.05 (s, 1H), 5.86 (bs, 2H), 5.82 (d, J=5.1Hz, 1H), 5.07 (dd, J=8.8, 5.1Hz, 1H), 4.20 (d, J=11.9Hz, 1H), 4.04-3.99 (m, 2H), 3.79 (dd, J=8.4, 4.3Hz, 1H), 2.70 (m, 2H), 2.13 (m, 1H), 2.11 (s, 3H), 1.84 (m, 1H), 1.08-1.00 (m, 28H); ^{13}C NMR (CDCl$_3$) δ 174.5, 155.5, 153.1, 149.0, 139.0, 120.1, 87.5, 81.9, 76.0, 68.5, 59.9, 53.2, 34.0, 30.5, 17.4, 17.3, 17.0, 16.8, 16.8, 15.2, 13.3, 12.9, 12.8, 12.4; HRMS calcd for C$_{27}$H$_{48}$N$_6$O$_6$SSi$_2$ 640.2895, found 640.2889.

2'-O-L-tryptophan 3',5'-O-[1,1,3,3-tetrakis(1-methylethyl)disiloxanyl]-adenosine: ^{1}H NMR (CDCl$_3$) δ 8.35 (bs, 1H), 8.27 (s, 1H), 7.88 (s, 1H), 7.61 (d, J=7.7Hz, 2H), 7.36 (d, J=7.8Hz, 2H), 7.15 (m, 4H), 5.86 (s, 1H), 5.85 (d, J=5.9Hz, 1H), 5.20 (dd, J=8.7, 5.8Hz, 1H), 4.18 (d, J=11.7Hz, 1H), 4.08-4.00 (m, 2H), 3.44 (dd, J=14.0, 3.6Hz, 1H), 3.01 (dd, J=13.8,8.7Hz, 1H), 2.12 (bs, 2H), 1.09-1.00 (m, 28H); ^{13}C NMR (CDCl$_3$) δ 173.8, 155.5, 153.1, 149.1, 139.4, 136.3, 127.4, 123.1, 122.2, 120.2, 119.8, 118.6, 111.3, 87.5, 81.9, 75.9, 68.9, 60.3, 55.2, 49.7, 31.0, 17.4, 17.3, 17.0, 16.9, 16.9, 13.3, 13.0, 12.8, 12.6; HRMS calcd for C$_{33}$H$_{49}$N$_7$O$_6$Si$_2$ 695.3283, found 695.3279.

2'-O-L-proline 3',5'-O-[1,1,3,3-tetrakis(1-methylethyl)disiloxanyl]-adenosine: ^{1}H NMR (CDCl$_3$) δ 8.24 (s,1H), 7.99 (s, 1H), 6.25 (bs, 2H), 6.03 (s, 1H), 5.81 (d, J=5.1Hz, 1H), 5.06 (dd, J=9.2,5.2Hz, 1H), 4.20-3.92 (m, 4H), 3.10-2.88 (m, 3H), 2.23-1.96 (m, 2H), 1.82-1.65 (m, 2H), 1.07-0.98 (m, 28H); HRMS calcd for C$_{27}$H$_{46}$N$_6$O$_6$Si$_2$ 606.3017, found 606.3009.

2'-O-L-pyroglutamic acid 3',5'-O-[1,1,3,3-tetrakis(1-methylethyl)disiloxanyl]-adenosine: ^{13}C NMR (CDCl$_3$) δ 178.6, 170.9, 155.9,

153.0, 148.7, 138.3, 119.7, 87.3, 81.8, 76.2, 68.4, 59.9, 55.4, 29.3, 24.9, 17.3, 17.2, 17.2, 16.9, 16.7, 16.6, 13.2, 12.8, 12.7, 12.5; HRMS calcd for $C_{27}H_{44}N_4O_6Si_2$ $[M+H]^+$ 621.2888, found 621.2899.

2'-O-L-methionine 3',5'-O-[1,1,3,3-tetrakis(1-methylethyl)disiloxanyl]-cytidine: HRMS calcd for $C_{26}H_{48}N_4O_7SSi_2$ 616.2782, found 616.2779.
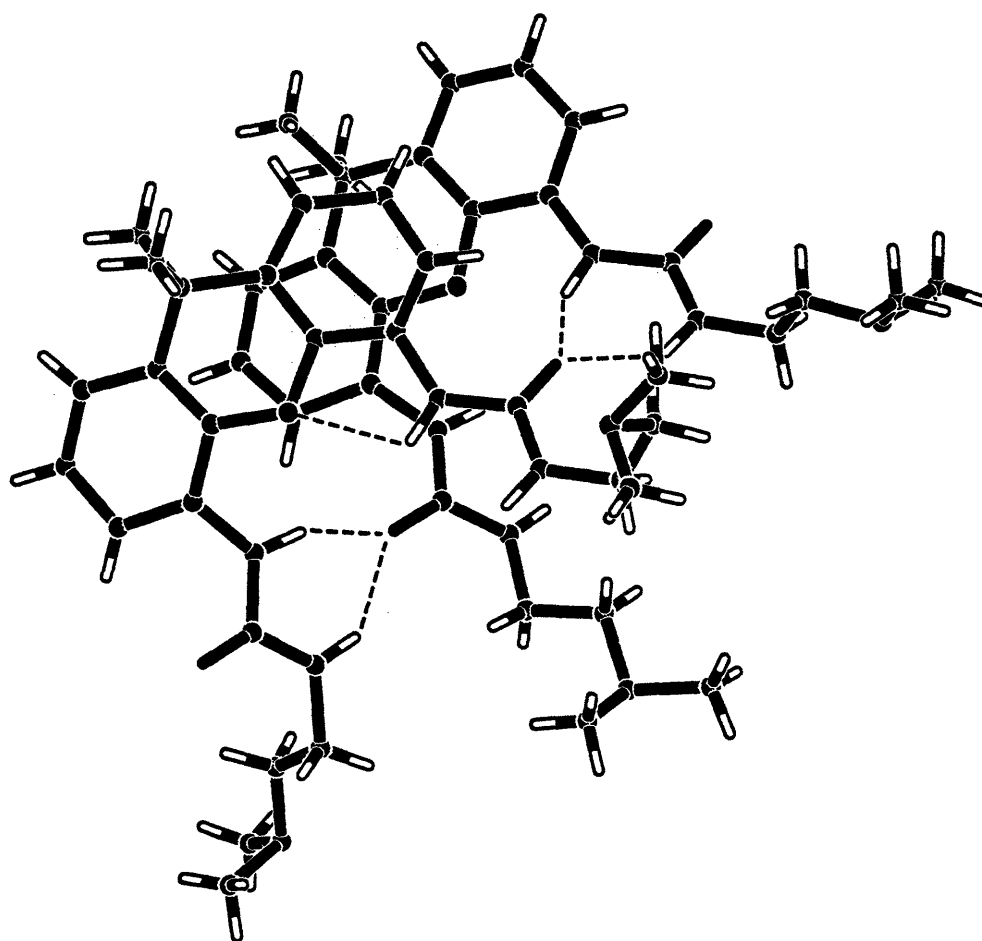
Fragments 1and 2 from crystal structure of **48**.
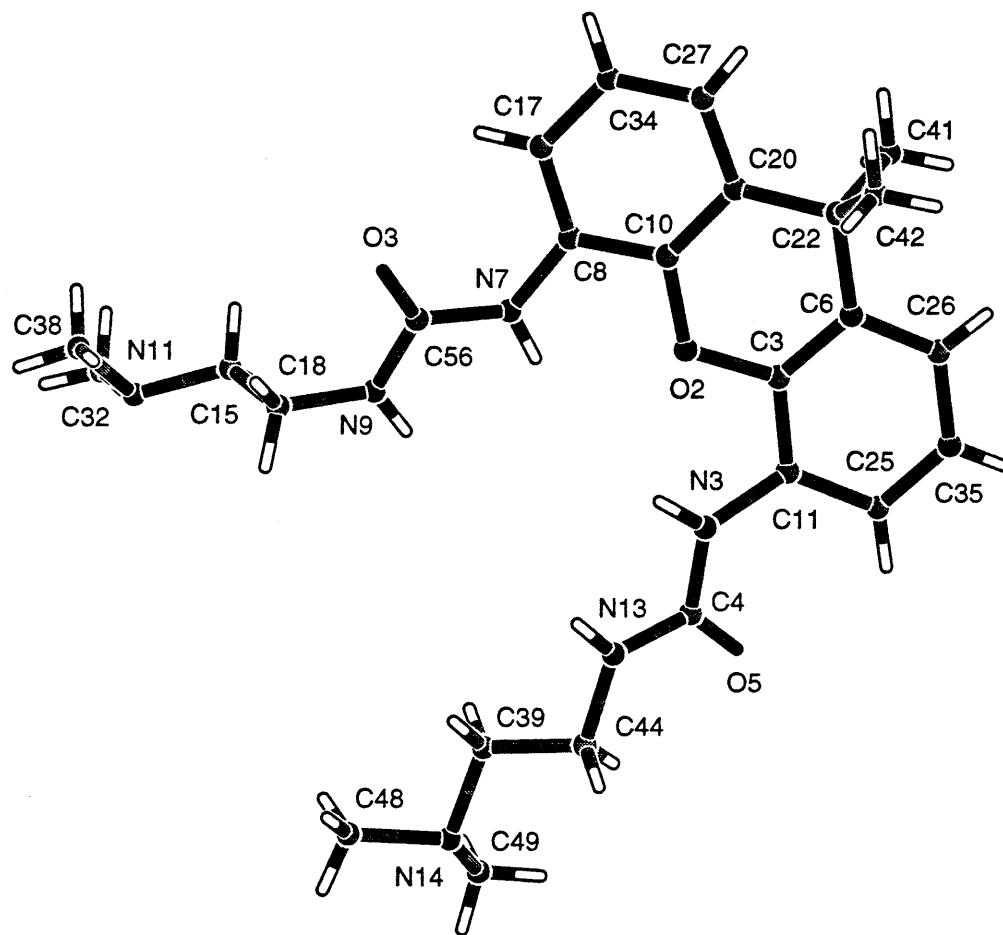
Fragment 1 from crystal structure of **48**.
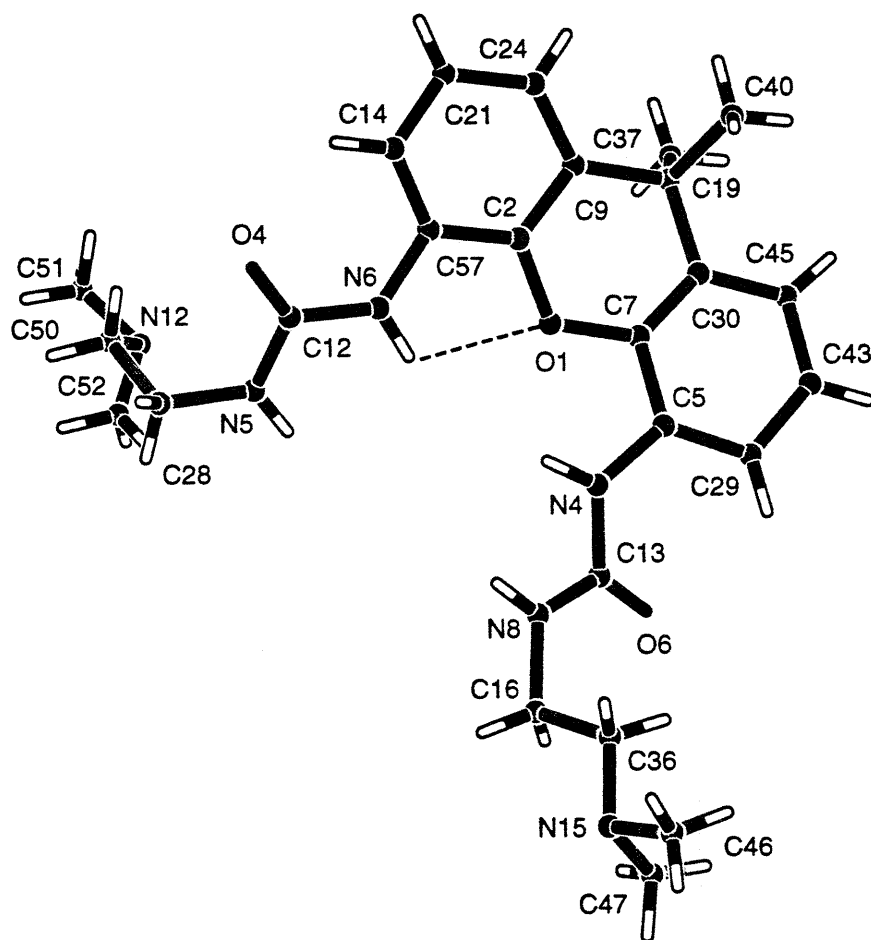
Fragment 2 from crystal structure of **48**.

Crystallographic Data for compound 48

Table 1:   Crystallographic parameters for compound 48.

Empirical formula[a]	$C_{41}H_{50}N_4O_3$
a (Å)	11.667(5)
b (Å)	24.22(1)
c (Å)	18.486(7)
β (deg)	96.86(2)
Volume ($Å^3$)	5186(3)
crystal size (mm)	0.4x0.2x0.2
space group,	$P2_1/n$
Z	8
ρ_{calc} (g/cm^3)	1.454
F_{000}	2408.00
μ (cm^{-1})	1.13
radiation, λ (Å)	Mo-Ka' (0.710690)
2θ limit (deg)	46.6
temperature (°C)	23.0
total reflections	18948
unique reflections	7499
no. of observations ($I>3\sigma$, $2.8\theta<40.3°$)	2911
no. of parameters	533
R (R_w)[a]	0.115 (0.096)
largest diff. peak and hole ($e^-Å^{-3}$)	0.05, -0.50

[a] $R = \sum \|Fo| - |Fc\| / \sum |Fo|$, $R_w = \sqrt{\left(\sum_w (|Fo|-|Fc|)^2 / \sum_w Fo^2\right)}$]

Positional parameters and B(eq)

atom	x	y	z	B(eq)
O(1)	0.0215(6)	0.3879(3)	-0.3796(4)	4.4(2)
O(2)	-0.0426(6)	0.3920(3)	-0.1163(4)	4.3(2)
O(3)	0.1725(7)	0.4749(3)	0.0814(5)	6.4(3)
O(4)	0.2017(7)	0.4847(3)	-0.1671(4)	6.0(2)
O(5)	-0.1429(6)	0.4993(3)	-0.3266(4)	5.3(2)
O(6)	-0.1743(6)	0.4860(3)	-0.5771(4)	5.9(2)
N(3)	-0.1288(7)	0.4634(4)	-0.2111(5)	4.4(3)
N(4)	-0.1138(7)	0.4492(4)	-0.4658(5)	4.6(3)
N(5)	0.2106(8)	0.5366(4)	-0.2687(5)	4.6(3)
N(6)	0.1375(7)	0.4503(4)	-0.2795(5)	3.4(2)
N(7)	0.1236(8)	0.4389(4)	-0.0316(5)	4.7(3)
N(8)	-0.1729(8)	0.5384(4)	-0.4750(5)	4.8(3)
N(9)	0.2034(8)	0.5253(4)	-0.0175(5)	4.8(3)
N(11)	0.4552(8)	0.6122(4)	0.0497(6)	5.4(2)
N(12)	0.472(2)	0.5463(9)	-0.270(1)	14.2(6)
N(13)	-0.1212(9)	0.5557(4)	-0.2281(5)	5.5(3)
N(14)	-0.036(1)	0.6977(7)	-0.2687(10)	12.4(4)
N(15)	-0.429(1)	0.6200(6)	-0.5487(9)	10.5(4)
C(2)	0.0798(9)	0.3602(5)	-0.3214(6)	3.7(3)
C(3)	-0.1179(10)	0.3684(5)	-0.1721(7)	4.2(4)
C(4)	-0.1317(9)	0.5056(5)	-0.2589(7)	3.7(3)
C(5)	-0.116(1)	0.3926(5)	-0.4802(7)	4.3(3)
C(6)	-0.1469(10)	0.3137(5)	-0.1735(7)	4.3(4)
C(7)	-0.0451(10)	0.3587(6)	-0.4315(6)	3.9(3)
C(8)	0.095(1)	0.3850(5)	-0.0150(7)	4.5(4)
C(9)	0.084(1)	0.3022(5)	-0.3192(7)	5.0(4)
C(10)	0.0092(10)	0.3572(6)	-0.0628(6)	4.2(4)
C(11)	-0.1569(8)	0.4064(5)	-0.2254(6)	3.4(3)
C(12)	0.1842(9)	0.4908(5)	-0.2335(7)	3.7(3)
C(13)	-0.1554(9)	0.4917(5)	-0.5110(7)	4.3(3)
C(14)	0.195(1)	0.3690(5)	-0.2081(7)	4.8(4)
C(15)	0.389(1)	0.5641(5)	0.0220(7)	5.5(3)
C(16)	-0.232(1)	0.5867(5)	-0.5110(7)	6.5(4)
C(17)	0.153(1)	0.3556(6)	0.0421(7)	6.1(4)
C(18)	0.2626(10)	0.5692(5)	0.0206(7)	5.5(4)
C(19)	0.028(1)	0.2688(5)	-0.3835(7)	5.7(4)
C(20)	-0.020(1)	0.3023(5)	-0.0564(7)	4.8(4)
C(21)	0.197(1)	0.3124(7)	-0.1993(8)	6.4(4)

Positional parameters and B(eq)

atom	x	y	z	B(eq)
C(22)	-0.111(1)	0.2758(5)	-0.1096(7)	5.1(4)
C(24)	0.144(1)	0.2796(5)	-0.2571(8)	5.5(4)
C(25)	-0.2272(9)	0.3869(6)	-0.2883(6)	5.0(3)
C(26)	-0.218(1)	0.2958(5)	-0.2335(8)	5.5(4)
C(27)	0.039(1)	0.2748(6)	0.0027(9)	7.3(5)
C(28)	0.276(1)	0.5799(5)	-0.2297(7)	6.0(4)
C(29)	-0.191(1)	0.3722(6)	-0.5373(9)	8.4(5)
C(30)	-0.048(1)	0.3035(6)	-0.4368(7)	5.5(4)
C(32)	0.576(1)	0.6080(6)	0.0345(8)	7.7(4)
C(34)	0.123(1)	0.3005(7)	0.0491(8)	7.4(5)
C(35)	-0.256(1)	0.3320(6)	-0.2890(8)	6.3(4)
C(36)	-0.366(1)	0.5759(6)	-0.5194(8)	8.2(4)
C(37)	0.129(1)	0.2461(6)	-0.4217(8)	9.0(5)
C(38)	0.453(1)	0.6176(6)	0.1268(9)	8.3(4)
C(39)	-0.033(1)	0.6441(7)	-0.2333(9)	9.7(4)
C(40)	-0.042(1)	0.2196(5)	-0.3559(7)	7.8(4)
C(41)	-0.064(1)	0.2209(5)	-0.1356(7)	6.8(4)
C(42)	-0.215(1)	0.2637(6)	-0.0706(9)	8.9(5)
C(43)	-0.191(1)	0.3135(8)	-0.5382(9)	8.9(6)
C(44)	-0.121(2)	0.6059(6)	-0.2688(9)	10.3(5)
C(45)	-0.122(2)	0.2796(6)	-0.4912(10)	8.8(6)
C(46)	-0.552(2)	0.6057(7)	-0.538(1)	11.6(5)
C(47)	-0.419(2)	0.6207(9)	-0.628(2)	16.2(7)
C(48)	0.036(2)	0.7344(9)	-0.219(1)	14.8(7)
C(49)	0.007(2)	0.6959(9)	-0.341(1)	15.8(7)
C(50)	0.399(2)	0.565(1)	-0.204(2)	18.0(8)
C(51)	0.562(4)	0.541(2)	-0.224(3)	32(1)
C(52)	0.452(3)	0.589(2)	-0.291(2)	27(1)
C(56)	0.1683(10)	0.4799(6)	0.0152(8)	4.8(4)
C(57)	0.1358(9)	0.3931(5)	-0.2661(6)	3.7(3)
H(1)	-0.107364997	0.472799987	-0.159383997	6.157680035
H(2)	-0.077500001	0.460211992	-0.416970998	6.173639774
H(3)	0.188951001	0.541262984	-0.322362989	6.058800220
H(4)	0.097179003	0.461739987	-0.326299995	4.756559849
H(5)	0.106388003	0.449259013	-0.082856998	5.872200012
H(6)	-0.148166001	0.541975975	-0.422583014	6.153600216
H(7)	0.191118002	0.528640985	-0.071011998	6.221640110
H(8)	-0.111102998	0.558934987	-0.175375000	6.953159809

Positional parameters and B(eq)

atom	x	y	z	B(eq)
H(9)	0.235669002	0.391681999	-0.169139996	5.983560085
H(10)	0.408428013	0.555918992	-0.026590001	7.083088875
H(11)	0.415118992	0.531740010	0.051507000	7.083088875
H(12)	-0.213938996	0.622098982	-0.484896988	8.250479698
H(13)	-0.203844994	0.593903005	-0.559215009	8.250479698
H(14)	0.213511005	0.373625010	0.076470003	8.046360016
H(15)	0.237919003	0.605230987	-0.002179000	7.568999767
H(16)	0.240714997	0.571328998	0.069204003	7.568999767
H(17)	0.238113001	0.295747995	-0.155252993	8.160719872
H(18)	0.146127999	0.238850996	-0.250187993	7.535039902
H(19)	-0.254732013	0.412001997	-0.328496993	7.135079861
H(20)	-0.242547005	0.257362008	-0.235113993	7.297200203
H(21)	0.024003999	0.236772999	0.010779000	8.954039574
H(22)	0.277027011	0.613569975	-0.261566997	8.486160278
H(23)	0.234887004	0.592038989	-0.190256998	8.486160278
H(24)	-0.241007999	0.395958990	-0.572535992	10.752599716
H(25)	0.613041997	0.574822009	0.057682000	8.912335396
H(26)	0.581560016	0.605107009	-0.015959000	8.912335396
H(27)	0.620908976	0.638679981	0.054088999	8.912335396
H(28)	0.166484997	0.279273003	0.090097003	9.097920418
H(29)	-0.305133998	0.318060994	-0.331566989	8.109479904
H(30)	-0.390556991	0.564751983	-0.473067999	11.034994125
H(31)	-0.383228987	0.541512012	-0.550575972	11.034994125
H(32)	0.183151007	0.223298997	-0.390325010	9.869761467
H(33)	0.102209002	0.222473994	-0.463281006	9.869761467
H(34)	0.172982007	0.275101990	-0.440030009	9.869761467
H(35)	0.489459008	0.588631988	0.155755997	10.714858055
H(36)	0.493992001	0.652136028	0.145559996	10.714858055
H(37)	0.375824004	0.622137010	0.140469998	10.714858055
H(38)	0.046395998	0.626999021	-0.233486995	12.392908096
H(39)	-0.039177999	0.647189021	-0.181067005	12.392908096
H(40)	-0.105232000	0.232253999	-0.333481997	9.818280220
H(41)	-0.072163001	0.195956007	-0.396952987	9.818280220
H(42)	0.004799000	0.195798993	-0.322466999	9.818280220
H(43)	-0.041009001	0.195653006	-0.095716000	8.306640625
H(44)	-0.117592998	0.201954007	-0.169842005	8.306640625
H(45)	0.005482000	0.227184996	-0.159193993	8.306640625
H(46)	-0.247955993	0.296957999	-0.051734000	9.551879883

Positional parameters and B(eq)

atom	x	y	z	B(eq)
H(47)	-0.278290004	0.245816007	-0.100831002	9.551879883
H(48)	-0.198484004	0.239444003	-0.027936000	9.551879883
H(49)	-0.247893006	0.296889007	-0.577816010	10.338359833
H(50)	-0.106803000	0.598812997	-0.319292992	11.997000694
H(51)	-0.196009994	0.624414027	-0.273185015	11.997000694
H(52)	-0.131426007	0.238892004	-0.498082012	11.180280685
H(53)	-0.606757998	0.632948995	-0.555338025	13.515004158
H(54)	-0.579590023	0.570463002	-0.560334027	13.515004158
H(55)	-0.560676992	0.600356996	-0.485639989	13.515004158
H(56)	-0.342848003	0.627381027	-0.638772011	17.507541656
H(57)	-0.454190999	0.592283010	-0.654904008	17.507541656
H(58)	-0.462698996	0.655960023	-0.648266971	17.507541656
H(59)	0.116293997	0.724067986	-0.210810006	16.600648880
H(60)	0.036448002	0.772728026	-0.238613993	16.600648880
H(61)	0.009721000	0.738520980	-0.171684995	16.600648880
H(62)	0.082062997	0.683902025	-0.343591988	19.208780289
H(63)	-0.043880001	0.671257019	-0.376327991	19.208780289
H(64)	-0.002060000	0.731939018	-0.367325991	19.208780289
H(65)	0.392816007	0.537755013	-0.168753996	23.084514618
H(66)	0.430714995	0.598556995	-0.177332997	23.084514618
H(67)	0.551011026	0.511263013	-0.184009001	38.314125061
H(68)	0.629085004	0.526628971	-0.243265003	38.314125061
H(69)	0.590505004	0.571892977	-0.191946000	38.314125061
H(70)	0.477815002	0.621752024	-0.261070997	31.968555450
H(71)	0.485983014	0.596081018	-0.337170005	31.968555450
H(72)	0.368849009	0.596651018	-0.305326998	31.968555450

Intramolecular Distances

atom	atom	distance	atom	atom	distance
O(1)	C(2)	1.38(1)	N(9)	C(18)	1.41(1)
O(1)	C(7)	1.36(1)	N(9)	C(56)	1.34(1)
O(2)	C(3)	1.40(1)	N(9)	H(7)	0.987
O(2)	C(10)	1.38(1)	N(11)	C(15)	1.45(1)
O(3)	C(56)	1.22(1)	N(11)	C(32)	1.47(1)
O(4)	C(12)	1.23(1)	N(11)	C(38)	1.43(2)
O(5)	C(4)	1.25(1)	N(12)	C(50)	1.62(3)
O(6)	C(13)	1.22(1)	N(12)	C(51)	1.27(4)
N(3)	C(4)	1.35(1)	N(12)	C(52)	1.12(4)
N(3)	C(11)	1.44(1)	N(13)	C(4)	1.34(1)
N(3)	H(1)	0.986	N(13)	C(44)	1.43(2)
N(4)	C(5)	1.40(1)	N(13)	H(8)	0.971
N(4)	C(13)	1.38(1)	N(14)	C(39)	1.45(2)
N(4)	H(2)	0.987	N(14)	C(48)	1.47(2)
N(5)	C(12)	1.34(1)	N(14)	C(49)	1.48(3)
N(5)	C(28)	1.44(1)	N(15)	C(36)	1.37(2)
N(5)	H(3)	1.000	N(15)	C(46)	1.51(2)
N(6)	C(12)	1.37(1)	N(15)	C(47)	1.49(2)
N(6)	C(57)	1.41(1)	C(2)	C(9)	1.41(1)
N(6)	H(4)	0.975	C(2)	C(57)	1.40(1)
N(7)	C(8)	1.39(1)	C(3)	C(6)	1.37(1)
N(7)	C(56)	1.38(1)	C(3)	C(11)	1.38(1)
N(7)	H(5)	0.978	C(5)	C(7)	1.41(1)
N(8)	C(13)	1.34(1)	C(5)	C(29)	1.38(2)
N(8)	C(16)	1.47(1)	C(6)	C(22)	1.52(2)
N(8)	H(6)	0.981	C(6)	C(26)	1.37(2)

Distances are in angstroms. Estimated standard deviations in the least significant figure are given in parentheses.

Intramolecular Distances

atom	atom	distance	atom	atom	distance
C(7)	C(30)	1.34(1)	C(21)	H(17)	0.981
C(8)	C(10)	1.42(1)	C(22)	C(41)	1.53(2)
C(8)	C(17)	1.38(2)	C(22)	C(42)	1.52(2)
C(9)	C(19)	1.52(2)	C(24)	H(18)	0.994
C(9)	C(24)	1.38(2)	C(25)	C(35)	1.37(2)
C(10)	C(20)	1.38(1)	C(25)	H(19)	0.985
C(11)	C(25)	1.42(1)	C(26)	C(35)	1.38(2)
C(14)	C(21)	1.38(2)	C(26)	H(20)	0.973
C(14)	C(57)	1.34(1)	C(27)	C(34)	1.38(2)
C(14)	H(9)	0.983	C(27)	H(21)	0.953
C(15)	C(18)	1.48(1)	C(28)	C(50)	1.50(3)
C(15)	H(10)	0.971	C(28)	H(22)	1.007
C(15)	H(11)	0.980	C(28)	H(23)	0.964
C(16)	C(36)	1.58(2)	C(29)	C(43)	1.42(2)
C(16)	H(12)	0.994	C(29)	H(24)	1.003
C(16)	H(13)	1.000	C(30)	C(45)	1.37(2)
C(17)	C(34)	1.39(2)	C(32)	H(25)	0.987
C(17)	H(14)	0.997	C(32)	H(26)	0.946
C(18)	H(15)	0.997	C(32)	H(27)	0.959
C(18)	H(16)	0.965	C(34)	H(28)	1.001
C(19)	C(30)	1.50(2)	C(35)	H(29)	0.979
C(19)	C(37)	1.54(2)	C(36)	H(30)	0.972
C(19)	C(40)	1.57(2)	C(36)	H(31)	1.018
C(20)	C(22)	1.50(2)	C(37)	H(32)	0.978
C(20)	C(27)	1.39(2)	C(37)	H(33)	0.978
C(21)	C(24)	1.41(2)	C(37)	H(34)	0.956

Distances are in angstroms. Estimated standard deviations in the least significant figure are given in parentheses.

Intramolecular Distances

atom	atom	distance	atom	atom	distance
C(38)	H(35)	0.950	C(48)	H(59)	0.963
C(38)	H(36)	1.002	C(48)	H(60)	0.999
C(38)	H(37)	0.976	C(48)	H(61)	0.963
C(39)	C(44)	1.48(2)	C(49)	H(62)	0.933
C(39)	H(38)	1.017	C(49)	H(63)	1.019
C(39)	H(39)	0.980	C(49)	H(64)	0.998
C(40)	H(40)	0.940	C(50)	H(65)	0.939
C(40)	H(41)	0.982	C(50)	H(66)	1.007
C(40)	H(42)	0.964	C(51)	H(67)	1.051
C(41)	H(43)	0.971	C(51)	H(68)	0.964
C(41)	H(44)	0.952	C(51)	H(69)	0.988
C(41)	H(45)	0.979	C(52)	H(70)	0.987
C(42)	H(46)	0.972	C(52)	H(71)	1.007
C(42)	H(47)	0.970	C(52)	H(72)	0.989
C(42)	H(48)	0.985			
C(43)	C(45)	1.38(2)			
C(43)	H(49)	1.008			
C(44)	H(50)	0.985			
C(44)	H(51)	0.973			
C(45)	H(52)	0.998			
C(46)	H(53)	0.946			
C(46)	H(54)	0.983			
C(46)	H(55)	0.998			
C(47)	H(56)	0.941			
C(47)	H(57)	0.916			
C(47)	H(58)	1.043			

Distances are in angstroms. Estimated standard deviations in the least significant figure are given in parentheses.

Intramolecular Bond Angles Involving the Nonhydrogen Atoms

atom	atom	atom	angle	atom	atom	atom	angle
C(2)	O(1)	C(7)	119.1(9)	O(2)	C(3)	C(11)	112(1)
C(3)	O(2)	C(10)	117.6(9)	C(6)	C(3)	C(11)	125(1)
C(4)	N(3)	C(11)	128(1)	O(5)	C(4)	N(3)	124(1)
C(5)	N(4)	C(13)	128(1)	O(5)	C(4)	N(13)	122(1)
C(12)	N(5)	C(28)	120(1)	N(3)	C(4)	N(13)	114(1)
C(12)	N(6)	C(57)	127.6(9)	N(4)	C(5)	C(7)	117(1)
C(8)	N(7)	C(56)	128(1)	N(4)	C(5)	C(29)	119(1)
C(13)	N(8)	C(16)	122(1)	C(7)	C(5)	C(29)	123(1)
C(18)	N(9)	C(56)	124(1)	C(3)	C(6)	C(22)	122(1)
C(15)	N(11)	C(32)	111(1)	C(3)	C(6)	C(26)	116(1)
C(15)	N(11)	C(38)	111(1)	C(22)	C(6)	C(26)	122(1)
C(32)	N(11)	C(38)	109(1)	O(1)	C(7)	C(5)	113(1)
C(50)	N(12)	C(51)	90(3)	O(1)	C(7)	C(30)	125(1)
C(50)	N(12)	C(52)	84(3)	C(5)	C(7)	C(30)	122(1)
C(51)	N(12)	C(52)	117(4)	N(7)	C(8)	C(10)	119(1)
C(4)	N(13)	C(44)	124(1)	N(7)	C(8)	C(17)	123(1)
C(39)	N(14)	C(48)	106(2)	C(10)	C(8)	C(17)	118(1)
C(39)	N(14)	C(49)	113(2)	C(2)	C(9)	C(19)	120(1)
C(48)	N(14)	C(49)	111(2)	C(2)	C(9)	C(24)	116(1)
C(36)	N(15)	C(46)	104(1)	C(19)	C(9)	C(24)	124(1)
C(36)	N(15)	C(47)	107(2)	O(2)	C(10)	C(8)	112(1)
C(46)	N(15)	C(47)	109(1)	O(2)	C(10)	C(20)	124(1)
O(1)	C(2)	C(9)	121(1)	C(8)	C(10)	C(20)	124(1)
O(1)	C(2)	C(57)	116(1)	N(3)	C(11)	C(3)	117(1)
C(9)	C(2)	C(57)	122(1)	N(3)	C(11)	C(25)	125(1)
O(2)	C(3)	C(6)	123(1)	C(3)	C(11)	C(25)	118(1)

Angles are in degrees. Estimated standard deviations in the least significant figure are in parentheses.

Intramolecular Bond Angles Involving the Nonhydrogen Atoms

atom	atom	atom	angle	atom	atom	atom	angle
O(4)	C(12)	N(5)	124(1)	C(41)	C(22)	C(42)	108(1)
O(4)	C(12)	N(6)	123(1)	C(9)	C(24)	C(21)	122(1)
N(5)	C(12)	N(6)	113(1)	C(11)	C(25)	C(35)	117(1)
O(6)	C(13)	N(4)	122(1)	C(6)	C(26)	C(35)	120(1)
O(6)	C(13)	N(8)	125(1)	C(20)	C(27)	C(34)	121(1)
N(4)	C(13)	N(8)	113(1)	N(5)	C(28)	C(50)	114(1)
C(21)	C(14)	C(57)	122(1)	C(5)	C(29)	C(43)	112(1)
N(11)	C(15)	C(18)	115(1)	C(7)	C(30)	C(19)	120(1)
N(8)	C(16)	C(36)	108(1)	C(7)	C(30)	C(45)	119(1)
C(8)	C(17)	C(34)	118(1)	C(19)	C(30)	C(45)	121(1)
N(9)	C(18)	C(15)	112(1)	C(17)	C(34)	C(27)	123(1)
C(9)	C(19)	C(30)	112(1)	C(25)	C(35)	C(26)	124(1)
C(9)	C(19)	C(37)	106(1)	N(15)	C(36)	C(16)	113(1)
C(9)	C(19)	C(40)	110(1)	N(14)	C(39)	C(44)	113(1)
C(30)	C(19)	C(37)	109(1)	C(29)	C(43)	C(45)	126(1)
C(30)	C(19)	C(40)	110(1)	N(13)	C(44)	C(39)	110(1)
C(37)	C(19)	C(40)	110(1)	C(30)	C(45)	C(43)	119(1)
C(10)	C(20)	C(22)	121(1)	N(12)	C(50)	C(28)	114(2)
C(10)	C(20)	C(27)	115(1)	O(3)	C(56)	N(7)	122(1)
C(22)	C(20)	C(27)	124(1)	O(3)	C(56)	N(9)	124(1)
C(14)	C(21)	C(24)	118(1)	N(7)	C(56)	N(9)	115(1)
C(6)	C(22)	C(20)	111(1)	N(6)	C(57)	C(2)	117(1)
C(6)	C(22)	C(41)	111(1)	N(6)	C(57)	C(14)	124(1)
C(6)	C(22)	C(42)	109(1)	C(2)	C(57)	C(14)	119(1)
C(20)	C(22)	C(41)	109(1)				
C(20)	C(22)	C(42)	108(1)				

Angles are in degrees. Estimated standard deviations in the least significant figure are gi·
in parentheses.

Torsion or Conformation Angles

(1)	(2)	(3)	(4)	angle	(1)	(2)	(3)	(4)	angle
O(1)	C(2)	C(9)	C(19)	3(2)	O(5)	C(4)	N(13)	C(44)	0(2)
O(1)	C(2)	C(9)	C(24)	-179(1)	O(5)	C(4)	N(13)	H(8)	-179
O(1)	C(2)	C(57)	N(6)	-7(1)	O(6)	C(13)	N(4)	C(5)	-19(2)
O(1)	C(2)	C(57)	C(14)	-179(1)	O(6)	C(13)	N(4)	H(2)	161
O(1)	C(7)	C(5)	N(4)	-5(1)	O(6)	C(13)	N(8)	C(16)	8(2)
O(1)	C(7)	C(5)	C(29)	-180(1)	O(6)	C(13)	N(8)	H(6)	-173
O(1)	C(7)	C(30)	C(19)	-2(2)	N(3)	C(4)	N(13)	C(44)	180(1)
O(1)	C(7)	C(30)	C(45)	178(1)	N(3)	C(4)	N(13)	H(8)	1
O(2)	C(3)	C(6)	C(22)	8(2)	N(3)	C(11)	C(3)	C(6)	173(1)
O(2)	C(3)	C(6)	C(26)	-177(1)	N(3)	C(11)	C(25)	C(35)	-173(1)
O(2)	C(3)	C(11)	N(3)	-8(1)	N(3)	C(11)	C(25)	H(19)	6
O(2)	C(3)	C(11)	C(25)	175.2(9)	N(4)	C(5)	C(7)	C(30)	174(1)
O(2)	C(10)	C(8)	N(7)	-7(1)	N(4)	C(5)	C(29)	C(43)	-173(1)
O(2)	C(10)	C(8)	C(17)	179(1)	N(4)	C(5)	C(29)	H(24)	6
O(2)	C(10)	C(20)	C(22)	1(2)	N(4)	C(13)	N(8)	C(16)	-171(1)
O(2)	C(10)	C(20)	C(27)	-177(1)	N(4)	C(13)	N(8)	H(6)	7
O(3)	C(56)	N(7)	C(8)	-11(2)	N(5)	C(12)	N(6)	C(57)	157(1)
O(3)	C(56)	N(7)	H(5)	166	N(5)	C(12)	N(6)	H(4)	-26
O(3)	C(56)	N(9)	C(18)	9(2)	N(5)	C(28)	C(50)	N(12)	58(2)
O(3)	C(56)	N(9)	H(7)	-174	N(5)	C(28)	C(50)	H(65)	-68
O(4)	C(12)	N(5)	C(28)	8(2)	N(5)	C(28)	C(50)	H(66)	-178
O(4)	C(12)	N(5)	H(3)	-175	N(6)	C(12)	N(5)	C(28)	-170.9(9)
O(4)	C(12)	N(6)	C(57)	-22(2)	N(6)	C(12)	N(5)	H(3)	7
O(4)	C(12)	N(6)	H(4)	155	N(6)	C(57)	C(2)	C(9)	172(1)
O(5)	C(4)	N(3)	C(11)	-12(2)	N(6)	C(57)	C(14)	C(21)	-176(1)
O(5)	C(4)	N(3)	H(1)	171	N(6)	C(57)	C(14)	H(9)	7

The sign is positive if when looking from atom 2 to atom 3 a clockwise motion of atom 1 would superimpose it on atom 4.

Torsion or Conformation Angles

(1)	(2)	(3)	(4)	angle	(1)	(2)	(3)	(4)	angle
N(7)	C(8)	C(10)	C(20)	174(1)	N(15)	C(36)	C(16)	H(12)	51
N(7)	C(8)	C(17)	C(34)	-174(1)	N(15)	C(36)	C(16)	H(13)	-61
N(7)	C(8)	C(17)	H(14)	5	C(2)	O(1)	C(7)	C(5)	169.1(9)
N(7)	C(56)	N(9)	C(18)	-173(1)	C(2)	O(1)	C(7)	C(30)	-9(2)
N(7)	C(56)	N(9)	H(7)	4	C(2)	C(9)	C(19)	C(30)	-12(2)
N(8)	C(13)	N(4)	C(5)	161(1)	C(2)	C(9)	C(19)	C(37)	106(1)
N(8)	C(13)	N(4)	H(2)	-20	C(2)	C(9)	C(19)	C(40)	-135(1)
N(8)	C(16)	C(36)	N(15)	176(1)	C(2)	C(9)	C(24)	C(21)	0(2)
N(8)	C(16)	C(36)	H(30)	51	C(2)	C(9)	C(24)	H(18)	176
N(8)	C(16)	C(36)	H(31)	-61	C(2)	C(57)	N(6)	C(12)	178(1)
N(9)	C(18)	C(15)	N(11)	170(1)	C(2)	C(57)	N(6)	H(4)	1
N(9)	C(18)	C(15)	H(10)	48	C(2)	C(57)	C(14)	C(21)	-3(2)
N(9)	C(18)	C(15)	H(11)	-67	C(2)	C(57)	C(14)	H(9)	179
N(9)	C(56)	N(7)	C(8)	171(1)	C(3)	O(2)	C(10)	C(8)	172.2(9)
N(9)	C(56)	N(7)	H(5)	-13	C(3)	O(2)	C(10)	C(20)	-8(1)
N(11)	C(15)	C(18)	H(15)	48	C(3)	C(6)	C(22)	C(20)	-13(2)
N(11)	C(15)	C(18)	H(16)	-66	C(3)	C(6)	C(22)	C(41)	-135(1)
N(12)	C(50)	C(28)	H(22)	-64	C(3)	C(6)	C(22)	C(42)	106(1)
N(12)	C(50)	C(28)	H(23)	-178	C(3)	C(6)	C(26)	C(35)	1(2)
N(13)	C(4)	N(3)	C(11)	168(1)	C(3)	C(6)	C(26)	H(20)	-178
N(13)	C(4)	N(3)	H(1)	-9	C(3)	C(11)	N(3)	C(4)	163(1)
N(13)	C(44)	C(39)	N(14)	-175(1)	C(3)	C(11)	N(3)	H(1)	-20
N(13)	C(44)	C(39)	H(38)	63	C(3)	C(11)	C(25)	C(35)	3(2)
N(13)	C(44)	C(39)	H(39)	-49	C(3)	C(11)	C(25)	H(19)	-178
N(14)	C(39)	C(44)	H(50)	62	C(4)	N(3)	C(11)	C(25)	-21(2)
N(14)	C(39)	C(44)	H(51)	-52	C(4)	N(13)	C(44)	C(39)	-139(1)

The sign is positive if when looking from atom 2 to atom 3 a clockwise motion of atom 1 would superimpose it on atom 4.

Torsion or Conformation Angles

(1)	(2)	(3)	(4)	angle	(1)	(2)	(3)	(4)	angle
C(4)	N(13)	C(44)	H(50)	-17	C(7)	C(30)	C(19)	C(40)	135(1)
C(4)	N(13)	C(44)	H(51)	100	C(7)	C(30)	C(45)	C(43)	-1(2)
C(5)	C(7)	C(30)	C(19)	-180(1)	C(7)	C(30)	C(45)	H(52)	-178
C(5)	C(7)	C(30)	C(45)	0(2)	C(8)	C(10)	C(20)	C(22)	-179(1)
C(5)	C(29)	C(43)	C(45)	-3(3)	C(8)	C(10)	C(20)	C(27)	2(2)
C(5)	C(29)	C(43)	H(49)	178	C(8)	C(17)	C(34)	C(27)	-1(2)
C(6)	C(3)	O(2)	C(10)	4(1)	C(8)	C(17)	C(34)	H(28)	179
C(6)	C(3)	C(11)	C(25)	-4(2)	C(9)	C(2)	C(57)	C(14)	-1(2)
C(6)	C(22)	C(20)	C(10)	9(2)	C(9)	C(19)	C(30)	C(45)	-168(1)
C(6)	C(22)	C(20)	C(27)	-172(1)	C(9)	C(19)	C(37)	H(32)	59
C(6)	C(22)	C(41)	H(43)	-179	C(9)	C(19)	C(37)	H(33)	178
C(6)	C(22)	C(41)	H(44)	-57	C(9)	C(19)	C(37)	H(34)	-62
C(6)	C(22)	C(41)	H(45)	63	C(9)	C(19)	C(40)	H(40)	66
C(6)	C(22)	C(42)	H(46)	-61	C(9)	C(19)	C(40)	H(41)	-175
C(6)	C(22)	C(42)	H(47)	60	C(9)	C(19)	C(40)	H(42)	-57
C(6)	C(22)	C(42)	H(48)	-180	C(9)	C(24)	C(21)	C(14)	-4(2)
C(6)	C(26)	C(35)	C(25)	-1(2)	C(9)	C(24)	C(21)	H(17)	179
C(6)	C(26)	C(35)	H(29)	179	C(10)	O(2)	C(3)	C(11)	-174.9(9)
C(7)	O(1)	C(2)	C(9)	9(2)	C(10)	C(8)	N(7)	C(56)	154(1)
C(7)	O(1)	C(2)	C(57)	-172.9(9)	C(10)	C(8)	N(7)	H(5)	-23
C(7)	C(5)	N(4)	C(13)	166(1)	C(10)	C(8)	C(17)	C(34)	0(2)
C(7)	C(5)	N(4)	H(2)	-13	C(10)	C(8)	C(17)	H(14)	179
C(7)	C(5)	C(29)	C(43)	2(2)	C(10)	C(20)	C(22)	C(41)	132(1)
C(7)	C(5)	C(29)	H(24)	-179	C(10)	C(20)	C(22)	C(42)	-110(1)
C(7)	C(30)	C(19)	C(9)	12(2)	C(10)	C(20)	C(27)	C(34)	-3(2)
C(7)	C(30)	C(19)	C(37)	-105(1)	C(10)	C(20)	C(27)	H(21)	-180

The sign is positive if when looking from atom 2 to atom 3 a clockwise motion of atom 1 would superimpose it on atom 4.

Torsion or Conformation Angles

(1)	(2)	(3)	(4)	angle	(1)	(2)	(3)	(4)	angle
C(11)	C(3)	C(6)	C(22)	-174(1)	C(17)	C(8)	C(10)	C(20)	0(2)
C(11)	C(3)	C(6)	C(26)	1(2)	C(17)	C(34)	C(27)	C(20)	3(3)
C(11)	C(25)	C(35)	C(26)	-1(2)	C(17)	C(34)	C(27)	H(21)	179
C(11)	C(25)	C(35)	H(29)	179	C(18)	C(15)	N(11)	C(32)	-168(1)
C(12)	N(5)	C(28)	C(50)	69(2)	C(18)	C(15)	N(11)	C(38)	71(1)
C(12)	N(5)	C(28)	H(22)	-171	C(19)	C(9)	C(2)	C(57)	-176(1)
C(12)	N(5)	C(28)	H(23)	-58	C(19)	C(9)	C(24)	C(21)	178(1)
C(12)	N(6)	C(57)	C(14)	-9(2)	C(19)	C(9)	C(24)	H(18)	-6
C(13)	N(4)	C(5)	C(29)	-19(2)	C(19)	C(30)	C(45)	C(43)	179(1)
C(13)	N(8)	C(16)	C(36)	79(1)	C(19)	C(30)	C(45)	H(52)	2
C(13)	N(8)	C(16)	H(12)	-158	C(20)	C(22)	C(6)	C(26)	172(1)
C(13)	N(8)	C(16)	H(13)	-44	C(20)	C(22)	C(41)	H(43)	58
C(14)	C(21)	C(24)	H(18)	-180	C(20)	C(22)	C(41)	H(44)	-180
C(14)	C(57)	N(6)	H(4)	174	C(20)	C(22)	C(41)	H(45)	-60
C(15)	N(11)	C(32)	H(25)	-60	C(20)	C(22)	C(42)	H(46)	60
C(15)	N(11)	C(32)	H(26)	59	C(20)	C(22)	C(42)	H(47)	-179
C(15)	N(11)	C(32)	H(27)	-178	C(20)	C(22)	C(42)	H(48)	-59
C(15)	N(11)	C(38)	H(35)	64	C(20)	C(27)	C(34)	H(28)	-177
C(15)	N(11)	C(38)	H(36)	-176	C(22)	C(6)	C(26)	C(35)	176(1)
C(15)	N(11)	C(38)	H(37)	-60	C(22)	C(6)	C(26)	H(20)	-3
C(15)	C(18)	N(9)	C(56)	96(1)	C(22)	C(20)	C(27)	C(34)	178(1)
C(15)	C(18)	N(9)	H(7)	-82	C(22)	C(20)	C(27)	H(21)	2
C(16)	C(36)	N(15)	C(46)	-169(1)	C(24)	C(9)	C(2)	C(57)	2(2)
C(16)	C(36)	N(15)	C(47)	76(2)	C(24)	C(9)	C(19)	C(30)	170(1)
C(17)	C(8)	N(7)	C(56)	-32(2)	C(24)	C(9)	C(19)	C(37)	-72(2)
C(17)	C(8)	N(7)	H(5)	151	C(24)	C(9)	C(19)	C(40)	47(2)

The sign is positive if when looking from atom 2 to atom 3 a clockwise motion of atom 1 would superimpose it on atom 4.

Torsion or Conformation Angles

(1)	(2)	(3)	(4)	angle	(1)	(2)	(3)	(4)	angle
C(24)	C(21)	C(14)	C(57)	6(2)	C(32)	N(11)	C(38)	H(36)	62
C(24)	C(21)	C(14)	H(9)	-176	C(32)	N(11)	C(38)	H(37)	178
C(25)	C(11)	N(3)	H(1)	156	C(36)	N(15)	C(46)	H(53)	179
C(25)	C(35)	C(26)	H(20)	178	C(36)	N(15)	C(46)	H(54)	-57
C(26)	C(6)	C(22)	C(41)	50(2)	C(36)	N(15)	C(46)	H(55)	59
C(26)	C(6)	C(22)	C(42)	-69(2)	C(36)	N(15)	C(47)	H(56)	-65
C(26)	C(35)	C(25)	H(19)	180	C(36)	N(15)	C(47)	H(57)	68
C(27)	C(20)	C(22)	C(41)	-50(2)	C(36)	N(15)	C(47)	H(58)	-177
C(27)	C(20)	C(22)	C(42)	68(2)	C(36)	C(16)	N(8)	H(6)	-100
C(27)	C(34)	C(17)	H(14)	179	C(37)	C(19)	C(30)	C(45)	75(2)
C(28)	C(50)	N(12)	C(51)	177(3)	C(37)	C(19)	C(40)	H(40)	-178
C(28)	C(50)	N(12)	C(52)	61(3)	C(37)	C(19)	C(40)	H(41)	-59
C(29)	C(5)	N(4)	H(2)	162	C(37)	C(19)	C(40)	H(42)	59
C(29)	C(5)	C(7)	C(30)	-1(2)	C(38)	N(11)	C(15)	H(10)	-165
C(29)	C(43)	C(45)	C(30)	2(3)	C(38)	N(11)	C(15)	H(11)	-51
C(29)	C(43)	C(45)	H(52)	180	C(38)	N(11)	C(32)	H(25)	62
C(30)	C(19)	C(37)	H(32)	179	C(38)	N(11)	C(32)	H(26)	-179
C(30)	C(19)	C(37)	H(33)	-61	C(38)	N(11)	C(32)	H(27)	-56
C(30)	C(19)	C(37)	H(34)	59	C(39)	N(14)	C(48)	H(59)	64
C(30)	C(19)	C(40)	H(40)	-59	C(39)	N(14)	C(48)	H(60)	-178
C(30)	C(19)	C(40)	H(41)	61	C(39)	N(14)	C(48)	H(61)	-60
C(30)	C(19)	C(40)	H(42)	178	C(39)	N(14)	C(49)	H(62)	-60
C(30)	C(45)	C(43)	H(49)	-178	C(39)	N(14)	C(49)	H(63)	62
C(32)	N(11)	C(15)	H(10)	-44	C(39)	N(14)	C(49)	H(64)	175
C(32)	N(11)	C(15)	H(11)	70	C(39)	C(44)	N(13)	H(8)	40
C(32)	N(11)	C(38)	H(35)	-58	C(40)	C(19)	C(30)	C(45)	-45(2)

The sign is positive if when looking from atom 2 to atom 3 a clockwise motion of atom 1 would superimpose it on atom 4.

Torsion or Conformation Angles

(1)	(2)	(3)	(4)	angle	(1)	(2)	(3)	(4)	angle
C(40)	C(19)	C(37)	H(32)	-60	C(48)	N(14)	C(49)	H(64)	-66
C(40)	C(19)	C(37)	H(33)	59	C(49)	N(14)	C(39)	H(38)	51
C(40)	C(19)	C(37)	H(34)	179	C(49)	N(14)	C(39)	H(39)	163
C(41)	C(22)	C(42)	H(46)	179	C(49)	N(14)	C(48)	H(59)	-59
C(41)	C(22)	C(42)	H(47)	-60	C(49)	N(14)	C(48)	H(60)	59
C(41)	C(22)	C(42)	H(48)	60	C(49)	N(14)	C(48)	H(61)	177
C(42)	C(22)	C(41)	H(43)	-60	C(50)	N(12)	C(51)	H(67)	61
C(42)	C(22)	C(41)	H(44)	62	C(50)	N(12)	C(51)	H(68)	175
C(42)	C(22)	C(41)	H(45)	-178	C(50)	N(12)	C(51)	H(69)	-55
C(44)	C(39)	N(14)	C(48)	167(2)	C(50)	N(12)	C(52)	H(70)	61
C(44)	C(39)	N(14)	C(49)	-71(2)	C(50)	N(12)	C(52)	H(71)	-180
C(45)	C(43)	C(29)	H(24)	179	C(50)	N(12)	C(52)	H(72)	-65
C(46)	N(15)	C(36)	H(30)	-44	C(50)	C(28)	N(5)	H(3)	-109
C(46)	N(15)	C(36)	H(31)	69	C(51)	N(12)	C(50)	H(65)	-63
C(46)	N(15)	C(47)	H(56)	-177	C(51)	N(12)	C(50)	H(66)	59
C(46)	N(15)	C(47)	H(57)	-43	C(51)	N(12)	C(52)	H(70)	-26
C(46)	N(15)	C(47)	H(58)	72	C(51)	N(12)	C(52)	H(71)	93
C(47)	N(15)	C(36)	H(30)	-159	C(51)	N(12)	C(52)	H(72)	-152
C(47)	N(15)	C(36)	H(31)	-46	C(52)	N(12)	C(50)	H(65)	-180
C(47)	N(15)	C(46)	H(53)	-67	C(52)	N(12)	C(50)	H(66)	-58
C(47)	N(15)	C(46)	H(54)	57	C(52)	N(12)	C(51)	H(67)	144
C(47)	N(15)	C(46)	H(55)	173	C(52)	N(12)	C(51)	H(68)	-102
C(48)	N(14)	C(39)	H(38)	-71	C(52)	N(12)	C(51)	H(69)	28
C(48)	N(14)	C(39)	H(39)	41	C(56)	N(9)	C(18)	H(15)	-143
C(48)	N(14)	C(49)	H(62)	59	C(56)	N(9)	C(18)	H(16)	-29
C(48)	N(14)	C(49)	H(63)	-179	C(57)	C(14)	C(21)	H(17)	-177

The sign is positive if when looking from atom 2 to atom 3 a clockwise motion of atom 1 would superimpose it on atom 4.

Torsion or Conformation Angles

(1)	(2)	(3)	(4)	angle	(1)	(2)	(3)	(4)	angle
H(3)	N(5)	C(28)	H(22)	12	H(24)	C(29)	C(43)	H(49)	-1
H(3)	N(5)	C(28)	H(23)	125	H(38)	C(39)	C(44)	H(50)	-60
H(6)	N(8)	C(16)	H(12)	23	H(38)	C(39)	C(44)	H(51)	-174
H(6)	N(8)	C(16)	H(13)	137	H(39)	C(39)	C(44)	H(50)	-171
H(7)	N(9)	C(18)	H(15)	39	H(39)	C(39)	C(44)	H(51)	75
H(7)	N(9)	C(18)	H(16)	154	H(49)	C(43)	C(45)	H(52)	-1
H(8)	N(13)	C(44)	H(50)	162					
H(8)	N(13)	C(44)	H(51)	-81					
H(9)	C(14)	C(21)	H(17)	1					
H(10)	C(15)	C(18)	H(15)	-75					
H(10)	C(15)	C(18)	H(16)	171					
H(11)	C(15)	C(18)	H(15)	171					
H(11)	C(15)	C(18)	H(16)	56					
H(12)	C(16)	C(36)	H(30)	-74					
H(12)	C(16)	C(36)	H(31)	174					
H(13)	C(16)	C(36)	H(30)	173					
H(13)	C(16)	C(36)	H(31)	62					
H(14)	C(17)	C(34)	H(28)	-1					
H(17)	C(21)	C(24)	H(18)	3					
H(19)	C(25)	C(35)	H(29)	0					
H(20)	C(26)	C(35)	H(29)	-3					
H(21)	C(27)	C(34)	H(28)	-1					
H(22)	C(28)	C(50)	H(65)	170					
H(22)	C(28)	C(50)	H(66)	60					
H(23)	C(28)	C(50)	H(65)	56					
H(23)	C(28)	C(50)	H(66)	-54					

The sign is positive if when looking from atom 2 to atom 3 a clockwise motion of atom 1 would superimpose it on atom 4.

Intermolecular Distances

atom	atom	distance	ADC(*)	atom	atom	distance	ADC(*)
O(1)	H(13)	2.564	56403	O(5)	H(2)	2.139	1
O(1)	C(16)	3.42(2)	56403	O(5)	N(8)	2.88(1)	1
O(1)	H(19)	3.515	1	O(5)	N(4)	2.90(1)	1
O(1)	O(5)	3.52(1)	1	O(5)	H(4)	2.945	1
O(1)	C(25)	3.53(1)	1	O(5)	H(68)	3.296	45501
O(1)	H(12)	3.566	56403	O(5)	C(13)	3.40(2)	1
O(2)	H(16)	2.715	56503	O(5)	N(6)	3.49(1)	1
O(2)	H(15)	3.344	56503	O(6)	H(3)	1.961	56403
O(2)	C(18)	3.42(1)	56503	O(6)	H(4)	2.447	56403
O(2)	C(14)	3.46(1)	1	O(6)	N(5)	2.88(1)	56403
O(2)	H(9)	3.501	1	O(6)	N(6)	3.14(1)	56403
O(3)	H(8)	2.122	56503	O(6)	H(2)	3.227	56403
O(3)	H(1)	2.128	56503	O(6)	C(12)	3.53(2)	56403
O(3)	N(3)	2.92(1)	56503	O(6)	H(72)	3.565	56403
O(3)	N(13)	2.94(1)	56503	N(3)	H(16)	3.181	56503
O(3)	C(4)	3.41(2)	56503	N(3)	H(68)	3.207	45501
O(3)	H(69)	3.429	66503	N(3)	N(6)	3.50(1)	1
O(3)	H(67)	3.558	66503	N(3)	H(4)	3.581	1
O(3)	H(68)	3.559	66503	N(4)	H(19)	3.310	1
O(4)	H(7)	2.088	1	N(4)	C(13)	3.52(1)	56403
O(4)	H(5)	2.194	1	N(5)	H(38)	3.032	1
O(4)	N(9)	2.93(1)	1	N(5)	H(24)	3.415	56403
O(4)	N(7)	2.98(1)	1	N(6)	H(13)	3.345	56403
O(4)	H(25)	3.130	66503	N(6)	C(4)	3.48(1)	1
O(4)	C(56)	3.44(2)	1	N(6)	H(56)	3.525	56403
O(5)	H(6)	2.048	1	N(7)	H(25)	3.184	66503

Contacts out to 3.60 angstroms. Estimated standard deviations in the least significant figure are given in parentheses.

Intermolecular Distances

atom	atom	distance	ADC(*)	atom	atom	distance	ADC(*)
N(7)	H(9)	3.206	1	C(6)	H(37)	3.211	56503
N(7)	H(27)	3.590	66503	C(7)	H(13)	3.147	56403
N(8)	H(50)	3.238	1	C(7)	H(19)	3.520	1
N(9)	H(25)	3.376	66503	C(7)	H(12)	3.585	56403
N(9)	H(1)	3.581	56503	C(8)	H(9)	3.459	1
N(11)	H(33)	3.143	55402	C(8)	H(27)	3.525	66503
N(11)	H(46)	3.273	56503	C(10)	H(15)	3.379	56503
N(13)	H(68)	2.978	45501	C(10)	H(16)	3.381	56503
N(13)	H(69)	3.529	45501	C(10)	H(9)	3.575	1
N(13)	H(14)	3.560	56503	C(11)	H(16)	3.204	56503
N(13)	H(6)	3.587	1	C(11)	H(37)	3.229	56503
N(14)	H(20)	2.972	45402	C(11)	C(57)	3.60(1)	1
N(14)	H(47)	3.260	45402	C(12)	H(7)	3.133	1
N(15)	H(21)	3.149	45402	C(12)	H(5)	3.194	1
N(15)	H(43)	3.292	45402	C(13)	H(3)	3.161	56403
N(15)	H(48)	3.477	45402	C(13)	H(4)	3.357	56403
C(2)	H(13)	2.995	56403	C(13)	H(2)	3.373	56403
C(2)	H(56)	3.255	56403	C(14)	H(5)	3.283	1
C(3)	H(16)	2.907	56503	C(14)	H(27)	3.362	66503
C(3)	H(37)	3.142	56503	C(14)	H(56)	3.489	56403
C(4)	H(68)	2.885	45501	C(15)	H(67)	3.504	66503
C(4)	H(6)	3.135	1	C(15)	H(65)	3.589	1
C(4)	H(2)	3.254	1	C(16)	H(34)	3.556	56403
C(4)	H(4)	3.257	1	C(17)	H(39)	3.028	56503
C(5)	H(19)	3.438	1	C(17)	H(8)	3.298	56503
C(5)	H(53)	3.439	46403	C(17)	H(26)	3.335	66503

Contacts out to 3.60 angstroms. Estimated standard deviations in the least significant figure are given in parentheses.

Intermolecular Distances

atom	atom	distance	ADC(*)	atom	atom	distance	ADC(*)
C(17)	H(27)	3.360	66503	C(29)	H(72)	3.449	56403
C(17)	H(41)	3.505	4	C(29)	H(63)	3.495	56403
C(17)	H(52)	3.548	4	C(29)	C(46)	3.50(2)	46403
C(18)	H(46)	3.301	56503	C(32)	H(9)	3.120	66503
C(18)	H(1)	3.465	56503	C(32)	H(41)	3.314	55402
C(21)	H(45)	3.196	1	C(32)	H(52)	3.323	55402
C(21)	H(27)	3.428	66503	C(32)	H(14)	3.416	66503
C(21)	H(49)	3.482	4	C(34)	H(39)	3.015	56503
C(21)	H(60)	3.571	54402	C(34)	H(61)	3.046	56503
C(21)	H(59)	3.597	54402	C(34)	H(52)	3.234	4
C(24)	H(45)	2.865	1	C(34)	H(41)	3.575	4
C(24)	H(59)	3.219	54402	C(35)	H(40)	3.152	1
C(25)	H(53)	3.317	46403	C(35)	H(53)	3.237	46403
C(25)	H(37)	3.414	56503	C(35)	H(58)	3.365	46403
C(25)	H(54)	3.532	46403	C(35)	H(37)	3.415	56503
C(25)	H(2)	3.586	1	C(35)	H(28)	3.549	45404
C(26)	H(40)	2.846	1	C(37)	H(48)	2.997	55404
C(26)	H(37)	3.324	56503	C(37)	H(46)	3.123	55404
C(27)	H(61)	3.256	56503	C(37)	C(42)	3.48(2)	55404
C(27)	H(49)	3.511	4	C(38)	H(67)	3.299	66503
C(28)	H(38)	2.903	1	C(38)	H(46)	3.341	56503
C(28)	H(7)	3.438	1	C(39)	H(23)	3.378	1
C(29)	H(62)	2.997	56403	C(40)	H(70)	3.235	54402
C(29)	H(55)	3.051	46403	C(40)	H(66)	3.235	54402
C(29)	H(53)	3.079	46403	C(40)	H(28)	3.429	45404
C(29)	H(3)	3.339	56403	C(40)	H(20)	3.542	1

Contacts out to 3.60 angstroms. Estimated standard deviations in the least significant figure are given in parentheses.

Intermolecular Distances

atom	atom	distance	ADC(*)	atom	atom	distance	ADC(*)
C(41)	H(71)	3.214	54402	C(47)	H(60)	3.294	46404
C(41)	H(70)	3.299	54402	C(47)	H(29)	3.546	46403
C(41)	H(18)	3.455	1	C(47)	H(61)	3.580	46404
C(42)	H(34)	3.027	45504	C(48)	H(58)	2.958	56504
C(42)	H(33)	3.097	45504	C(48)	H(20)	3.474	45402
C(42)	H(64)	3.446	44402	C(48)	H(28)	3.564	56503
C(42)	H(15)	3.469	56503	C(48)	H(29)	3.582	45402
C(42)	H(37)	3.498	56503	C(49)	H(47)	3.005	45402
C(43)	H(62)	2.659	56403	C(49)	H(49)	3.348	56403
C(43)	H(64)	3.208	56403	C(50)	H(10)	3.284	1
C(43)	C(49)	3.29(3)	56403	C(50)	H(42)	3.383	55402
C(43)	H(53)	3.346	46403	C(51)	H(35)	3.463	66503
C(43)	H(63)	3.347	56403	C(52)	H(42)	3.323	55402
C(43)	H(17)	3.454	45404	C(52)	H(24)	3.331	56403
C(44)	H(6)	3.220	1	C(52)	H(44)	3.477	55402
C(44)	H(68)	3.564	45501	C(52)	H(45)	3.522	55402
C(45)	H(64)	3.150	56403	C(52)	H(43)	3.562	55402
C(45)	H(62)	3.267	56403	C(56)	H(1)	3.063	56503
C(45)	H(28)	3.356	45404	C(56)	H(8)	3.252	56503
C(45)	H(63)	3.507	56403	C(56)	H(25)	3.301	66503
C(45)	C(49)	3.57(3)	56403	C(56)	H(26)	3.570	66503
C(46)	H(19)	3.163	46403	C(57)	H(56)	3.193	56403
C(46)	H(21)	3.226	45402	C(57)	H(13)	3.431	56403
C(46)	H(29)	3.320	46403	H(1)	H(16)	2.639	56503
C(46)	H(24)	3.348	46403	H(1)	H(68)	3.524	45501
C(46)	H(43)	3.379	45402	H(2)	H(19)	3.020	1

Contacts out to 3.60 angstroms. Estimated standard deviations in the least significant figure are given in parentheses.

Appendix A

Intermolecular Distances

atom	atom	distance	ADC(*)	atom	atom	distance	ADC(*)
H(3)	H(24)	2.596	56403	H(11)	H(11)	3.289	66503
H(3)	H(38)	3.230	1	H(11)	H(65)	3.375	66503
H(4)	H(13)	2.911	56403	H(11)	H(26)	3.380	66503
H(5)	H(9)	2.709	1	H(12)	H(63)	2.904	1
H(5)	H(25)	3.303	66503	H(12)	H(34)	2.918	56403
H(6)	H(50)	2.357	1	H(12)	H(48)	3.039	45402
H(6)	H(63)	3.431	1	H(12)	H(50)	3.215	1
H(6)	H(51)	3.506	1	H(12)	H(47)	3.396	45402
H(7)	H(23)	2.783	1	H(13)	H(34)	3.194	56403
H(7)	H(65)	3.141	1	H(14)	H(26)	2.806	66503
H(7)	H(25)	3.380	66503	H(14)	H(41)	3.007	4
H(8)	H(14)	2.822	56503	H(14)	H(39)	3.012	56503
H(8)	H(68)	3.235	45501	H(14)	H(69)	3.219	66503
H(8)	H(69)	3.473	45501	H(14)	H(27)	3.280	66503
H(9)	H(27)	2.648	66503	H(15)	H(46)	2.568	56503
H(9)	H(25)	2.674	66503	H(15)	H(23)	3.487	1
H(9)	H(35)	3.222	66503	H(15)	H(33)	3.498	55402
H(9)	H(36)	3.307	66503	H(16)	H(46)	3.209	56503
H(10)	H(65)	2.649	1	H(17)	H(49)	2.656	4
H(10)	H(66)	3.012	1	H(17)	H(27)	2.827	66503
H(10)	H(11)	3.031	66503	H(17)	H(45)	3.175	1
H(10)	H(25)	3.223	66503	H(17)	H(52)	3.226	4
H(10)	H(10)	3.517	66503	H(17)	H(36)	3.356	66503
H(10)	H(23)	3.543	1	H(17)	H(64)	3.426	54402
H(11)	H(67)	2.648	66503	H(17)	H(62)	3.428	54402
H(11)	H(25)	3.269	66503	H(17)	H(60)	3.509	54402

Contacts out to 3.60 angstroms. Estimated standard deviations in the least significant figure are given in parentheses.

Intermolecular Distances

atom	atom	distance	ADC(*)	atom	atom	distance	ADC(*)
H(18)	H(45)	2.502	1	H(23)	H(59)	3.487	1
H(18)	H(59)	2.968	54402	H(23)	H(39)	3.488	1
H(18)	H(22)	3.164	54402	H(23)	H(32)	3.592	55402
H(18)	H(70)	3.202	54402	H(24)	H(72)	2.559	56403
H(18)	H(49)	3.390	4	H(24)	H(55)	2.667	46403
H(19)	H(54)	2.682	46403	H(24)	H(71)	3.139	56403
H(19)	H(53)	2.753	46403	H(24)	H(53)	3.199	46403
H(19)	H(57)	3.375	46403	H(24)	H(62)	3.205	56403
H(19)	H(68)	3.541	45501	H(24)	H(54)	3.508	46403
H(20)	H(40)	2.634	1	H(25)	H(65)	3.419	66503
H(20)	H(51)	3.307	44402	H(26)	H(41)	2.721	55402
H(20)	H(28)	3.396	45404	H(26)	H(66)	3.281	1
H(20)	H(61)	3.407	44402	H(26)	H(52)	3.297	55402
H(20)	H(60)	3.426	44402	H(26)	H(69)	3.365	1
H(21)	H(53)	2.783	44402	H(26)	H(33)	3.554	55402
H(21)	H(61)	3.105	56503	H(27)	H(52)	2.648	55402
H(21)	H(58)	3.352	·44402	H(27)	H(41)	3.208	55402
H(21)	H(55)	3.371	44402	H(27)	H(33)	3.559	55402
H(21)	H(49)	3.387	4	H(28)	H(61)	2.726	56503
H(21)	H(29)	3.584	4	H(28)	H(29)	2.766	4
H(22)	H(38)	2.820	1	H(28)	H(40)	2.876	4
H(22)	H(24)	3.054	56403	H(28)	H(39)	2.967	56503
H(22)	H(62)	3.091	1	H(28)	H(52)	3.054	4
H(22)	H(42)	3.452	55402	H(28)	H(41)	3.089	4
H(22)	H(59)	3.461	1	H(29)	H(53)	2.514	46403
H(23)	H(38)	2.403	1	H(29)	H(58)	2.762	46403

Contacts out to 3.60 angstroms. Estimated standard deviations in the least significant figure are given in parentheses.

Intermolecular Distances

atom	atom	distance	ADC(*)	atom	atom	distance	ADC(*)
H(29)	H(61)	3.074	44402	H(36)	H(60)	2.809	56504
H(29)	H(40)	3.127	1	H(36)	H(64)	2.819	56504
H(29)	H(60)	3.318	44402	H(36)	H(46)	3.403	56503
H(29)	H(54)	3.529	46403	H(36)	H(47)	3.554	56503
H(29)	H(57)	3.535	46403	H(37)	H(46)	2.859	56503
H(30)	H(71)	3.135	45501	H(37)	H(67)	3.414	66503
H(30)	H(54)	3.359	46403	H(37)	H(47)	3.444	56503
H(30)	H(43)	3.543	45402	H(40)	H(44)	3.133	1
H(31)	H(54)	3.458	46403	H(40)	H(45)	3.327	1
H(31)	H(55)	3.576	46403	H(40)	H(70)	3.436	54402
H(32)	H(59)	2.815	54402	H(41)	H(66)	3.104	54402
H(32)	H(48)	3.167	55404	H(41)	H(69)	3.444	54402
H(32)	H(46)	3.219	55404	H(41)	H(70)	3.494	54402
H(32)	H(66)	3.586	54402	H(42)	H(70)	2.360	54402
H(33)	H(46)	2.576	55404	H(42)	H(66)	2.473	54402
H(33)	H(48)	2.890	55404	H(42)	H(45)	3.112	1
H(33)	H(47)	3.138	55404	H(42)	H(69)	3.223	54402
H(33)	H(64)	3.393	56403	H(42)	H(44)	3.314	1
H(34)	H(48)	2.366	55404	H(42)	H(72)	3.562	54402
H(34)	H(46)	2.935	55404	H(43)	H(71)	2.821	54402
H(34)	H(47)	3.134	55404	H(43)	H(55)	2.928	44402
H(34)	H(56)	3.307	56403	H(43)	H(70)	3.350	54402
H(35)	H(67)	2.532	66503	H(43)	H(49)	3.401	4
H(35)	H(65)	3.352	66503	H(43)	H(53)	3.453	44402
H(35)	H(57)	3.484	65601	H(44)	H(70)	2.926	54402
H(35)	H(68)	3.586	66503	H(44)	H(51)	2.970	44402

Contacts out to 3.60 angstroms. Estimated standard deviations in the least significant figure are given in parentheses.

Intermolecular Distances

atom	atom	distance	ADC(*)	atom	atom	distance	ADC(*)
H(44)	H(71)	2.984	54402				
H(45)	H(70)	2.967	54402				
H(45)	H(49)	3.138	4				
H(45)	H(71)	3.178	54402				
H(45)	H(72)	3.579	54402				
H(46)	H(64)	3.490	44402				
H(47)	H(64)	2.582	44402				
H(47)	H(63)	2.745	44402				
H(49)	H(62)	2.597	56403				
H(49)	H(64)	3.275	56403				
H(49)	H(72)	3.547	56403				
H(49)	H(53)	3.581	46403				
H(51)	H(68)	3.217	45501				
H(51)	H(69)	3.312	45501				
H(52)	H(64)	3.169	56403				
H(52)	H(62)	3.577	56403				
H(55)	H(71)	2.736	45501				
H(55)	H(72)	3.528	45501				
H(56)	H(60)	3.259	46404				
H(58)	H(60)	2.402	46404				
H(58)	H(61)	2.606	46404				
H(58)	H(59)	3.299	46404				

Contacts out to 3.60 angstroms. Estimated standard deviations in the least significant figure are given in parentheses.

(*)footnote

The ADC (atom designator code) specifies the position of an atom in a crystal. The 5-digit number shown in the table is a composite of three one digit numbers and one two digit number: TA(1st digit) + TB(2nd digit) + TC(3rd digit) + SN(4th and 5th digit). TA, TB, & TC are the crystal lattice translation digits along cell edges a, b, and c. A translation digit of 5 indicates the origin unit cell. If TA=4, this indicates a translation of one unit cell length along the a axis in the negative direction. Each translation digit can range in value from 1 to 9 and thus (+/-)4 lattice translations from the origin (TA=5,TB=5,TC=5) can be represented.

The SN or symmetry operator number refers to the number of the symmetry operator used to generate the coordinates of the target atom. A list of the symmetry operators relevant to this structure are given below.

For a given intermolecular contact, the first atom (origin atom) is located in the origin unit cell (TA=5,TB=5,TC=5) and its position can be generated using the identity operator (SN=1). Thus, the ADC for an origin atom is always ADC=55501. The position of the second atom (target atom) can be generated using the ADC and the coordinates of that atom in the parameter table. For example, an ADC of 47502 refers to the target atom moved through operator two, then translated -1 cell translations along the a axis, +2 cell translations along the b axis, and 0 cell translations along the c axis.

An ADC of 1 indicates an intermolecular contact between two fragments (i.e.cation and anion) that reside in the same asymmetric unit.

Symmetry Operators:
(1)+X , +Y , +Z (2) 1/2-X ,1/2+Y ,1/2-Z (3)-X , -Y , -Z (4) 1/2+X ,1/2-Y ,1/2+Z

Hydrogen Bonds

A	H	B	A...B	A-H...B
N(3)	H(1)	O(3)	2.92(1)	137
N(4)	H(2)	O(5)	2.90(1)	133
N(5)	H(3)	O(6)	2.88(1)	152
N(7)	H(5)	O(4)	2.98(1)	137
N(8)	H(6)	O(5)	2.88(1)	142
N(9)	H(7)	O(4)	2.93(1)	143
N(13)	H(8)	O(3)	2.94(1)	141
N(6)	H(4)	O(6)	3.14(1)	128
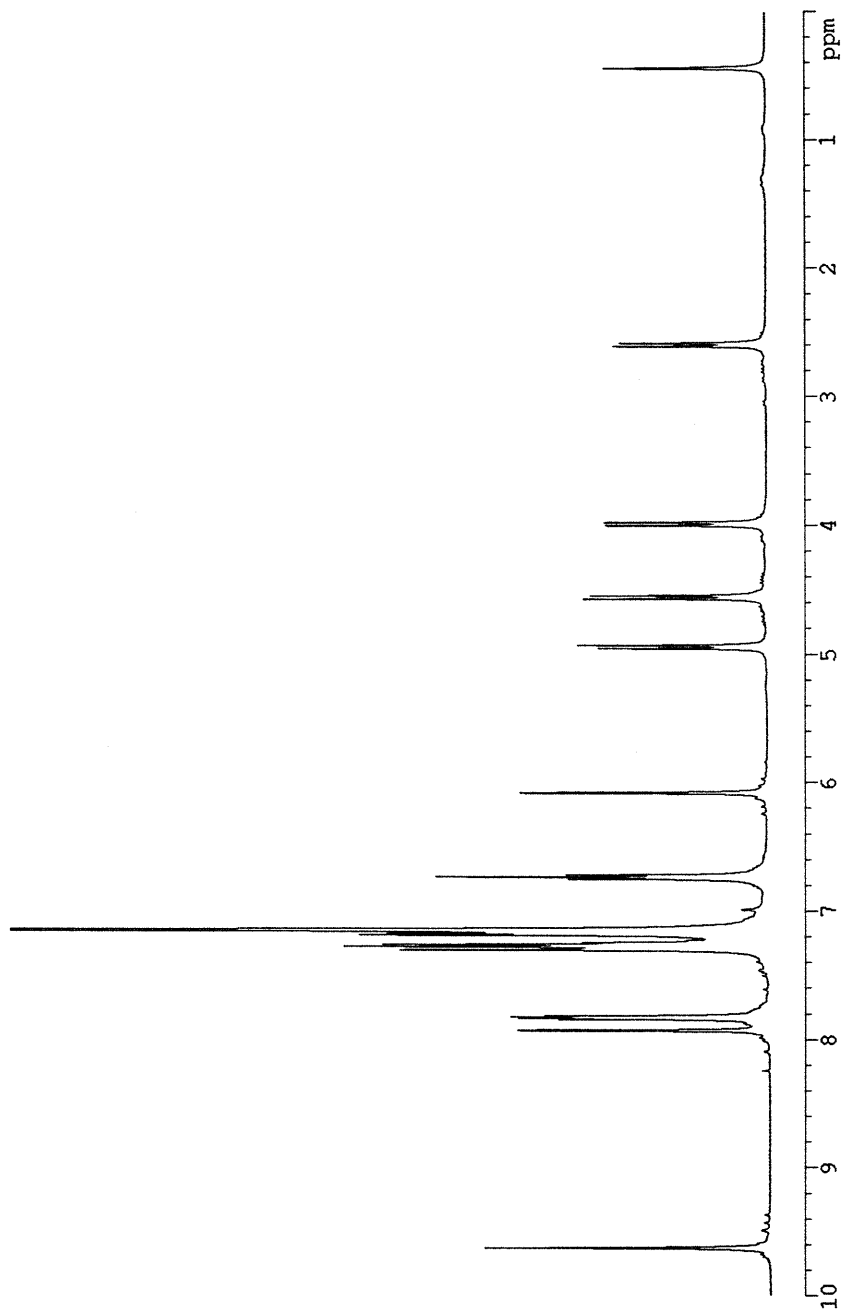
Dimer 71·71 in benzene-d_6.
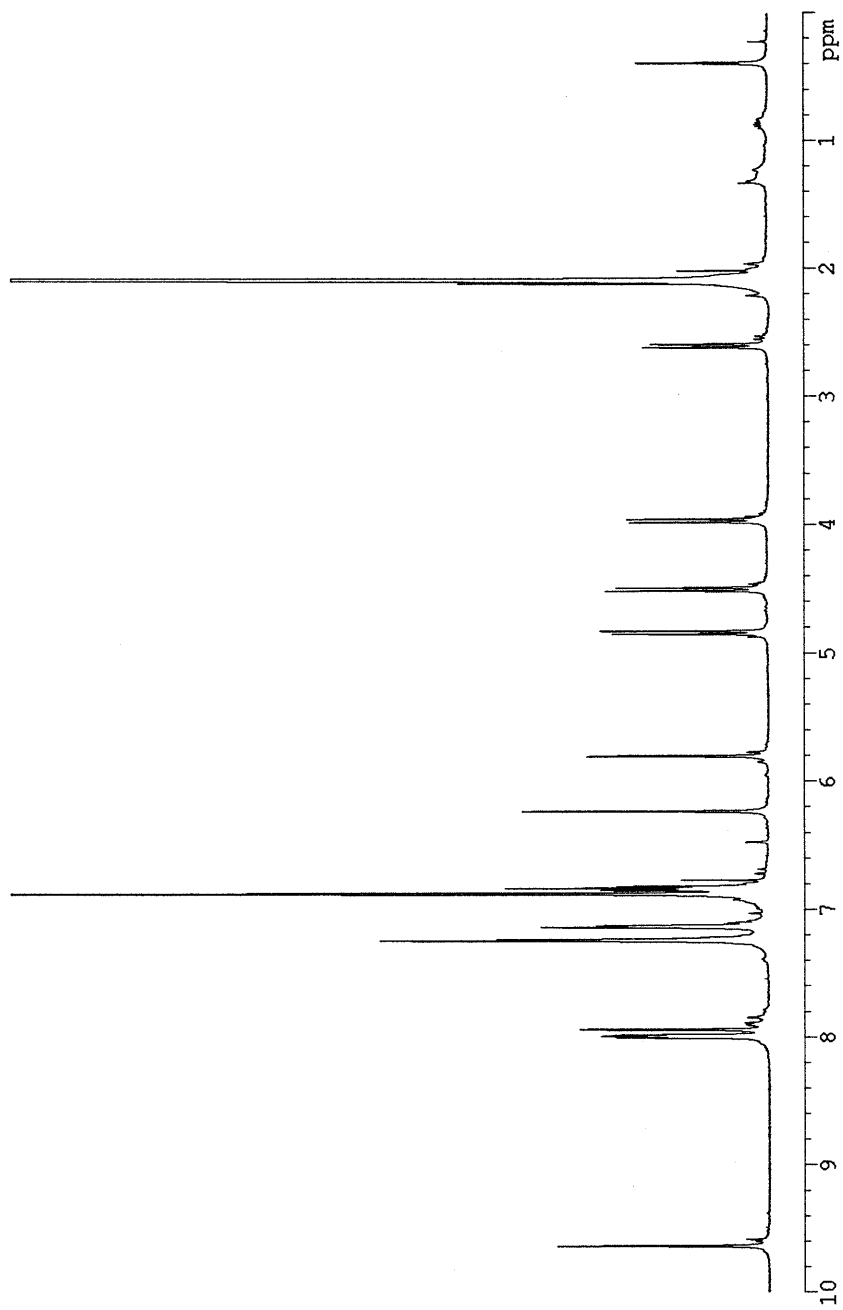
Dimer **71·71** in *p*-xylene-d_{10}.
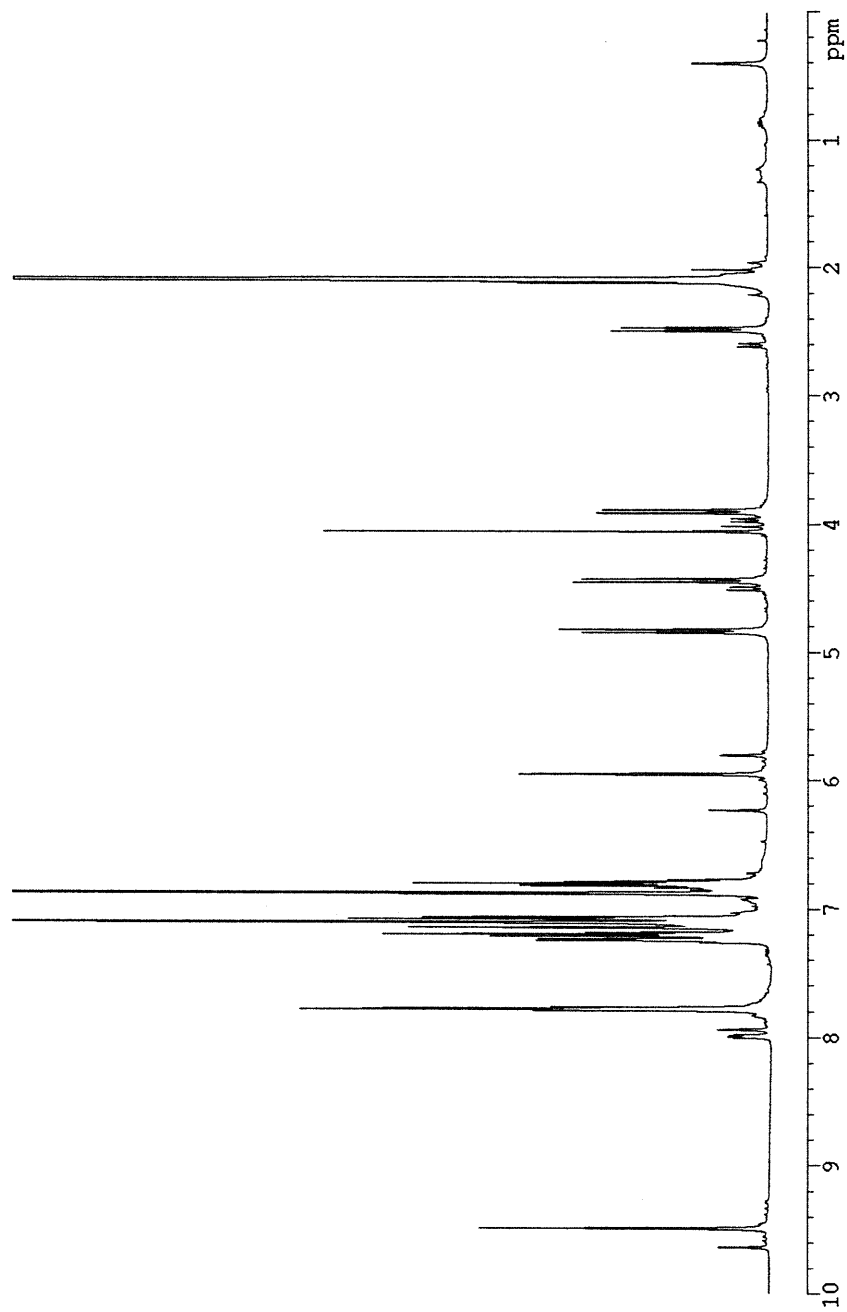
Dimer **71·71** with encapsulated benzene and *p*-xylene-d_{10}.
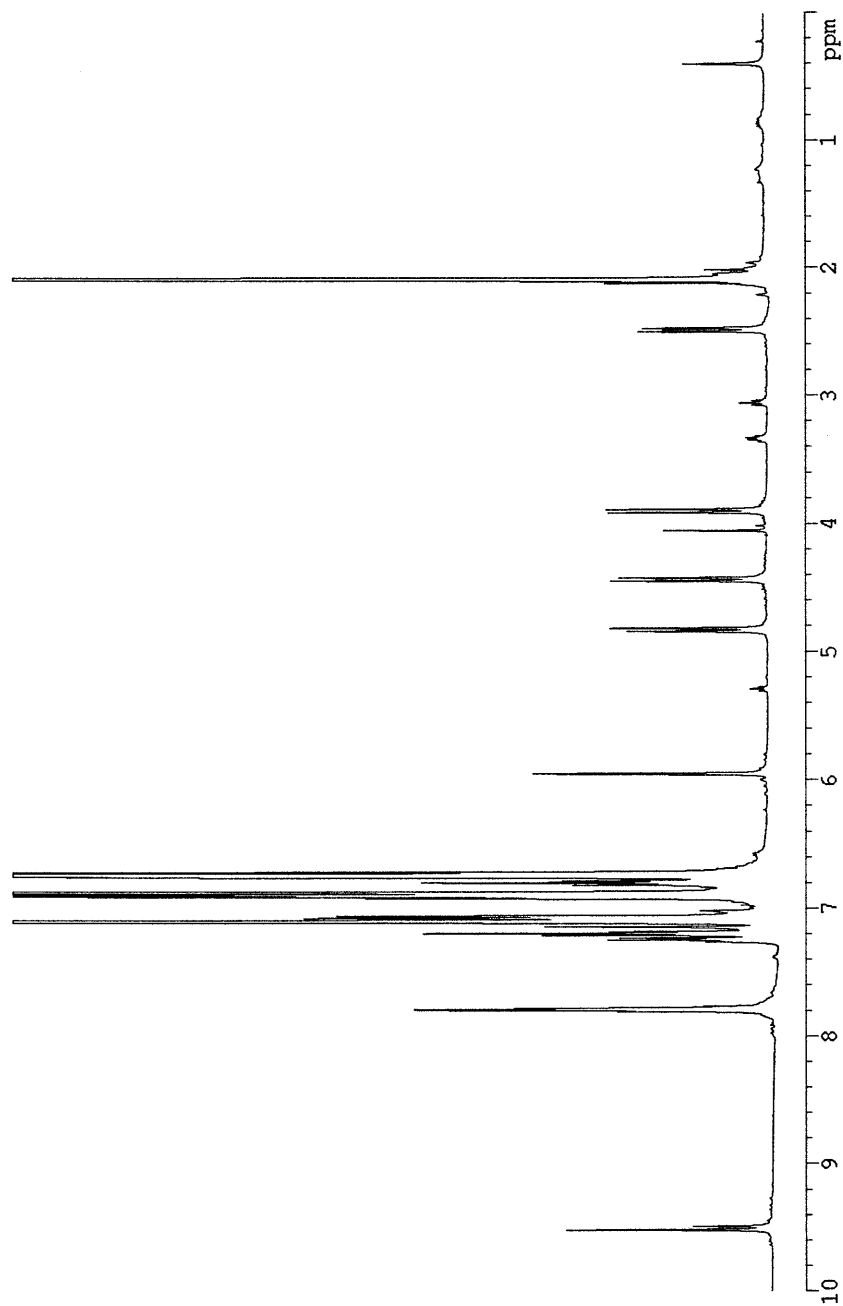
Dimer **71·71** with encapsulated benzene and fluorobenzene in *p*-xylene-*d*$_{10}$.
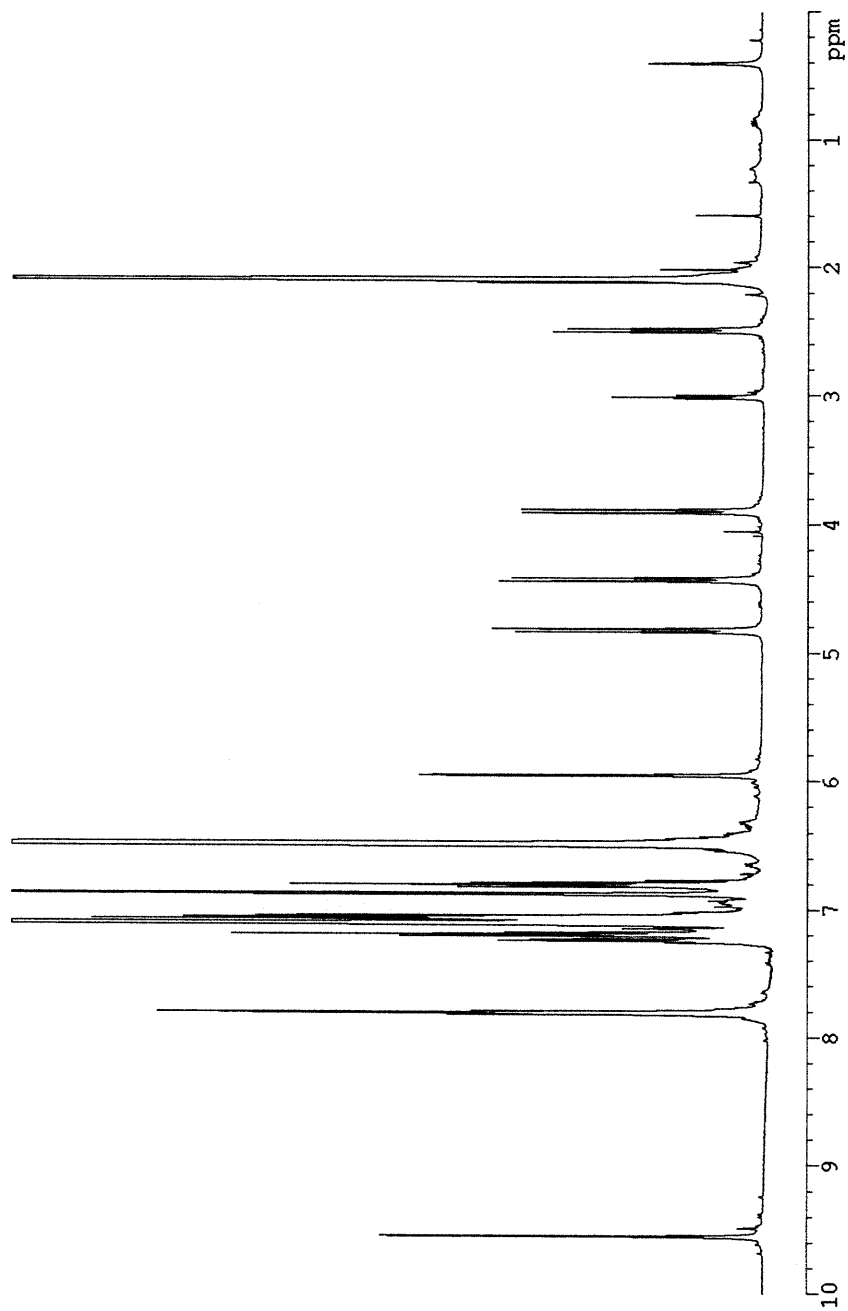
Dimer **71·71** with encapsulated benzene and 1,4-difluorobenzene in *p*-xylene-d_{10}.
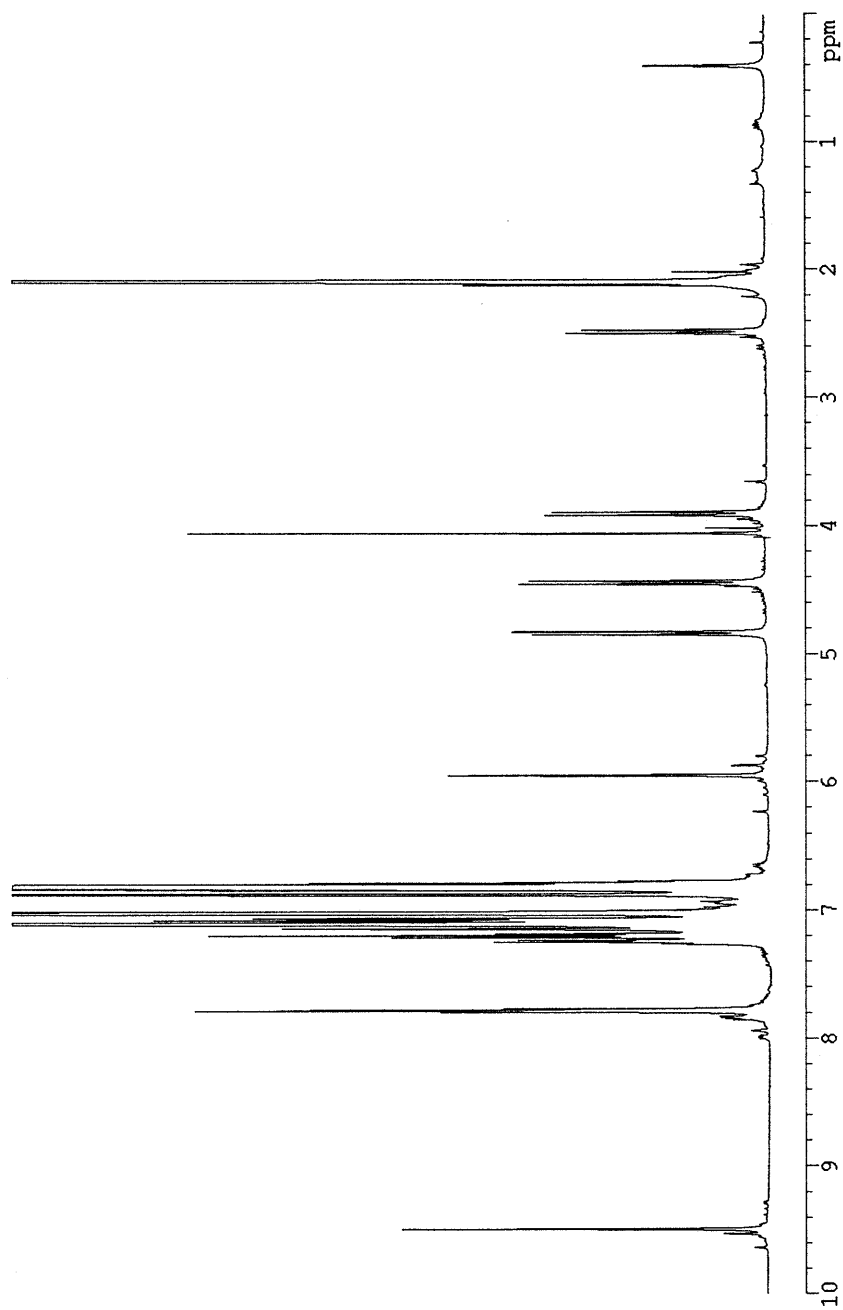
Dimer **71·71** with encapsulated benzene and chlorobenzene in *p*-xylene-*d*$_{10}$.
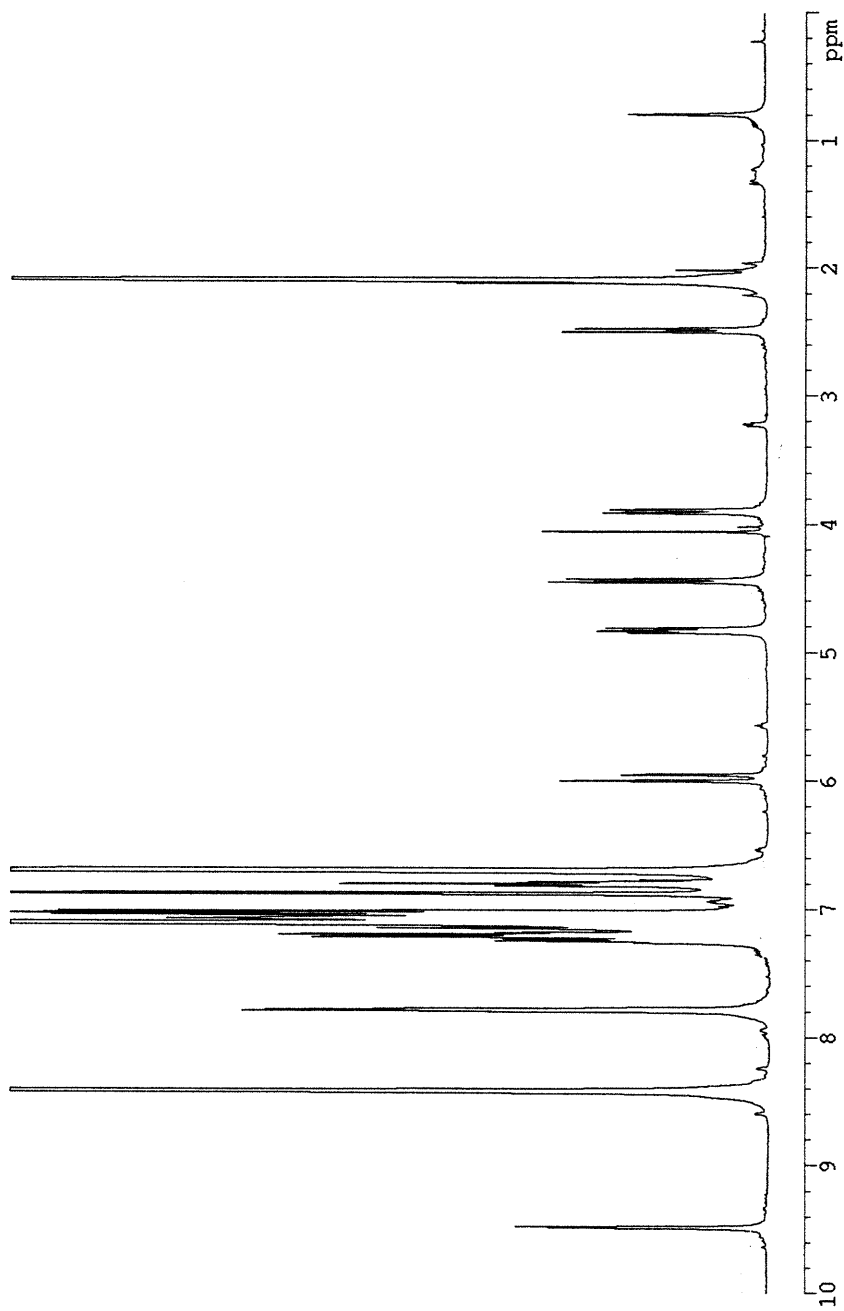
Dimer **71·71** with encapsulated benzene and pyridine in *p*-xylene-*d*10.
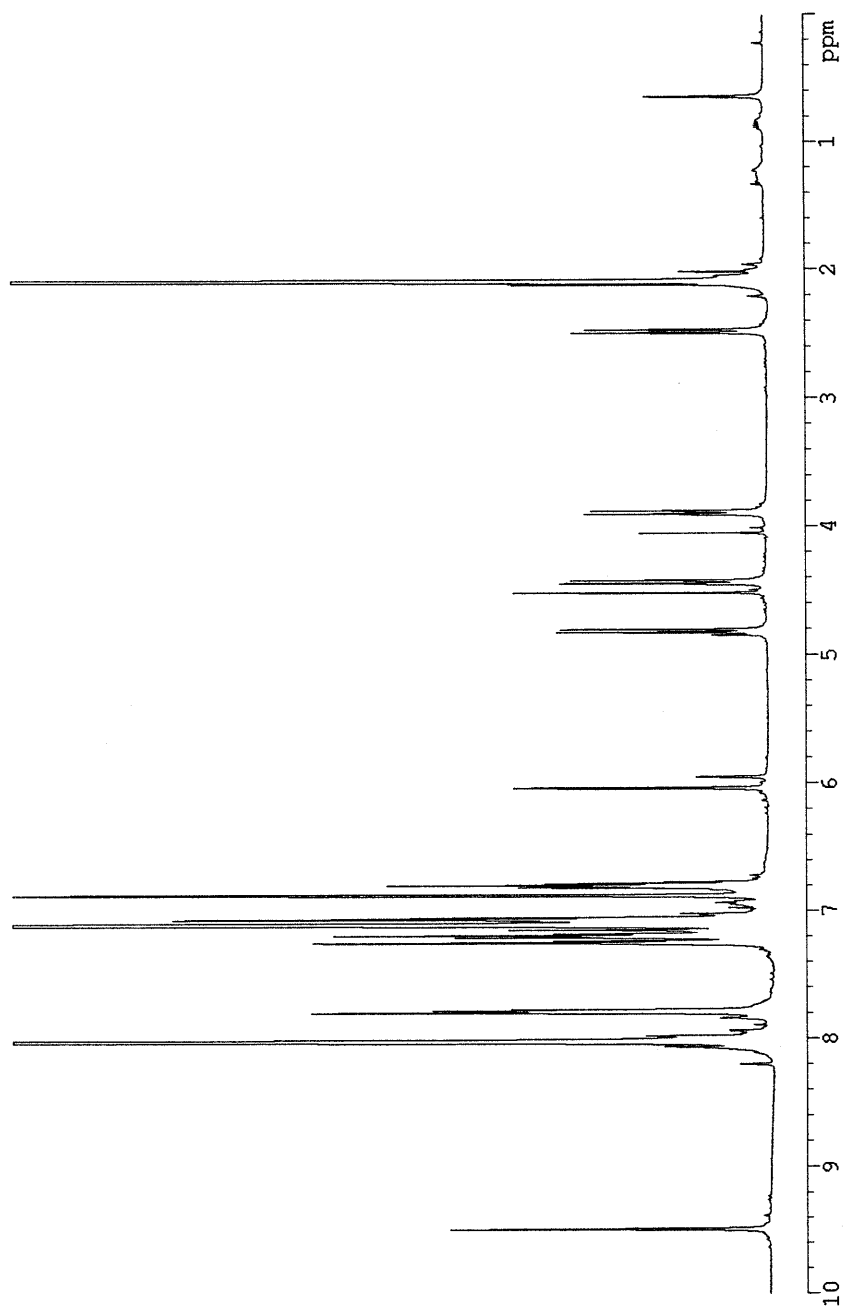
Dimer **71·71** with encapsulated benzene and pyrazine in *p*-xylene-*d10*.
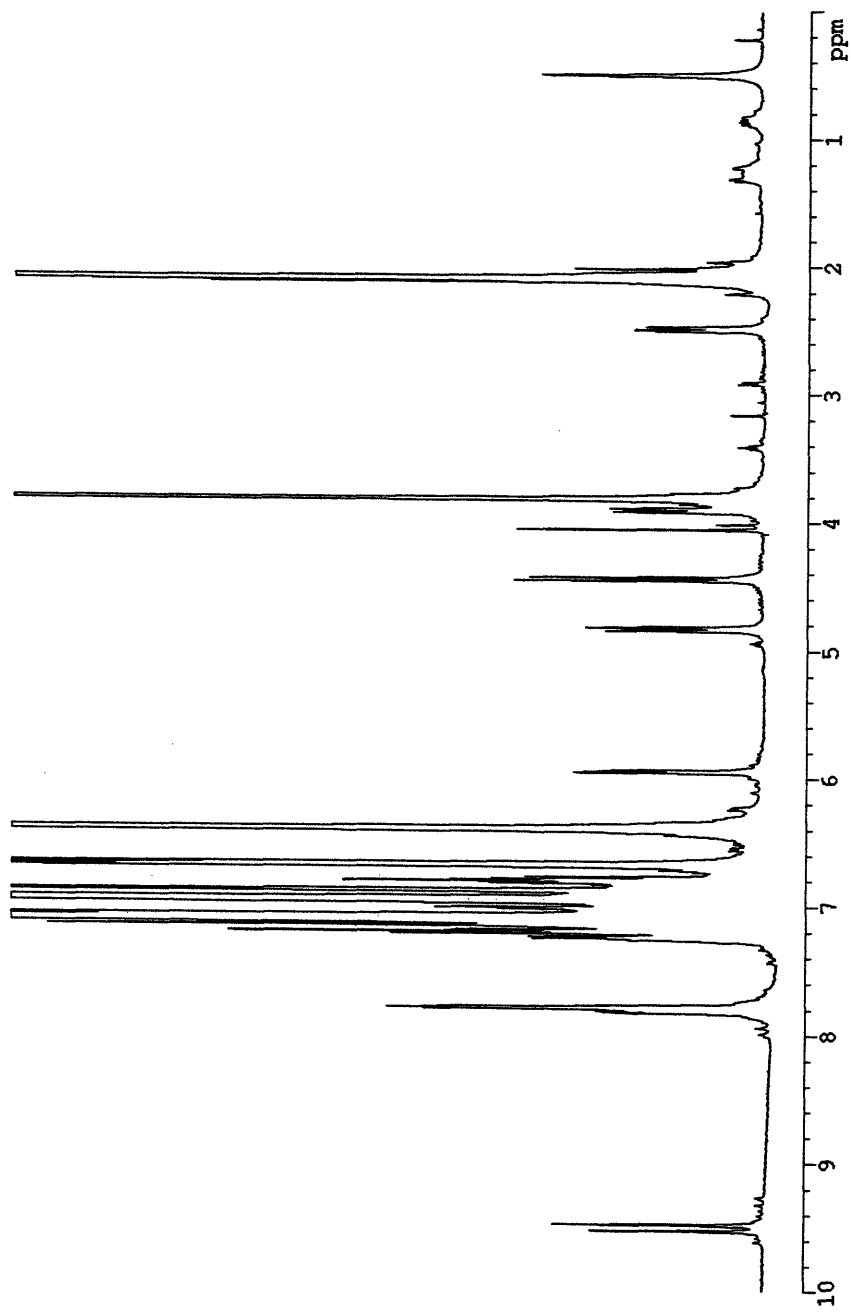
Dimer **71·71** with encapsulated benzene and phenol in *p*-xylene-*d*$_{10}$.
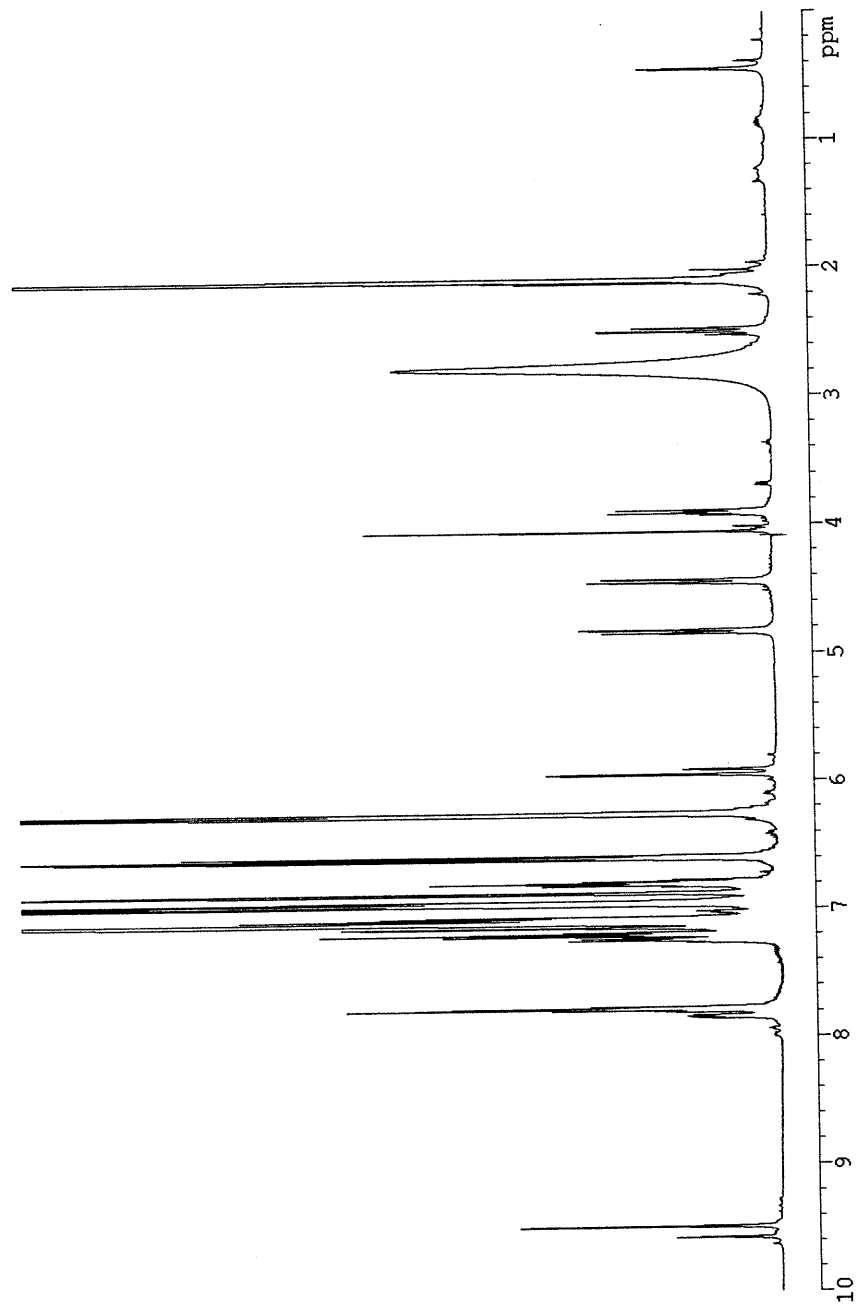
Dimer **71·71** with encapsulated benzene and aniline in *p*-xylene-*d*10.
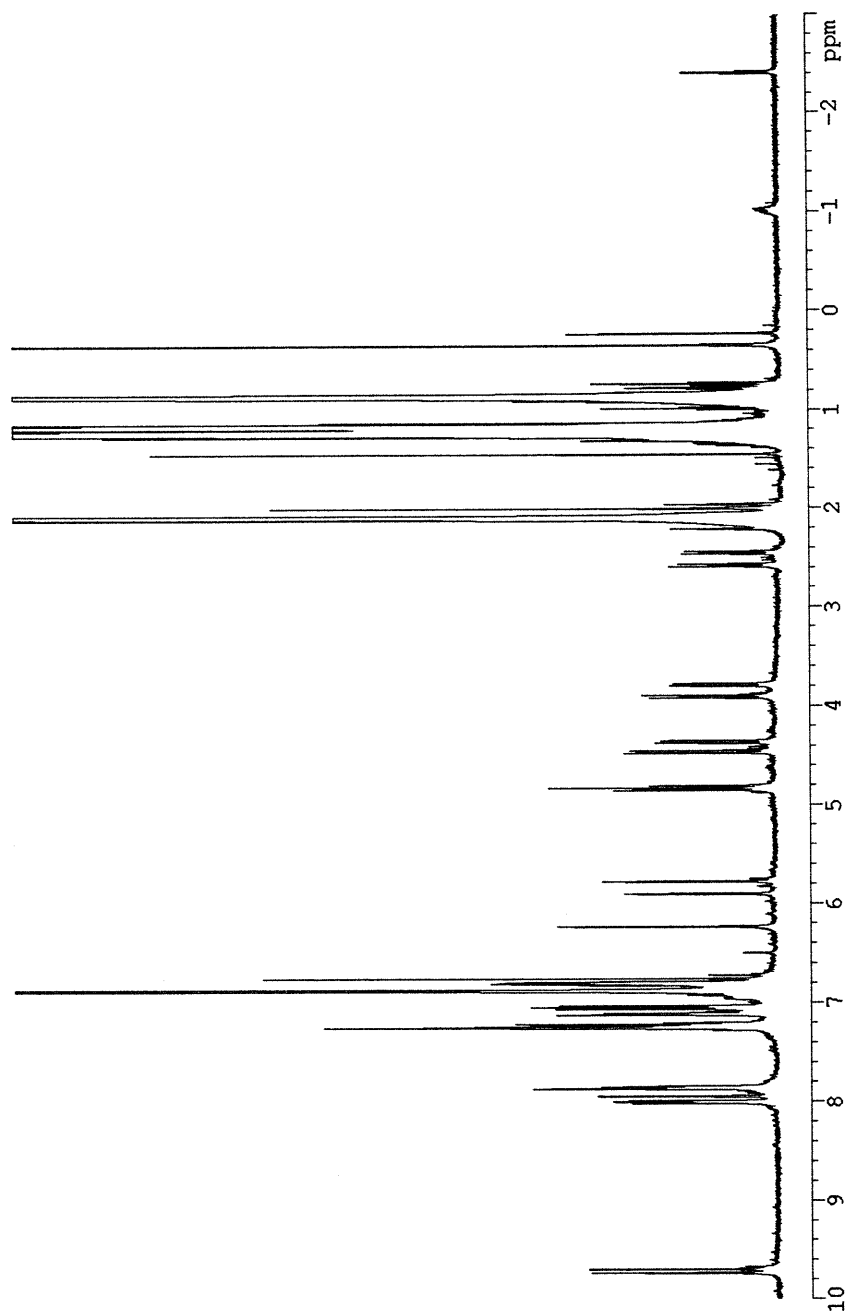
Dimer **71·71** with encapsulated *n*-pentane in *p*-xylene-*d*₁₀.
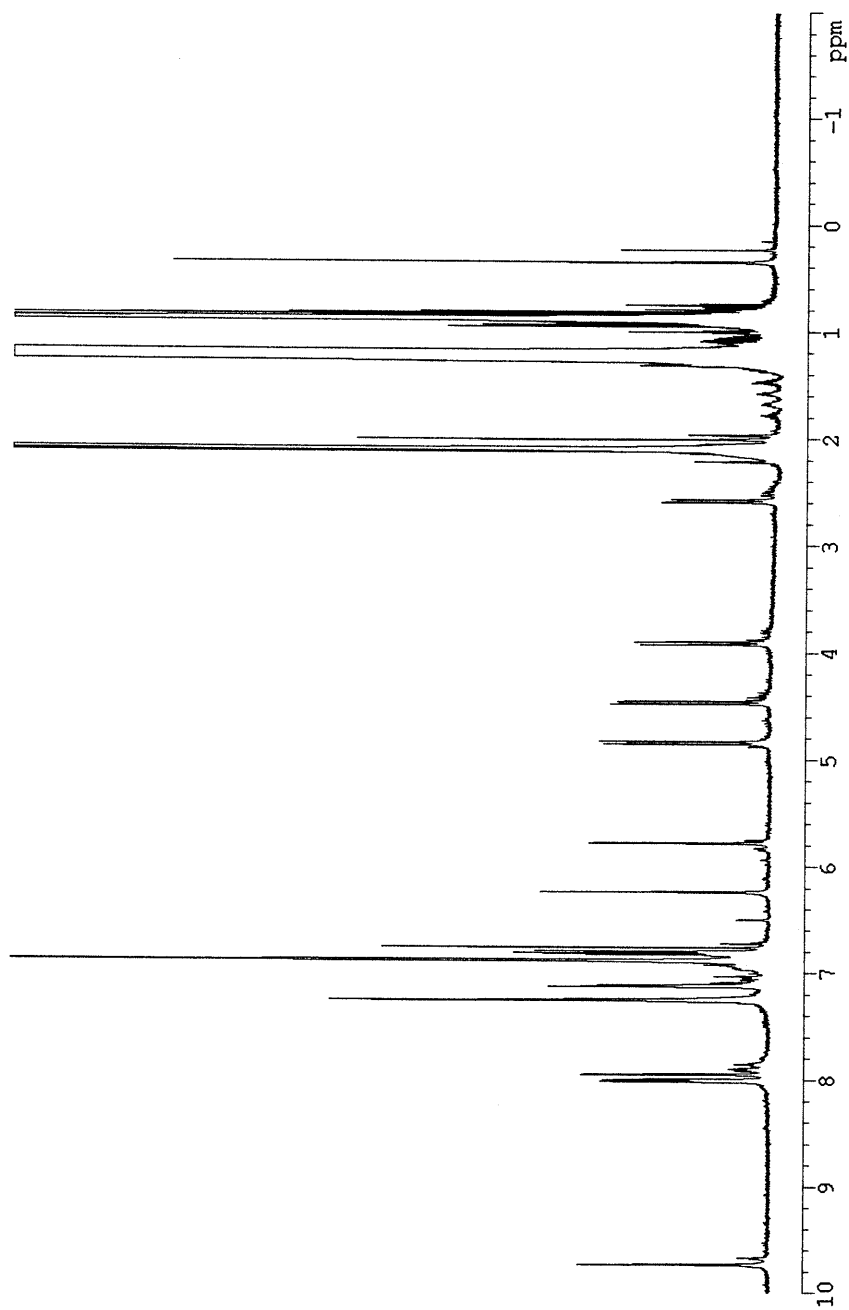
Dimer **71·71** with encapsulated *n*-hexane in *p*-xylene-d_{10}.
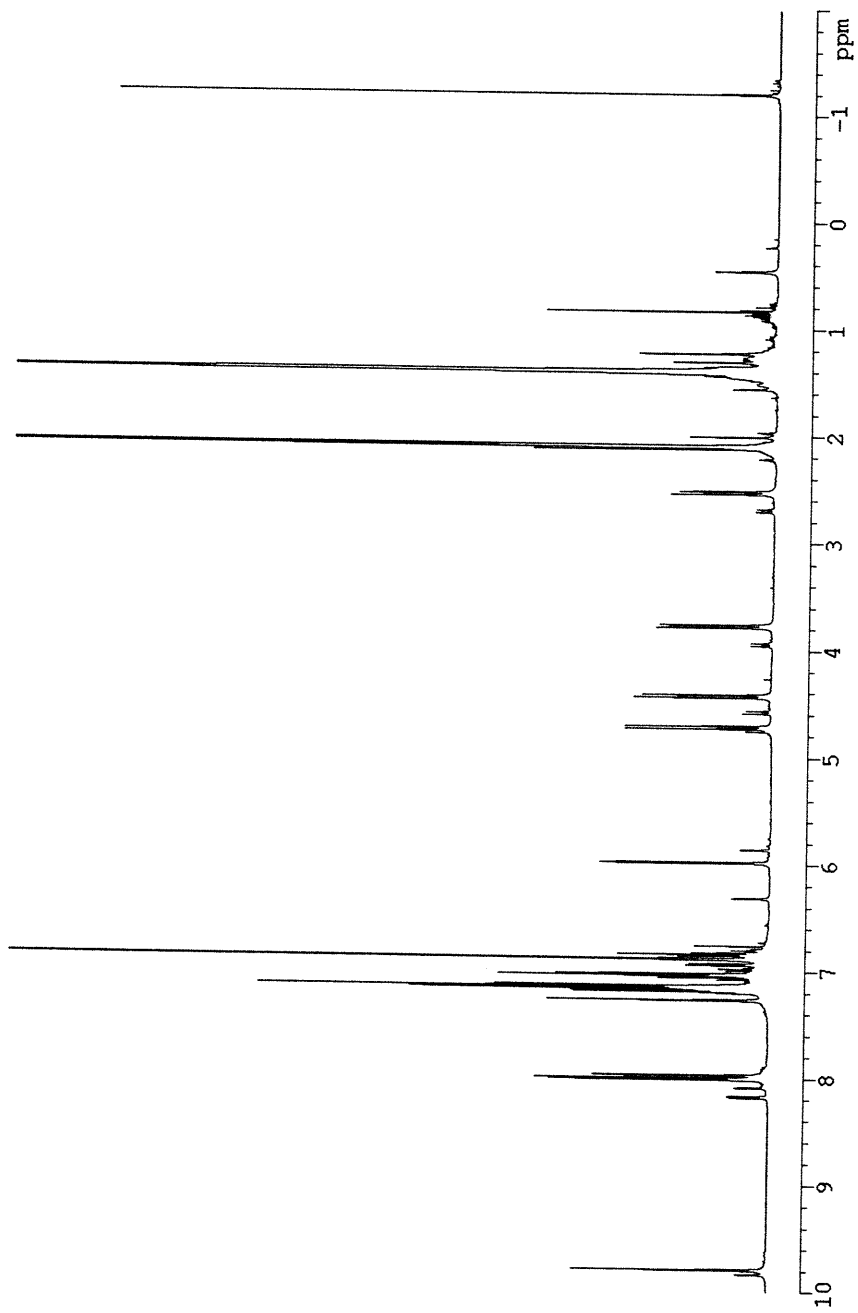
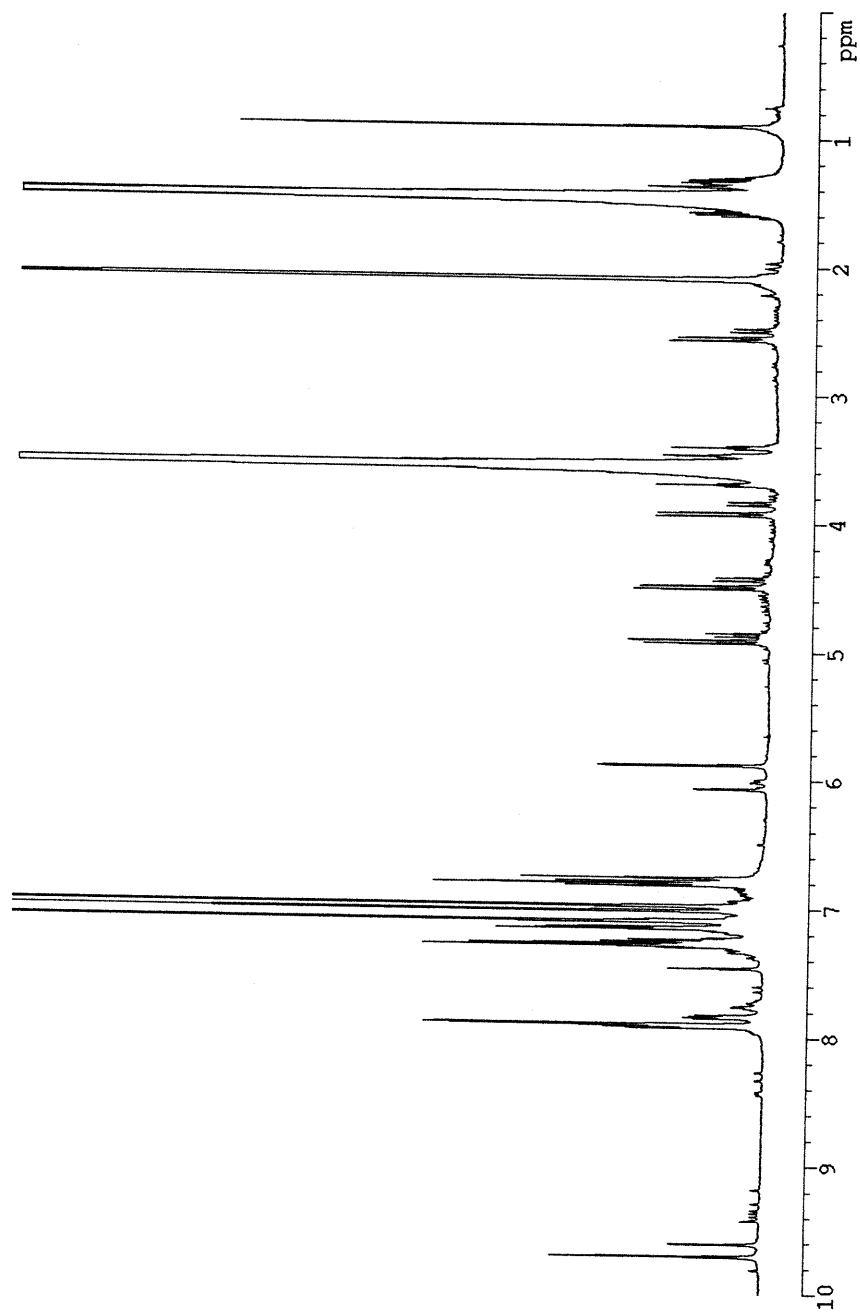Dimer **71·71** with encapsulated cyclohexane in *p*-xylene-*d*10.
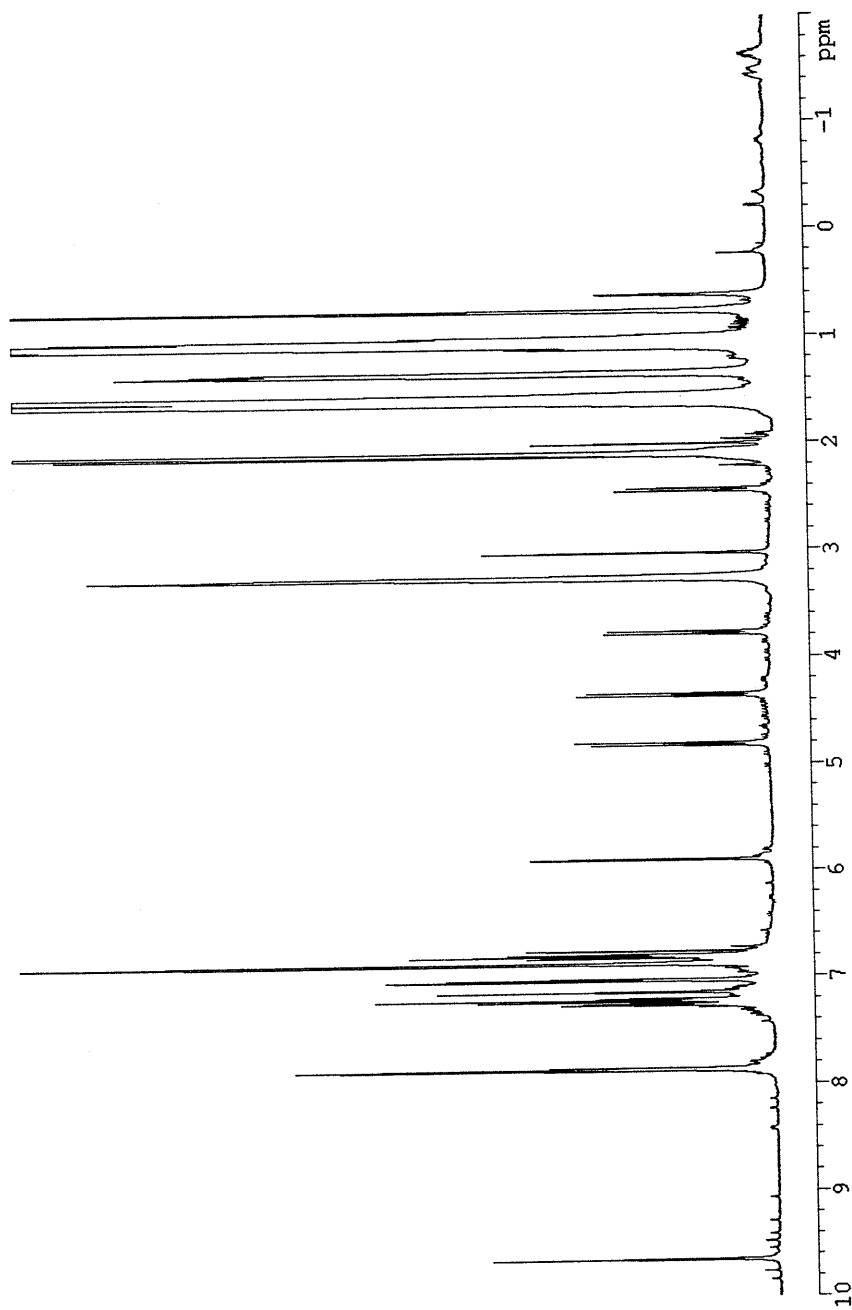
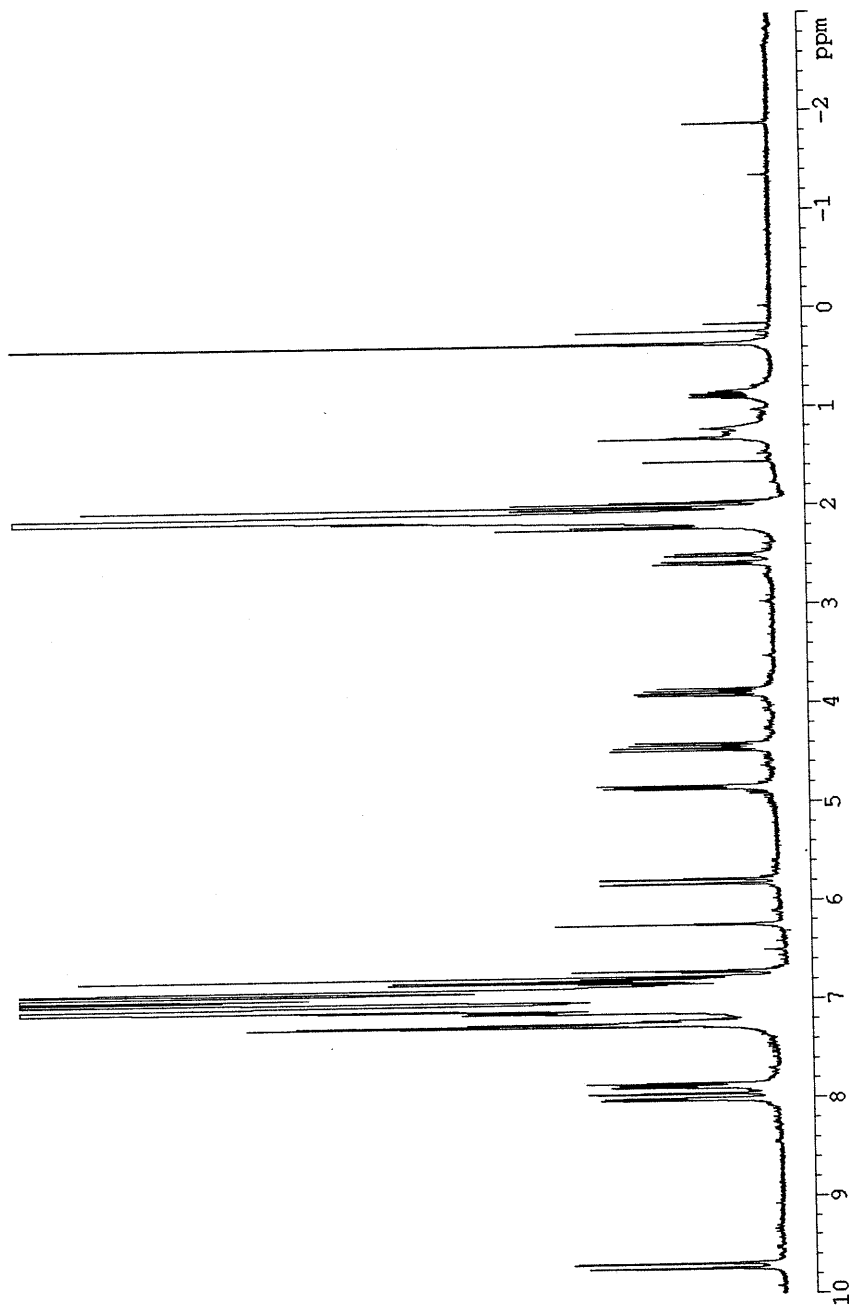Dimer **71·71** with encapsulated cyclohexanol in *p*-xylene-*d10*.
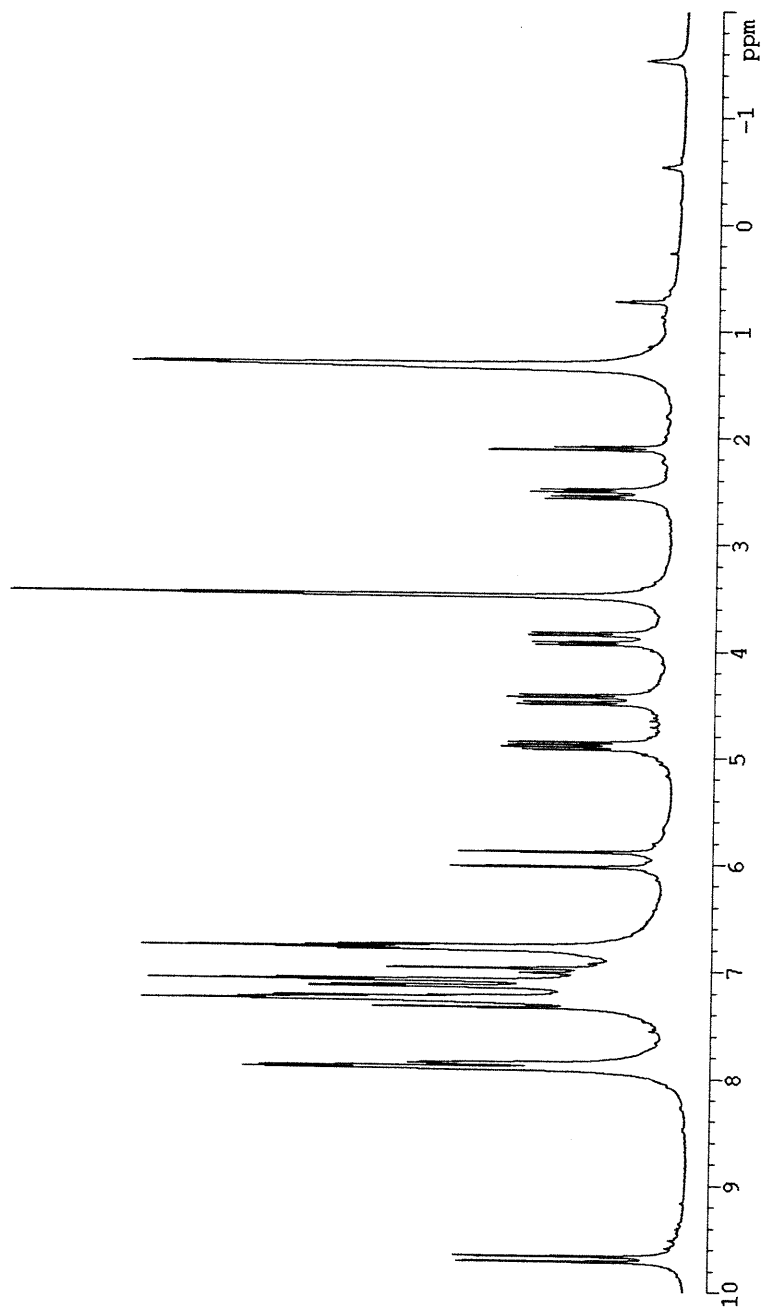
Dimer **71·71** with encapsulated tetrahydropyran in toluene-d_8.
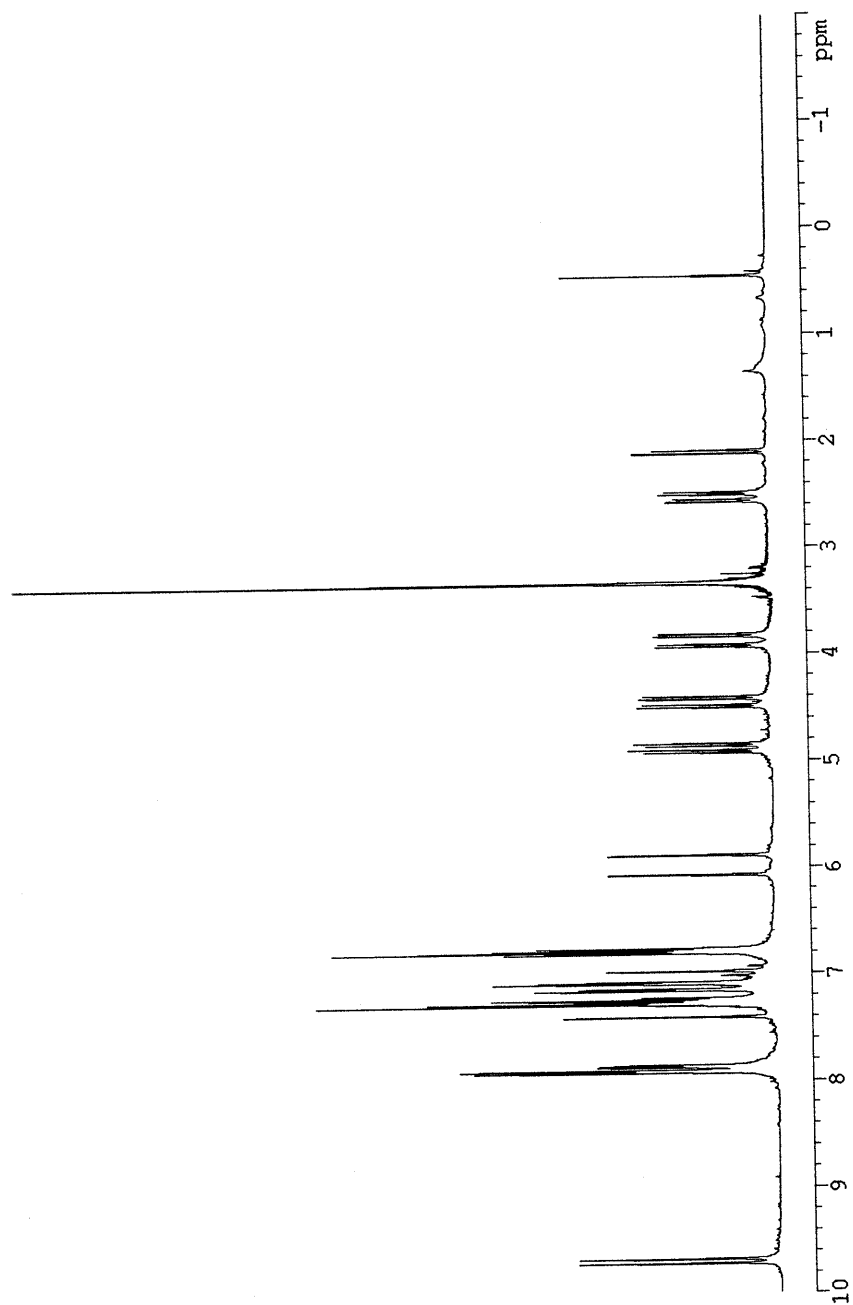
Dimer 71·71 with encapsulated 1,4-dioxane in toluene-*d8*.

Dimer **71·71** with encapsulated tetrahydrofuran in *p*-xylene-d_{10}.

Dimer **71·71** with encapsulated toluene in *p*-xylene-*d₁₀*.

7131-83